UMTRI 96-19

INTERPRETATION OF ROAD ROUGHNESS PROFILE DATA

FINAL REPORT

Prepared for

Federal Highway Administration
Contract DTFH 61-92-C00143

Michael W. Sayers
Steven M. Karamihas

June 1996

UMTRI The University of Michigan Transportation Research Institute

Technical Report Documentation Page

1. Report No.	2. Government Accession No.	3. Recipient's Catalog No.
FHWA-RD-96-101		

4. Title and Subtitle	5. Report Date
Interpretation of Road Roughness Profile Data	6. Performing Organization Code
	8. Performing Organization Report No.
7. Author(s)	
M. W. Sayers and S. M. Karamihas	
9. Performing Organization Name and Address	10. Work Unit No. (TRAIS)
The University of Michigan Transportation Research Institute 2901 Baxter Road Ann Arbor, Michigan 48109	11. Contract or Grant No.
	13. Type of Report and Period Covered Final Report Nov. 1992 - Jan. 1996
12. Sponsoring Agency Name and Address Office of Engineering Research and Development Federal Highway Administration 6300 Georgetown Pike McLean, Virginia 22101-2296	14. Sponsoring Agency Code

15. Supplementary Notes

This research was conducted in collaboration with Soil and Materials Engineers, Inc. via participation and contributions of Dr. Starr Kohn and Dr. Rohan Perera. Mr. Harry Smith also contributed as a private consultant.

16. Abstract

The majority of States own high-speed devices for measuring longitudinal road profiles that are potentially rich in information about the pavement surface condition. The primary objective of this research was to advance the state of practice for extracting this information. A secondary objective was to assist users in resolving common measurement errors.

Vast amounts of measured profile data were acquired to evaluate various analysis methods in terms of their usefulness and validity when applied to profiles obtained from different types of instruments. Methods for determining an index called Rideability Number (RN) were studied in detail. A practical algorithm was developed for computing RN without bias from profiles obtained from a variety of equipment, with the exception of those that use ultrasonic sensors. Other analyses studied in the project include the International Roughness Index (IRI), power spectral density (PSD), high-pass filters, and cross correlation.

The research was coordinated with activities of the Road Profiler User Group (RPUG). A critical problem facing road profiler users is a lack of knowledge involving the technology. Accordingly, a 2-1/2 day course on profile measurement and analysis was prepared, along with the first draft of a companion document called "The Little Book of Profiling." The course introduces new users to the basics of what profilers are, how they work, and what can be done with their data. A user-friendly profile analysis software package called RoadRuf was developed that includes many profile analysis methods. The software had been provided to participating States, and is available on the Internet.

17. Key Words	18. Distribution Statement
Road roughness, longitudinal profile, profile measurement, profile analysis, power spectral density, International Roughness Index (IRI), Ride Number (RN)	No restrictions. This document is available to the public through the National Technical Information Service, Springfield, Virginia 22161.

19. Security Classif. (of this report)	20. Security Classif. (of this page)	21. No. of Pages	22. Price
Unclassified	Unclassified	177	

TABLE OF CONTENTS

TABLE OF CONTENTS
(Continued)

TABLE OF CONTENTS
(Continued)

Page

TABLE OF CONTENTS
(Continued)

Page

LIST OF FIGURES

LIST OF FIGURES
(Continued)

LIST OF FIGURES

(Continued)

LIST OF TABLES

LIST OF ACRONYMS

AASHTO	American Society of State Highway and Transportation Officials
APL	Longitudinal Profile Analyzer
ASTM	American Society for Testing and Materials
CPCC	Continuous Portland Cement Concrete
DLC	Dynamic Load Coefficient
DOT	Department of Transportation
FFT	Fast Fourier Transform
FHWA	Federal Highway Administration
GMR	General Motors Research
GPS	General Pavement Study
GUI	Graphical User Interface
HCS	Half-Car Simulation
HPMS	Highway Performance Monitoring Network
HRI	Half-Car Roughness Index
ICC	International Cybernetics Corporation
IRI	International Roughness Index
IRRE	International Road Roughness Experiment
JPCC	Jointed Portland Cement Concrete
LCPC	Laboratoire Central des Ponts et Chaussees
LTPP	Long-Term Pavement Performance
MPR	Mean Panel Rating
NASA	National Aeronautics and Space Administration
NCHRP	National Cooperative Highway Research Program
NHI	National Highway Institute
PCC	Portland Cement Concrete
PI	profile index
PSD	Power Spectral Density
PSI	Present Serviceability Index
PSR	Present Serviceability Rating
QI	Quarter-car Index
RMS	root mean squared
RMSD	Root-Mean-Squared Deviation
RMSVA	Root-Mean-Squared Vertical Acceleration
RN	Rideability Number
RPUG	Road Profiler User Group
RQI	Ride Quality Index
SD	South Dakota
SDI	South Dakota Index
SHRP	Strategic Highway Research Program
TRB	Transportation Research Board
TRIS	Transportation Research Information Service
TRRL	Transport and Road Research Laboratory
UMTRI	University of Michigan Transportation Research Institute

1. INTRODUCTION

High-speed road profiling is a technology that began in the 1960s when Spangler and Kelly developed the inertial profiler at the General Motors Research (GMR) Laboratory.[1] In the past decade, profiling instruments based on the GMR design have become everyday tools for measuring road roughness. The majority of States now own road profilers. As profiling capability has become the rule, rather than the exception, the most widely used summary index is the International Roughness Index (IRI). IRI has considerable merit as a summary profile-based roughness index. However, it was tailored to be measurable by a wide range of equipment, including response-type systems, rather than to be the best profile-based measure of any specific pavement quality.[2]

State agencies with profiling instruments are building a data base of measurements that contain potential riches of information about the pavement surface condition. However, existing technology for extracting practical information from profiles often goes unused. With the vast amount of data being acquired, users are now asking (other than IRI) what can be learned from the profile data? An even more basic issue for many users involves the quality of the IRI data now being collected. Roughness measures that are supposedly on the standard IRI scale are submitted yearly to FHWA for the national Highway Performance Monitoring System (HPMS) data base, and discrepancies in profile-based data are being identified. This leads to questions of how to control the quality of IRI and other profile-based measures. For example, many State agencies use algorithms developed in-house for estimating serviceability, and the relationship of these indices to each other and to IRI is not well known.

This report documents the research conducted under FHWA Contract DTFH 61-92-C00143, supported with funds pooled from 17 States. The primary objective of the research was to advance the state of practice for extracting information from profile data. A secondary objective was to assist State profiler users in resolving common sources of profile measurement error. To address these needs, the research program covered three areas: (1) profile analysis methods were studied; (2) technology was transferred to the States through several novel methods; and (3) standardization was promoted by providing tested computer code to the States and the American Society for Testing and Materials (ASTM).

ANALYSIS METHODS

The technical approach taken in the research was to acquire vast amounts of measured profile data, and then study profile analysis methods in terms of the usefulness of the information they extract and their validity when applied to profiles obtained from different types of instruments. The profile measurements were organized into the data sets listed in table 1. Over 200,000 analyses were run on these profiles during the project.

Table 1. Summary of data sets used in this research.

Data Set	Purpose	Number of	
		Sections	Measurements
Correlation Matrix	Correlate profile indices	88	400
Portability Matrix	Determine the portability of various profile analysis algorithms	30	158
Measurement Error Matrix	Identify common measurement errors	30	2,458
Minnesota Data	Verify ride number algorithms	96	285
Ohio Data	Evaluate alternative ride numbers	140	700
LTPP Study GPS Section Data[1]	Identify common measurement errors, test the IRI algorithm	180	1,010
State Department of Trans. Data	Identify common measurement errors	27	27

[1] Long-Term Pavement Performance Study (LTPP) General Pavement Study (GPS) Data

The focus of the work was on ride quality because the participating States identified rideability as the pavement condition of greatest interest. Methods for determining an index called Rideability Number (RN) were studied quite thoroughly. Previous research sponsored by the National Cooperative Highway Research Program (NCHRP) was continued to develop a practical algorithm for computing an RN.[3,4]

Although the primary technical achievement of the project was the development of a portable RN algorithm, many other analyses were investigated and demonstrated. The IRI analysis was further studied and refined. Several profile analyses useful for research programs were considered and are described. These include band-pass filters, power spectral density (PSD) transforms, and the cross-correlation transform.

TRANSFER OF TECHNOLOGY

Many of the concerns of the State profiler users involve inadequate technology transfer rather than a lack of tools for interpreting profiles. The research was coordinated with activities of the Road Profiler User Group (RPUG). Data collected for RPUG were analyzed, and preliminary research results were presented at three consecutive RPUG annual meetings. Most of the measurement problems were identified by users at RPUG. Analysis methods were used to identify measurement problems and to illustrate how pavement condition can be diagnosed in more detail.

The project included several novel approaches to promote technology transfer:

1. During the project, the researchers worked directly with State users, through RPUG and contacts with the pooled-fund States. The research direction was strongly influenced by practitioners, and RPUG provided a means for transferring useful technology to the users as it was developed during the project.

2. Analysis methods were transferred in the form of ready-to-run software that was made available to users during the project.

3. The major problem facing users was identified as being a lack of information about existing technology, rather than a lack of technology. Accordingly, the researchers prepared lectures for RPUG and developed a short course on profiling.

Two technical papers were prepared for the Transportation Research Board (TRB). The first, "On the Calculation of IRI from Longitudinal Road Profile," was recently published and provides a single, short, archival reference for the IRI analysis.[5] The second, "Estimation of Rideability by Analyzing Longitudinal Road Profile," describes the new RN analysis developed in the research and is awaiting final publication.[6]

STANDARDIZATION OF PRACTICE

The Pavement Division of FHWA has initiated a major emphasis on standardization of procedures for evaluating the condition of the Interstate Highway System. All of the States are currently required to report measured IRI values for a portion of their network for the national HPMS data base. When this project started, wide discrepancies were noted in the reported IRI roughness levels between the States.[7] Standardization is needed in two areas: (1) guidelines for obtaining profile measurements are needed to ensure that the measures are valid; and (2) analyses applied to the profiles must function as expected.

Organizations such as ASTM and the American Association of State Highway and Transportation Officials (AASHTO) currently serve as the normal source of standards for profiling practice. However, the technology for evaluating road roughness profiles has developed much more rapidly than these organizations put standards into print. Standardization of profile analyses is accomplished most directly if the same software is used by most States. This was a major motivation for preparing the user-friendly software package. The computer source code is listed in this report and has been incorporated into several draft ASTM standards now in review.

ORGANIZATION OF THE REPORT

Chapter 2 concentrates on the interpretation of road profiles without regard to how they are obtained. It summarizes analysis methods that are commonly applied to profiles, such as IRI and PSD, and presents the new RN algorithm developed in this project. Chapter 3 focuses on the measurement of profiles, as needed to support the analyses described in chapter 2. It begins with an introduction to profiling, and discusses factors in current practice that sometimes prevent the accurate measurement of road profile. Chapters 4 and 5 cover the standardization and transfer of technology; chapter 4 describes the user-friendly software package, and chapter 5 briefly summarizes the National Highway Institute (NHI) short course. Chapter 6 presents the conclusions and recommendations.

Appendices A through I provide technical details about the analyses, sources of data, derivations, etc.

2. ANALYSES

This chapter summarizes the analysis methods used in the project. Two of the analyses produce roughness indices for summarizing pavement roughness condition for pavement management and evaluating new construction. The first is the IRI, which is presently the standard roughness index used by all States for data submitted to HPMS. The second method, developed as a part of this project, is the portable RN.

Other analyses are described that have application in the more specialized tasks of (1) diagnosing the condition of specific sites and determining appropriate remedies; and (2) studying the condition of specific sites for research. These analyses include adjustable filters, PSD functions, and the cross-correlation transform.

This chapter focuses on uses that can be made of measured profiles. In general, the descriptions that follow are based on the assumption that valid profiles have been measured. The quality of the measurement is also important and will be covered in chapter 3.

INTERNATIONAL ROUGHNESS INDEX

The IRI is a profile-based roughness statistic that has become a standard indicator of road roughness in the United States and elsewhere around the world. The research foundation for the IRI occurred under an NCHRP project in the late 1970s, described in NCHRP Report 228.[8] A main objective of that research program was to develop a time-stable means for calibrating response-type systems. A mathematical transform of measured longitudinal profile was proposed as a calibration reference. The analysis method was further developed, simplified, and standardized under funding from The World Bank. The index obtained with the standardized method was called IRI, and guidelines were prepared for measuring it with a variety of equipment, including profilers.[2,9]

Technically, the IRI is a mathematical representation of the accumulated suspension stroke of a vehicle, divided by the distance traveled by the vehicle during a test. Thus, it has units of slope. Instead of accumulating the suspension stroke with a test vehicle, the IRI is calculated from a measured longitudinal road profile using a quarter-car simulation. The quarter-car simulation is meant to be a theoretical representation of the response-type systems in use at the time the IRI was developed. Coefficients in the equations were found in the NCHRP research to obtain maximum correlation to the output of those systems.

Since the publication of guidelines for obtaining IRI in 1986, it has become the most widely-used reproducible indicator of road roughness.[2] The IRI is required for all data submitted to the FHWA HPMS data base and is stored in the LTPP data base.[10] Virtually all road profiling systems used in the United States are equipped with software for computing IRI, and an ASTM standard (test method E 1364-90) exists for computing IRI from rod and level instruments. In several past research projects, the algorithm used to compute IRI has been shown to be largely independent of profile characteristics—more so than any of the other proposed roughness indices evaluated.[9]

Figure 1 shows some sample scatter plots obtained from the portability data acquired in this project. Each plot includes a line of equality. Ideally, all points would lie on the line of equality. Scatter about the line is expected because of random sources of variation. Systematic bias is a potential problem because management decisions would be based on an incorrect overall view of a network's condition. The plots show little bias, indicating that IRI values from the different profilers are directly comparable. Thus, similar management decisions would be made based on data from any of them.

Although the IRI is in widespread use, there has been a lack of consistency in the procedure for measuring the IRI for HPMS and LTPP. This was revealed in a survey of the States conducted during the planning stages of this pooled-fund project (see appendix B). It was found that some States average the left- and right-hand profiles prior to

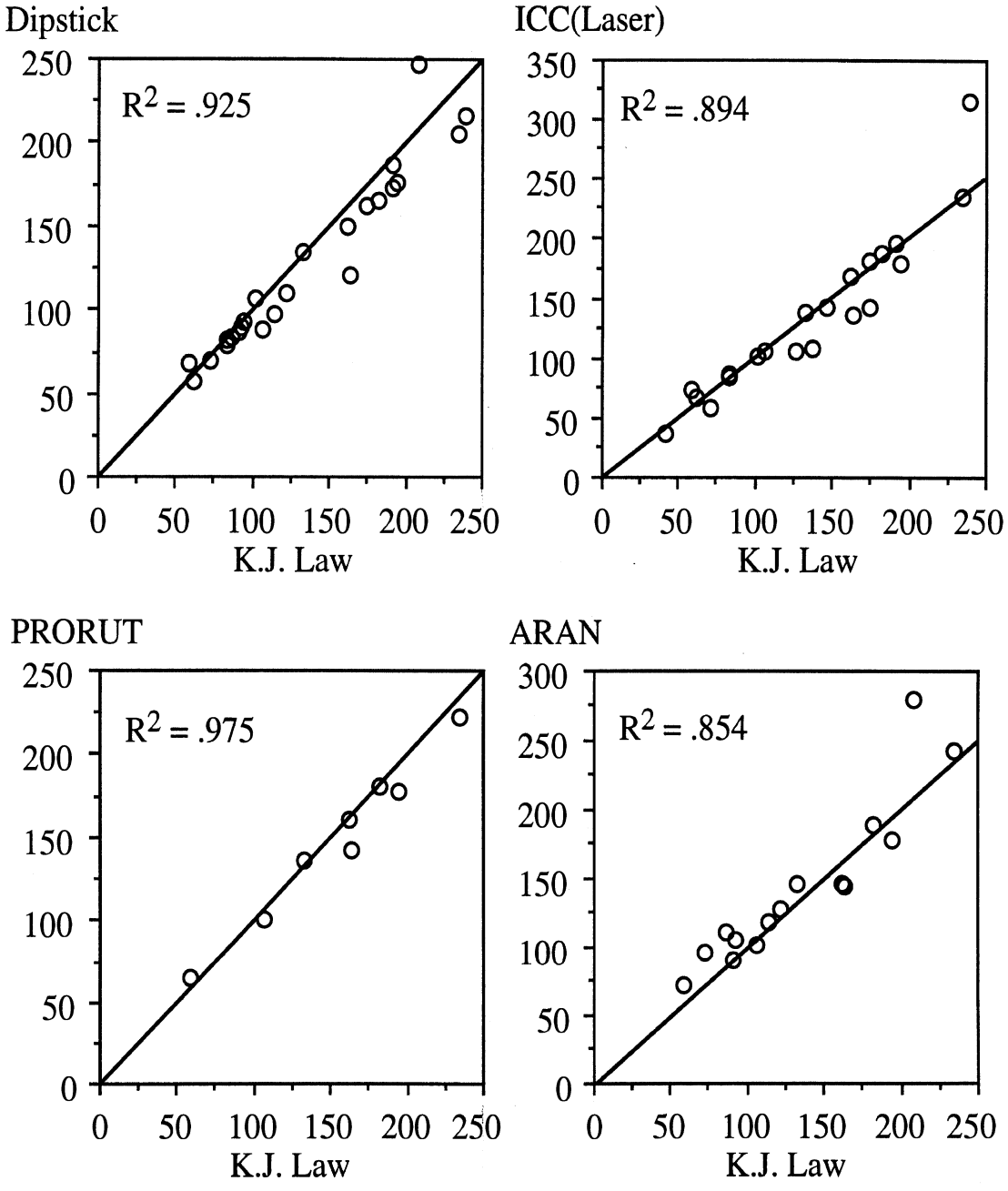

Figure 1. Comparison of IRI measures from different profilers.

processing, thereby obtaining the Half-car Roughness Index (HRI) rather than the IRI.[11] (The difference between the HRI and IRI will be discussed later in this chapter.) This was verified in informal discussions at the 1993 and 1994 meetings of the RPUG, and has been documented in recent surveys of the States aimed at identifying impediments to standardization for the HPMS.[7,12]

Another issue in the calculation of the IRI involves the use of a 9.8-in (250-mm) moving average, which is part of the specification for calculating the IRI. Digital Profilometers made by K.J. Law, Inc., already include a moving average of 12 in (305 mm). Therefore, users of Law Profilometers should omit the moving average portion of the IRI algorithm. The result of performing the smoothing twice is that the short wavelengths are filtered excessively, leading to IRI numbers that are too small. For example, the IRI values reported for 737 measurements of 139 GPS sections were found to be systematically lower than the correct values by 1.4 percent because they were filtered twice. This error is more significant in road sections with large, short duration bumps, such as faulted joints or potholes. Although the error in procedure causes an average bias of only 1 to 2 percent, the error can be as high as 10 percent on sections with large bumps.

In response to concerns expressed by participating States and RPUG members, the definition of the IRI was reviewed during this project and found to be technically sound. IRI calculations have been made for all profiles analyzed in the project, and no errors have been identified that were not the result of errors in the original profile. The problems mentioned above indicate a need for education about the IRI. Profiler users had been hampered in their adoption of a standard procedure for calculating IRI because the pertinent information was scattered through three lengthy reports published from different sources: NCHRP Report 228, and World Bank Technical Papers 45 and 46.[2,8,9] A further complication is that some papers and reports have been published over the last few years that contain errors and misconceptions about IRI. New users and equipment developers wishing to calculate IRI find that there has been no single, short, reference document to aid them.

Several steps have been taken to reduce future error in IRI measurements.

- A paper entitled "On the Calculation of IRI from Longitudinal Road Profile" was written and has been published by TRB.[5] The paper provides a single reference document that contains the history and theoretical basis of the recommended IRI algorithm in detail. It includes previously unpublished details about how the algorithm works and theoretical analyses of the effects of sample interval. Hopefully, by fully defining the IRI and its calculation methods in one place, new users and equipment and software developers will find it easier to understand.
- Software for computing IRI has been prepared for public distribution as part of the user-friendly software package described in chapter 4.
- Fortran computer code for calculating IRI is listed in appendix F of this report. The Fortran code has been supplied to ASTM and is in a pending standard for computing IRI.

- Dr. Sayers, the developer of the IRI, made presentations at the 1993, 1994, and 1995 RPUG meetings describing the basic theory of the IRI and helped with minor problems some of the States were having.

HALF-CAR ROUGHNESS INDEX

Given two profiles, one for the left-hand wheel track and one for the right-hand wheel track, there are two ways to process them with a quarter-car model. One method, used for IRI, is to process each profile separately and obtain a roughness index for each. Then, the two IRI values are averaged.

The other method is to take a point-by-point average of the two profiles first, and then process the averaged profile with a quarter car filter. As shown in figure 2, the second method is the same as simulating a half-car model (with some restrictions on parameters) when roughness is characterized by a simulated road meter located at the center of the vehicle model. When the IRI quarter-car analysis is applied to the averaged profile, the resulting index has been called the HRI.[11]

There is a subtle difference in the way roughness is filtered by IRI and HRI. Consider a sinusoidal input. If both sides receive the same sinusoid, in phase, then the whole vehicle bounces in response. It does not roll at all. In this case, IRI and HRI would be identical.

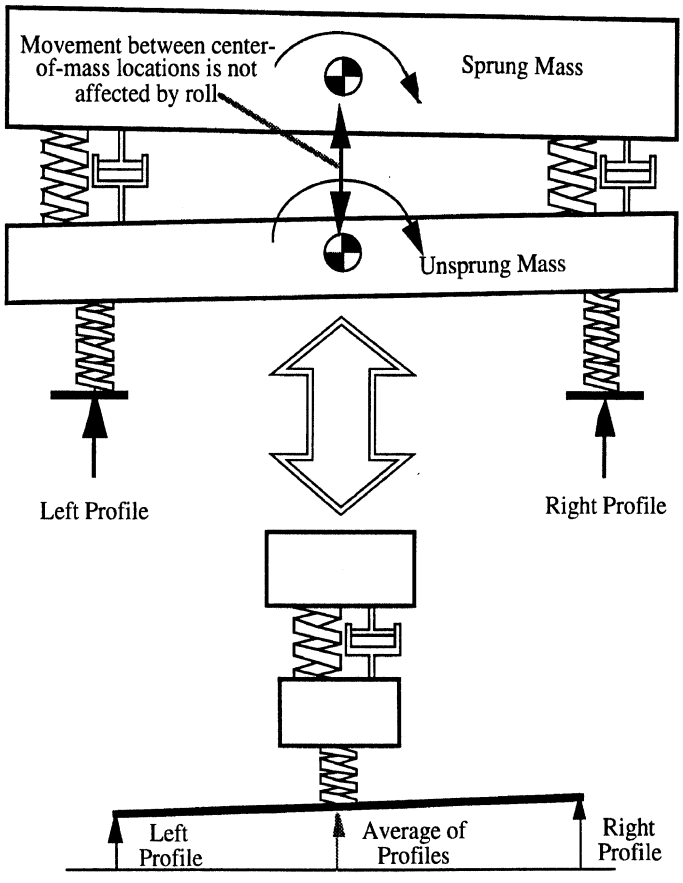

Figure 2. Half-car model.

However, if the sinusoids are 180 degrees out of phase, such that the left side goes up when the right side goes down, the vehicle rolls but does not bounce. With the road meter installed at the center of the axle, it senses bounce but not roll. In this case, the HRI would be zero, but not the IRI. In real roads, there is a mixture of bounce and roll. The bounce part gets through, but the roll part does not. Consequently, the roughness as calculated with an HRI analysis must be less than or equal to the result obtained from the IRI analysis.

A potential advantage of the half-car analysis is that it more closely matches the way road meters are installed in passenger cars. If the intent is to predict passenger ride, then it is not clear which model is better. Passengers do not sit at the center of the vehicle—they sit on one side. The HRI analysis eliminates roll responses that are experienced by the passenger. The IRI quarter car does include a roll component, but it is probably not an accurate representation.

A disadvantage of the half-car analysis is that for it to work, the two profiles must be perfectly synchronized before they are averaged. For profilers that measure profiles in two wheel tracks simultaneously, the two are properly synchronized and this is not a problem. However, for profilers that profile only one line, it is extremely difficult and time consuming to make two passes (measuring the profiles of the left and right wheel track) and then align the two profiles within a foot (0.305 m) as needed for the analysis. Practically speaking, the HRI analysis can only be used for systems that profile two wheel tracks simultaneously.

Statistically, there is not much difference between the HRI and the average of the IRIs calculated independently for the two wheel-track profiles. Figures 3 and 4 compare the indices for Portland cement concrete (PCC) and asphalt sections from the correlation matrix assembled in this project.

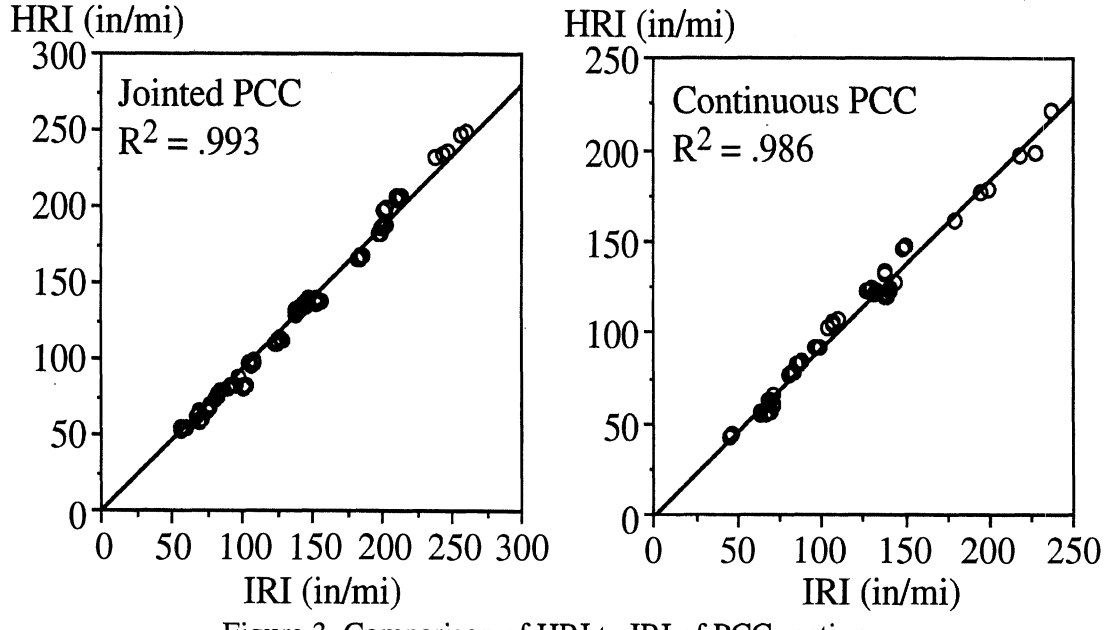

Figure 3. Comparison of HRI to IRI of PCC sections.

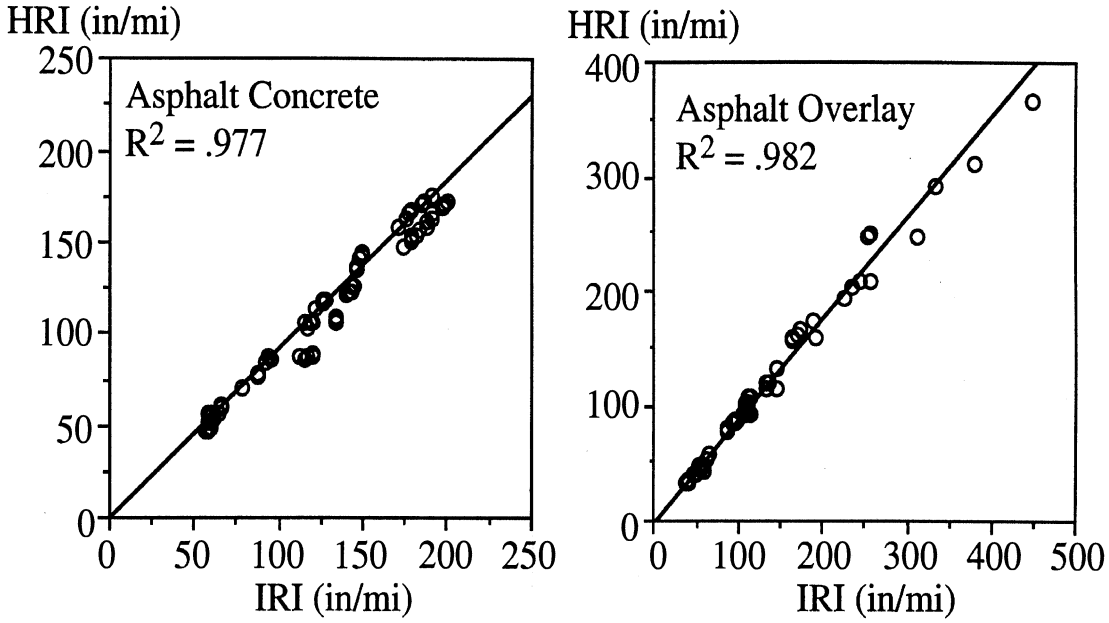

Figure 4. Comparison of HRI to IRI of asphalt sections.

RIDE NUMBER

"Ever since roads and highways have been constructed, the people who use them have been keenly aware of the relative degrees of comfort or discomfort experienced in traveling."[13] Long before high-speed profiling technology existed, engineers attempted to estimate the general opinion of the traveling public of specific roadways using a variety of road-roughness measuring instruments and methods. As soon as road profiling became a feasible technology for highway agencies, research began to establish a link between profile properties and rideability.

Concern about public opinion is as great today as it ever was. A poll of the States participating in this project ranked rideability measurement as the most important function desired in a road profiler system (see appendix B). Since the invention of the high-speed profiler three decades ago, researchers have worked to link public opinion to amplitudes and wavelengths in the profiles. Dr. Holbrook of the Michigan Department of Transportation (DOT) designed psychological testing methods to define public opinion, which he linked to wavelengths in roughness PSD functions in the late 1960s.[14] The NCHRP-sponsored two research projects by Dr. Michael Janoff in the 1980s that investigated the effects of road surface roughness on ride comfort, as described in NCHRP Reports 275 and 308.[3,4] Simultaneously, the Ohio DOT funded research by Elson Spangler and William Kelly of Surface Dynamics, Inc., on the same topic.[15,16] During two studies, spaced at about a 5-year interval, Janoff ran human rating experiments on 142 test sites in Ohio and determined mean panel ratings (MPR) on a 0-to-5 scale for each section. The Ohio DOT measured road profiles that were analyzed as part of the research.

Each rideability study resulted in the development of a profile analysis algorithm to predict MPR from measured profile. Based on Holbrook's work, John Darlington of the Michigan DOT developed an electronic filter to produce a profile-based statistic called Ride Quality Index (RQI).[17] RQI has been revised several times since then and has been used

in several internal research projects conducted by the Michigan DOT. (Technical details of the newer versions of RQI had not been published when this report was prepared.) Janoff and others developed a method for estimating panel rating from PSD functions taken for both left- and right-hand wheel-track profiles.[4] Although the basic theory of the method was presented, the method is complex, and a ready-to-run algorithm has not been published. Spangler and Kelly developed a simpler algorithm for predicting panel rating from profile that is more fully explained and is intended for use with profiles measured with K.J. Law Profilometers.[15] A review of the Janoff and Spangler/Kelly algorithms for predicting panel rating is given in appendix D. Neither analysis method was in common use at the time of this research.

The algorithms published by Janoff and Spangler for computing RN were tested on the portability matrix described in appendix C. Initial results showed that different results were obtained for data measured with different profiling systems. Consequently, the scope of work was extended to include data from three experiments in which panel ratings could be correlated to measured road profiles. The experiments included the two Ohio DOT studies mentioned earlier, and a recent study performed by Fred Maurer of the Minnesota DOT. Two data sets (see appendix C) were analyzed with the objective of devising a method for processing measured profile to obtain an index that is suitable for widespread use. A computational algorithm was developed with three objectives in mind: (1) relevance, as established by correlation between MPR and RN computed from profile; (2) portability, as determined by the ability of different profiling systems to obtain comparable RN values for profiles taken on the same pavement; and (3) simplicity, as determined by programming effort.

Analysis Approach

A variety of algorithms were considered and tested for computing RN. The criteria used to develop the recommended algorithm are as follows:

- The computed RN should be nearly optimal for the Ohio DOT data set, which is thought to provide the best statistical link between profile and panel ratings.
- The computed RN should also show good results for the Minnesota data.
- Values of RN computed from profiles measured by different systems on the same test sites should be comparable, with minimal bias and random error. (These comparisons were made using the portability data set.) Further:
  - Good agreement is expected between K.J. Law Profilometers, other high-speed profilers with optical sensors, and static devices such as the Dipstick.
  - The algorithm must be relatively insensitive to sample interval and should remain valid for improved profilers that can sample the profile at intervals shorter than 6 in (152 mm).
  - If possible, the algorithm should give meaningful results when applied to profiles obtained with low-cost ultrasonic sensors.
- If possible, RN should be defined such that users can apply the algorithm even if they have profiles measured in only one wheel track.

- The algorithm should be relatively simple to reduce programming errors and to encourage its use.

The study of the link between profile characteristics and rideability was done in three stages. First, as was done in the NCHRP rideability studies, PSD analyses were used to identify the waveband of road roughness that correlates best with MPR. Second, various numerical filters were tested whose basic sensitivity to wave number matched the desired waveband. Third, the portability of the algorithms to common profiling systems was tested by applying the algorithms to profiles from the portability matrix.

Using computer searching, thousands of coefficient sets were tested on hundreds of profiles. The best algorithm is discussed in detail below. Further details are given in appendixes H and I, with other algorithms included for comparison.

Initial Waveband Study

PSD analyses were used to identify the waveband of road roughness that correlates best with MPR. PSD functions of measured road profiles from the Ohio and Minnesota DOT panel rating experiments were converted to a series of root-mean-square (RMS) values over one-third octave bands. (PSD analysis is discussed in more detail later in this chapter.) The RMS values were combined over various wavebands in a search for the wave number range that yielded the best estimate of panel rating.

A profile index (PI) was defined for several combinations of RMS values in one-third octave bands, including various ranges of bands and weightings. To account for the nonlinear relationship between PI and MPR, a transform was applied each time PI was correlated to MPR. The transform has the form:

$$RN = 5\, e^{-A(PI)^B} \qquad (1)$$

For each road site, five sets of RMS slope values were calculated: (1) the left wheel-track profile alone; (2) the right wheel-track profile alone; (3) the point-by-point average of the two profiles; (4) the point-by-point difference between the two profiles; and (5) the RMS average of the RMS values computed for the left and right wheel-track profiles. Of the five sets of RMS values computed for each pair of profiles, the best correlations were obtained for both the Ohio and Minnesota DOT data sets with two of the five sets of RMS values: (1) the RMS average of the RMS of the left profile and the RMS of the right profile; and (2) the RMS of the averaged profiles.

Figure 5 shows a plot of R^2 (the coefficient of determination, also known as the squared correlation coefficient) versus wave number for the Ohio DOT data set, obtained using PIs defined as the average of the RMS of the left and right profiles in 28 individual one-third octave bands. High correlation ($R^2 > 0.65$) is obtained for wavelengths shorter than 20 ft (6.10 m). Lesser agreement is obtained for wavelengths up to 64 ft (19.51 m), and very little correlation is shown for longer wavelengths. For the range of wave numbers covered, the high wave numbers are clearly more important for predicting MPR than the low wave numbers. This finding corroborates the conclusions of Janoff, Spangler, and others.

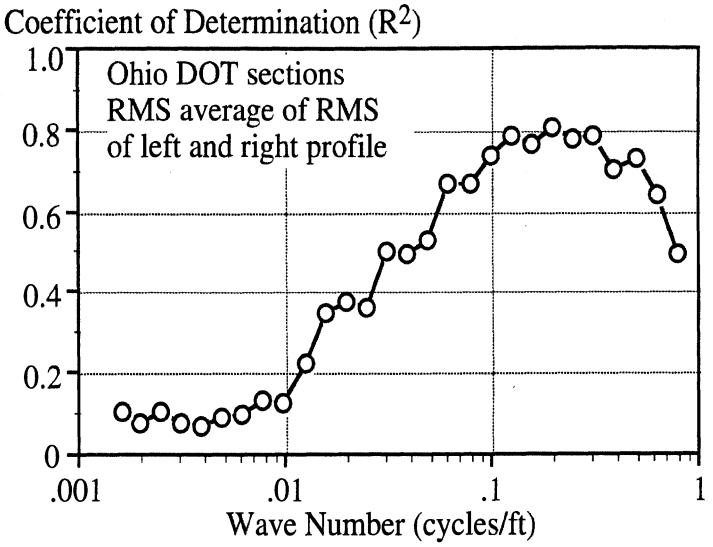

Figure 5. Correlation between MPR and third-octave RMS slope.

Having established correlations between MPR and individual third-octave RMS values, the next step was to roughly determine the range of wave numbers that should be included in a single PI that is intended to predict MPR. The strategy was to define a PI calculated from the highest third-octave waveband, then define a second PI that includes lower wave numbers to include two-thirds of an octave, and then a third PI that includes a full octave, and so on. Figure 6a compares the correlations for over 28 PIs, differing by the lower limit (longest wavelength, λ). The PI for the highest one-third octave band alone shows fair correlation with MPR. As the bandwidth is extended to include longer wavelengths, the correlation with MPR improves up to a point, after which roughness because of the longest wavelengths degrades the correlation. The best results ($R^2 = 0.85$) are obtained using the range of wavelengths from 1.1 to 36 ft (0.34 to 10.9 m).

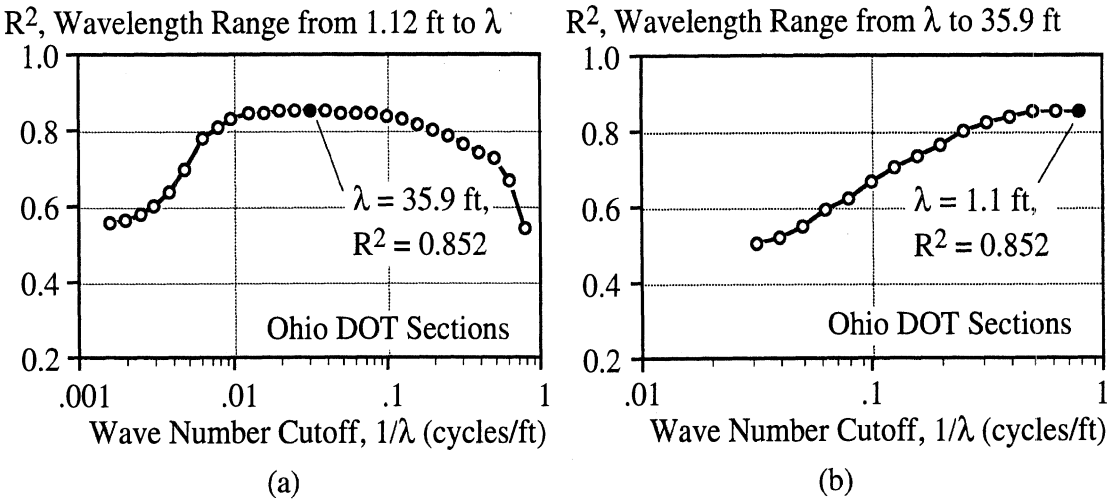

Figure 6. Correlation between MPR and PI for various wavebands.

Given an approximate limit for the longest wavelength that should be included for predicting panel rating, the question then becomes: What is the shortest wavelength that should be included? The same general sensitivity study was repeated, except that this time the PI was initially defined for the optimum long wavelength band alone, and higher third-octave bands were added until the highest wave numbers were included. As shown in Figure 6b, correlation improved until the highest band was added. This suggests that an RN algorithm should include wavelengths ranging from 1.1 to 36 ft (0.34 to 10.9 m).

In an attempt to guide the development of a digital filter for calculating RN, further searching was conducted to identify an optimal frequency weighting function that could be applied to the RMS values over one-third octave bands. The best weighting function could be used as a target filter shape. Several attempts were made to improve the correlation over that shown in figure 6 for the box-car weighting function, but only slight improvements were achieved.

Further information about the waveband study is presented in appendix G.

The New Algorithm for Computing Ride Number

The results of the PSD analyses were used to devise a variety of filters that were then tested. Some are described in appendixes E and F. One was the basic IRI calculation method. However, the filter coefficients were set to new values to change the sensitivity to wavelength, and different initialization and averaging methods were used. The changes result in an output considerably different from IRI. The new RN statistic is defined as follows.

- RN is an exponential transform of an RMS slope statistic called PI with dimensionless units of slope (in/in), according to the equation:

$$RN = 5e^{-160(PI)} \tag{2}$$

- If two profiles are processed, PI is the RMS value of the PI for the left and right profile:

$$PI = \sqrt{\frac{PI_L^2 + PI_R^2}{2}} \tag{3}$$

  However, if only a single profile is measured, its PI is used in eq. 2.

- PI for an individual profile is calculated using a modified version of the IRI algorithm. A Fortran version of the algorithm is provided in appendix F. The differences between the calculation of PI and IRI are:

  — The coefficients of the IRI are replaced with the following:

$$k_1 = 5120,\ k_2 = 390,\ c = 17,\ \mu = 0.036$$

  — The initialization length is changed from 36.1 ft (11.0 m) for IRI to 62.3 ft (19.0 m) for PI.

  — The accumulation is done by RMS, rather than mean absolute.

Note that the transform listed in eq. 2 uses a "B" value (see eq. 1) of 1.0. The optimal value was found to be 0.975. Given that the best value was so close to unity, a transform in which B is defined as 1.0 was also tested, and the difference was negligible. The value of 1.0 is used in the RN definition to simplify the equation.

Figure 7 shows the sensitivity of the PI filter to wave number. The gain, shown on the Y axis of the plot, is the ratio of the amplitude of a sinusoid output to the amplitude of a sinusoid input. Because the IRI filter involves processing of the slope profile, rather than the elevation profile, the PI produced by this filter has units of slope.

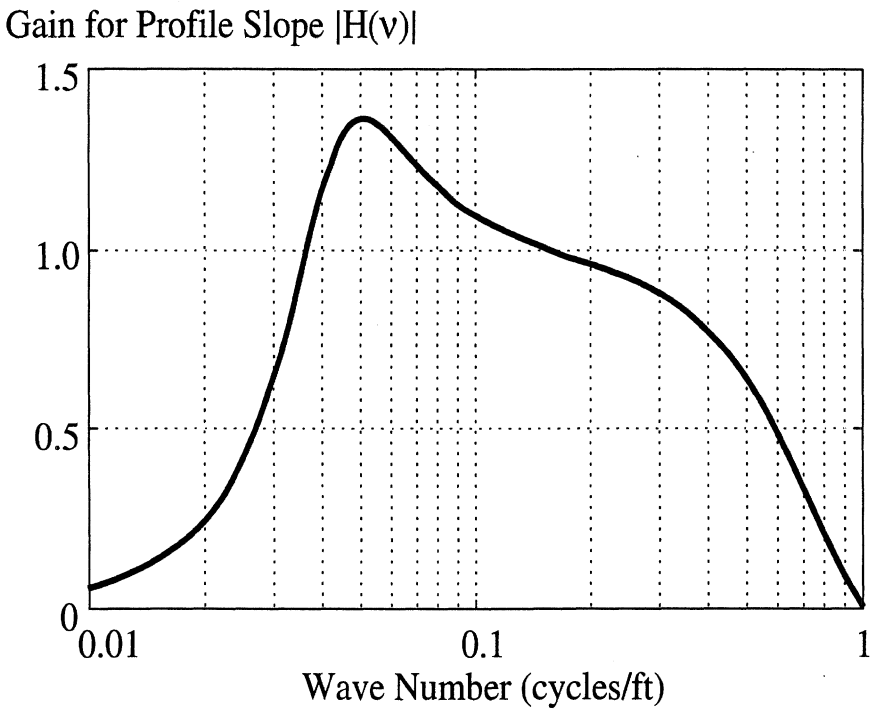

Figure 7. Wave-number response of the quarter-car filter for PI.

The choice of accumulating the square of the filtered slope (i.e., RMS averaging) was made after testing other powers (average rectified slope, root mean cubed, etc.). Mean-square accumulation was found to give noticeably better correlation with MPR than absolute value accumulation. Powers other than two were also tested, and the best correlation was found at about 2.2. However, the improvement gained was slight, and a power of two was chosen because it is compatible with variance-based statistics such as PSD functions.

Relevance of the New Algorithm

The relevance of the RN algorithm can be quantified by its correlation with MPR. Figure 8 shows scatter plots linking MPR to RN. Each plot also shows both a linear regression line and a line of equality. The new algorithm correlates to MPR ($R^2 = 0.85$) as well as any other analyses that have been reported.[18] The correlation for the Minnesota data is somewhat better ($R^2 = 0.88$), partly because the Minnesota data have more rough sections, which tends to improve the R^2 statistic regardless of the underlying relationship

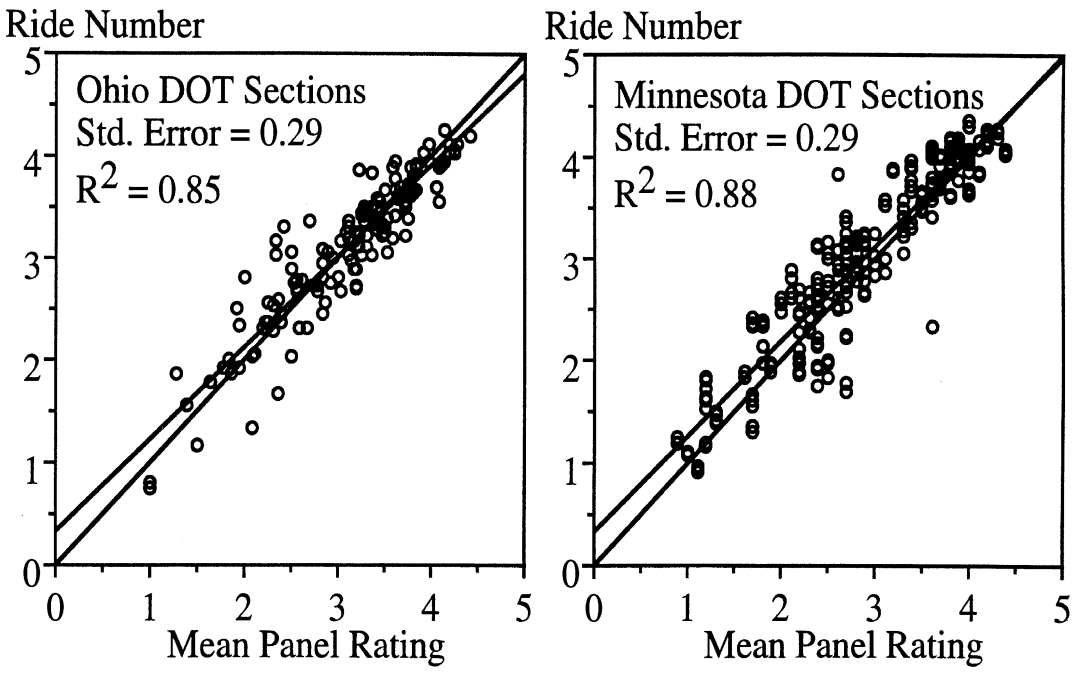

Figure 8. Correlation of Ride Number to Mean Panel Rating.

between the two variables being correlated. Appendix H provides details of the study of this and other algorithms.

Portability of the New Algorithm

The correlation obtained for the Ohio data set is about the same as that obtained independently by Janoff, Spangler, and others for the same data set. But what about the portability of the method? If an RN analysis is applied to profiles obtained by different instruments are comparable results obtained?

A subset of data from this project was used to determine the portability of profile-based algorithms to variety in the equipment. The new RN algorithm and other algorithms were applied to the portability matrix (see appendix C). Table 2 provides a summary of the normalized bias and normalized RMS difference values for four roughness statistics, relative to a K.J. Law Profilometer. (The Law system is used as the reference, because the Ohio data used to derive the algorithm were based on profiles from a Law system.) The IRI is included in the table as a reference. The others are PI algorithms as described by Janoff, and Spangler and Kelly.[4,12] The bias and RMS errors are taken for the PI values, rather than the RN values obtained by exponential transform. IRI and all three PI statistics are linearly related to profile amplitude, and thus statistical comparisons between them are simpler to understand. A detailed analysis of the portability of these algorithms is provided in appendix I.

The algorithm for the new PI shows the lowest errors of the three. The large differences seen for the Spangler/Kelly algorithm were investigated, and it was found that the algorithm includes an error that causes a significant bias as a function of sample interval (see appendix D).

Table 2. Comparison of various profilers to K.J. Law system.

Normalized Bias (%)	Dipstick	ICC (L)	PRORUT	ARAN	Pave Tech	ICC (U)	SDType
IRI	-5.6	-1.3	-3.1	8.3	26.6	16.3	6.5
Janoff PI	8.6	9.1	4.9	32.1	106.3	49.0	62.6
Spangler/Kelly PI	86.0	24.6	21.8	56.8	268.2	179.7	199.5
New PI	**0.3**	**-1.9**	**2.2**	**9.6**	**71.6**	**20.0**	**45.4**
Normalized Total Error (%)							
IRI	10.6	13.3	6.9	17.0	51.1	35.0	17.1
Janoff PI	21.5	21.1	11.6	45.4	167.5	105.8	73.5
Spangler/Kelly PI	94.6	39.8	31.8	71.5	407.5	315.3	222.3
New PI	**15.6**	**23.4**	**8.5**	**16.2**	**122.6**	**78.6**	**59.5**

Remaining Questions

Although the prediction of rideability is a long-standing objective of planners and engineers, the supporting research is scattered and is in some ways inconclusive and contradictory.

Frequency Range of Interest

The Ohio DOT data show that correlation between RN and MPR improves as shorter and shorter wavelengths are added to the profile index used to compute RN. On the other hand, the Minnesota profiles do not include those short wavelengths, and still give high correlations with MPR. This apparent contradiction is the heart of the problem with understanding rideability. Rideability projects such as those conducted by NCHRP and the Ohio DOT suggest that users mainly object to roughness associated with short wavelengths, corresponding to frequencies of 10 Hz and higher at normal highway speeds. On the other hand, shaker tests with human subjects have been performed in the controlled conditions of the laboratory by the National Aeronautics and Space Administration (NASA) and military researchers. (Conditions in aircraft and military ground vehicles can be so harsh that considerable research has been done to study the response of a human to full-body vibrations typical of those environments.) Results from the tests generally show that test subjects are most vulnerable to vibrations between 1 and 10 Hz, with maximum sensitivities in the 2 to 5 Hz range, depending on many factors such as posture, direction of the vibration, physical body type of the subject, and nature of the task being performed by the subject.[19,20,21] At normal highway speeds of 88 ft/sec (26.8 m/sec), the 2 to 5 Hz frequency range corresponds to wavelengths in the road ranging from 17.6 to 44 feet (5.4 to 13.4 m).

Although a great deal of test data support the idea that humans are most sensitive to lower-frequency vibrations (2 to 5 Hz), a possible explanation for the rideability ratings may be that users associate those vibrations more with the vehicle than the road, reserving blame of the road to higher frequencies.

Vehicle Type

The NCHRP panel rating data were collected using 1982 Plymouth Reliants (members of the Chrysler K-Car series), and the Minnesota panel data were collected using 1993 Chevrolet Luminas. Different classes of vehicle provide distinctly different levels of isolation from road roughness. Small economy cars transmit more high frequency (short wavelength) inputs to the car occupants, whereas larger and more expensive cars are tuned to provide better isolation. In addition, advances have been made in car design for ride quality between the time of the NCHRP and Minnesota studies. Physically, the small economy cars used in the NCHRP research were surely subjecting the test subjects to proportionally more harsh, high-frequency vibrations than the larger, more expensive cars used in the Minnesota study. After conducting a preliminary study, involving only asphalt tests sites, the NCHRP researchers concluded that the vehicle type did not influence panel rating, and limited all of the subjective rating vehicles to the K-Cars. However, other panel rating studies have concluded that vehicle type is an important factor in determining panel rating.[22,23]

Profiler Limits

The PSD study described in appendix G shows that the range of wavelengths that is most relevant to MPR for the Minnesota data is 4.5 to 90 ft (1.4 to 27.4 m). The Minnesota DOT sections were measured with ultrasonic profilers at a sample interval of about 13 in (330 mm). The shortest wavelength that can be measured at this sample interval is greater than 2 ft (610 mm). Another limit is that ultrasonic systems have difficulty measuring short wavelengths accurately, particularly on sections of coarse macrotexture.[5,24] The likelihood that the short-wavelength contributions to PI are inaccurate helps explain why adding these wavelengths degrades the correlation with MPR for the Minnesota data. Although the short wavelength measuring capability of the K.J. Law Profilometer is thought to be accurate for wavelengths down to a few centimeters, the data acquisition system attenuates the content for wavelengths shorter than 3 ft (0.914 m). Even with compensation for the filtering, the significance of wavelengths shorter than about 1.1 ft (0.34 m) cannot be determined because of the 6-in (152-mm) sample interval.

Instructions to the Panel

Subjective panel ratings depend strongly on the instructions given to the members of the panel to define what property or quality is being judged.[25] The instructions must train the rater. Yet, in a research program, the physical properties are not fully known—that is the point of the research. A primary objective of the NCHRP project was to develop a methodology for obtaining valid ratings. Instructions were read to the raters, but no physical examples of smooth or rough were given. The raters were told to consider the feel of bumps alone as degrading ride from perfect. The Minnesota study was done using the same scaling method (a form with the same look as in the NCHRP work), but the raters were exposed to physical examples of smooth or rough before they started. Because the IRI was in use as a measure of rough and smooth, it is possible that the example roads roughly trained the raters to estimate IRI, thereby explaining the high correlation seen between the IRI scale and the MPR data.

Relationship to IRI

Using the profiles from the correlation matrix to calculate IRI and PI, the calculated R^2 was 0.83. Thus, the PI statistic used to define RN is highly correlated to IRI. However, the two are not interchangeable—the new RN statistic provides a measure of pavement condition that is partially independent of IRI.

MOVING AVERAGE FILTER

To make practical use of a profile measurement, it is almost mandatory to filter the sequence of numbers that make up the profile. For example, figure 9 shows three profile plots for the same imaginary line along one of the sites included in the portability matrix. The profiles from the inertial devices were taken at normal highway speeds, so chances are that the exact lateral location of the profile was not exactly the same for the three measures. But still, this does not explain the completely different appearances among the profiles. The Dipstick shows a positive grade of 1 ft (0.305 m) vertical per 100 ft (30.5 m) longitudinal. The Strategic Highway Research Program (SHRP) instrument shows a fairly level profile, and the PRORUT shows a negative grade. (The grade seen by the static Dipstick device is assumed to be the closest to the truth.)

Details of the profile roughness are all but invisible in the plots of the unfiltered profiles. Figure 10 shows the same three profiles after they have been filtered to remove the road grade and very long undulations. Not only does the figure show profile variations, it also shows that the three measured profiles agree closely. Notice the bump at 260 ft (79.2 m). It is barely visible in the first figure, because the scaling is set to cover several feet of elevation change. When the grade and long undulations are removed mathematically, the bump is much easier to see. With a 0.06-ft (18.3-mm) magnitude, this is actually a severe disturbance in the road that will get the attention of anyone driving over it.

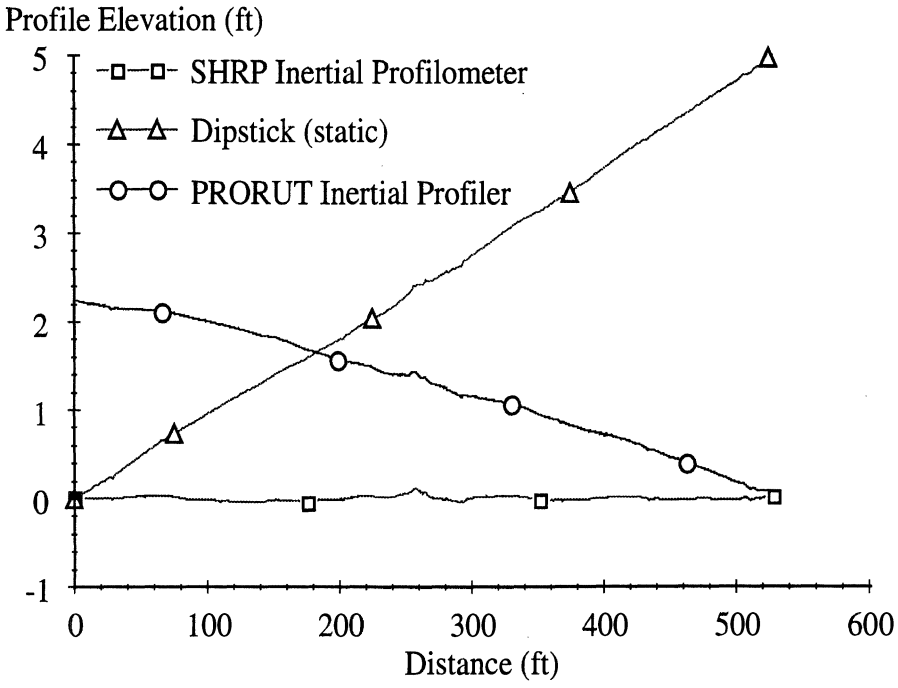

Figure 9. Three profiles measured with different devices.

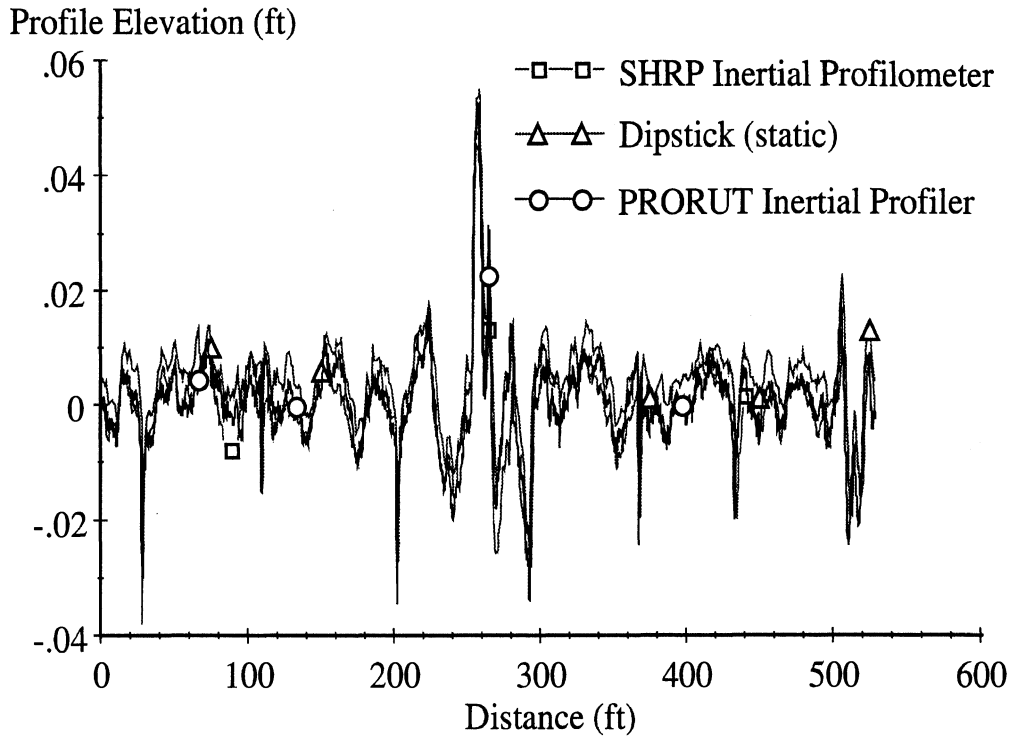

Figure 10. The same three profiles with long wavelengths removed by filtering.

To compare profiles from different profilers, it is necessary to filter the data to remove grade and long undulations. Filtering is particularly important when viewing data from high-speed inertial profilers and should be viewed as a fundamental part of the measurement process.

Appendix F contains computer code for two kinds of filters that remove both long and short wavelengths, leaving a band of wavelengths. (These are called bandpass filters.) One is based on the quarter-car differential equations and is used in the IRI and RN analyses described earlier. The other is called a Butterworth filter and is commonly used in electronics.

A much simpler filter, commonly used in profile analysis, is called the moving average. A moving average filter simply replaces each profile point with the average of several adjacent points within some base length. For a profile p that has been sampled at interval Δ, a moving average smoothing filter is defined by the summation:

$$p_f(i) = \frac{1}{N_{ave}} \sum_{j=i-B/(2\Delta)}^{i+B/(2\Delta)} p(j) \qquad (4)$$

where p_f is the smoothed profile, B is the base length of the moving average, and N_{ave} is the number of samples included in the summation. (The ratio $B/(2\Delta)$ is often not an integer. The round-off method influences the effective base length of the moving average.)

The effects of a moving average filter is demonstrated in figure 11. The long wavelength component of the original profile is not altered much. However, the short wavelength component is averaged out, smoothing the filter output.

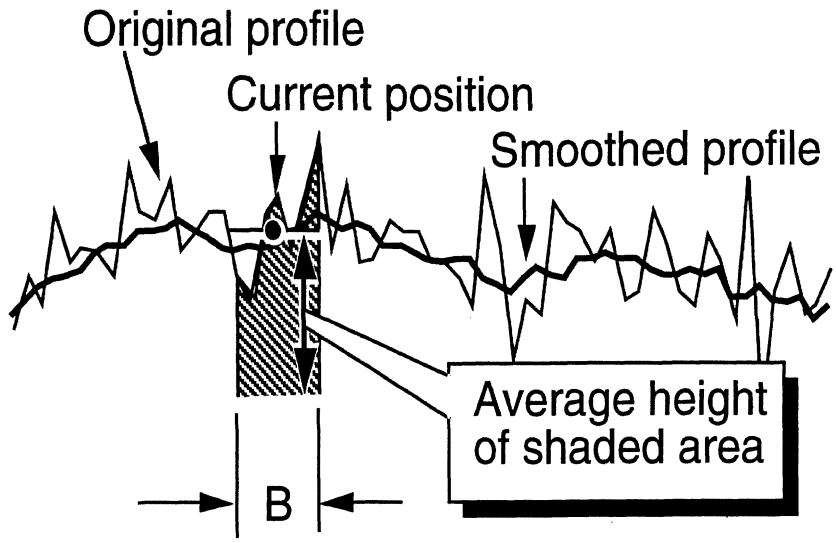

Figure 11. The moving average filter.

Figure 12 shows the wave-number response plot for a moving average filter. The X axis has been scaled by the product of wave number and base length (i.e., base length/wavelength). For each value of base length/wavelength, the plot shows how the moving average scales a sinusoid. Note that the output is zero when the wavelength equals the base length or any integer multiple of the base length. This is because the positive part of the sinusoid is exactly canceled by the negative part within the averaging interval. Because the filter attenuates sinusoids with high wave numbers, but passes sinusoids with low wave numbers, it is called a low-pass filter.

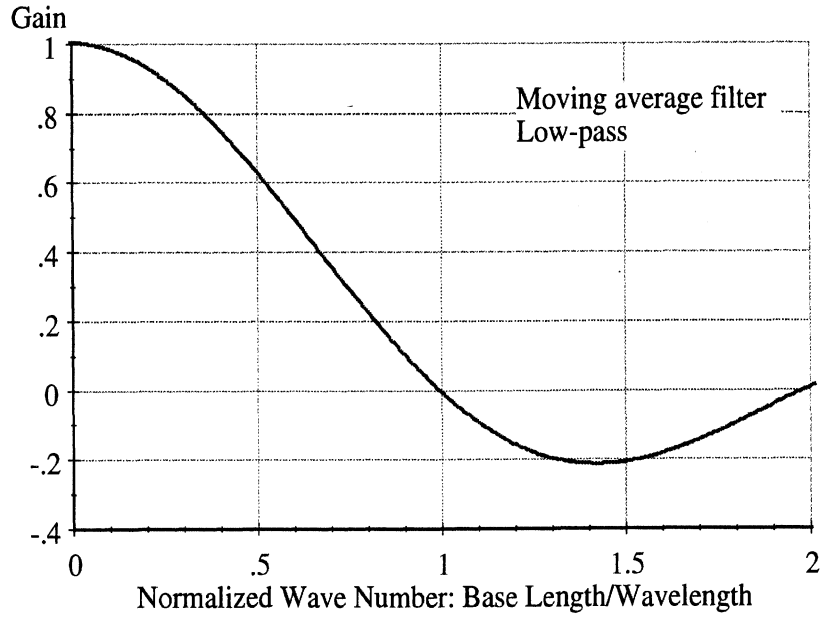

Figure 12. Wave-number response of the low-pass moving average filter.

The moving average can be converted to function as a high-pass filter that attenuates sinusoids with low wave number but passes sinusoids with high wave number. The high-pass version involves subtracting a smoothed profile from the original. Figure 13 shows the wave-number sensitivity for a high-pass version of a moving average. For any wave

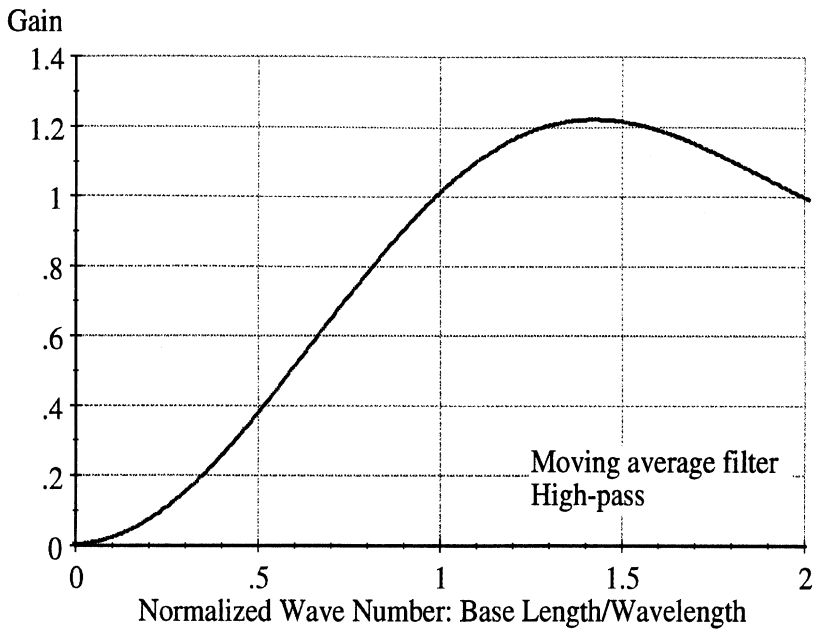

Figure 13. Wave-number response of the high-pass moving average filter.

number, the output of the high-pass moving average filter is one minus the output of the low-pass moving average filter.

A high-pass filter is an essential tool for viewing plots of road profiles. For example, a high-pass filter with a 30-ft (9.14-m) base length was used in figure 10 to compare profiles from different instruments. The filter also allows an engineer to see the features in the road that are of interest. There is no single best base length for profile interpretation; the best setting depends on the use to be made of the data. For example, figure 14 shows the profile of a faulted PCC pavement section filtered three different ways. The first plot in the figure was filtered with a 3-ft (0.914-m) moving average. This plot shows only the very short-duration bumps in the profile. The faults, spaced about 15 ft (4.57 m) apart, are very obvious when this filter is applied. The second plot shows the profile after a band-pass filter (high-pass, then low-pass filtered with a moving average) with base lengths of 3 and 20 ft (0.914 and 6.10 m) was applied. In this plot the faults are not visible because the short-wavelength content was removed, but the upward curling shape of the PCC slabs is very obvious. The third plot shows the band-pass filtered profile with base lengths of 20 and 100 ft (6.10 and 30.5 m). This plot shows the longer wavelength trends in the road, without the faulting or slab shapes. These plots illustrate the use of the moving average to understand the road features that contribute to roughness.

The moving average filter is an intuitive way to smooth a profile that is easy to understand and program. It is also efficient computationally and is bundled into the plotter provided in the user-friendly software package described in chapter 4. Although it can be used to separate different kinds of roughness (high wave number, low wave number), it is not an ideal tool for separating sinusoids with different wavelengths. As shown in figure 13, the transition from full attenuation to unity occurs gradually. Also, the filter amplifies the amplitudes of sinusoids with some wavelengths by over 20 percent.

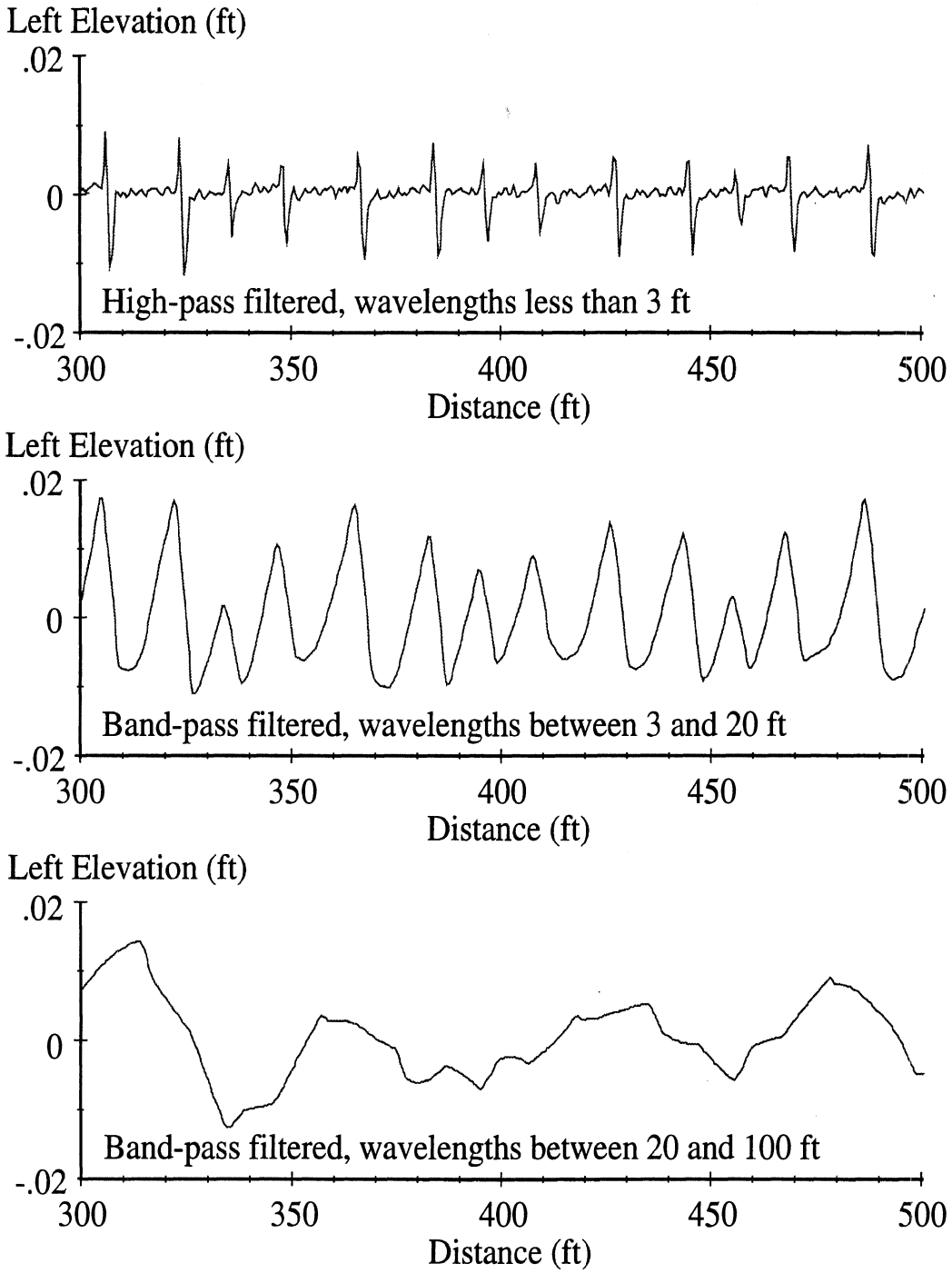

Figure 14. Filtered profiles of a faulted PCC pavement section.

A better analytical tool for investigating the distribution of roughness over different wave numbers is the power spectral density, described next.

PSD ANALYSIS

Mathematically, an arbitrary profile can be constructed from a series of sinusoids with different wavelengths, amplitudes, and phases. This is shown in figure 15 for just four sinusoids. To get the sharpness and detail seen in measured profiles, it is necessary to add many more sinusoids with shorter wavelengths.

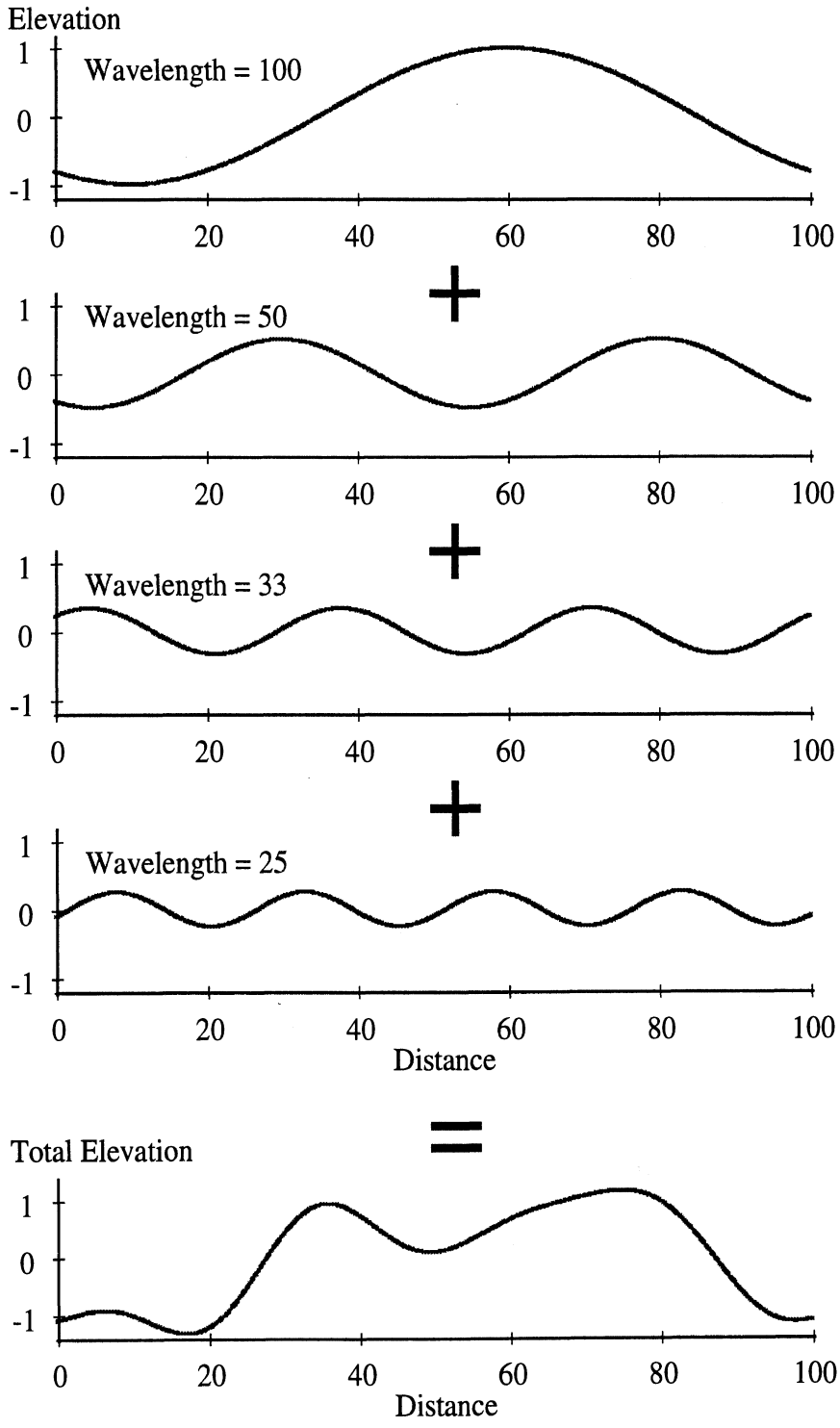

Figure 15. Mathematical construction of a profile from sinusoids.

On one hand, road profiles usually do not contain identifiable sinusoids. On the other hand, an arbitrary profile shape can be constructed artificially by adding together a series of sinusoids. If a profile is defined with N equally spaced elevation points, then it can be duplicated mathematically with N/2 sinusoids. Because there are so many sinusoids being added, their individual amplitudes are not large. A mathematical transform called a Fourier transform can be used to compute the amplitudes of the sinusoids that could be added together to construct the profile. The Fourier transform can be scaled such that it shows how the variance of the profile is distributed over wave numbers associated with sinusoids. When scaled in this manner, the transform is called a PSD function.[26]

The word power in PSD comes from its application in electronics, where it is applied to voltages. The variance of a voltage is proportional to power in a resister, so the PSD illustrates the distribution of electrical power over frequency. The same mathematical calculations developed for characterizing voltage variations can be applied to road profiles. Two differences between a road profile PSD and one measured for a voltage are (1) the variance has units of elevation squared, rather than volts squared; and (2) the distribution is over wave number (cycles/ft or cycles/m) rather than frequency (cycles/sec).

Calculation of Road PSDs

A profile constructed from a small number of sinusoids has nearly identical values at the start and end, and nearly the same slope. This can be seen for the example profile constructed in figure 15. The Fourier transform has a built in assumption that the profile repeats perfectly. However, this is not the case for profiles of real roads. For example, figure 16 shows how profiles from two sources are assumed to look beyond the 528-ft (160.9-m) distance measured. The assumed repeat of the profile shape causes an artificial discontinuity at the beginning and end of the measured profile. If the profile is filtered to exclude long wavelengths, as is the case for inertial profilers, the discontinuities might be minor. However, unfiltered profiles can introduce a large discontinuity, as shown in the figure for the Dipstick data. The roughness in the profile is barely visible, in comparison to a large sawtooth profile shape. Because the discontinuity occurs at the edge of the measurement, it is sometimes called an edge effect. Notice that the range covered on the Y axis is 6 ft (1.8 m) for the Dipstick, and only 0.2 ft (0.061 m) for the inertial profiler. Clearly, higher amplitudes can be expected from the Dipstick data unless mathematical techniques are used to reduce the effects of the sawtooth wave form.

There are two mathematical techniques used in general PSD applications (i.e., applications other than profile analysis) to reduce the edge effects. One is to calculate the linear trend in the profile with linear regression between elevation and distance, and then subtract the trend. This process is called detrending. It is particularly effective in eliminating the sawtooth wave form shown in the figure. However, when applied to a profile with a vertical curve, the detrended profile has a distinct parabolic shape, which introduces a different type of artifact in the computed PSD.

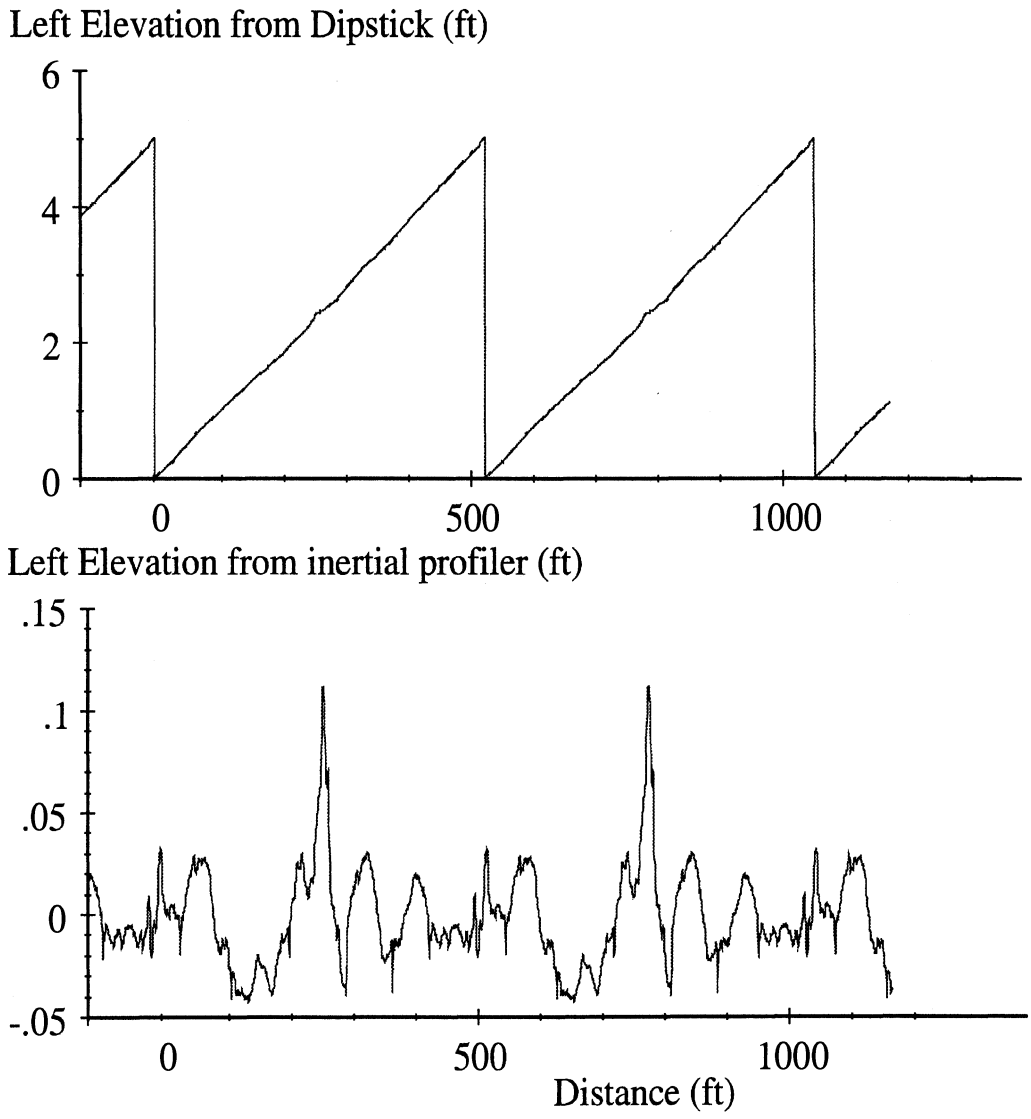

Figure 16. Wave forms assumed by Fourier transform for profile.

Another method is to "window" the data. (The name implies that the data is limited to what can be seen through a mathematical window.) A mathematical shaping function is multiplied by the profile values, to attenuate the elevations near the edges while leaving the values intact near the middle of the profile. The effect is similar to having a knob controlling the gain of the profiler and turning it on gradually at the start of the run, and then turning it down near the end of the run. One of the simplest mathematical functions is called a cosine taper.

Figure 17 compares PSD functions computed for the Dipstick data, processed in five different ways. First, the profile was processed with no conditioning. The figure shows that the sawtooth wave form results in a PSD function that is very high relative to the others. Effects of road roughness are rendered negligible in comparison to the roughness of the 6-ft (1.8-m) sawtooth. When used alone, both the cosine taper and the linear detrending transforms introduce artifacts at the lowest wave numbers, but result in similar PSD

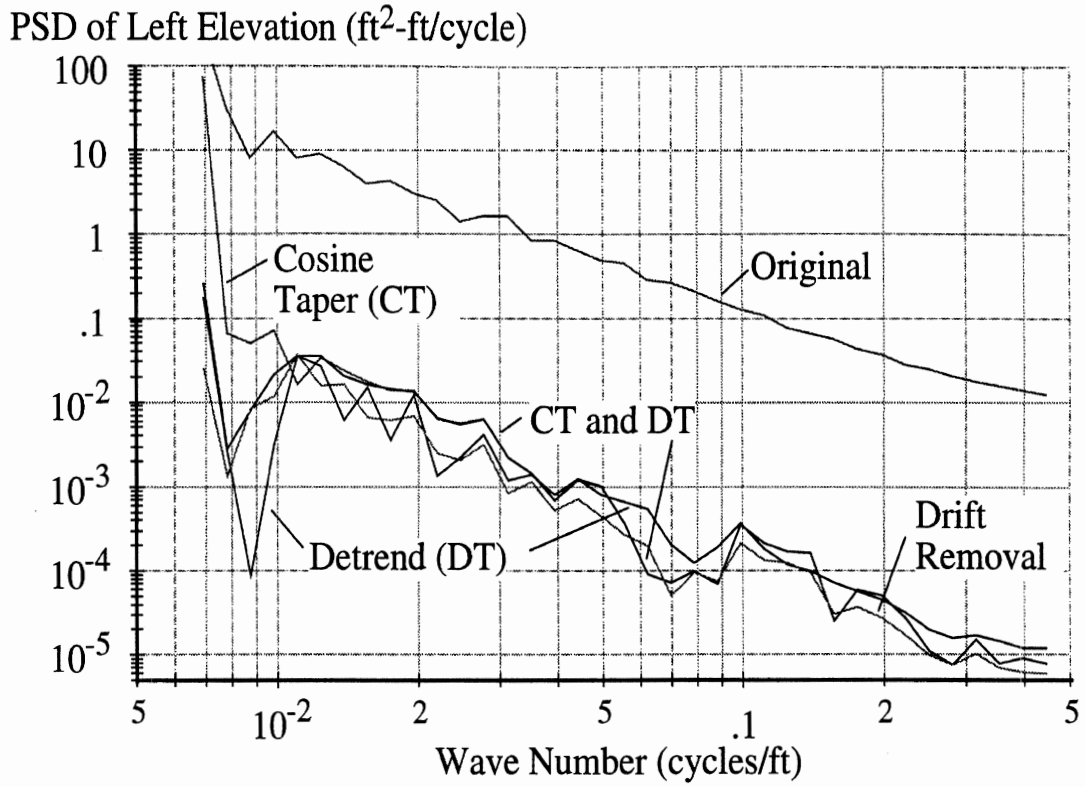

Figure 17. Effects of various profile conditioning methods.

functions for higher wave numbers. When used together, the PSD is less sensitive to the edge effects.

Figure 17 shows a fifth PSD function obtained by using a process called drift removal, which was developed to compare PSD functions for profiles obtained by different instruments in the International Road Roughness Experiment (IRRE).[2] The drift-removal method involves four steps:

1. The elevation profile is replaced with a slope profile, obtained point-by-point by subtracting adjacent elevation values and dividing by the sample interval.
2. The Fourier transform is applied to the slope profile.
3. The PSD amplitudes are corrected to account for the finite difference algorithm used in step 1, to convert to a PSD function based on the original units of the profile (e.g., elevation). The correction factor is a function of wave number (ν).

$$\text{Correction Factor} = \frac{\Delta^2}{4\,\sin(\pi\,\Delta\,\nu)^2} \tag{5}$$

4. The numbers obtained after step 3 are averaged. Some considerations in averaging are discussed later in this section.

The method is effective because edge effects are insignificant when a Fourier transform is performed on a road slope profile.

For the example Dipstick profile, the drift removal method gives a PSD that is similar to the PSD obtained using both the cosine taper and the trend removal. However, in some

cases, the drift removal method eliminates a problem that exists with the cosine taper method (and other windowing methods). The PSD obtained from a windowed profile represents the roughness properties in the middle, with little or no contribution from the beginning and end. The windowing method is suitable when the roughness properties of the profile are uniform over its length. However, if the roughness near the edges is different than in the middle, then the windowing can change the PSD significantly in a way that does not correlate to summary indices such as IRI and RN. With the drift removal method, the entire profile contributes equally to the PSD.

PSD Amplitudes in Road Profiles

The PSD shows a characteristic of road roughness that is very important in understanding some measurement problems. Notice that the PSD amplitudes in figure 17 cover many orders of magnitude. For low wave numbers (long wavelengths), the amplitudes are much higher than for high wave numbers (short wavelengths). The PSD plot supports results seen from filtered profile plots. When profiles are filtered using software that is known to attenuate long wavelengths, the resulting profiles show very small variations. For example, an unfiltered profile might show variations of several feet. When filtered to remove grade and long undulations, the range of variations might cover only a few hundredths of a foot. This confirms that long wavelengths are associated with high amplitudes of elevation variation.

The exact relationship between amplitude and wave number is an individual property of each profile. However, many roads of matching construction show a similar PSD signature. A typical relation for roads is that PSD amplitude is inversely proportional to the square of wave number.

PSD of Slope Profiles

PSD plots that cover many orders of magnitude can be confusing and difficult to interpret. For example, four of the PSD functions appear very similar in figure 17 in the wave-number range covering 0.05 to 0.1 cycles/ft (0.16 to 0.33 cycles/m). Yet, the actual difference is up to a factor of four. Allowing for the fact that PSD amplitudes are squared, this implies a difference in roughness of a factor of two, which is certainly significant. Given the characteristic dependence of PSD elevation amplitude on wave number, a much more convenient view of the road properties is provided by a PSD function computed for slope profile. For example, figure 18 shows slope PSD functions for the two profiles, shown in figure 16, and obtained by different instruments.

PSD Averaging

The PSD function was originally defined as the Fourier transform of another statistical function called the autocorrelation function. It was developed to characterize random data, such as wind speed. To a moving vehicle, a road input appears as a random variable. Of course, it is not. If the vehicle makes a second trip in which it follows an identical path on the same road, it experiences the same input. However, tools such as PSD analysis that were developed for analyzing random variables are still very useful.

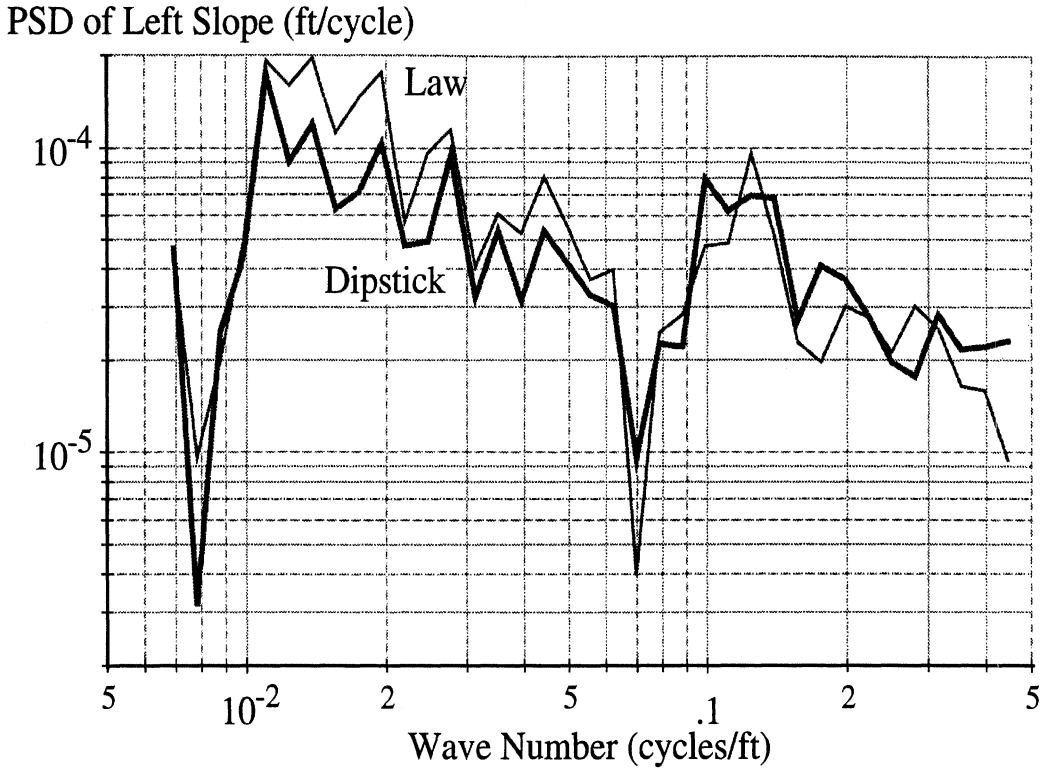

Figure 18. Slope PSD functions from two profilers.

For a truly random variable, it has been proven that the PSD is also equal to the expected value of the properly scaled numbers produced by the Fourier transform algorithm.[26] However, individual values have a random error whose variance is equal to the PSD. To obtain the expected value, averaging is performed. Two methods are commonly used: ensemble averaging and frequency averaging. The frequency averaging method is recommended for PSD functions of road profiles. (The ensemble averaging method is used for repeated tests, or for analyzing very large data sets on computers with limited memory.) Figure 19 compares the PSD functions obtained for the Dipstick data with and without averaging.

Averaging over adjacent wave numbers, as done in figure 19, is valid only if the expected values of the PSD function are approximately constant over the band. The slope PSD is approximately uniform, and the averaging introduces little bias. However, elevation PSD amplitudes change so much with wave number that averaging over wave number can add a bias, causing the averaged PSD values to increase with the amount of averaging.

For truly random variables, the accuracy of the averaged PSD value improves with averaging; the estimate of the expected value improves with more averaging. However, detail is lost with respect to wave number. There is a basic trade-off: averaging improves accuracy on the Y axis at the expense of resolution on the X axis. To improve both, the length of the test must be increased to provide more information. (Decreasing the sample interval extends the band width to include shorter wavelengths but does nothing to provide more information about long wavelengths.)

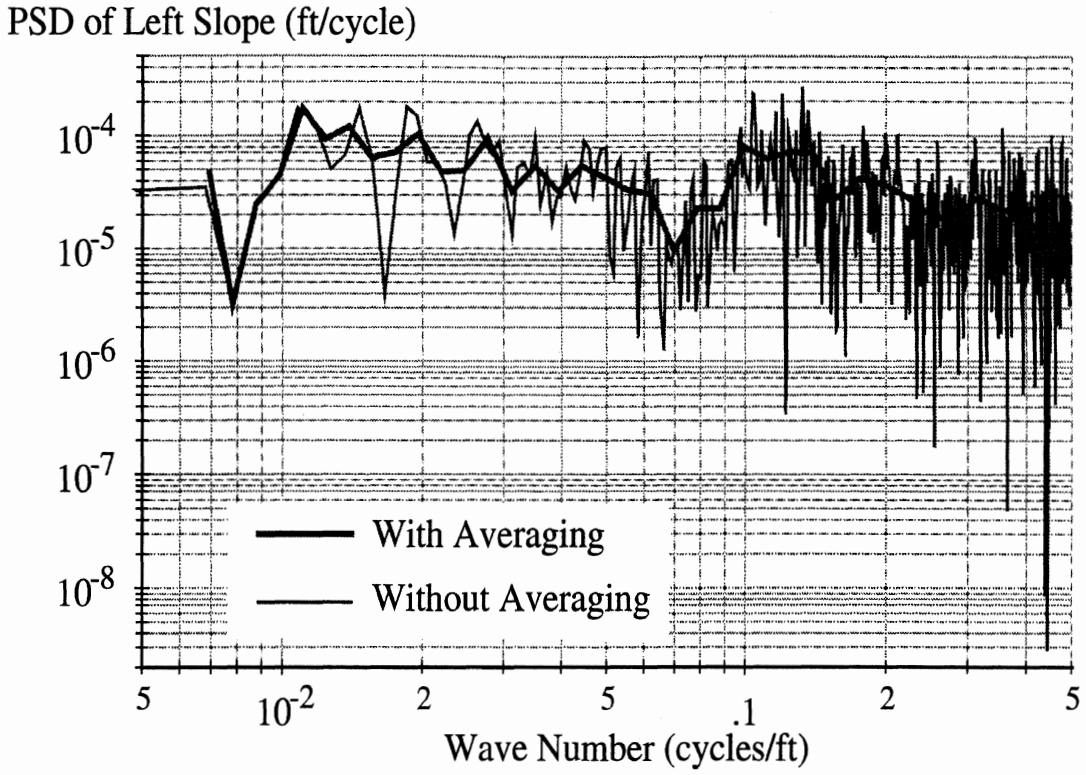

Figure 19. Effect of averaging on PSD function.

For road profiles, a similar trade-off exists. However, if one is interested in a specific section of pavement, then it is not possible to improve the results by adding length. If the profile is extended, then the resulting PSD is influenced by the roughness properties of the added pavement. One might be tempted to artificially increase the length of the profile by repeating the measurement or copying numbers. However, the problem involves information, not the number of samples. Unless the added numbers provide new information, the trade-off between resolution and accuracy cannot be avoided. Further, some methods for copying data introduce unintended artifacts (i.e., errors).

True Profile PSD

Just as there is a concept of a true profile, there is a corresponding concept of a true PSD. Different profilers produce data sets that cover different bandwidths and are based on different sample intervals. For the example data used in the previous few figures, the Dipstick data, taken at a 12-in (305-mm) interval, had no inherent filtering to limit the bandwidth. The inertial profiler data, taken at a 6-in (152-mm) interval, were filtered with a Butterworth high-pass filter whose cut-off wave number corresponds to a 300-ft (91.4-m) wavelength. The profile was also filtered with a moving average low-pass filter with a 12-in (305-mm) base length. Therefore, it is expected that the PSD functions should match for wave numbers between 0.01 and 0.5 cycles/ft (0.033 and 1.64 cycles/m). If the analysis can produce identical PSD functions in this range, it can be considered the true PSD.

The method used to determine the slope PSD functions is less sensitive to sample interval and bandwidth than other methods that have been tried. The software package described in chapter 4 includes the capability for computing PSD using the four-step

method described earlier. For all practical purposes, the results obtained using this method can be considered the true PSD when applied to sampled elevation data taken for the true profile, in the limit for a sample interval approaching zero.

Uses of Road PSD functions

Because the PSD is not a single summary index, it is not particularly useful for reducing profile data to a standard index. (PSD analysis was used to develop IRI, RN, and other profile indices. However, once an index is defined, simpler algorithms can usually be written for performing the calculations in routine use.) On the other hand, PSD analysis is one of the best available diagnostic tools for interpreting pavement properties and measurement capabilities of profilers.

Surface Characterization

Studies have been done that use PSDs to classify the wavelength content of road profiles and represent them mathematically.[27,28,29] In some cases, enough road profile data were available for a range of surface types to identify specific characteristics of each.[29] Figure 20 shows PSD functions for a faulted PCC and a wavy surface-treated road. The PSD for the surface-treated road is higher on the left-hand side of the plot (low wave numbers = long wavelengths) because the treatment removed all of the sharp bumps, but left the long wavy roughness. The PSD for the PCC road is high on the right-hand side of the plot (high wave numbers = short wavelengths) because it is faulted. The plot also shows several spikes that correspond to the periodic effect from the uniformly-spaced faults.

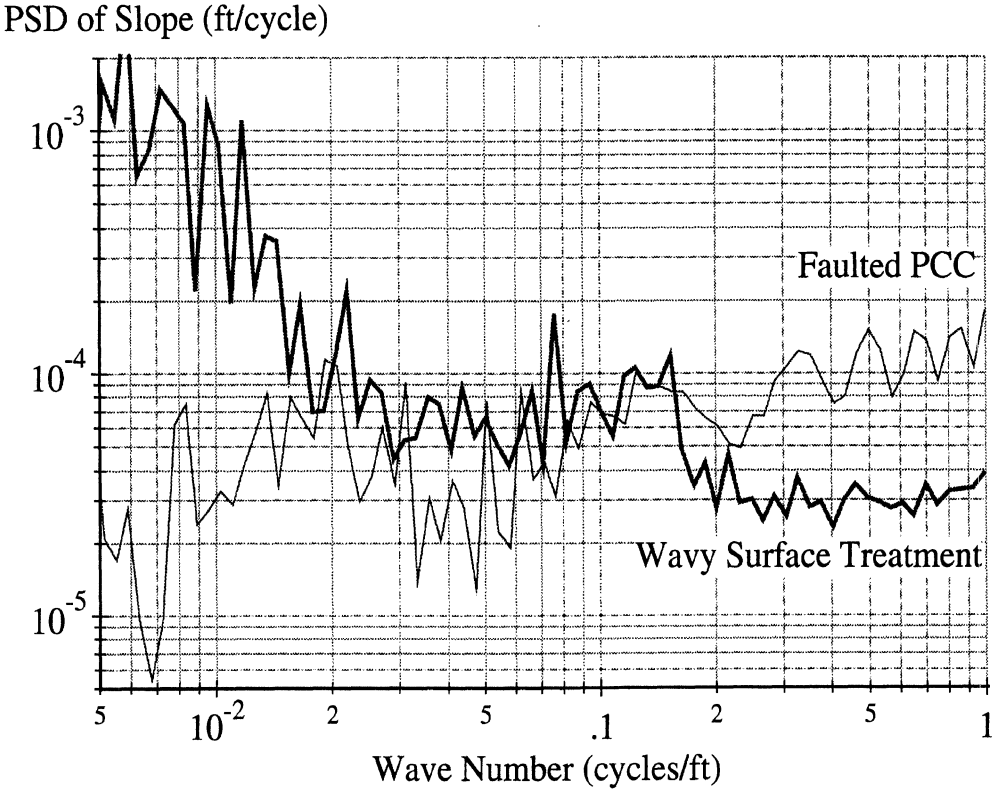

Figure 20. PSD of a faulted PCC and wavy surface-treated road.

PSD functions help identify failures in roads that contribute to roughness. Roads where the long wavelengths are dominant have poor foundations. Old dirt roads that were paved without significant grading tend to have high PSD amplitudes at the low wave numbers. Roads where the high wave numbers are dominant tend to have cracks, faulting, and other forms of surface distress.

Links to Subjective Measures

Several studies have been done that use PSD functions to link road roughness in different wavebands to subjective evaluations of ride quality. (See references 3, 4, 14, 17, and 30.) In these studies, panel ratings of ride quality were correlated to the mean squared roughness level over various wavebands, calculated from PSD functions. The same method, detailed in appendix G, was used to develop the algorithm for calculating RN that was described earlier.

Error Diagnosis

PSD functions can help reveal measurement errors when profiling devices are compared. Inertial profilers use an accelerometer and a height sensor (ultrasonic, laser, optical, etc.). Measurement errors in the height sensor tend to affect the PSD functions for high wave numbers. Errors in the accelerometer or the software that processes the accelerometer tend to affect PSDs for low wave numbers. Examples of using PSD functions for measurement error detection and diagnosis appear in chapter 3 of this report and a report by Perera.[24]

CROSS CORRELATION

Cross correlation functions are a statistical measure of the dependence of one variable on another.[26] The cross correlation function of repeat measurements of road profiles provides a way to synchronize them and rate their agreement. For two measures of road profile, the cross-correlation function is defined as:

$$Rpq(\delta) = \lim_{L\to\infty} \frac{1}{L} \int_0^L p(x)q(x+\delta)dx \tag{6}$$

where p and q are each measurements of road profile as a function of distance x with length L. The correlation function, R, exists as a continuous function of the offset distance δ between the profiles. Since actual measures of road profile are finite in length and sampled at discrete intervals, the integral is replaced with a summation. A correlation coefficient also exists and is defined as the correlation function normalized by the standard deviations of p and q. The definition for sampled variables p and q is:

$$\rho_{pq}(\delta) = \frac{1}{\sigma_p \sigma_q} \sum_{i=1}^{N} p(x_i)q(x_i+\delta) \tag{7}$$

where N is the number of points common to both profiles at an offset distance δ (equal to an integer multiple of the sample interval), and σ represents the standard deviation of each

profile. If the profiles are in exact agreement, ρ will have a value of 1. If they are exactly opposites, ρ will be -1. If they are uncorrelated, ρ is zero.

It is essential that the same filters be applied to both profiles before applying this analysis. If the profiles are not filtered similarly, the filtering, rather than the profiles, will dictate the results. It is also helpful to convert the profiles from elevation to slope before computing the correlation coefficient. If elevation is used, the agreement for the longest wavelength range included in the analysis has a disproportionate influence on the results.

Synchronization

For research studies that involve several measurements of the same road section by a single device or a collection of devices, it is often desirable to make sure that all of the systems are measuring exactly the same stretch of road. In the 1993 and 1994 RPUG calibration studies, an artificial bump was placed before and after each road section to help isolate the section of interest.[24] A simple bump finder could then be used to synchronize the sections, as will be described in chapter 3. For studies in which no such reference bumps are available (or to check the synchronizing provided by the reference bumps), the following synchronization procedure can be used.

The procedure is based on matching two measurements of a section of road and finding the offset associated with the highest cross-correlation. If a static measurement of the road profile is available, it should be used as the reference. If the profile measurements are properly filtered and normalized, the output of the algorithm is a number between -1.0 and 1.0 that describes the agreement of the two measurements at each offset. In the 1993 RPUG study, most of the profilers measured up to 2,000 ft (610 m) of road. The reference measure made by the Dipstick was only as long as the section of interest: 528 ft (160.9 m). Figure 21 shows the cross-correlation between a measurement from the study and the Dipstick measurement, as a function of offset. Both were high-pass filtered with a cut-off of 30 ft (9.14 m). Because the shape of roads changes so randomly with distance, the level of agreement is very poor except where the measurements are synchronized. The function has a value less than 0.2 everywhere except the vicinity of 1,000 ft (305 m), where the segments are nearly synchronized. The analysis shows the correct offset to be 1,003.5 ft (305.9 m), where the correlation coefficient is 0.945.

Repeatability Measure

If the measurements compared in figure 21 agreed perfectly, the maximum correlation coefficient would be unity. However, measurement variations lower the coefficient. Thus, once the measurements are synchronized, the result of the algorithm provides a quantitative rating of the agreement between the measurements. This can be used to assess the ability of a device to make repeat measurements or evaluate the agreement between unlike instruments. The process is to (1) filter the profiles identically; and (2) cross-correlate them to see how well they agree in the waveband of the filter.

The cross-correlation evaluation is a much more demanding comparison than a summary roughness index such as IRI or RN. Two profilers might produce the same IRI even though the profiles are completely different. In contrast, the cross-correlation analysis

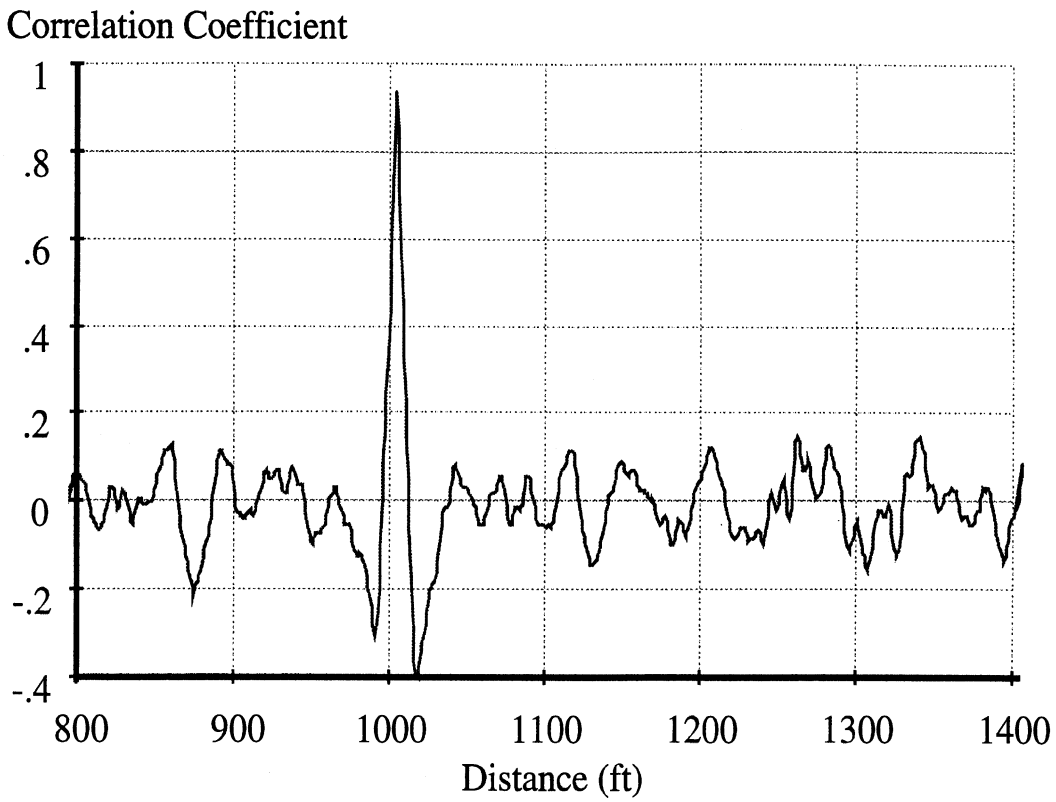

Figure 21. Cross-correlation of two repeat measurements used for synchronization.

will yield a low correlation coefficient. Thus, one can assess repeatability without having to measure the many sections needed for valid statistical comparison of the IRI values.

This method also offers the ability to diagnose measurement errors by considering a variety of wavebands, as controlled by the filtering done before the cross-correlation calculations. For example, bad agreement for short wavelengths but good agreement for long wavelengths suggests a problem with the height sensors and the opposite suggests a problem with the accelerometer signal.

Table 3 shows some results from cross-correlation analysis of repeat measurements of a section made for the 1993 RPUG study. The slope profiles from these measurements were compared in two wavebands: (1) from 20 to 100 ft (6.10 to 30.5 m); and (2) from 4 to 20 ft (1.22 to 6.10 m). The table provides the results for a Law system and an ultrasonic system. For each system, one of the repeats is compared to nine others and a measurement by the Dipstick. The comparison of repeat measures by the same device represents the repeatability of the measurement (in each waveband). Comparison to the Dipstick reference is an indication of accuracy.

In the 20- to 100-ft (6.10- to 30.5-m) range, the Law measurements correlate to each other almost perfectly ($\rho \approx 0.999$). This implies that plots of the repeats must look almost exactly alike if they are filtered to include this range. Figure 22 confirms this. All ten repeats are shown, as well as the Dipstick measurement. The ten repeats from the Law system overlay so well that they look like one line. The Dipstick measurement does not agree as well. This is reflected in the fact that the correlation coefficient between the Dipstick measurement and the Law system for this wavelength range is lower (0.878).

Table 3. Cross-correlation between repeat measurements.

Repeat Number		Correlation Coefficient	
First	Second	(20 to 100 ft)	(4 to 20 ft)
D	U1	.858	.456
U1	U2	.987	.422
U1	U3	.986	.421
U1	U4	.984	.398
U1	U5	.985	.415
U1	U6	.983	.361
U1	U7	.986	.403
U1	U8	.986	.457
U1	U9	.987	.398
U1	U10	.984	.423
D	L1	.878	.687
L1	L2	.999	.971
L1	L3	.999	.974
L1	L4	.999	.972
L1	L5	.999	.972
L1	L6	.999	.977
L1	L7	.999	.949
L1	L8	.997	.934
L1	L9	.999	.968
L1	L10	.999	.948

L = Law D = Dipstick U = Ultrasonic

In the 4- to 20-ft (1.22- to 6.10-m) range, the Law measurements also correlate well to each other (0.95–0.97), and only moderately well to the Dipstick. The corresponding filtered plots are shown in figure 23. Again, the 10 repeat measurements from the Law system look very similar. Overall, the agreement between these repeats in both ranges is very good. Thus, the IRI, which is sensitive to wavelengths from 5 to 100 ft (1.52 to 30.5 m), is expected to be nearly the same for all ten repeats. Indeed, they are all within 2 percent of the average.

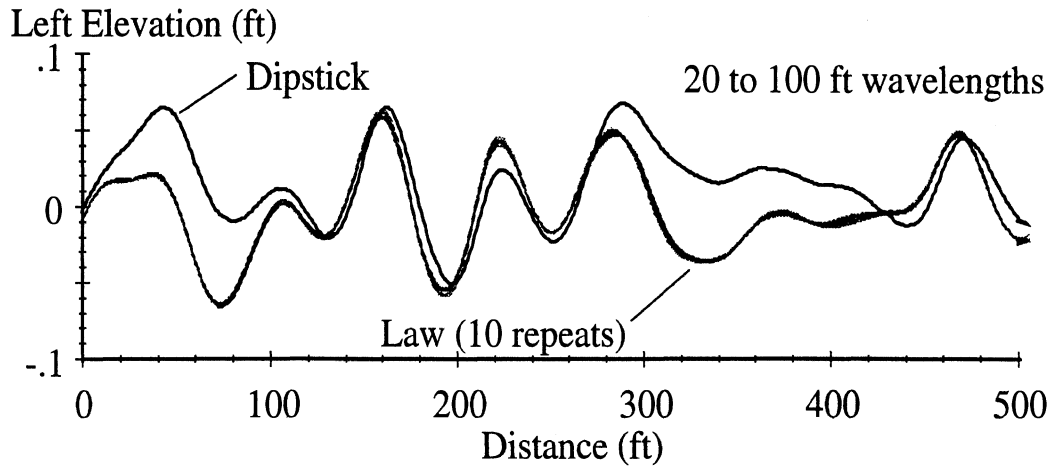

Figure 22. Ten Law repeats, band-pass filtered (20 to 100 ft).

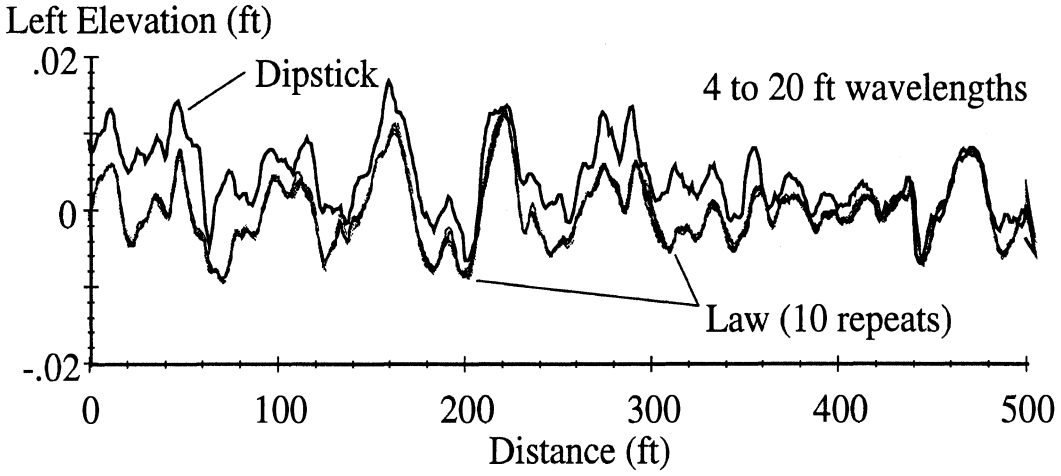

Figure 23. Ten Law repeats, band-pass filtered (4 to 20 ft).

Figure 24 shows the same set of plots for the measurements made by the ultrasonic device. In the 20- to 100-ft (6.10- to 30.5-m) wavelength range, the repeats are very similar, as would be expected knowing the correlation coefficients listed in the table ($\rho \approx$ 0.98 to 0.99). In the 4- to 20-ft (1.22- to 6.10-m) range, on the other hand, the correlation coefficients are less than 0.5, and the filtered plots do not agree very well. The lack of agreement is reflected in the IRI values, which vary by more than 5 percent from the mean value in some cases. The poor correlation in the short wavelength range suggests a problem with the height sensors. The road section used in this example is an asphalt concrete surface of coarse texture, which is known to cause measurement errors in systems with ultrasonic sensors.

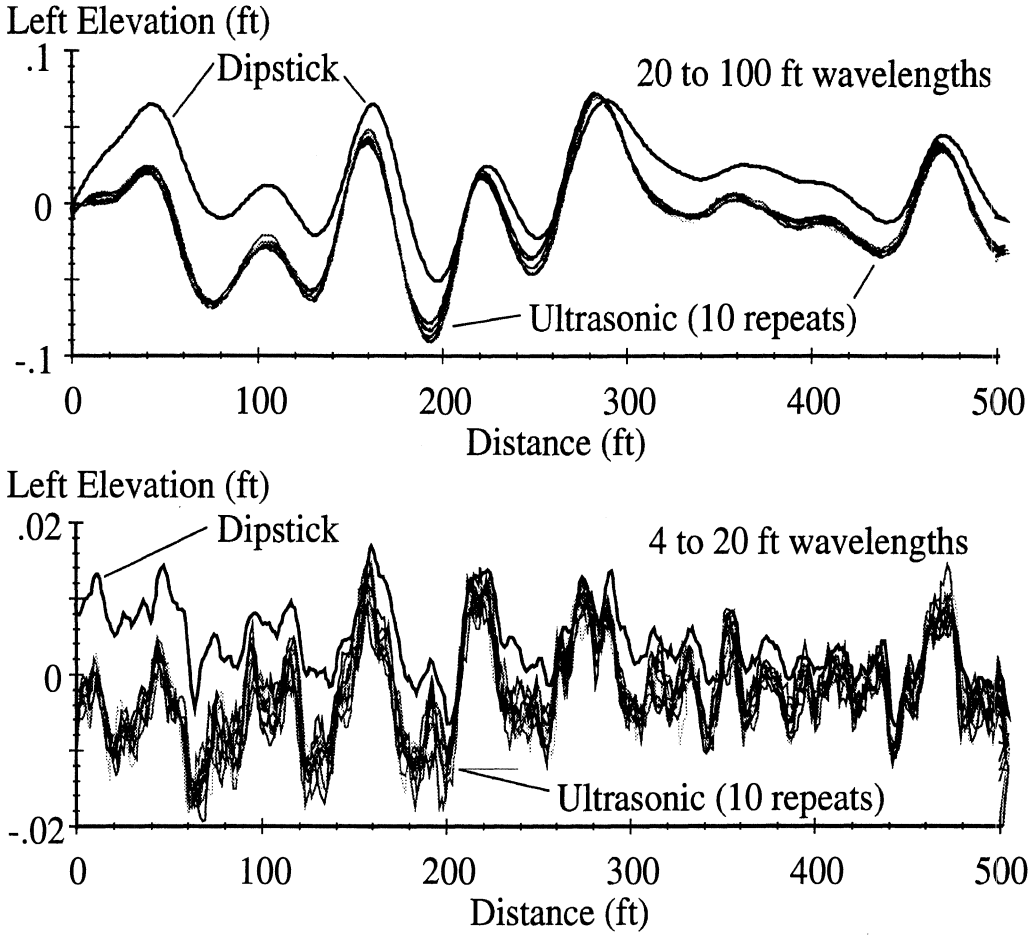

Figure 24. Filtered plots of repeat measurements made with an ultrasonic system.

3. MEASUREMENT ERRORS

Understanding the sources of variation in measurements obtained by profilers is one of the most important problems faced by users of road profilers. For the past several years, the RPUG has organized experiments where users can run their equipment over sets of test sites, located in four regions in the country. Data from the 1993 and 1994 studies were analyzed by Perera and Kohn to quantify the statistical differences observed in IRI and other summary indices.[24,31] The 1993 RPUG data were also analyzed in this study, with the objective of diagnosing the causes of measurement variation and error.

PROFILER OPERATION

Before considering sources of variation and measurement error, it is helpful to review some basic concepts of profiling.

A profile is a two-dimensional slice of the road surface, taken along an imaginary line. Profiles taken along a lateral line show the super elevation and crown of the road design, plus rutting and other damage. Longitudinal profiles show the design grade plus roughness. (See figure 25.)

A profile of a road, pavement, or ground can be measured along any continuous imaginary line on the surface. If a measurement is repeated, the same profile can only be expected if the same imaginary line is followed. It is possible to measure the profile for a curved line. Normally, the expectation for a road is that the line is a constant distance from the centerline or some other reference that follows the road geometry. Frequently, profile is measured along two lines per lane, one in each wheel track. For greater detail any number of lines can be measured.

For any line on the road, there is a true profile. The concept is simple: It is easy to see that for a line drawn on a physical surface, a true profile exists.

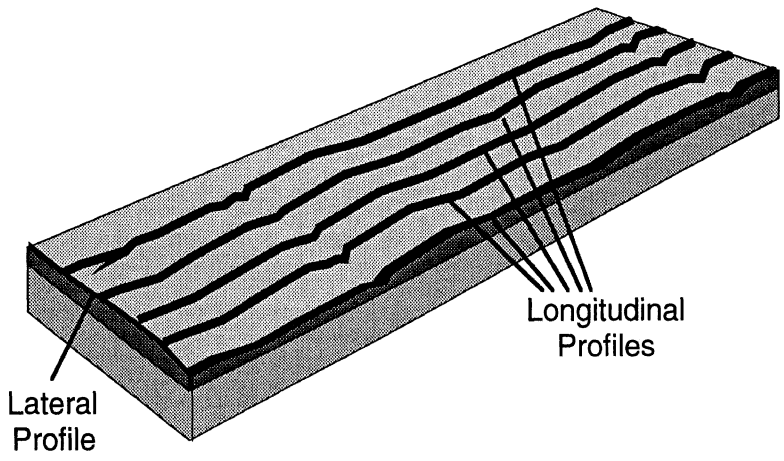

Figure 25. Profiles in a pavement.

A profiler is an instrument used to produce a series of numbers related in a well-defined way to a true profile. As seen by examples in chapter 2, the numbers obtained from some profilers are not necessarily equal to true elevation. A profiler measures the components of true profile that are needed for a specific purpose. It works by combining three ingredients: (1) a reference elevation; (2) a height relative to the reference; and (3) longitudinal distance. Nearly all high-speed profilers used in the United States are based on the inertial profiler design originally developed by Spangler and Kelly at the GMR Laboratories. Figure 26 shows a simplified view of the three ingredients in a GMR-type inertial profiler.

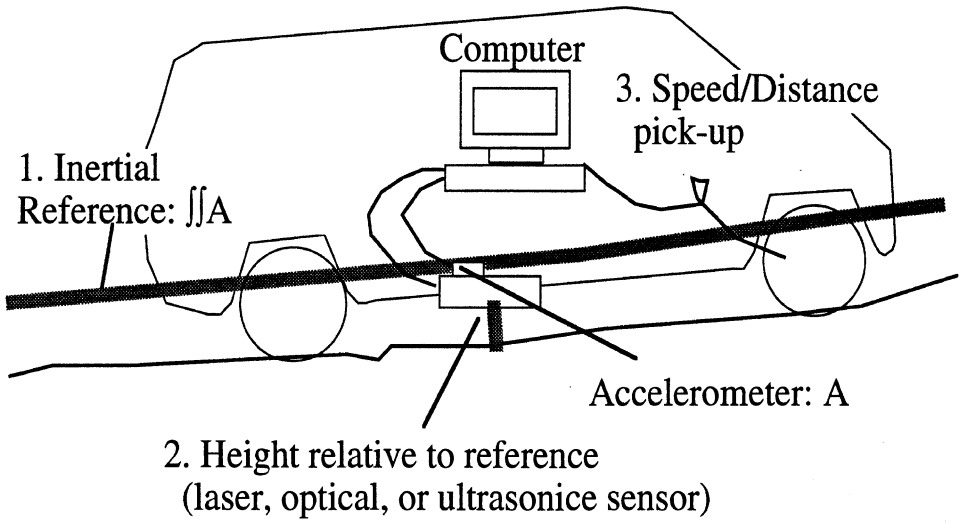

Figure 26. The inertial profiler.

The inertial reference is provided by an accelerometer (a sensor that measures acceleration) that is oriented vertically. Data processing algorithms convert the vertical acceleration measure to an inertial reference that defines the instant height of the accelerometer in the host vehicle. The height of the ground relative to the reference is therefore the distance between the accelerometer (in the vehicle) and the ground directly under the accelerometer. This height is measured with a non-contacting sensor, such as a laser or an ultrasonic transducer. The longitudinal distance of the instruments is usually picked up from the vehicle speedometer.

The original GMR design has been updated with new sensors and computers. Early inertial profilers sensed the height of the vehicle relative to the ground using an instrumented follower wheel. The design worked, but the follower wheels were fragile, and required testing at speeds low enough to avoid bouncing. All profilers that are sold today use non-contacting sensors instead of follower wheels. Early systems performed the profile calculations electronically and required that the vehicle operate at constant forward speed. Modern inertial profilers correct for minor variations in speed and perform the calculations numerically with on-board computers.

An inertial profiler must be moving to function. This type of instrument not only works at highway speed, it requires a certain speed even to operate properly. For example, even the best inertial profilers do not work well at speeds less than 10 mi/h (4.5 m/sec).

The inertial reference from a profiler qualifies as useful, but it is not as easy to visualize as the reference used in the static rod and level or Dipstick. The agreement between the profile obtained with an inertial system and one obtained statically is good in some respects but not in others. The static measures include the grade of the road, but measures from an inertial profiler do not. Long undulations, covering hundreds of feet, are included in the static measures but not in those from the inertial profilers. Because of these differences, plots of elevation versus distance from an inertial profiler do not agree with plots made from statically measured data, even though the measures are made over the same line and are based on the same true profile. Further, different plots may be obtained for repeated measures of the same true profile, if the measures are made with inertial profilers made by different manufacturers. It is even possible to get different plots from the same instrument, just by choosing different settings before each test.

The analyses described in chapter 2 are intended to extract the same information from the measures of a profiler that would be obtained from the true profile. Filters such as the moving average are used to process the measures for close comparison of the ability of different devices to measure profile characteristics that are of interest.

FEATURES OF A VALID PROFILER

The true profile includes a great deal of information. It tells whether the road is going up or down a hill. It gives roughness information. It has texture information. It is neither economical nor useful to measure the true profile with enough detail to extract texture information and also view large-scale landscape features such as hills and valleys. The amount of data storage needed to capture a mile of profile with detail down to the texture level would fill computer storage capabilities rapidly, and make the management of the data base difficult. Profilers are designed to measure only a part of the information in a true profile.

A valid profiler provides measurements that, when analyzed, give the same results that would be obtained by analyzing the true profile. Thus, the validity of a profiler depends on the use that will be made of the data. Although profilers do not measure all of the information needed for a true profile, they should measure the information that is of interest. A profiler is considered valid for obtaining a profile property if the statistics obtained from its measures are neither high nor low, on the average, compared with statistics that would be calculated from the true profile.

Statistics from two or more valid profilers are directly comparable, with no conversion required. Because statistics computed from the measures of a valid profiler are not biased relative to the true profile, it is not necessary to convert statistical data from a valid profiler to compare them with data obtained from a different valid profiler. Statistics from valid profilers are stable over time. Because the concept of a true profile is timeless, profile statistics calculated this year have the same significance as those calculated last year and will be comparable with statistics calculated 100 years from now.

What if the statistics calculated from a profiling device are systematically biased relative to an accepted reference? Say they tend to be 20 percent high for some tests. Then, quite simply, the device does not qualify as a valid profiler for that analysis. It is not a good

practice to apply a scaling factor to try to correct for the 20-percent error, because the source of the error probably depends on unknown factors. (Instead, call the manufacturer.) A profiler is not valid for measuring a property of true profile if (1) its measures are systematically biased; or (2) the random error for an individual measurement is unacceptably high.

STATE OF MEASUREMENT PRACTICE

The major finding of the 1993 and 1994 RPUG correlation studies was that an unacceptable level of error exists in the routine measurement of the IRI. Evidence of the problem is obtained by choosing any section profiled by different instruments to obtain IRI measures. For example, figures 27 and 28 show repeated measures of IRI from 10 devices for a single test site. (Ten repeat tests were made for each of the 9 inertial profilers.) The results plotted in the figures are representative of the RPUG data, and show:

1. The IRI values from the Dipstick are often lower than mean values from the inertial profilers.
2. Measures for ultrasonic systems are often systematically higher than those from other profilers.
3. Although the mean values obtained with different devices can differ significantly, they are often reasonably repeatable (within ±3 percent of their mean values).
4. For tests sites with coarse textures, the profilers with ultrasonic sensors measure IRI values that are systematically high. Also, they are less repeatable.

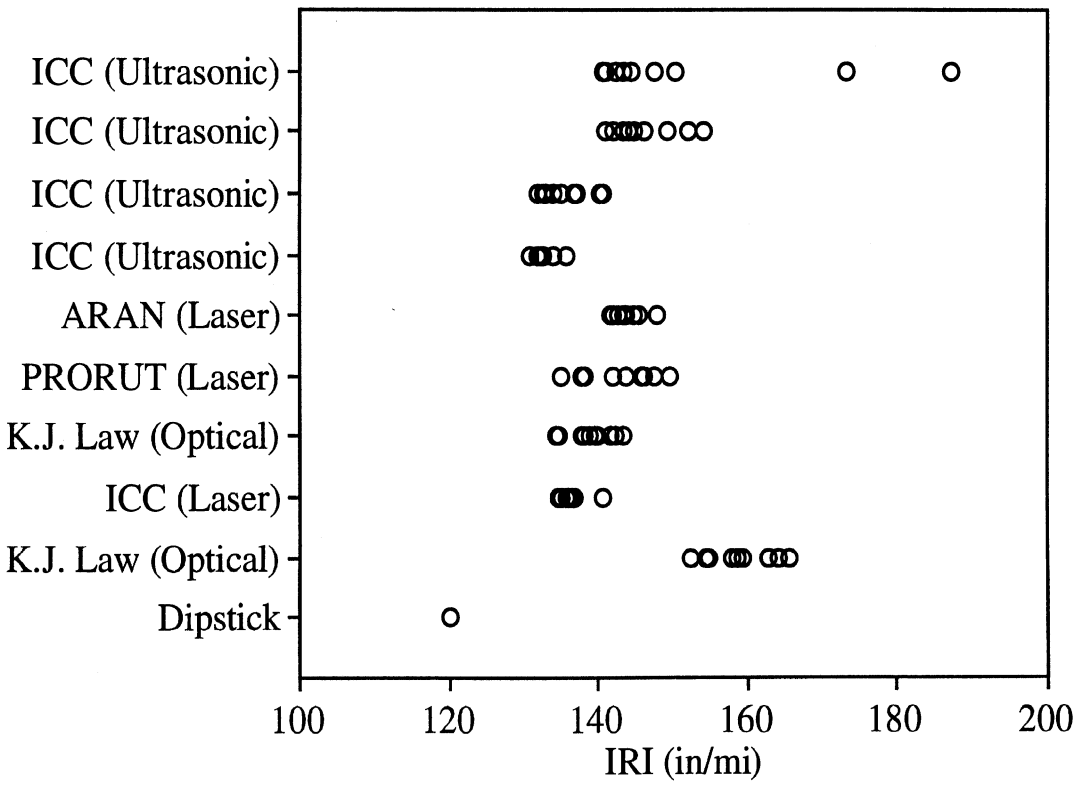

Figure 27. Repeat IRI measures from different profilers (PCC with regular texture).

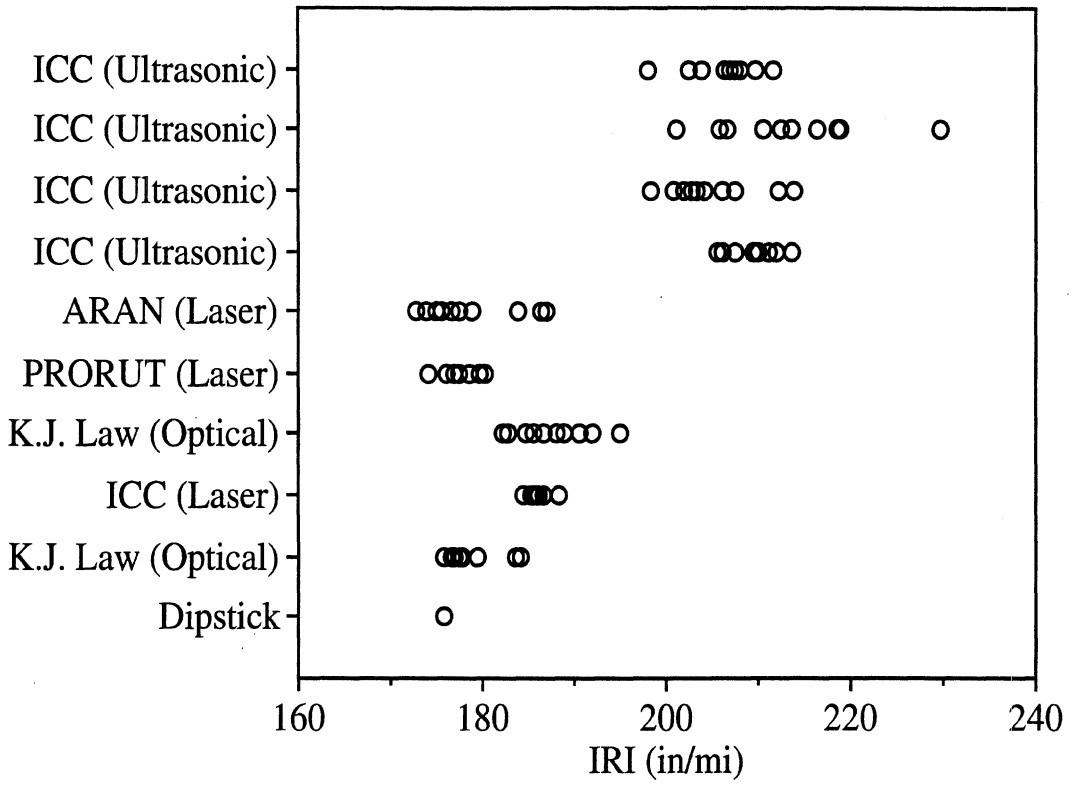

Figure 28. Repeat IRI measures from different profilers (PCC with coarse texture).

At one instant of time, a line on the pavement has a single true profile and thus, a single true IRI value. One would expect that profilers should be capable of producing measures of IRI that are close to the true value. The differences seen in figures 27 and 28 can be due to three factors: (1) the user might have made an error, typically running the instrument over a different line on the pavement than intended, and therefore obtaining a different profile; (2) the instrument might be in error, because of limitations of the sensors, the electronics, and the software used to compute profile from the transducer signals; and (3) the true profile of the pavement might have changed between runs, because of temperature and other environmental effects. Realistically, all three factors are present in any single measurement. However, the first and third can be controlled with tightly controlled testing methods. For example, changes in the true profile are minimized when all measures are taken within a short period of time. With a static device such as the Dipstick, errors involved in locating the line on the pavement to be profiled are minimized.

The RPUG data are sufficient to show the amount of variations that exist in profile measurements. The experiment was not controlled sufficiently to quantify the sources of variation. Also, the profiles were not all taken within a short time frame, leaving the possibility that the true profile had changed between measures made by different instruments. NCHRP Project 10-47, entitled "Standards for Profile Measurement Accuracy," starts in 1996 and will include tests designed explicitly to determine the roles of sources of variation.

In some cases, sources of variation from the RPUG data could be identified. These sources are described below.

SOURCES OF VARIATION

A major source of variation in profiler measures is that different lines on the road are being profiled each time. The different lines have different true profiles, and the measured profiles reflect this. For profiles collected with static methods, this source of variation is easy to avoid. However, for high-speed profiling equipment, the lateral position and longitudinal starting position are difficult to control. Thus, a set of repeat measurements of the same section may all be different, because of subtle changes in the actual location of the profile that was measured.

The 1993 and 1994 RPUG tests were designed to ensure that profiles all began at the same longitudinal location. An artificial bump was placed on the road before each test site, and the bumps in the measured profiles were used to synchronize them to the profile from the Dipstick. The bumps in the profile were about 0.25 in (6.35 mm) high, and were located 100 ft (30.5 m) upstream and 50 ft (15.2 m) downstream of the section of interest. Although a bump of 0.25 in (6.35 mm) is fairly severe from the point of view of a driver, it is not always visible in an unfiltered profile. Since the artificial bumps were 18 in (0.46 m) long, they could be isolated using a high-pass filter with a short-wavelength cutoff. Figure 29 shows a sample profile from the RPUG study after it has been high-pass filtered with a base length of 3 ft (0.914 m). Note that the filter removes most of the normal roughness features of the profile, leaving the artificial bumps.

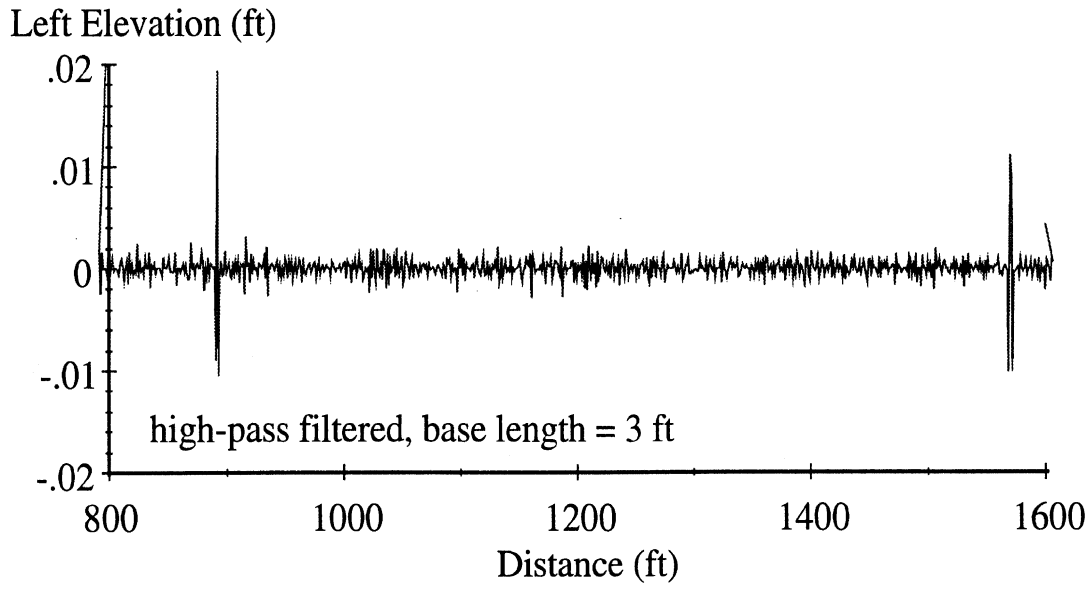

Figure 29. Use of filtering to locate artificial bumps in a measured profile.

The participants in the 1993 RPUG study were asked to submit the profiles with longitudinal distance adjusted so that the sections of interest begin at a location of 1,000 ft (304.8 m). Thus, the bumps in figure 29 are approximately in the correct locations: 900 and 1,578 ft (274.3 and 481.0 m). The majority of the profiles were synchronized properly

within a few feet. However, verifying them with the high-pass filter and the cross-correlation method described in chapter 2 showed that a small fraction of them were off by 10 to 100 ft (3.05 to 30.5 m). For example, 40 sections were submitted with synchronization errors that were distributed as shown in figure 30.

If undetected, synchronization errors cause small differences in the IRI computed for those measurements. Figure 31 shows the distribution of IRI error for the same set of 40 measurements in percent and gives an idea of the significance of the synchronization for 528-ft (160.9-m) sections.

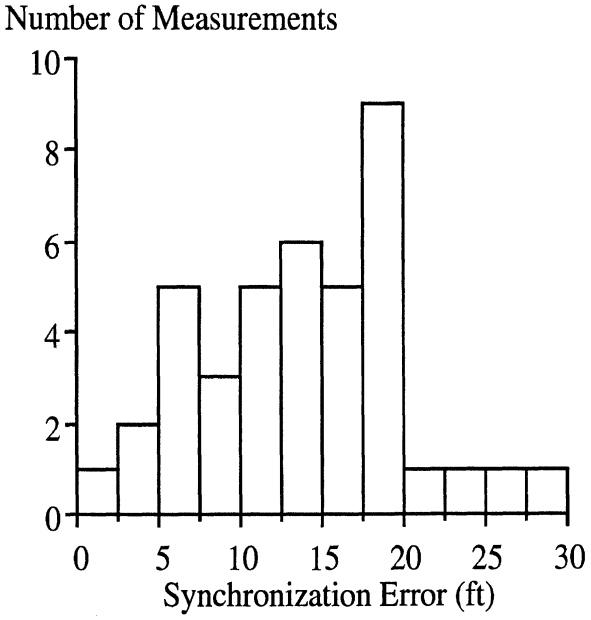

Figure 30. Synchronization errors found for one device in the 1993 RPUG study.

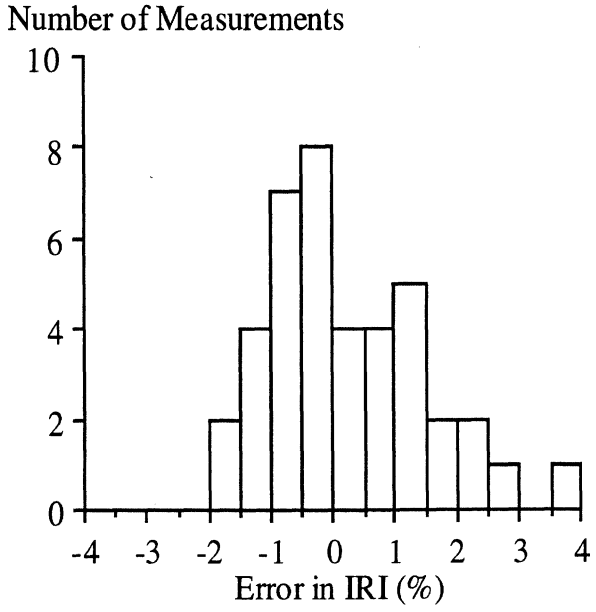

Figure 31. IRI errors caused by incorrect synchronization of one device.

The synchronization brings the profiles into agreement within the amount of the sample interval, which is a little over a foot for some of the ultrasonic-based systems. Even this amount of discrepancy can affect IRI repeatability by several percent on a 528-ft (160.9-m) section when the profile includes discrete events such as patches, potholes, and cracks.

Even when longitudinal positioning of the profiles is controlled, the lateral positioning can still differ between runs, introducing another source of variation. For example, figure 32 shows a set of ten repeat measurements made by the FHWA PRORUT over a section of PCC. The section is spalled in some locations, including a narrow patch about 10 in (0.254 m) long at a distance of 115 ft (35.1 m) from the start of the section. Because the PRORUT collects samples at an interval of about 2 in (50 mm), the dip in the profile is detected in every run in which the lateral location of the profile passed over the spalled area. The figure shows a 0.25-in (6.35-mm) depression in the profile for 8 of the 10 repeats. (The measurements are high-pass filtered to make the dips more visible.) The other two repeats are thought to be runs in which the lateral location of the profile did not include the spalled area.

Figure 33 shows a set of ten repeat measurements made by an ultrasonic profiling device. This device has a sample interval of about 13 in (330 mm). Three of the repeats have a large dip in the location of the spalling. In this case, the dip is indicated by a single point in the profile, because the sample interval of the device is larger than the longitudinal dimension of the spalled area. Some of the measurements may have missed this feature because of the lateral location of the profiles that were measured. Others, however, may have missed the dip because the profile was sampled on either side (longitudinally) of the dip.

Note that the ultrasonic measurement of the spalled area only includes one sample (at most), so very little information is available about what road feature caused the dip. The PRORUT measurement includes up to five samples, so the dip can be distinguished from faulting or cracking.

COMMON MEASUREMENT ERRORS

Although variations in profile measures can be expected even with an instrument having perfect accuracy, profiler instruments are in fact not perfect. Some of variations are due to errors introduced in the measurement process.

Extraneous Spikes

The spikes in the profiles shown in figures 32 and 33 always occur in the same longitudinal location, indicating that they are caused by a defect in the pavement. In other cases, spikes appeared at random. Figure 34 shows an example of a set of 10 repeat measurements made by a profiling device with laser sensors. Several spikes appear in the data, including four in one measurement alone (the top line in the figure). None of the spikes appear in the same location in different repeated measurements. They were also not present in the Dipstick measurement or measurements made by other profiling devices. For this reason, these spikes are thought to result from a source of error within the profiling device itself.

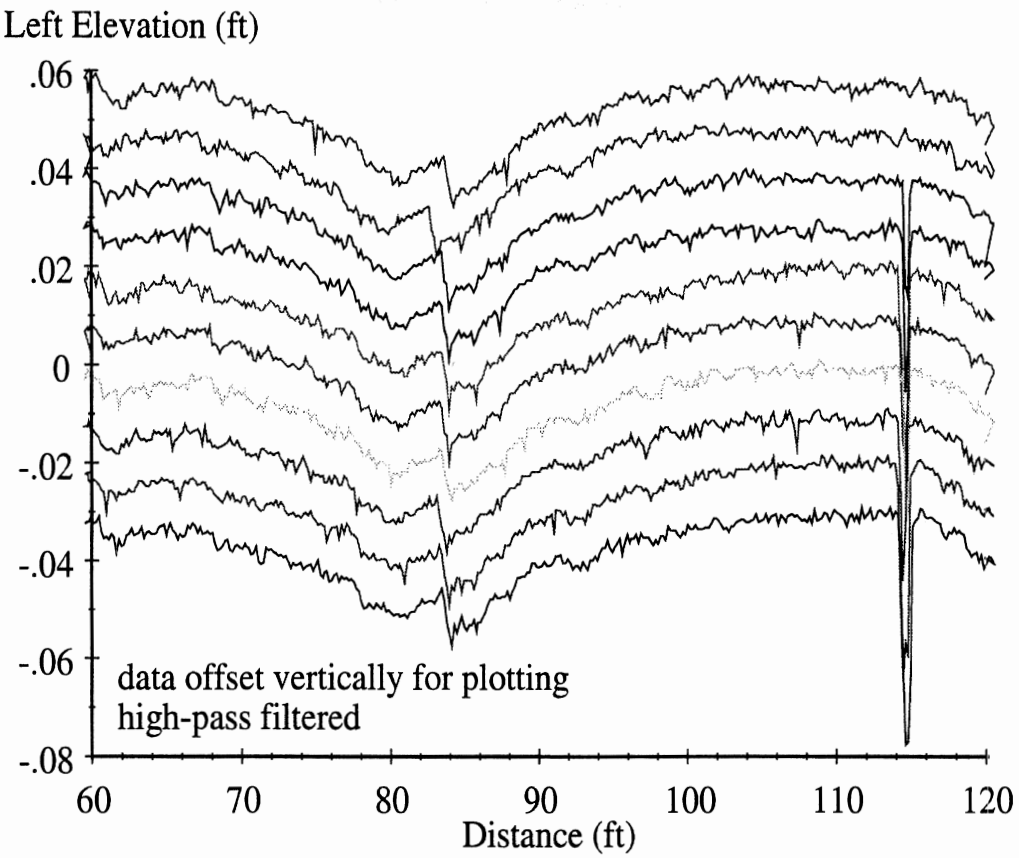

Figure 32. Repeat measures of spalled PCC by the PRORUT.

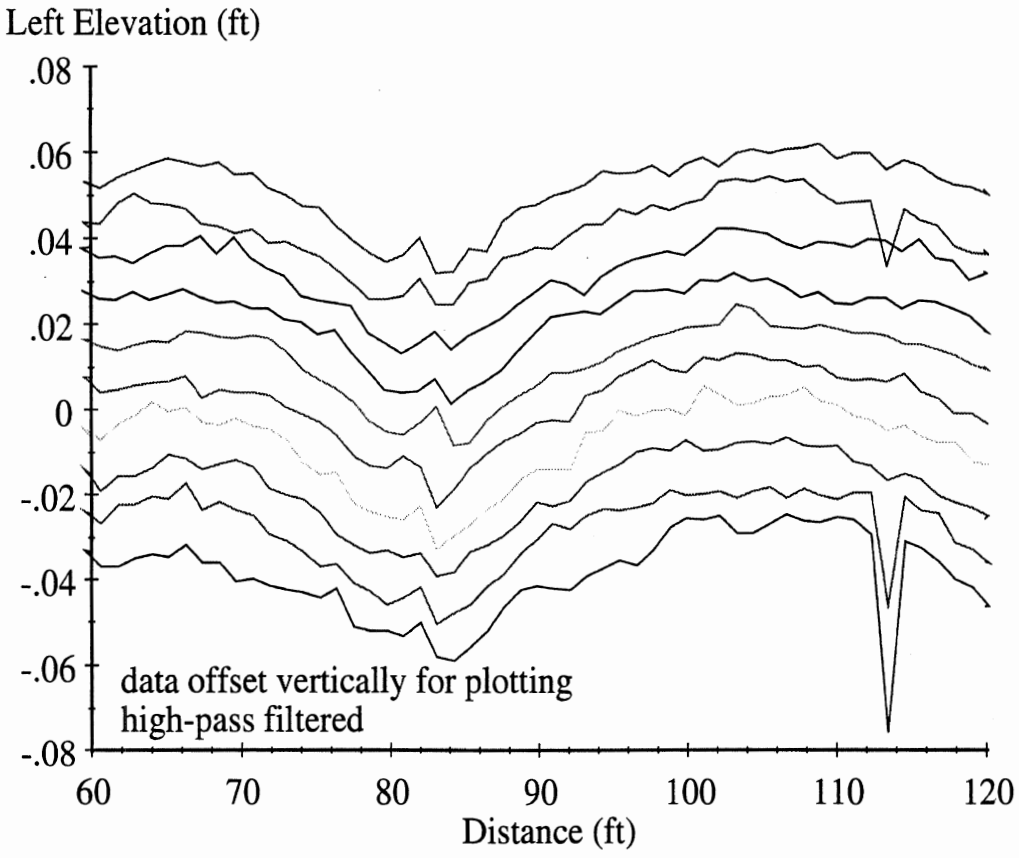

Figure 33. Repeat measures of spalled PCC by an ultrasonic system.

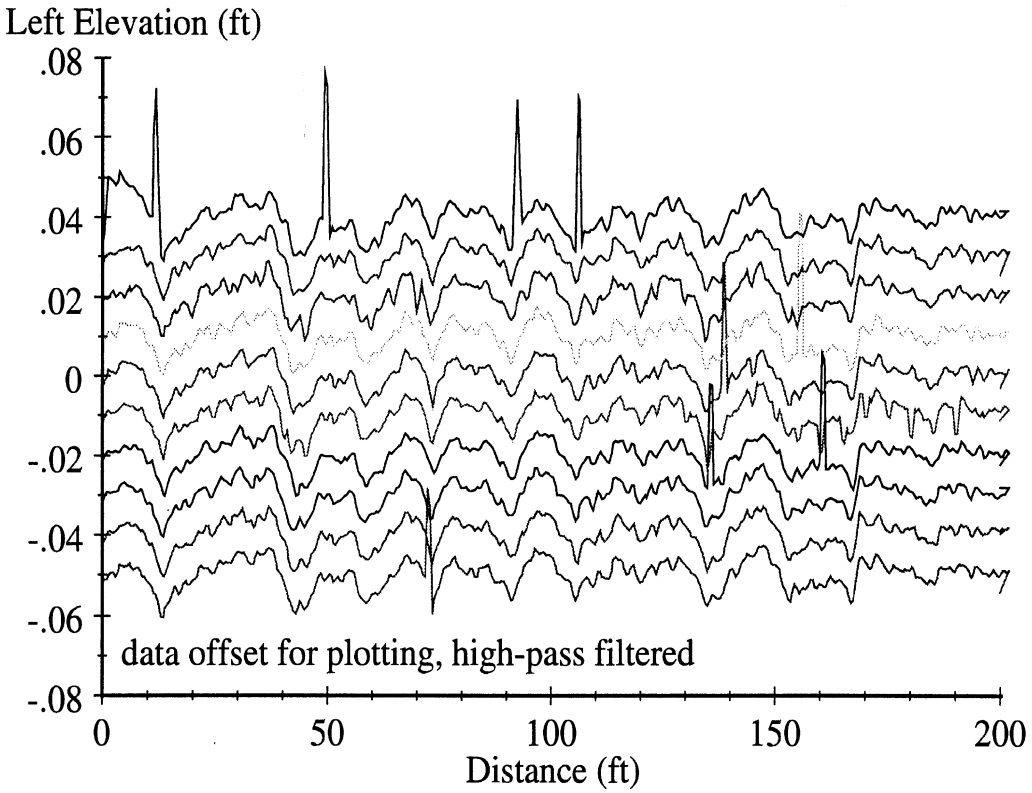

Figure 34. Repeat measurements containing spikes caused by measurement error.

Laser height sensors work by projecting an image on the ground, detecting its position when viewed at an angle, and determining the distance by triangulation. This technique fails if the image cannot be detected. It is suspected that this is the cause of the spikes shown in figure 34.

The extraneous spikes shown in figure 34 affect the measured IRI of the section as well as the measured frequency content. The IRI of the site shown with four spikes (second from the bottom) was about 15 percent higher than other repeats with no spikes. Figure 35 shows the PSD functions computed for two of the repeat measures: one with extraneous spikes and one without. The plot covers the wave-number range where the greatest difference occurs. For some wave numbers, the PSD of the repeat with the spikes is a factor of 5 greater than the profile measurement without them. Recall from chapter 2 that RN is sensitive to roughness in this wave-number range. Clearly, the spikes lead to significant error in the calculation of the RN.

Surface Texture

Coarse surface texture has become a well known source of measurement error in road profile measurement, particularly with profilers that use ultrasonic height sensors. This was demonstrated in the 1993 RPUG study when nearly all of the participating devices with ultrasonic sensors measured high IRI values on sections with coarse surface texture.[24] Ultrasonic height sensors work by emitting a short sound pulse and listening for the returning echo. The time between the emission of the pulse and its return is proportional to the distance covered. This technique fails (1) if the surface does not reflect the sound well enough to detect; or (2) if the surface reflects the sound many times, such that the multiple echoes confuse the sensor logic.

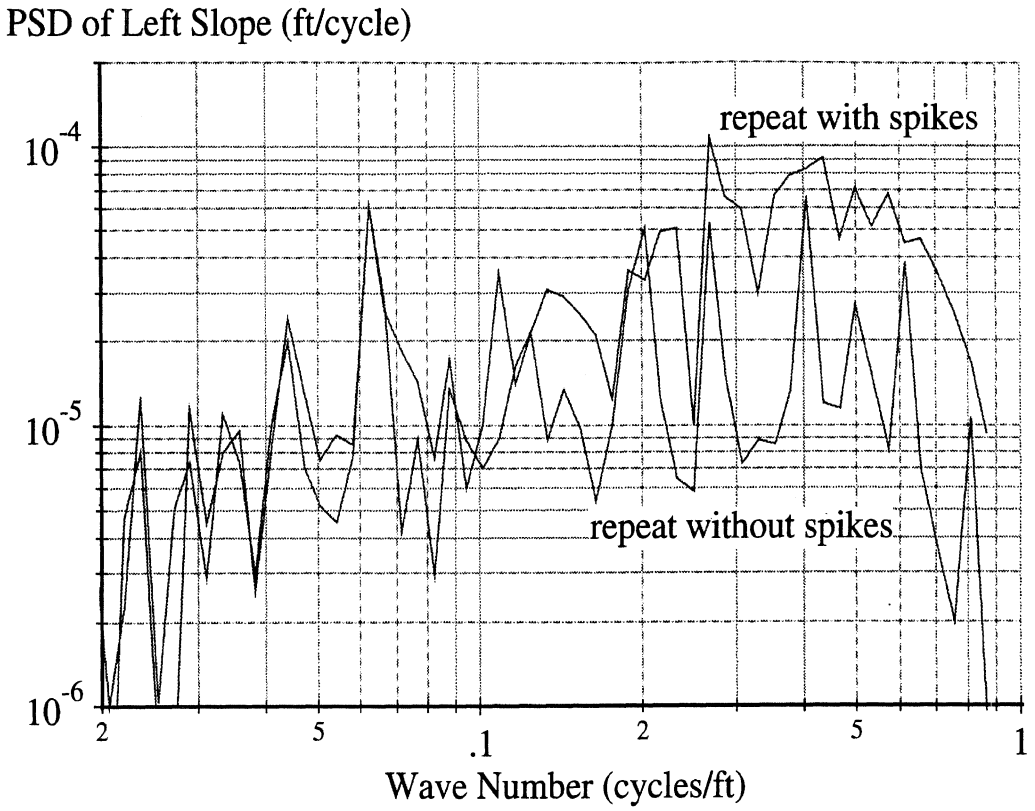

Figure 35. PSD of repeat measurements with and without spikes.

In some cases, IRI values from the ultrasonic profilers were 70 percent higher than the IRI from the Dipstick. Figure 36 compares four measurements made by a device with ultrasonic sensors and the Dipstick for the same pavement section. The repeats made by the ultrasonic device possess a component not present in the Dipstick measurement that has a high frequency (short wavelength) and low amplitude. In addition to this artificial jaggedness, the repeats show a level of visual agreement less than typical of the same device on fine surface texture roads. For this specific example, the IRI values from the ultrasonic system were consistently 20 percent higher than the IRI from the Dipstick.

Measurement errors related to surface texture are the most significant for high wave numbers (short wavelengths). For example, figure 37 shows the PSD of each of the repeats shown in figure 36. All of the measurements agree in the range of wave numbers up to 0.1 cycles/ft (0.33 cycles/m). In the higher wave-number range, the PSDs of the ultrasonic measurements are greater than the PSD of the Dipstick measurement by up to a factor of ten.

The effects of the errors on specific indices such as IRI and RN depend on the sensitivities to wave number of the filters used to compute the indices. The errors in high wave-number amplitudes seen in figure 35 affect both IRI and RN. However, because RN is the most sensitive to short wavelengths, the errors are more significant for RN than they are for IRI. The PSD plots in figures 35 and 37 support the statistical findings in chapter 2 that ultrasonic profilers are marginal in their capability to measure RN.

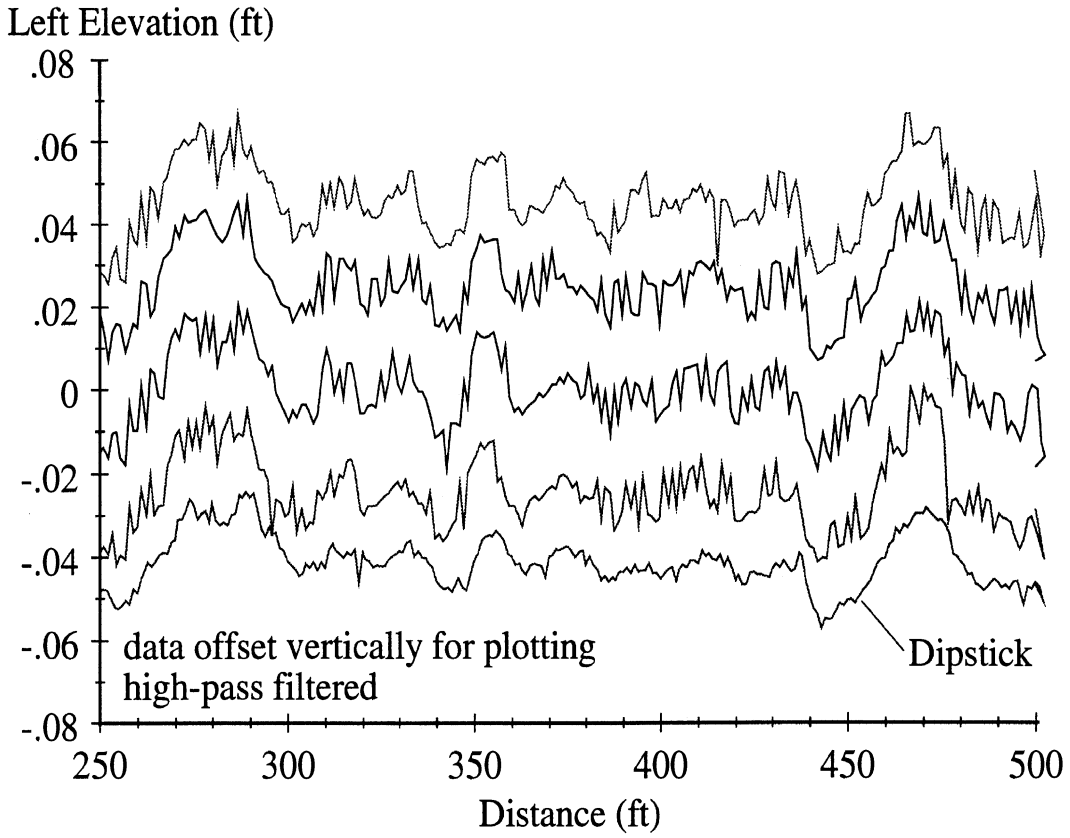

Figure 36. Repeat measurements of a section of coarse surface texture.

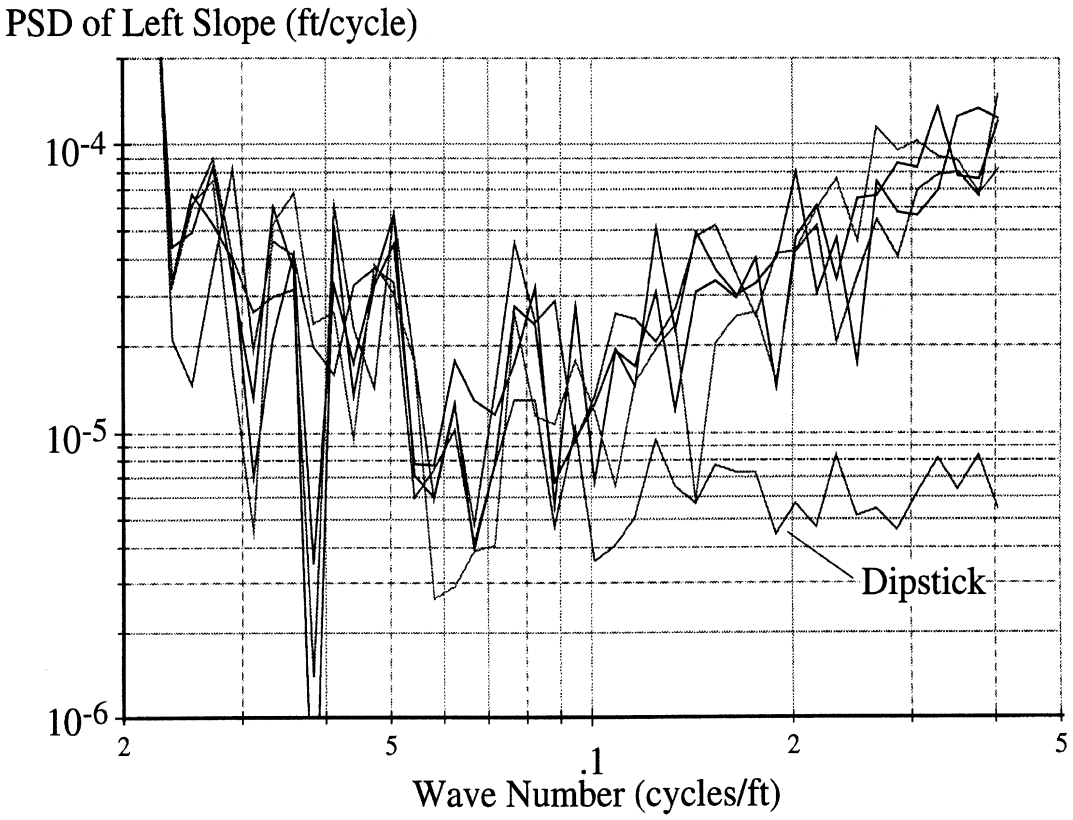

Figure 37. PSDs of repeat measurements of a section of coarse surface texture.

Although devices with ultrasonic sensors are particularly prone to errors caused by coarse surface texture, devices with other types of sensors also showed a recognizable level of error.

Missing Accelerometer Signal

Some data were submitted that only contained the output of the height sensor, without the contribution from the accelerometer. Once the error was detected, the data were corrected and resubmitted. Figure 38 shows the corrected and uncorrected measurements. A profile plot shows a much different signature than normal. The height sensor signal alone deviates very little from zero. The longer wavelengths only appear in the corrected profile, because the longer wavelengths in a road profile are detected by an inertial profiler almost entirely by the accelerometer.

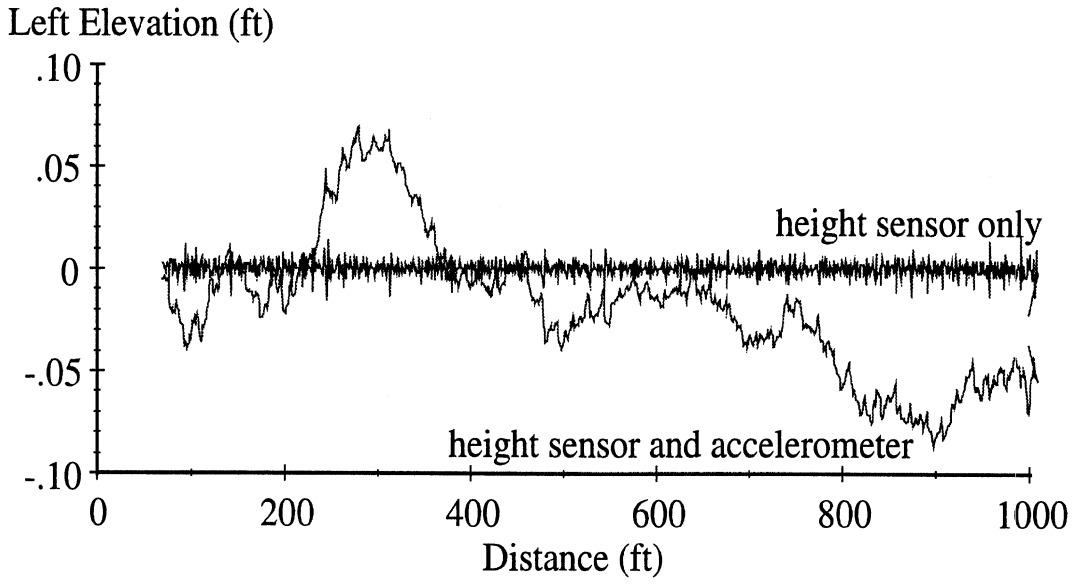

Figure 38. Profiles measured with and without an accelerometer.

The IRI computed from the height sensor signal alone is about 97 in/mi (1.53 m/km), whereas the IRI computed from the corrected profile is about 140 in/mi (2.21 m/km). Although these values are very different, the IRI value from the height sensor signal is in the expected range, and might not cause any notice when entered into a data base. Without a profile plot, this error could go undetected.

The PSD can also be used to diagnose a problem with the accelerometer (or the absence of its contribution from the computed profile). For example, figure 39 shows the PSD of the two measurements. The PSD of the corrected profile is fairly typical—uniform slope amplitude with respect to wave number. The PSD of the height sensor signal alone is very low in the low wave-number (long wavelength) range, where the contribution of the accelerometer is most significant. For high wave numbers, the agreement of the PSD functions is still poor. During the analog-to-digital conversion, the measure from the height sensor is rounded off. The round-off adds an error that is negligible in comparison to profile variations detected with the accelerometer. However, the error is significant with

respect to the height sensor alone, causing the PSD to be too high for very high wave numbers (short wavelengths).

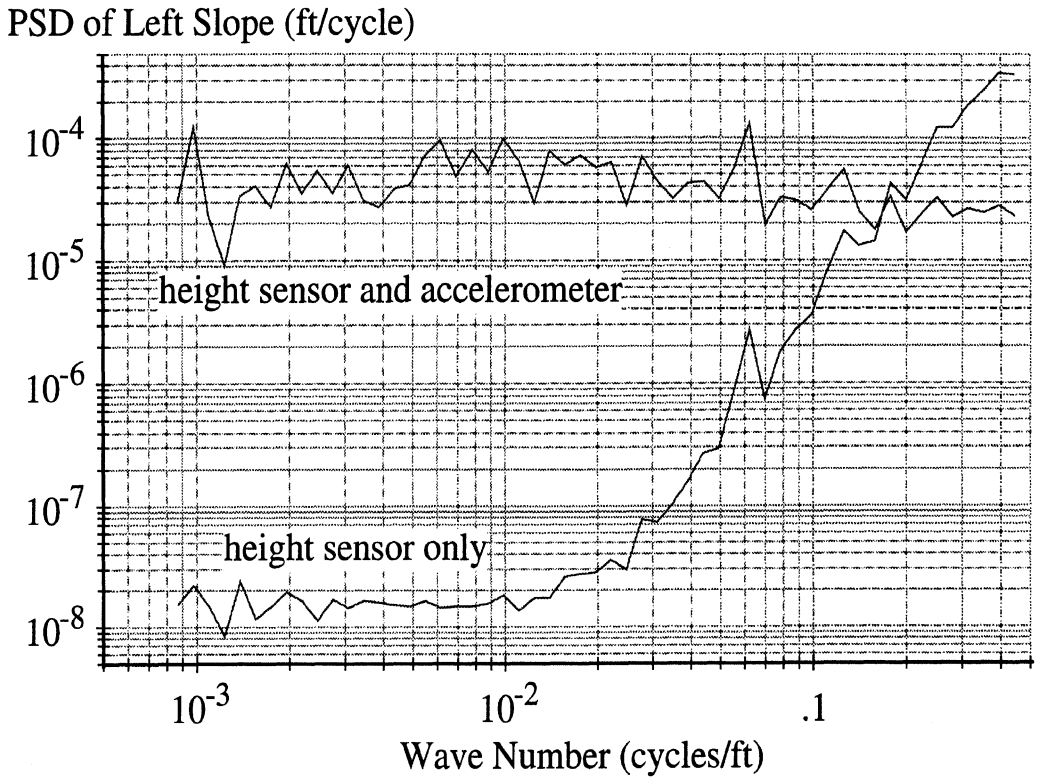

Figure 39. PSD of profiles measured with and without an accelerometer.

4. SOFTWARE

Some of the computer tools used in this project are of general interest to road profiler users. A road profile analysis software package called *RoadRuf* was prepared to transfer technology and promote standardization. RoadRuf is free and can be obtained from the Internet.

CAPABILITIES OF ROADRUF

RoadRuf is an integrated set of computer tools for interpreting longitudinal road roughness profile data. The tools include an X-Y plotter with filters, the IRI, RN, some general application filters with adjustable settings, and a spectrum analyzer for calculating PSD functions. The software is easy to use because the various analysis tools are integrated through a common graphical user interface (GUI). Together these tools allow the user to:

- Overlay plots of repeat measurements of the same road from different instruments.
- Calculate the IRI and RN of many profiles in a single batch run.
- Generate sets of standard plots.
- Apply moving average filters to profile plots.
- Diagnose profile measurement errors and find large bumps (faults, potholes, etc.) in measured profiles.
- View the wavelength content of various road surfaces using PSD functions.
- Calculate arbitrary profile indices by specifying their sensitivity to wave number.

The Simulation Graphical User Interface

All of the tools that are included in RoadRuf are integrated with a system called the simulation graphical user interface (SGUI), developed for vehicle dynamic simulation programs.[32] (Except for the IRI, the analyses in RoadRuf would generally not be called simulations. However, the word simulation is kept in SGUI for compatibility with literature involving similar software packages.) The SGUI works with a graphical data base that includes analysis settings, sets of data files, and options for viewing outputs. Inputs and outputs can be viewed graphically or in table form by clicking buttons on a master control screen, shown in figure 40.

Interactive X-Y Plotter with Filters

A plotter called EP (engineering plotter) is an essential part of the RoadRuf software. It has adjustable low-pass, high-pass, and band-pass moving average filters, with full batch capabilities for automatically plotting large numbers of files. It also includes options for zooming with the mouse, using a movable cross-hair to display numerical values, viewing with linear or log axes, and formatting labels, lines, and plot symbols. Figure 41 shows a

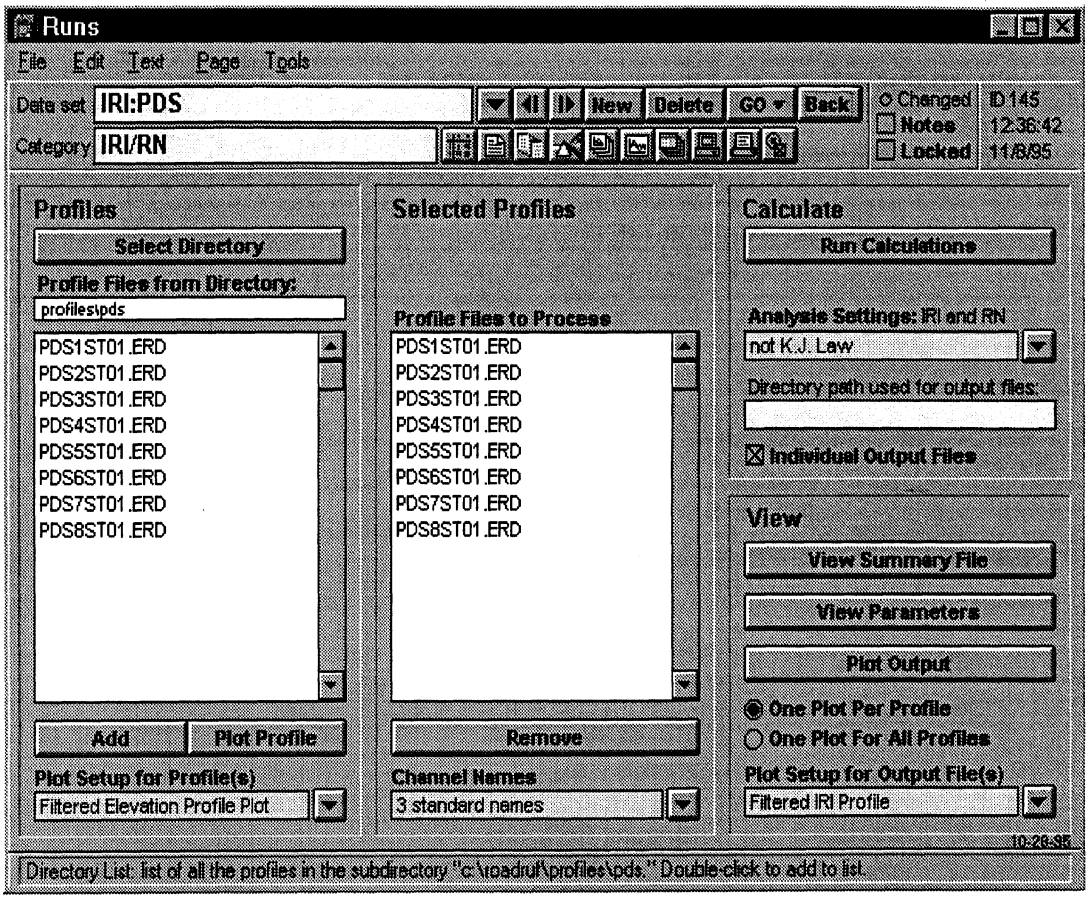

Figure 40. The master control screen in RoadRuf.

sample profile plot in which measures from three profilers are filtered identically and overlaid.

International Roughness Index and Ride Number Calculations

In RoadRuf, the user can calculate the IRI and RN of a batch of profiles from a single directory by using menus to select the directory, and the settings provided for the IRI and RN, and then clicking a button. RoadRuf writes a summary of the results into a text file for import into a spreadsheet program. The summary file contains the IRI and RN of the profiles in each file, and subsections of the profiles. The starting point and length of the subsections are specified by the user. Table 4 shows part of a sample summary file.

Customized Roughness Index Calculation

RoadRuf also includes two general application band-pass filters that attenuate long and short wavelengths. One is a quarter-car filter and the other is a four-pole, Butterworth band-pass filter as described in appendix E and chapter 2. The coefficients for these filters can be set by the user to define roughness indices other than the standard ones. The filters also include accumulators that calculate summary indices based on user-specified powers. Most of the analyses described in this report can be reproduced by researchers using the adjustable filters in RoadRuf, without writing any new code.

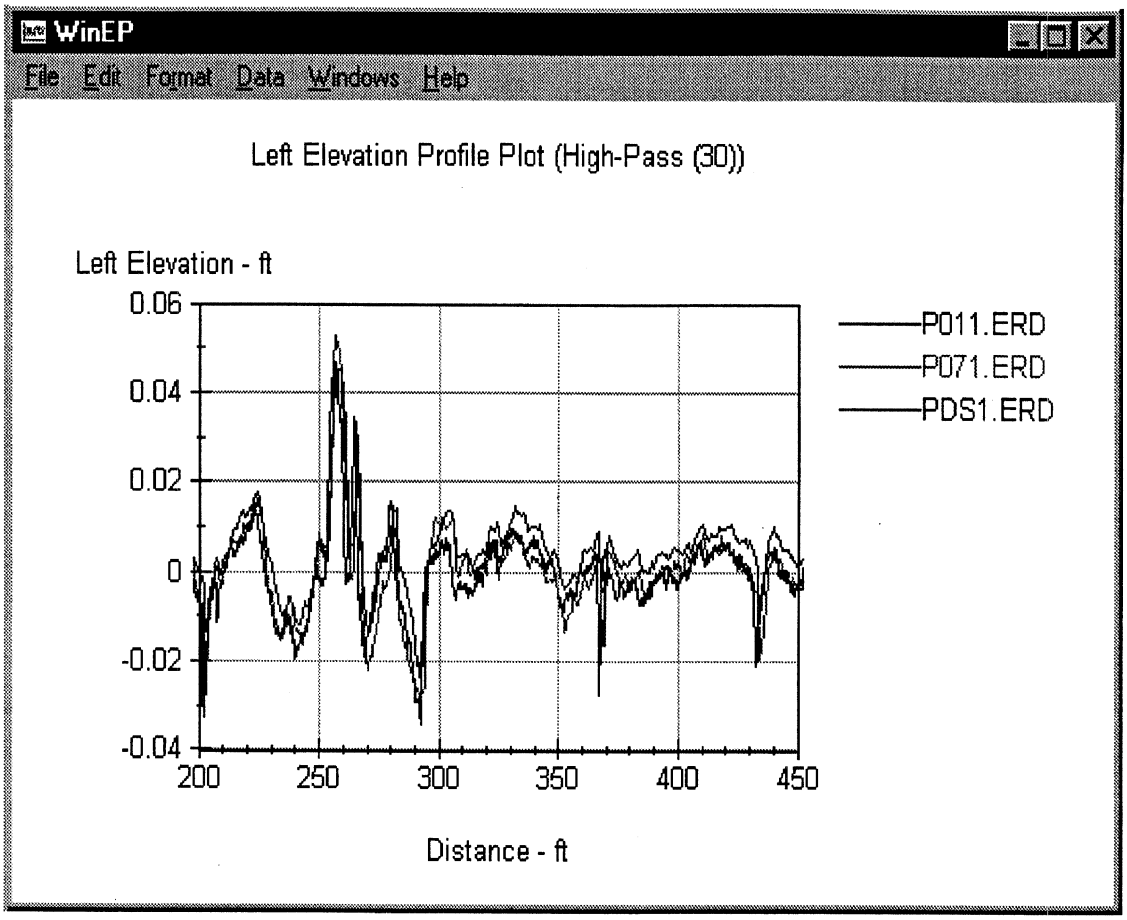

Figure 41. Filtered road profile plots.

Table 4. Summary IRI and RN table from RoadRuf.

```
IRI and Ride Number Calculation
Last modified at UMTRI Oct 20, 1995
Copyright (c) 1995 The Regents of the University of Michigan. All Rig…

Input files from directory "c:\roadruf\profiles"

Filename      Start: ft  End: ft    IRI: in/mi          RN: 0-5
                                    LElev.    RElev.    LElev.    ...
-------------------------------------------------------------------- ...
MDS1ST01.ERD      0.00     526.00     79.60     82.11      3.78   ...
                  0.00      50.00     66.42     61.84      3.99   ...
                 50.00     150.00     77.28     72.70      3.86   ...
                150.00     250.00     96.13     89.47      3.55   ...
                250.00     350.00     55.72     73.55      4.05   ...
                350.00     450.00     99.69    125.18      3.61   ...
                450.00     526.00     73.33     52.01      3.87   ...
MDS2ST01.ERD      0.00     526.00     56.49     65.55      4.11   ...
                  0.00      50.00     57.83     64.96      4.00   ...
                 50.00     150.00     44.01     46.38      4.19   ...
                150.00     250.00     67.66     71.53      4.00   ...
                250.00     350.00     50.06     55.80      4.16   ...
                350.00     450.00     62.14     87.26      4.12   ...
...
```

Spectrum Analyzer

RoadRuf includes a spectrum analyzer that uses a Fast Fourier Transform (FFT) to convert road elevation stored as a function of distance into a PSD function that indicates how the roughness is distributed over wave number. For example, figure 42 shows how the PSD functions compare for measures of a single profile made by two devices. The spectrum analyzer includes several options for calculating PSDs, including preprocessing capabilities developed specifically for analyzing road profiles. (Details of the analysis method were covered in chapter 2.)

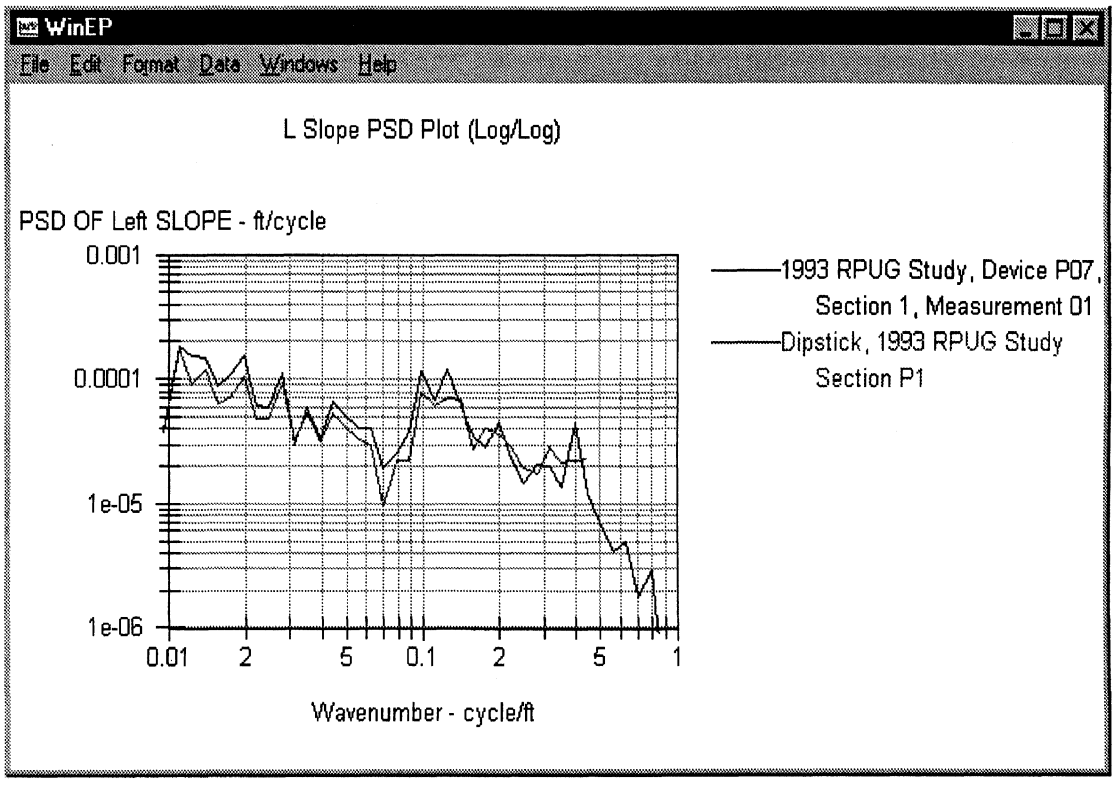

Figure 42. Example PSD functions for two devices.

Standard File Format

The analysis tools all use a universal data file format called the *ERD file*, which contains labeling information that is used by programs to automate the processing of the file.[33] This format was developed to support automated processing of data collected in the 1984 Road Profiler Meeting sponsored by FHWA. For example the IRI values for all of the data from the 1993 RPUG correlation study (more than 2,400 files) can be calculated in less than 2 hours on a 486 PC.

SOFTWARE AVAILABILITY

RoadRuf is free to the public. To find RoadRuf and its documentation on the Internet, start with the University of Michigan Transportation Research Institute (UMTRI) Web site: `http://www.umtri.umich.edu`. The address for information about road roughness is `http://www.umtri.umich.edu/erd/roughness/rr_home.html`.

5. SHORT COURSE

In the three decades since the invention of the inertial profiler, a substantial body of knowledge has been developed in the field of profiler design and technology. There are also many proven methods for analyzing and interpreting data similar to the measures obtained from profilers. The available information exists largely in the form of research reports and technical papers, which all describe *additions* to the state of knowledge. However, the authors are not aware of any single book or report that satisfactorily *summarizes* the current state of knowledge. Users have instructions provided by the manufacturers to operate the equipment, but little else to go on.

Some road profiler users from different States met in 1989 and formed the RPUG. RPUG has been meeting annually since then to provide a forum for issues involving the measurement and interpretation of road profiles. Following the 1994 annual meeting in Lake Tahoe, Nevada, representatives from the pooled-fund States and FHWA met with the researchers to review the project and discuss applications of the research. The group agreed that a lack of standards and training hinders users from making effective use of their equipment. FHWA provided funding to prepare a short course called "Measuring and Interpreting Road Profiles" (Contract DTFH61-95-P-00917) through the NHI. The first session of the course was held from November 14-16, 1995, in Ann Arbor, Michigan.

SUMMARY OF COURSE

The course covered $2^1/_2$ days. The lectures were mainly made by Dr. Sayers and Mr. Karamihas, based on a document called *The Little Book of Profiling*. In addition, Dr. Thomas Gillespie provided a lecture on vehicle dynamics, and Dr. Starr Kohn talked about applications of profiler data. The 17 participants received a notebook with The Little Book (prepared as part of the course), two TRB draft papers, and a tutorial for using the RoadRuf software described in chapter 4. The attendees also received the RoadRuf software on floppy disks. Table 5 lists the contents of The Little Book. In addition to listening to explanations of the basics of measuring and analyzing profiles, the participants spent several hours using the RoadRuf software in a computer lab adjacent to the classroom.

FUTURE OF THE COURSE

The presentation of course material concluded at about 10:30 on the third day. For about 2 hours after that, the participants conferred with the organizers on how the course should be developed. It was unanimous that the course was useful and should be continued. The total number of potential students is about the same as the attendance at the annual RPUG meeting—about 150. However, there is a great deal of turnover each year, so there should be a continued need to provide the course to about 40 or 50 engineers per year. Any particular agency would only have a few potential students, so it is probably not feasible to repeat the course at each State. Obtaining out-of-State travel approval is difficult in some States, so providing the course at a central location such as Ann Arbor is not ideal,

Table 5. Contents of *The Little Book of Profiling.*

Contents

either. One idea is to combine the course with the annual RPUG meeting. For example, if the RPUG runs from Tuesday to Thursday, the course could be held Sunday and Monday. That way, new course attendees would be familiar with the basics of profiling to better understand the RPUG presentations.

TECHNICAL LEVEL OF COURSE

Several of the participants had years of profiling experience and were hoping the course would cover more advanced material than it did. Others were new to profiling, and found it a challenge to keep up. Those new to the material thought that an extra half-day would have

been better to allow them to absorb the new concepts, although no one complained that the pace was unreasonable.

Those hoping to cover more advanced material were interested in learning more about signal processing, and particularly, details of popular filtering methods. However, they also recommended that the basic course be kept at the same technical level, because new students for the course would also be new to profiling. The thinking was that only a few users were ready for advanced material, and that it is probably best to provide introductory material. It was noted that this course is the only comprehensive resource available for new users.

One possibility would be to create a shorter course—say, a half day—covering more advanced material. If combined with RPUG, the advanced course could be given at the end of the conference.

COURSE CONTENT AND THE LITTLE BOOK OF PROFILING

No one suggested removing anything from the material presented. The course closely followed the contents shown in table 5. The close correspondence between the book and the lectures was viewed as a good way to structure the course. The following additions were proposed by the attendees:

- A glossary of terminology.
- A recommended reading list.
- Material on vehicle dynamics presented by Dr. Gillespie.
- History of roughness measuring, including profilographs.
- Guidelines for filtering.
- Inclusion of the South Dakota Index (SDI).
- Wave number responses of historical equipment (response-type systems, profilographs, etc.).

Although the general consensus was that the main content of the course should not be more advanced technically than the current version, it was suggested that a few additional equations could be provided to show how some of the examples were worked out. Also, an appendix was suggested that would contain equations for filters used in analyzing profiles, along with graphical representations of the frequency responses. (These would be similar to the figures and equations that are in this report.)

The Little Book of Profiling can be downloaded from the Internet from the web page `http://www.umtri.umich.edu/erd/roughness/litbook.html`.

ROADRUF SOFTWARE

There were some suggestions for minor changes to the software itself, mainly involving the generation of reports. It was also proposed that more worked examples be

included, along with more standard setups. This would allow new users to generate standard reports with very little learning time.

For the next session, it was suggested that students with laptop computers could bring them, install the software, and run the examples during the course. This would have two advantages: (1) the students would leave with the software already installed and running, with any examples completed during the course; and (2) fewer computers would need to be rented or borrowed, which would lower the cost of running the course.

6. CONCLUSIONS AND RECOMMENDATIONS

The development by South Dakota of an inertial profiler that uses a low-cost ultrasonic height sensor in the early 1980s triggered a rapid movement by the States away from response-type road roughness measuring systems towards profiling systems.[7,12] The majority of States now own road profilers, and profiler use is still growing. The research conducted in this project has shown that the rapid growth in profiler use has not been without problems. Interactions with the pooled-fund users and those attending the annual RPUG meetings have indicated that there is a major need for education about profiling in general. There is also a need for standardization of analysis methods.

The RPUG is, by itself, a source of progress in these areas. As experiences are accumulated and shared, some of the problems have been identified and reduced. The project overlapped three RPUG meetings (1993, 1994, and 1995), and progress has been noted at those meetings. For example, FHWA has been collecting IRI data for the HPMS for several years now and has standardized more variables, leading to more consistent results. The difference between HRI and IRI is now understood by more users, with the result that errors associated with the mixing of the two statistics have been reduced. As another example, the importance of using high-pass filters to visually compare profiles from different systems is now recognized by a higher portion of the user community than was the case several years ago.

ASSEMBLY OF PROFILE TEST MATRICES

A significant accomplishment of this project was the assembly of over 5,000 profiles into 7 data sets, each suitable for different types of analyses. (See table 1 and appendix C.) All of the profiles are stored in a standard file format called the ERD file, which has been in use for over 10 years for automated analysis of profile data. The test matrices can be used by researchers to evaluate new profile analyses. The correlation matrix is particularly well suited for determining experimental correlations between different profile properties. Further, free software has been prepared for viewing the profiles graphically and applying the most common analyses.

Test matrices that involve repeats from different types of instruments are useful for showing the portability of new profile analyses. They can also give insight into the accuracy of different types of profilers. However, there are limits as to how much information the existing data can provide about sources of variation in the profiles. The measures were not made under tightly controlled conditions, particularly with respect to accounting for possible changes in the pavement surface because of temperature and other environmental effects. The 1996 NCHRP project 10-47, "Standards for Profile Measurement Accuracy," could result in a new portability matrix in which the measures are made under more precisely defined conditions.

INTERPRETATION OF PROFILE

The participating pooled-fund States were surveyed, and they identified passenger car ride quality as the pavement performance quality of greatest interest. Although research has been done to link public opinion to measurable profile characteristics, some findings are still inconclusive and contradictory. Rideability research indicates that the public is most critical of wavelengths of about 8 ft (2.44 m), although other studies indicate that the maximum sensitivity should be for wavelengths near 30 ft (9.14 m). Results from recent NCHRP studies show that short wavelengths are very important up to the limit of the profile measuring system. The question of whether or not the public is critical of roughness in wavelengths shorter than about 1.2 ft (0.37 m) cannot be determined from existing data because of limitations in the original profile measurements. The mechanical properties of the vehicle are known to strongly influence the vibrations experienced within the vehicle. However, findings from some rideability studies have indicated that the type of vehicle in use is not significant. Instructions and examples given to the panel members influence their responses so strongly that it is difficult to compare results from different studies.

Even though many research questions remain, the information in the NCHRP rideability data set contributes substantially to the present state of knowledge. Existing algorithms for estimating rideability were tested, but were found to be impractical for most profilers in use. After this finding was made, data collected in the 1980s under the sponsorship of NCHRP were obtained and used to develop a practical algorithm for computing an RN.

The new RN algorithm defines a ride number statistic that is independent of IRI and gives a useful measure of pavement quality. RN correlates well with the MPR data collected in the 1980s, and the new algorithm has been tested with data from a variety of profilers. The relationship between MPR and RN is not dependent on surface type. Most of the new algorithm for calculating RN is the same as used for calculating IRI, so users and profiler manufacturers with working software for computing IRI can make a minor modification to the software to add RN as an output option.

The development of a portable RN algorithm was the primary achievement of the project with respect to adding to our knowledge of how to interpret profiles. It has been described in a TRB paper distributed at the 1996 meeting, and the computer code for computing RN has been incorporated into the free RoadRuf software package.(6) Also, the computer source code has been included into the most recent draft of an ASTM standard being developed for estimating rideability from measured profile.

The bias and random error associated with the new algorithm are similar to errors associated with the IRI for several optical and laser high-speed profilers, and for the quasi-static Dipstick. However, when applied to profiles obtained with ultrasonic devices, the errors are significantly higher than for IRI. Although results from some profile data indicate that ultrasonic systems can produce useful measures of RN, users of ultrasonic systems should be aware that the majority of the ultrasonic data available in this study showed errors that are too high for most uses.

The IRI analysis was also reviewed, and found to be technically sound. Problems associated by users with IRI are generally caused by problems in the profile data, or

software errors. To remedy problems associated with misunderstanding of how IRI is computed, a TRB paper was prepared to provide a short, archival description of the IRI along with tested Fortran computer code.(5)

TRANSFER OF TECHNOLOGY

During the project, the researchers participated in RPUG meetings and presented lectures and new findings to the user community. As noted above, two TRB papers were prepared (one has been published and the other is in review). The project also resulted in two new resources for transferring technology to users. First, a user-friendly profile analysis software package called *RoadRuf* was developed that calculates IRI, RN, filtered profile, and PSD functions, and includes a plotter with filters. Second, a $2^1/_2$ day course on profile measurement and analysis was prepared, along with a 90-page document called *The Little Book of Profiling* that introduces new users to the basics of what profilers are, how they work, and what can be done with their data.

Both the software and the short course are the first resources of their kind to be made available to the profiler user community. It is early to comment on their long-term significance, as both made their debut in November 1995. However, both were well received, and the researchers anticipate that they will prove valuable to many users in the years to come.

STANDARDIZATION OF PRACTICE

Analyses of the collected data show that standardization is needed in two areas. First, standardization is needed for the methods used to analyze the profile data. Standardization of profile analyses is accomplished most directly if the same software is used by most States. This was a major motivation for preparing the RoadRuf software package. The computer code used in RoadRuf is also listed in this report, and has been incorporated into several draft ASTM standards now in review.

The second need is for obtaining profile measurements that are valid. Unexplained variation in profile measurements is perhaps the number one problem facing profile users today. A major contribution to this problem is the fact that most users have little experience to prepare them for the technology in high-speed profilers. A typical background in civil engineering does little to prepare the engineer for the link between a rapidly-moving vehicle and the static properties of the road surface. The Little Book is a start towards providing the basics of how profilers work and the uses that can be made of the data.

It is clear that profilers from different manufacturers have different capabilities in terms of accuracy and ease of use. Systems that use ultrasonic height sensors cannot measure short-wavelength, low-amplitude profile features, as well as systems that use laser and optical sensors. Specifications have been published in the past to classify profilers. For example, the World Bank report and HPMS requirements define Class 1 and Class 2 systems. The ASTM standard for inertial profilers defines four classes. Data analyzed in this research show that profilers that qualify on paper as Class 1 do not produce measures that repeat to the degree expected. The existing specifications are well suited for static

profilers but may not be appropriate for inertial ones. A major factor in determining accuracy requirements is that accuracy is linked to wavelength. For example, consider the three sinusoids as summarized in table 6 with different wavelengths and amplitudes.

Table 6. Comparison of three profile sinusoids.

Wavelength	Amplitude	Slope Amplitude	IRI
200 ft	1 in	165.9 in/mi	9.5 in/mi
50 ft	0.25 in	165.9 in/mi	160 in/mi
10 ft	0.05 in	165.9 in/mi	150 in/mi

Suppose the amplitude of the sinusoid is in error by 0.005 in (0.127 mm), and consider the effect on IRI. There would be a 10-percent, or 15 in/mi (0.24 m/km), error for the 10-ft (3.05-m) sinusoid; a 2-percent, or 3.2 in/mi (0.05 m/km), error for the 50-ft (15.2-m) sinusoid; and a 0.5-percent (negligible) error for the 200-ft (61.0-m) sinusoid. Clearly, a tolerance for amplitude error is nearly meaningless unless a wavelength is also specified.

NCHRP Project 10-47, "Standards for Profile Measurement Accuracy," starts in 1996 and is intended to produce new methods for evaluating profiler accuracy.

RECOMMENDATIONS

The most critical problem facing road profilers is the lack of knowledge involving profiler technology. The short course and *The Little Book of Profiling*, developed as an extension of this research, are resources available to users that can provide access to the existing base of knowledge. Feedback from the 17 attendees of the first short course suggests that the course is basically sound but could use more worked examples and be extended to cover some derivations. Although the total number of profile users is limited to several persons per State, the annual turnover is significant. There is now a potential base of a few hundred students for the course, with a continued addition of 50 or so new users per year. The current curriculum is appropriate for the majority of users. However, advanced users would benefit from a shorter course covering signal processing, with worked-out examples involving filters such as moving average, quarter car, and Butterworth. Also, managers and planners would benefit from a shorter course giving a less technical overview.

Recommendation: The profiling short course should be taught on an annual basis, and scheduled to coincide with the RPUG meeting. For the next 2 years, it should be budgeted to cover updates and improvements in the lectures and the accompanying Little Book.

Recommendation: Two shorter versions of the course should be spun-off. One should be for the advanced user, covering signal processing and describing how common profile filters work. The other should be for planners and managers, covering the uses that can be made of profilers. This version would leave out the technical details. Both spin-off versions should be based on the same Little Book.

The IRI analysis is technically sound, and is compatible with most profilers. However, some users are computing the statistic from a point-by-point average of two profiles, resulting in a different statistic called HRI. HRI numbers are lower than IRI by 10 to 20 percent. Theoretically, HRI is a slightly better representation of a car equipped with a road meter. It is not a better representation of the ride experienced by a driver or passenger, because it does not account for the roll vibrations of the vehicle. Work done in this project indicates that IRI and HRI are so highly correlated that there is no statistical support to choose one over the other.

Recommendation: All users making quarter-car analyses should use the IRI in the spirit of standardization. HRI can be computed as an additional measure, but it should not be used in place of IRI.

The new method for computing RN, presented in chapter 2, provides a closure for the research sponsored by NCHRP in the 1980s to link profile characteristics to the public perception of rideability. No other 0 to 5 rideability scale has the same demonstrated portability.

Recommendation: The algorithm for computing RN should be applied by users wishing to rate roads on a 0 to 5 rideability scale and who have profilers with laser or optical sensors.

Ultrasonic sensors have limited resolution that introduces errors in the short-wavelength, low-amplitude range of roughness. These errors become unacceptable for roads that are very smooth, for roads with coarse texture, and for any roads that will be processed using analyses such as RN that emphasize short wavelengths.

Recommendation: Profiler users interested in evaluating profiles of smooth roads or applying the RN analysis should move to replace their ultrasonic sensors with lasers or optical sensors.

Profiling analyses are more complex than most algorithms described in road standards such as those published by ASTM and AASHTO. The best way to standardize typical profile analyses is by direct distribution of computer software and source code. With the rising connectivity of State agencies through the Internet, access to standard computer code is becoming simpler than access to written reports and technical papers.

The RoadRuf software is a free, user-friendly software package for computers that runs on Microsoft Windows. It includes IRI, RN, plotting, moving average, PSD, and custom filters. RoadRuf was put on the Internet in late 1995. (At the same time, floppy disks with the software were sent to the pooled-fund States.) The experience to date indicates that the package fulfills a real need, offering many users their first opportunity to view and compare measured profiles. However, users have also found bugs and areas where more documentation is needed.

Recommendation: Users should obtain the RoadRuf software and, as a minimum, confirm that their own profile analysis software gives comparable IRI values.

The RoadRuf software has been tested and is much easier to use than other road profile analysis software that has been publicly available in the past. Considerable time was spent

during this project testing and debugging the software. However, even after this testing, attendees at the short course found a few bugs and identified simple changes that would improve the software. The experience of preparing the software for the short course has shown that testing and documenting software with the complexity of RoadRuf is a time consuming process. It is also a process that should continue after RoadRuf has gone into use, to take into account recommendations of users.

Recommendation: The RoadRuf software should be maintained and supported. Distribution of the software (and updates) through an Internet site appears to be a good way to make the software available world wide. A source of funding will be needed to maintain the software and its documentation.

Comparisons of profile statistics derived from different instruments measuring the same roads show that variations between instruments are larger than would be expected. Published specifications for Class 1 instruments are not sufficient to define the absolute accuracy that can be expected for all possible analyses. For example, specification of accuracy in measuring profile slope would be better for instruments mainly used to obtain IRI. Variations tend to average out over length, which means that results obtained from short profiles tend to show more variation than similar results obtained for long profiles. For example, an instrument might show a standard deviation in IRI of 0.5 percent for 1-mile (1.6-km) sections, but for 200-ft (61.0-m) sections, the standard deviation could be 5 percent.

The type of analysis is also a factor. For example, an ultrasonic profiler might be shown to measure IRI with errors less than ±3 percent and RN with errors less than 55 percent, while a laser profiler might have IRI errors within ±2 percent and RN errors within ±8 percent. The errors would be obtained for a fixed profile length, such as 0.1 mi (0.16 km).

A new NCHRP research project (Project 10-47) starts in 1996 and is intended to produce new methods for evaluating profiler accuracy.

Recommendation: Until research findings come in from NCHRP Project 10-47, specifications of profiler accuracy should be made in terms of specific analyses (e.g., IRI, RN) and profile lengths (e.g., 0.1 mi, 0.5 mi).

APPENDIX A. LITERATURE SURVEY

A literature search was made to determine the current state of knowledge about profiling technology and how profiles are linked to pavement performance qualities (ride quality, pavement performance, etc.). The existing knowledge of the research team was supplemented by computer searches through the UMTRI library and the Transportation Research Information Service (TRIS) data base. A summary of the knowledge from the literature is provided under the topical headings that follow.

PROFILE ANALYSES

A major study of profile analyses and indices was made for the 1982 IRRE, described in World Bank Technical Paper 45.[9] The data from this experiment were used to compare a variety of profile-based roughness analyses in use at that time. The analyses included PSD, IRI, a Brazilian Quarter-car Index (QI), a Half-Car Simulation (HCS), root-mean-squared vertical acceleration (RMSVA), an index called root-mean-squared deviation (RMSD) that was proposed by the British Transport and Road Research Laboratory (TRRL), and several waveband indices used in Europe. Subjective panel ratings were also obtained and correlated with IRI. The significant product of this project was a standardized index and methods for measuring it. Two concepts defined in that work that are now widely used are (1) the IRI; and (2) the definition of separate classes of roughness measuring methods (Class 1 profile, Class 2 profile, Class 3 calibrated response-type systems, and Class 4 subjective rating and estimates). Both concepts are described in World Bank Technical Paper 46.[2] The IRI is described in chapter 2 and appendix F of this report.

In the past 5 years, there has been a strong movement towards using the IRI in the United States and elsewhere. It is required for all data submitted to the FHWA HPMS data base. Virtually all road profiling systems used in the United States are equipped with software for computing IRI. Appendix J, "Roughness Equipment, Calibration and Data Collection," of the HPMS Field Manual references World Bank Technical Paper 46 with regard to procedures for direct profile measurements and computation of IRI.[10] The HPMS Field Manual recommends that the profile of the right wheel track be used to compute IRI for use in the HPMS data base. The manual also suggests that HPMS efforts should be coordinated with other related activities such as the LTPP study and State pavement management system activities.

The other profile index that has generated interest recently in the United States is the RN proposed by Janoff.[4] It is based on experimentally determined correlations between profile PSD functions and subjective ratings of rideability. The experience with RN is not yet as widespread as with IRI. Development of an RN calculation method is described in chapter 2 and was one of the major accomplishments of the current research.

Although many profile indices have been proposed and studied over that past 20 years, they are all based on mathematical algorithms that were proposed for characterizing profile measurements in the 1970s. Those algorithms that are still in use for processing a single profile fall into just a few categories. The process essentially involves two steps: (1) *transform* the original profile; and (2) *summarize* the transformed profile by averaging.

The typical effects of a transform are to remove long wavelengths and to change the significance of the wavelengths in the profile. Some transforms that are most commonly used are the quarter-car simulation (e.g., the IRI), other vehicle simulations (e.g., truck dynamic loading), finite difference (approximate slope calculation), mid-chord deviation (typified by the RMSVA), moving average smoothing (low-pass filter), moving-average removing (high-pass filter), waveband RMS measures, and RN.

Statistics obtained from filtered profiles are typically summarized using either (1) RMS; or (2) average rectified values (e.g., accumulated response measure divided by length of profile).

In addition to choosing a method for transforming the profile and averaging the results, there are a few other issues involved in using profiles to characterize road condition:

- Which profile should be measured in a traveled lane (left, right, center, or other)?
- How are left and right profiles combined for processing? (e.g., process independently, average the profiles then process, or process the profiles then average the results?)
- What is an acceptable profile test length?

A Fourier transform changes a profile from a function of distance to a function of wave number. This type of transformation is often called *spectral analysis*. A typical form of output of a Fourier transform is a PSD function. The PSD is a function rather than a summary index. RMS statistics can be obtained from a PSD for a waveband of interest by integrating under a portion of the function.[1]

EXPERIMENTAL LINKS TO PERFORMANCE INDICES

Analyses to derive experimental correlations between profile properties and measures of performance require data that are hard to come by. The major areas of research have involved pavement performance, automotive ride quality, and dynamic loads imposed by heavy trucks. Because pavement performance can be classified as functional and structural, there is an inter-relationship between ride quality, pavement performance, and dynamic loads.

---

[1] The mean value should be subtracted from a profile signal before spectral analysis. When this is done, the variance equals the mean-square value and the standard deviation equals the RMS value.

Ride Quality

Several studies that link road roughness to experimental measures of ride quality have been performed. Probably the most significant works involving new experimental data that have resulted in a strong correlation between ride quality and profile roughness are Janoff's studies for the NCHRP, described in Reports 275 and 308.[3,4] These reports link profile properties to the subjective panel ratings of rideability. Janoff recommended processing road profiles to obtain an RN, using spectral analysis and a weighting function that emphasizes wavelengths in the range of 1.6 to 8 ft (0.49 to 2.44 m). Another of Janoff's findings was that the correlation between RN and IRI is good for flexible pavements but poor for rigid pavements.

During the NCHRP studies of pavement roughness and rideability, both passenger car and truck ride quality were initially considered. It was determined at the time that passenger car ride quality was the primary consideration. Heavily traveled highways that carry the majority of high-speed truck traffic generally are not permitted to develop a level of pavement roughness that will result in substantial truck ride quality complaints. The noted exception is jointed PCC pavements with significant joint faulting.

Ride quality is of great interest to the manufacturers of cars, trucks, and busses. In the vehicle dynamics arena, there is presently no consensus as to how the ride quality perceived by a driver or passenger can be predicted from experimental measures of vehicle motions. The relationship between accelerations of the human body and the human's evaluation of the vehicle ride or the pavement rideability is not well understood. Nonetheless, the basic first-order effect is simple: higher levels of vibration generally are assumed to indicate a lower opinion of ride.

Although the link between the vibrational environment of a human and the human's opinion of that environment is not simple, the link between road profile and the vibrational environment is handled well by fairly simple vehicle dynamics models. Passenger car vibrations are predicted well to the first order with quarter-car models, and truck vibrations are predicted well with pitch-plane (bicycle) models if they include the essential components.

Dynamic Pavement Loading

Dynamic pavement loading caused by road roughness has been measured experimentally by Sweatman and Ervin.[34,35,36] In each of these studies, road roughness was linked to a dynamic load coefficient (DLC) of truck tire loads for several suspension designs. Another study of dynamic pavement loading caused by road roughness is contained in NCHRP Report 353.[37] In this work, experimentally measured truck tire loads were used to validate a pitch-plane vehicle simulation and measured pavement strains caused by dynamic loading were used to validate the ILLI-SLAB pavement structural model. The study went on to relate dynamic loading (characterized using DLC) to road roughness using vehicle simulation models. The study also demonstrated the ability of pitch-plane models to duplicate dynamic loading behavior over the frequency range of 0 to 15 Hz.

Functional Pavement Performance

Pavement performance is commonly described as *functional* or *structural*. The accepted definition of functional performance was developed in the AASHO Road Test, completed in 1960:[38]

> "The level of a particular pavement's ability to serve the traveling public has been termed its serviceability, and it is the trend of serviceability with time or load applications that has been defined as pavement performance."

The Present Serviceability Rating (PSR) was described as the subjective public perception of pavement serviceability; Present Serviceability Index (PSI) was an estimate of PSR computed from objective measurements.[39] It was determined at the Road Test that pavement roughness was the most significant factor in determining the PSI of a pavement. The PSI concept, based primarily on measured roughness, has been used by many State highway agencies to (1) monitor pavement performance and condition; (2) determine the need for maintenance and rehabilitation; and (3) predict remaining life. With the development and implementation of pavement management systems in recent years to more formally record, evaluate, and forecast pavement conditions, it has become apparent that the ability to collect and analyze the longitudinal profiles of the pavement wheel paths provides improved methods for determining pavement condition and serviceability. Consequently, the ability to realistically measure pavement profiles and compute various ride and roughness statistics is an increasingly important element in the determination of highway pavement functional performance.

As noted above, FHWA requires that all roughness data submitted to the HPMS data base be in the form of IRI. However, there is not yet standardization as to how pavement serviceability is represented in pavement management system data bases maintained by the individual States. Most States that profile their networks obtain IRI values, which is the basis for the serviceability indices put into their data bases. Some re-scale IRI to units of PSI; some re-scale IRI to estimates of earlier roughness measures, such as a Mays meter response-type system or slope variance; and some use IRI directly.[7]

Structural Pavement Performance

Structural performance of pavements is described as the ability to support current and anticipated wheel loads with realistic maintenance and rehabilitation activities and expenditures. Some attempts have been made to identify inadequate structural capacity and performance by analysis of longitudinal pavement profiles. However, on heavily traveled highways with a substantial percentage of truck use, the development of pavement roughness related to structural performance occurs at a time beyond the optimum for the planning and programming of structural rehabilitation. Many States use records of pavement surface distress development and non-destructive deflection testing as the preferred method of evaluating structural performance. (By the time a pavement gets rough, it is already past the optimum point for maintenance.)

Novak and Defrain of the Michigan DOT performed some studies relating to the seasonal variation in the profile.[40] They found that cracks in overlays can change significantly as frost action takes place. This generally increases roughness, and once it

occurs, it keeps increasing. It might be that seasonal variations in profile could be correlated more directly with distress than the profiles themselves. The researchers showed that these types of distress roughness interactions occur in a cyclic pattern. Thus, spectral analysis might be used to identify the presence of these patterns, which can then be related to certain performance characteristics.

PROFILE MEASUREMENT TECHNOLOGY

Measurement of road profiles is a highly specialized area of technology that has been developed mainly to serve the highway community. A variety of equipment has also been used over the years at universities and in the military. However, it is the systems used for highway applications that have seen the most development and validation.

Road profile can be measured at highway speeds using inertial profilers, which are vehicle-mounted instrumentation systems intended to measure vertical deviations of the road surface along the direction of travel. They have been in existence for three decades, and millions of dollars have been spent thus far on their purchase and operation. In recent years, the variety in hardware and design available to the highway community has increased dramatically. These devices are playing an increasing role in the routine evaluation of pavement condition by States, and in Federally-coordinated research projects.

The importance of profile measurements has also led to a new interest in measuring profiles manually. Manual measures are appropriate when the scope of the measurement activity is limited and the high cost of obtaining a high-speed system cannot be justified.

Manual Methods

The most obvious method for measuring ground profiles is with a surveyor's rod and level. Although laborious, measurement of a profile by this method is straightforward and contains no surprising sources of error. The accuracy of the measurements is primarily determined by the precision of the level instrument (together with the skill of the survey team) and the interval between measures. Typical land surveying equipment is used for readings of 0.01 ft (3 mm), which is too coarse for all but the roughest pavements. In some cases, rod and level measures are made on road sites used to calibrate other roughness measuring instruments. For this application, the level should have a resolution of about 0.039 in (1 mm). This resolution is adequate for measuring the IRI on all but the smoothest pavements. On very smooth road surfaces, a resolution of 0.020 in (0.5 mm) is needed. The sample interval originally recommended for computing the correct IRI value is 19.7 in (500 mm) if the road has no significant localized roughness features (tar strips, potholes, etc.) that would not be seen at that interval. A closer spacing of 9.8 in (250 mm) was recommended. A more recent analysis of the requirements for obtaining accurate IRI estimates indicates that the spacing should be 12 in (305 mm) or less.[5]

Specification of accuracy and sample interval is trivial for a rod and level measurement. What is not trivial is the actual measurement process. This method is tedious and time consuming, taking several days to measure both wheel tracks for a mile of road. The time required to make the measurement is roughly proportional to the number of samples per mile, so there is a strong motivation to use the longest interval that will give a useful

profile. After the measures are made in the field, they must be entered into a computer system. The main problem with the rod and level method is that it often requires the manual logging of a large amount of data, such that the chances for human error are high.

At least two other static profiling methods are in use, based on commercial systems designed to offer greater efficiency and eliminate the manual logging of the measures. One of these is a device developed by the overseas unit of TRRL in England, called the TRRL Beam. It consists of an aluminum box beam about 9.8 ft (3 m) in length supported at each end by a fixed tripod. The beam is leveled by an adjustment at one end, thereby defining a fixed horizontal datum. Measurement of the ground-to-beam distance is made with an instrumented assembly that contacts the ground through a small pneumatic tire, and which slides along the beam on precision rollers. The moving assembly contains a microcomputer that digitizes the signal at preset intervals and records the data. After the sliding fixture is moved over the length of the beam, it is picked up and moved down the road so that the new starting position matches the old end position. The TRRL Beam was designed for use in developing countries to calibrate other roughness measuring systems.

Potentially, this design introduces a small random error each time the beam is moved. This error was demonstrated to be negligible when a prototype was used in the 1982 Brazil experiment. In that experiment, the TRRL Beam demonstrated a level of accuracy that is hard to match.[9]

A different approach is used for a device called the Dipstick made by the Face Company. This device is supported by two legs nominally separated by a distance of 1 ft (0.305 m), and held by the operator with long vertical handle. The separation between the legs can be adjusted to lengths other than 1 ft (0.305 m) in some models. The instrument measures the inclination angle between the feet, thereby providing the difference in elevation. The instrument records the difference in elevation and signals the operator, who then walks the device along the road by alternately pivoting it about each leg. This instrument is commonly used in the United States to validate measures from inertial profilers. The Dipstick has been successfully compared to the rod and level as a reference device for the IRI.[41]

The General Motors Design

Most high-speed profiling systems are based on a design from the GMR Laboratory that was developed in the 1960s.[1] In this design, shown in figure 43, a vehicle is instrumented with an accelerometer and a height sensor. The accelerometer senses the vertical motions of the vehicle body, relative to an inertial reference. The height sensor follows the road by sensing the distance between the vehicle and the road surface. The signals from the accelerometer and the height sensor are used together to compute the profile of the road. By eliminating the vehicle motions, a profile is obtained relative to an inertial reference. This profile computation is a form of data processing that is specific to GM-type Profilometers, and requires some type of computer capability.

Several systems are in use today that are based on the GM-type design. Most of the newer systems feature on-board computers for digital analysis, non-contacting height sensors, and software that allows a variable measurement speed.

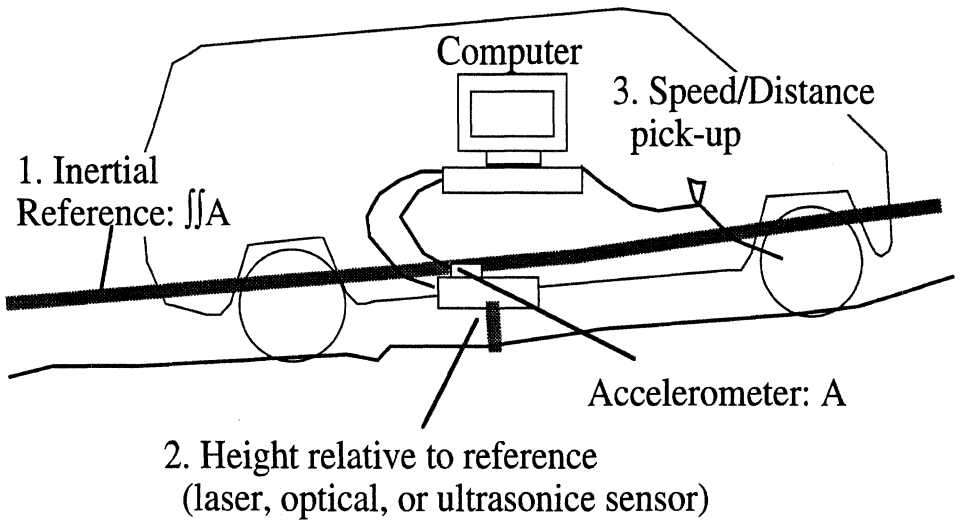

Figure 43. GM-type Profilometer.

The South Dakota DOT designed and built a novel GM-type profiling system in 1981.[42] SDDOT provided plans for the system to other States, and offered help at nominal cost for States wishing to build similar systems. Several States and commercial manufacturers have built systems based on the SDDOT design since. It is now the most commonly used profiling system in the United States.

The original GM-type Profilometer used a mechanical follower wheel, spring-loaded against the ground. A problem with a mechanical follower wheel is that it can sometimes bounce when it hits a bump or hole. The result is that the profile obtained traces the path of the wheel through the air, rather than the surface. The design of follower wheels used on GM-type profilometers has limited their valid measurement range to exclude rough roads, and imposes limits on the operating speed on even slightly rough roads. A more serious problem, from the perspective of the users, is that the mechanical follower wheel is easily damaged. In modern GM-type profilometers, follower wheels have been replaced by non-contacting sensors that measure height using ultrasound, laser beams, or optical images.

Height can be measured using ultrasound in at least two ways:

1. A speaker emits a short burst of sound, and the time needed for the sound to reach the pavement and be reflected back to a microphone is measured. By knowing the speed of sound through air, the distance can be computed from the time interval.

2. A speaker emits a continuous tone, and the reflected sound is monitored. The height is determined by the phase relationship between the original and reflected sound.

Measuring height with ultrasound requires that a number of problems be solved that have nothing to do with the surface quality, such as effects of wind and changes in air pressure. Surface condition can also challenge an ultrasonic system if it is a poor reflector of sound, such that a detectable sound is not returned to the sensor. Generally, open texture and bumps with sharply sloping surfaces are poor reflectors that cause problems with ultrasonic height sensors. Smooth roads also pose a challenge, because the ultrasound

sensors typically have limited resolution—an effect that adds a small amount of roughness to the measurement.

Laser beams are used in some systems to measure vehicle height by triangulation. A laser beam is projected straight down onto the surface resulting in a small, bright spot of light. The spot is seen by a photo detector mounted to the side. Optics and a linear detector are used to relate the light spot location to an angle, from which the distance from the vehicle to the ground is determined. The laser uses a single frequency (monochromatic light), and the detector can include filters to exclude effects of ambient light. Thus the system may be made insensitive to variations in light intensity, both the ambient and that reflected from the laser. One problem that can occur with a laser sensor is that the spot can go into a crack or hole, where it cannot be seen by the detector. Another property of this design is that it may include texture in the measure, which can add a random error to a profile if not properly dealt with in the digital data-acquisition system by anti-aliasing filters. Most of the laser sensors used in profiling systems are manufactured by a Swedish company named Selcom.

Several designs of non-contacting height sensors use conventional light sources (i.e., not laser) to project an image on the ground. A successful optical system has been developed by K.J. Law, Inc., and the Michigan DOT. An optical non-contact sensor was also developed in FHWA-supported research using an infrared light beam with two photo detectors viewing the image from an angle. The relative amount of illumination falling on detectors is used to establish the angle to the light spot, and hence the distance from the detector to the road surface. This design is not completely successful at eliminating effects of changes in reflectiveness, although the practical effect is negligible on most pavements.

The French APL Design

The Longitudinal Profile Analyzer (APL) is a towed trailer developed by the Laboratoire Central des Ponts et Chaussees (LCPC) in France for rapid checking of road unevenness.[43] The trailer frame acts as a sprung mass supported by a wheel that follows the road surface. An inertial reference is provided by a horizontal pendulum supported on a Bendix-type bearing. The pendulum is centered by a coil spring and damped magnetically. A displacement transducer is located between the inertial pendulum and the trailing arm of the road wheel, such that its signal is proportional to profile over the frequency range of 0.5 to 20 Hz as the trailer travels along the road. A digital distance transducer on the road wheel measures the distance traveled and the towing speed.

The British Three-Laser Design

The TRRL in England has developed a unique laser profiling system.[44] The distance to the road surface is sensed at three points along the length of a trailer. As the trailer progresses forward, road elevation at the leading sensor is referenced to that at the other sensors so that a continuing profile can be developed. The design requires hardware that is much more expensive than the other designs. The positions of the three lasers must be known to a high degree of accuracy, such that thermal expansion within the trailer must be controlled. The system has never been used in North America.

Profiler Comparisons

In 1984, FHWA sponsored a full-scale experimental and analytical investigation of the abilities of profiling systems to measure various roughness indices.[45] The so-called Ann Arbor Road Profilometer Meeting involved 12 profiling systems that were used to produce raw profiles for analysis. In this study, every high-speed profiler design in use in North America at the time was represented. These included several Law 690 DNC systems, two GM-type systems with mechanical follower wheels, the PRORUT system (run in two configurations, with laser and infrared sensors), the prototype South Dakota ultrasound profiler, the Swedish Road Surface Tester laser system, and the Law 8300 ultrasound unit. Further, the French APL system participated, and static profile measures were made by rod and level. The results showed that 10 of the 12 high-speed profiling systems could generate indices comparable to those obtained from rod and level, and 9 of the 12 could generate profile plots that matched those from rod and level when identical post-processing filters were applied. The indices included IRI, waveband numerics, PSD functions, and a statistic proposed by Hudson and others at the University of Texas called RMSVA.[46]

Findings from the 1984 study regarding accuracy and repeatability appear to still be relevant. Ultimately, limits in reproducibility of the systems with optical and laser sensors were due almost exclusively to operator effects. Although the operators and drivers of profiler systems are generally experts at what they do, the requirements of a correlation research program are different from those of routine survey work, and extra measures are needed to control the testing. Errors that are negligible in survey work involving miles of road are much more significant when closely inspecting profiles of short test sites. Even with a half-day training exercise in which the operators adjusted their lateral position until the sensors were directly over the painted wheel track markers, differences in lateral position of 18 in (0.46 m) occurred on the test sites. Unless data acquisition is triggered automatically by a method such as reflective markers at the start of the test site, measures from different operators can differ by over 100 ft (30.5 m).

In the 10 years since the Ann Arbor meeting, the major new developments in profiler technology have been towards making the technology cheaper and more accessible. Two significant changes in the available hardware since 1984 are:

1. The majority of profilers now in use are based on the South Dakota design.[42]
2. The Dipstick has made high-quality static profiling a widespread option for verifying the operation of high-speed profilers.[47]

Although the South Dakota prototype participated in the 1984 study, a software error introduced errors that were significant on smooth roads. Therefore, its capabilities were not completely evaluated. The Dipstick had not been configured for road profiling in 1984, and was not included in the study.

The general accuracy associated with high-speed profilers has not changed. If anything, the widespread use of ultrasonic probes tends to imply a fleet of profilers with less resolution than the laser and optical sensors that were installed on almost all of the small fleet of existing profilers in 1984. The general use of static profiling was almost non-existent in the United States in 1984. Today, two methods are now used for verifying

profile measurements. One is the Dipstick, and the other is the use of standard rod and level according to the ASTM's "Standard Test Method for Measuring Road Roughness by Static Rod and Level Method."[48]

Since 1984, several correlation experiments have been conducted with multiple profiling systems. In 1987, FHWA sponsored a workshop on pavement smoothness in Fort Collins, Colorado, that included demonstrations of various profilers over test sites in the area.[49] The RPUG has collected similar data in 1993 and 1994, which concluded that devices with ultrasonic sensors do not produce IRI reproducibly.[24,31] Other studies have involved a single instrument, generally compared with an existing profiler or profiles measured statically by rod and level or the Dipstick. In all cases, resources were limited for thoroughly analyzing the results, and the comparisons have not been as comprehensive as in the results reported in 1984. The results of the survey reported in appendix B show that the reproducibility of IRI measurements obtained from South Dakota systems and the Dipstick are still not fully established.

The current FHWA LTPP study offers a large amount of valuable road profile data. The GPS sections are profiled annually with K.J. Law 690 DNC Profilometers. There are four LTPP regions, each with its own dedicated Profilometer. A short test program is performed annually to run the Profilometers over a set of test sections to confirm that the four systems are performing within acceptable specifications.

The LTPP program affords the States with at least two opportunities. The first is that any profiler could run over GPS sections to compare measurements from the profiler with the most recent LTPP data. A second opportunity is that States close to the annual comparison sites could run those sections and compare their results with those from all four of the LTPP Profilometers.

APPENDIX B. USER SURVEY

State highway agencies participating in this pooled-fund project were informally surveyed to:

- Determine which performance qualities relating to longitudinal pavement profiles were of greatest interest.
- Identify issues related to the collection of accurate pavement profiles.
- Identify the availability of pavement profile data for use in project analysis activities.

An information collection form to conduct the survey was prepared and approved by the FHWA Contracting Officer's Technical Representative. A copy of the form is included at the end of this appendix. It was mailed to the contact person for each participating State with a cover letter explaining that collection of the desired information would be by telephone interviews based on the form enclosed with the letter. Telephone interviews with 17 of the participants were completed.

PERFORMANCE QUALITIES

Table 7 lists the rankings of various performance qualities by the participants. The rankings show that automobile ride quality is of paramount interest. Subsequent conversations with representatives from the participating States on the phone and at annual meetings of the RPUG verified that ride quality is considered the most important pavement quality. The rankings also show that pavement performance, heavy truck ride quality, and highway safety are of interest. However, many of the participants continue to indicate that they would favor a single profile-based index for use in their pavement management systems to avoid cumbersome data handling. This argues for a general pavement index that primarily relates to ride quality.

Table 7. Importance of profile-based performance qualities.

Performance Quality	Number of States that Assigned Rank						
	1	2	3	4	5	6	7
Ride Quality (Automobile)	11	2	4				
Ride Quality (Truck)		6	5	3			
Pavement Performance	4	7	5				
Dynamic Loads		1	2	5	2		1
Highway Safety	3			4	3	1	
Vehicle Wear				1	3	4	
Cargo Damage					2	3	4

Note: Some States ranked only the top three or four objectives.

The concern with automobile ride quality goes back to the earliest measures of pavement roughness, which have mostly been designed to reflect rideability. The IRI that is already in widespread use has been experimentally linked with subjective ratings of rideability, and an RN developed by the NCHRP was designed to be a direct link to subjective ratings of rideability. The continued interest in ride quality was the motivation for the evaluation and further development of RN in this project.

Pavement performance covers a category of properties that can be classified as functional and structural. Functional performance is the level of pavement serviceability, which in practice is strongly linked with IRI roughness and rideability. Structural performance has been mainly evaluated by methods other than profile analysis. Although profile roughness can identify structural failures, particularly with flexible pavements, there is no established methodology for using monitored profile histories to predict failures. The authors hypothesize that seasonal variations in profile may highlight certain types of failure earlier than would be observed in profiles taken at the same time of year, but this remains to be demonstrated.

Recently developed methods reported by the NCHRP combine vehicle dynamic models with pavement structure models to predict pavement fatigue failures.[37] When pavements are new and smooth, the interaction between dynamic loads and pavement profile is minimal. As pavements increase in roughness, the dynamics of tire-pavement interaction of heavy vehicles can accelerate structural deterioration of pavements. Although prediction of dynamic loads was seen by the participating States as less important than rideability and pavement performance, the dynamic loads are required to predict fatigue damage with structural models. The NCHRP vehicle dynamics and structural pavement model analytical approach is presently the only available analytical method to link profile measurements with structural performance.

Many other aspects of structural performance have no established link to profile. Pavement structural defects often do not necessarily appear on the surface first. In addition, characterizing most surface defects would require several profiles along the width of the pavement with a close lateral spacing and a very fine sample interval. Using currently available equipment, it is not possible to make a complete assessment of pavement structural condition without the assistance of some other means, such as video imagery.

Truck ride quality, pavement loading, and several aspects of highway safety involve variables that can be obtained from a relatively small set of vehicle dynamics models. The prediction of cargo damage and vehicle wear requires use of vehicle dynamics models to predict vibrations and some semiempirical damage models to translate those vibrations into damage. However, these predictions were not considered by the States to be as important as other issues, and therefore the search for information to assemble vehicle and cargo damage models was not done.

Other objectives, not included in the survey, but mentioned by the participants, were:

- Influence of jointed pavement faulting on ride quality (2 States).
- Correlation with Mays meters (1 State).
- Use of roughness numerics in pavement management (1 State).

- Correlation among profilers (1 State).
- How to resolve smooth pavements in ruts (1 State).
- Relationships between various ride/roughness numerics (1 State).
- High speed crack identification by laser sensors (1 State).
- Acceptance testing of new construction using ride/roughness numeric (2 States).

With regard to construction acceptance, the 1994 NCHRP Project 1-31, "Assessment of Ride Quality Specifications for Asphalt and Portland Cement Concrete Pavements" targeted this subject, so it was not addressed in research covered by this report.

The subject of correlation with Mays meters and other response-type systems has been addressed extensively in past research and publications. (See references 2, 18, 45, and 49-52.) World Bank Technical Report 46 describes in detail the measures needed to establish valid correlations using the IRI.

PROFILE MEASUREMENT PROBLEMS

Table 8 lists the rankings of priority for various measurement problems by the participating States. Other concerns mentioned by the States are:

- The influence of coarse surface texture (3 States).
- The required accuracy and repeatability for routine data collection (3 States).
- The profiler sample interval (2 States).
- The effects of the data analysis algorithm and filter applied to the profiles (3 States).
- The profiler sensor type and number (1 State).
- The influence of wind and power lines on ultrasonic sensors (1 State).
- The influence of rough spots on ride and roughness values for a segment (1 State).

Some of the measurement problems identified by the participants have known solutions that can be communicated through cooperation with RPUG and the short course described in chapter 5. However, the problem that was identified most often was that reproducibility of profiles with different profilers has been poorer than expected. This is a serious problem: If measured profiles are invalid, then none of the analytical methods for interpreting the data are of any use.

It was apparent from conversations with representatives from the participating States and issues raised at RPUG meetings that a major concern in the profiling community was encouragement of nationwide consistency in profile measurement and the use of a pavement ride and roughness numeric computed from a measured longitudinal profile. The information collected from the States participating in this project indicates substantial inconsistencies between the reporting of IRI values to the Federal HPMS, use of profile data in the LTPP study, and use of ride and roughness numerics in State's pavement management system programs. The IRI values currently being reported to the FHWA-

Table 8. Importance of measurement problems.

Measurement Problem	Number of States that Assigned Rank			
	1	2	3	4
Equipment Type	7	1	1	
Lateral Placement	4	6	1	1
Speed Effects	2	1	2	1
Other Test Variables	4	3	5	2

HPMS data base by States are being computed by a variety of procedures. Some States measure IRI in the left wheel track, some in the right wheel track, some measure in both and report the average, and some average left and right profiles before processing, thereby obtaining the HRI. Only a few States use the IRI numeric in their pavement management system data base directly. Several States use local correlation equations to convert IRI into PSI or a historical Mays index before entering the numbers in the pavement management system data base. Several forms of technology transfer were pursued in this research to promote standardization of IRI measurement.

AGENCY PROFILING ACTIVITIES

The 17 participating States were surveyed concerning their profiling activities and their ability to supply profile measurements for the project. Their responses are summarized in table 9.

Some States have more than one profiling unit, and others collect profile data by contract. A total of 27 profilers were considered including those used by contractors to collect data. The majority of the profilers were of the South Dakota (SD) type built by the agency or by International Cybernetics Corporation (ICC). Others included K.J. Law 690, ARAN, PRORUT (agency built), K.J. Law 8300, and three units built by Pave Tech essentially using the South Dakota design but with the addition of joint fault measuring sensors.

As indicated in the table, all but two of the profilers were equipped with ultrasonic sensors. Laser sensors were used on the two exceptions. Profile measures are provided in digital form from all profilers. Digital Equipment Corporation computers were used in six profilers. The others use Intel or compatible computers. The lateral spacing between sensors was reported as 69 in (1.75 m) for 20 profilers and 59 to 64 in (1.50 to 1.63 m) for 6 profilers. All interviewed States, except one with equipment not functioning, collect profile data in at least one lane in both directions on interstate and most other multilane highways. They also collect profile data on most State-maintained roads, generally in one direction only on two-lane roads. Sixteen profilers were reported as collecting profile data in both wheel tracks and 11 in the left wheel track only. Most profilers do not collect profile wavelengths over 1,000 ft (305 m). During processing to obtain a ride or roughness numeric, 10 agencies reported filtering out wavelengths over 300 ft (91.4 m) and seven used some other filter setting. The most commonly used sample interval is approximately

Table 9. State agency profiling system and practice.

Profiler Type:	*SD (Agency)* 5	*SD (ICC)* 14	*Other* 8
Sensor Type:	*Ultrasonic* 25	*Laser* 2	*Other* 0
Computer:	*DEC* 6	*IBM /compatible* 21	*Other* 0
Number of Sensors:	*3* 18	*5* 5	*Other* 4
Wheel track Spacing:	*69 in* 20	*64 in* 4	*59 to 62 in* 3
Profile Position:	*Left* 11	*Right* 0	*Both* 16
Sample Interval:	*Approx.1.1 ft* 18	*Other* 1	*Unknown* 8
Filter During Processing:	*Over 300 ft* 10	*Other* 3	*Unknown* 4
Unfiltered Data Availability:	*Yes (1993)* 14	*Yes (Pre-1993)* 10	*No* 2

1 ft (0.305 m) but one was reported as 3 in (76.2 mm) and several were unknown. No agency reported filtering out very short wavelengths.

Profile data collected in 1993 were available from 14 States. Only 10 States have retained unfiltered data for one or more years previous to 1993. The profile equipment is not operational in one State and actual profile data is not collected in two other States. Data collected over the past 2 to 4 years are available from 10 States. The storage space is reused in other States, and the actual profile data not retained.

Calibration and verification procedures varied extensively. Most agencies have selected some special sections for periodic validation and profile readings. These sections vary in length, are used from once a week to once a year, generally are both asphalt and concrete surfaces, and in most cases repeat runs are made at more than one speed. There apparently is no standardization except for static calibration of the sensors and computers.

SURVEY FORM

SUBJECT: Interpretation of Road Roughness Profile Data
FHWA Contract DTFH61-92-C-00143
FROM: University of Michigan Transportation Research Institute

INFORMATION COLLECTION FORM

Agency:_____

Interviewer:_____ Date:_____

Objectives: The primary project objectives are to develop relationships between longitudinal pavement profiles and ride quality, pavement performance, dynamic loads, highway safety, and vehicle and cargo wear. A secondary objective is to investigate the effects of speed and other test variables on measured profiles and the profile analysis.

GENERAL INFORMATION

How do you rank primary objectives?

_____ Ride quality (automobile)
_____ Ride quality (truck)
_____ Pavement performance
_____ Dynamic loads
_____ Highway safety
_____ Vehicle wear
_____ Cargo damage
_____ Other (*list* _____)

What data can you provide to facilitate these objectives?

_____

How important are secondary objectives?

_____ Speed effects
_____ Lateral placement
_____ Equipment type
_____ Other test variables (*list* _____)
_____ Other test variables (*list* _____)

What data can you provide to facilitate these objectives?

_____

Other problems you suggest for investigation:

_____

_____

Ability to fund additional investigations:

_____

_____

AGENCY PROFILING ACTIVITIES

Profiling System

Profiler Type: SD (agency built) _____ SD (Cybernetics) _____

Law Profilometer _____

Other (specify) _____

If other:
Road sensor type: Ultrasonic _____ Laser _____ Other _____

Data acquisition system: Analog _____ Digital _____

On-board computer: DEC _____ IBM _____ Other _____

If capable of 2-track measures:
Lateral sensor spacing: Inches _____

Profiling Practice

Road systems profiled: Interstate _____ Primary-Secondary _____

Profile position: Left wheeltrack _____ Right wheeltrack _____ Both _____

Sample interval (inches): _____

Profiling speed: Maximum _____ Minimum _____

Profile filter settings: _____

Calibration procedures: _____

Test length: Maximum _____ Minimum _____

Total number of measures (original plus repeats):
Routine sections _____ Special sections _____

OTHER DATA COLLECTED/AVAILABILITY

Rut depth: _____ Surface distress: _____

Road classification: _____ Lanes: _____

Traffic volume: _____ Accident data: _____

Truck factor: _____

Pavement types: _____ Pavement design: _____

Weather: _____ Pavement temperatures: _____

Other: _____

_____

DATA AVAILABILITY

Do you retain unfiltered actual profile that can be provided on diskette? _____

Would you be able to provide unfiltered data for this study? _____

APPENDIX C. PROFILE DATA

This appendix describes the various sets of longitudinal road profile data used in the project. Seven separate sets of profile data were compiled for five specific types of studies. These data sets are summarized in table 10. Through the course of the research more than 25, and in some cases more than 1,000, analyses were applied to each data set. Altogether, over 200,000 valid profile analyses were run. The actual number of runs was much higher, because of repeats made for error detection and corrections made when programming errors were found. Automated methods were used. All profiles were converted into a standard file format originally developed for handling profiler data in a 1984 profiler correlation study conducted in Ann Arbor. Each analysis resulted in a summary index, which was automatically written into a text file in a format that was compatible with spreadsheet software.

Data for the project came from several sources: State transportation departments, regional contractors for the LTPP study, recent RPUG correlation studies, and private contractors. In all the data cover 3,900 measurements of 470 sections (see table 10).

Table 10. Summary of data sets used in this research (repeated).

Data Set	Purpose	Number of:	
		Sections	Measurements
Ohio Panel Rating Data	develop and verify a ride quality index	139	139
Minnesota Panel Rating Data	develop and verify a ride quality index	96	285
Correlation Matrix	determine relationships between summary indices	88	400
Portability Matrix	test the portability of analyses to various types of equipment	30	158
Measurement Error Matrix	identify common measurement errors	30	2,458
LTPP Study GPS Data	identify common measurement errors, test the IRI algorithm	180	1,010
State DOT Data	identify common measurement errors	27	27

PANEL RATING DATA

The development and verification of an RN required subjective panel ratings of ride over road sections with known profiles. This provided the means of testing the ability of a proposed profile-based summary index to estimate ride quality. Panel ratings of ride quality require significant time and effort to collect and, as such, this type of data is rare. Data were available from two sources, covering three experiments in which MPR were obtained for roads that were also profiled in both the left- and right-hand traveled wheel tracks. Two of the experiments were linked to NCHRP projects: a rideability study held in 1983, and a follow-up study held in 1988.[3,4] The sites were about a half mile (0.80 km) in length, and all were measured by the Ohio DOT. The third experiment was made in the fall of 1993 by the Minnesota DOT. The distributions of roughness for the two data sets are illustrated in figure 44. Both of these data sets were used to evaluate existing and proposed algorithms for estimating pavement ride quality.

Ohio DOT Data

The Ohio DOT data set is composed of 139 road sections: 52 sections from the 1983 study and 87 sections from the 1988 study. The sections were classified as asphalt concrete (51), PCC (47), or composite (41). The sections range in IRI levels from 40 to 570 in/mi (0.63 to 9.00 m/km). (See figure 44.) The MPR values for the Ohio data were determined during the NCHRP research by Janoff, as described in the NCHRP reports.[3,4] A 36-member citizen panel judged each section. The vehicles used were late model Plymouth Reliants, members of the Chrysler K-Car series. After conducting a preliminary study, involving only asphalt test sites, the researchers concluded that the vehicle type did not influence panel rating and limited all of the subjective rating vehicles to the K-Cars. Measures of longitudinal profile of each section were made with a K.J. Law Profilometer at a 1-in (25.4-mm) sample interval. The profilometer applied a 12-in (305 mm) moving-average low-pass anti-aliasing filter and recorded elevation values each 6 in (152 mm). (In the NCHRP research, a few sites were measured with a research profiler owned by Pennsylvania State University (PSU). There were some discrepancies with data from the PSU system so those sites were not included in the analyses.)

Minnesota DOT Data

In the fall of 1993, Fred Maurer of the Minnesota DOT conducted an informal ride panel study. The study included 96 quarter-mile (0.40 km) pavement sections ranging in IRI levels from 40 to 450 in/mi (0.63 to 7.10 m/km). Most of these had IRI values between 50 and 200 in/mi (0.79 to 3.16 m/km). (See figure 44.) The sections were classified as either asphalt concrete (51) or PCC (45). Each section was judged by a citizen panel of 30. A fleet of new (less than 1,000 mi) 1993 Chevrolet Lumina four-door vehicles was used in the study. The panel ratings were collected over 2 days. For each, the mean, standard deviation, high, and low panel ratings are available. The Minnesota DOT measured the left and right wheel track profiles of each section three times using a Pave Tech profiler with ultrasonic sensors. The sample interval of the Pave Tech device was about 13 in (330 mm).

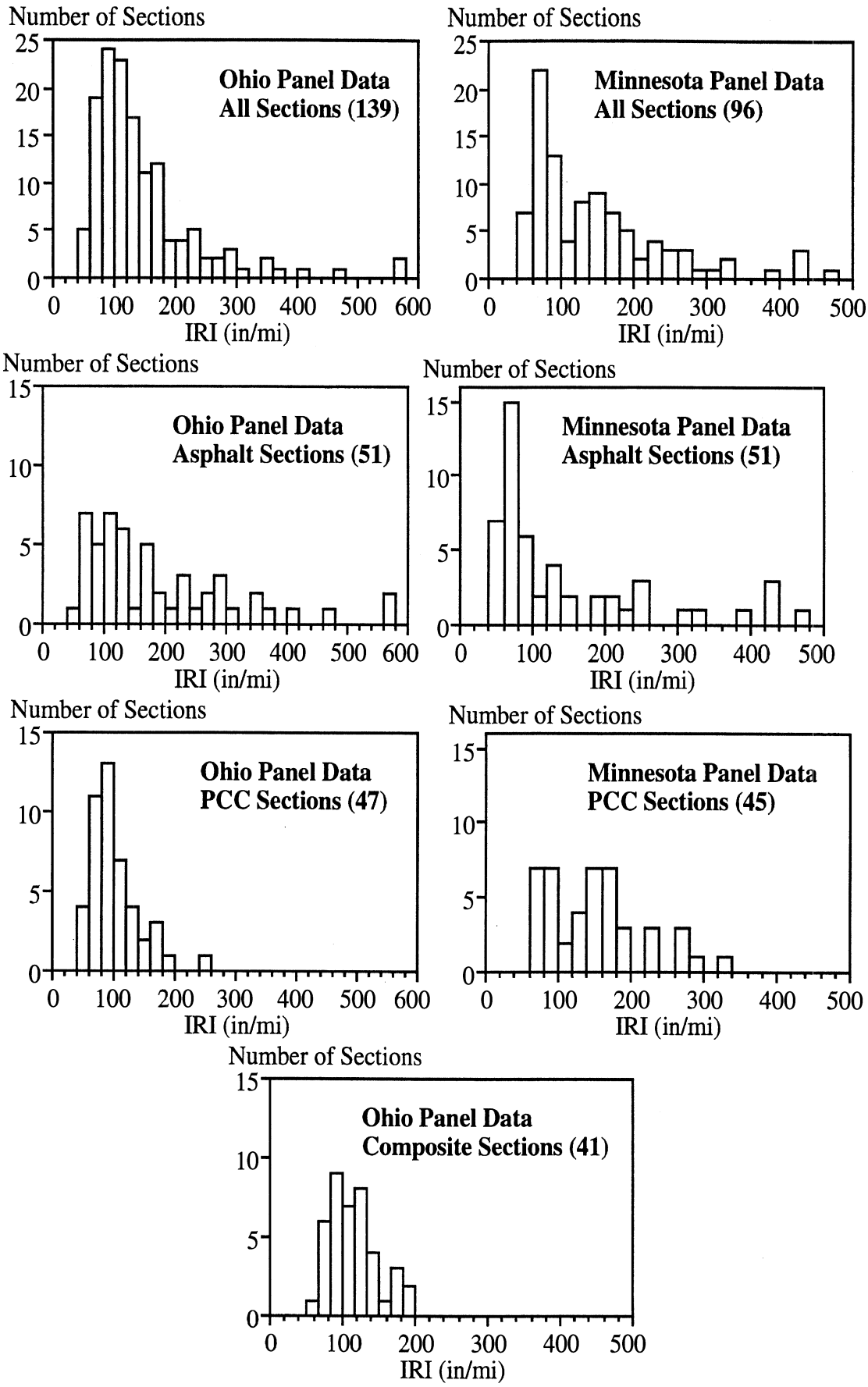

Figure 44. Distribution of roughness in the panel rating data sets.

THE CORRELATION MATRIX

A matrix of profile measurements was compiled to support studies involving statistical comparisons between alternative roughness indices. This *correlation matrix* is made up of measurements from a single profiler design that cover a broad range of roughness levels and road construction types.

The matrix is made completely of measurements by the LTPP study's regional contractors using K.J. Law Profilometers. Measurements from a single profiler design are used to remove the effect of sample interval and sensor type from the comparisons. The LTPP regional contractors were chosen because they routinely collect accurate profiles of a multitude of pavement sections of known construction type.

The matrix covers four construction types: continuous Portland cement concrete (CPCC), jointed Portland cement concrete (JPCC), asphalt overlay of PCC, and asphalt concrete with fine surface texture. Each of these construction types is common in the United States road network and has characteristics that affect their spectral signatures. Often, studies of profile-based road-roughness indices consider only two surface types: asphalt and concrete. However, in this matrix, asphalt was split into two categories: asphalt over a typical base and asphalt overlay on PCC. The distinction was made because overlay pavements often take on some of the roughness characteristics of the concrete underneath, making their roughness properties different from pure asphalt pavements. PCC pavements were split into two categories (continuous and jointed) because the presence or absence of joints is known to affect profile characteristics, even very early in the life of a PCC pavement. In addition, the two construction types exhibit different types of distress. (Faulting is of particular interest.)

The matrix covers IRI levels over the range of 40 to 300 in/mi (0.63 to 4.73 m/km). Seven roughness ranges are given in table 11. The median target roughness level for each range is shown in bold typeface. To ensure that regression statistics (e.g., coefficient, standard error, etc.) between roughness indices are valid over a broad range of roughness, each roughness level should be equally represented for each surface type. Thus, an attempt was made to fill each cell in the matrix with measurements of at least three sections, and no more than five sections.

The table shows the number of sections contained in the matrix for each category of surface type and roughness level. Sections were shuffled into the matrix according to the IRI of the left wheel track. The smooth to intermediate range of roughness, IRI of 40 to 182 in/mi (0.63 to 2.87 m/km), is completely covered. On the other hand, the roughest portion of the matrix is not completely filled, because the profiles were hard to find.

Most of the matrix is composed of measurements of LTPP GPS sections from within the States participating in the project. These sections are all 500 ft (152.4 m) long. Up to five repeat measures are included for these sections. The rest of the matrix is made up of extra measurements taken by special request by the LTPP regional contractors (North Central, North Western, Western, and Southern). In most cases, these sections are 528 ft (160.9 m) long, and only include one repeat. Tables 12 to 15 list the specific sections, their locations, and the average IRI values.

Table 11. The correlation matrix of profiles.

Surface Type	Roughness Targets and Ranges in IRI (in/mi)						
	60	**95**	**130**	**165**	**200**	**235**	**270**
	40-78	79-112	113-147	148-182	183-217	218-252	253-300
Continuous PCC	4	4	4	4	2	2	0
Jointed PCC	4	4	5	4	4	1	1
Asphalt overlay on PCC	5	5	4	4	2	4	3
Asphalt (fine texture)	5	4	4	4	1	0	0

Shaded data indicates a reduced number of sections for a cell.

Table 12. Continuous PCC sections in the correlation matrix.

Location	Source	State	Reps	IRI (in/mi)	
				Actual	Target
GPS 465020	North Central	South Dakota	5	67	60
GPS 315052	North Atlantic	Nebraska	5	66	
GPS 415021	North Central	Oregon	5	65	
GPS 185518	North Central	Indiana	5	44	
GPS 195046	North Central	Iowa	5	96	95
GPS 195042	North Central	Iowa	5	107	
GPS 175849	North Central	Illinois	5	88	
GPS 465025	North Central	South Dakota	5	79	
GPS 465040	North Central	South Dakota	5	128	130
GPS 175908	North Central	Illinois	5	121	
GPS 185043	North Central	Indiana	5	136	
GPS 165025	Western	Idaho	5	144	
GPS 184042	North Central	Indiana	5	148	165
Dauphin Co., I-81 N, MP 79.4	North Atlantic	Pennsylvania	1	180	
Cumberland Co., I-81 N, MP 64.5	North Atlantic	Pennsylvania	1	164	
Cumberland Co., I-81 S, MP 68.1	North Atlantic	Pennsylvania	1	156	
Cumberland Co., I-81 S, MP 67.6	North Atlantic	Pennsylvania	1	201	200
Dauphin Co., I-81 N, MP 79.7	North Atlantic	Pennsylvania	1	186	
Cumberland Co., I-81 S	North Atlantic	Pennsylvania	1	226	235
Dauphin Co., I-81 N	North Atlantic	Pennsylvania	1	218	

Table 13. Jointed PCC sections in the correlation matrix.

Location	Source	State	Reps	IRI (in/mi)	
				Actual	Target
GPS 174082	North Central	Illinois	5	72	60
GPS 203015	North Central	Kansas	5	65	
GPS 313033	North Central	Nebraska	5	60	
GPS 463052	Western	South Dakota	5	58	
GPS 203013	North Central	Kansas	5	104	95
GPS 313024	North Central	Nebraska	5	89	
GPS 163017	Western	Idaho	5	104	
GPS 566032	Western	Wyoming	5	89	
GPS 184021	North Central	Indiana	5	140	130
GPS 193009	North Central	Iowa	5	147	
GPS 204052	North Central	Kansas	5	124	
GPS 323010	Western	Nevada	5	137	
GPS 323013	Western	Nevada	5	126	
GPS 463012	North Central	South Dakota	5	183	165
GPS 563027	Western	Wyoming	5	181	
GPS 553010	North Central	Wisconsin	4	157	
GPS 393801	North Central	Ohio	5	155	
GPS 193006	North Central	Iowa	5	200	200
GPS 463009	North Central	South Dakota	5	186	
Linn Co., SR 13, MP 18	North Central	Iowa	1	201	
GPS 553014	North Central	Wisconsin	5	206	
GPS 553008	North Central	Wisconsin	5	245	235
Linn Co., SR 13	North Central	Iowa	1	261	270

Table 14. Asphalt overlay on PCC sections in the correlation matrix.

Location	Source	State	Reps	IRI (in/mi)	
				Actual	Target
GPS 199116	North Central	Iowa	5	62	60
GPS 207085	North Central	Kansas	5	56	
GPS 317040	North Central	Nebraska	5	57	
GPS 179327	North Central	Illinois	5	54	
GPS 175217	North Central	Illinois	5	42	
GPS 277090	North Central	Minnesota	5	95	95
GPS 317050	North Central	Nebraska	5	84	
GPS 467049	North Central	South Dakota	5	107	
GPS 177937	North Central	Illinois	5	102	
GPS 417019	Western	Oregon	5	111	
GPS 317017	North Central	Nebraska	5	114	130
GPS 276251	North Central	Minnesota	5	129	
Cumb. Co., SR944, PMS seg. 670	North Atlantic	Pennsylvania	1	127	
Linn Co., I-5, MP 239.3-239.4	North Atlantic	Oregon	1	132	
GPS 557030	North Central	Wisconsin	5	158	165
York Co., SR24, PMS segment 160	North Atlantic	Pennsylvania	1	172	
York Co, SR216, PMS segment 230	North Atlantic	Pennsylvania	1	149	
North. Co., SR147, PMS seg. 10	North Atlantic	Pennsylvania	1	182	
York Co., SR24, PMS segment 160	North Atlantic	Pennsylvania	1	193	200
York Co., SR24, PMS segment 160	North Atlantic	Pennsylvania	1	192	
GPS 393013	North Central	Ohio	5	252	235
York Co., SR24, PMS segment 160	North Atlantic	Pennsylvania	1	229	
York Co., SR24, PMS segment 320	North Atlantic	Pennsylvania	1	252	
York Co., SR214, PMS segment 20	North Atlantic	Pennsylvania	1	234	
York Co., SR24, PMS segment 320	North Atlantic	Pennsylvania	1	287	270
York Co., SR214, PMS segment 20	North Atlantic	Pennsylvania	1	267	
York Co., SR24, PMS segment 320	North Atlantic	Pennsylvania	1	303	

Table 15. Asphalt concrete (fine texture) sections in the correlation matrix.

Location	Source	State	Reps	IRI (in/mi)	
				Actual	Target
GPS 171003	North Central	Illinois	5	62	60
GPS 561007	Western	Wyoming	5	58	
GPS 321020	Western	Nevada	5	63	
GPS 321030	Western	Nevada	5	63	
GPS 322027	Western	Nevada	5	66	
GPS 271087	North Central	Minnesota	5	105	95
GPS 562017	Western	Wyoming	5	91	
GPS 191044	North Central	Iowa	5	111	
1993 RPUG Section Miss. 01	Southern	Mississippi	1	80	
GPS 181037	North Central	Indiana	5	125	130
GPS 271016	North Central	Minnesota	5	125	
GPS 271023	North Central	Minnesota	5	125	
GPS 271028	North Central	Minnesota	5	128	
GPS 182008	North Central	Indiana	5	171	165
GPS 271085	North Central	Minnesota	5	170	
GPS 271018	North Central	Minnesota	5	152	
1993 RPUG Section Penn. 01	North Central, Ohio DOT	Pennsylvania	2	166	
GPS 201005	North Central	Kansas	5	190	200

THE PORTABILITY MATRIX

The *portability matrix* was compiled for studies assessing the validity of profile-analysis algorithms for profiles measured by a variety of equipment. The matrix provides multiple measurements of a few pavement sections by multiple devices. This way, an algorithm's sensitivity to sample interval, sensor type, and profile measurement errors characteristic of specific devices could be investigated.

The portability matrix is a subset of the measurements made for the 1993 RPUG correlation study. Each section was measured by several profiling devices that normally operate in its region, such as devices owned by State DOTs, LTPP regional contractors, manufacturers, and other private operators. Each profiler took up to 10 measurements of each correlation section. In many cases, several profilers of the same type measured the same section. Overall, more than 2,000 measurements were made. All of the RPUG profiles were supplied by the contractor who conducted the correlation and analyses for the RPUG.[24] Thirty calibration sections were measured in the study in four regions around the United States. These sections are described in table 16.

For each of the sections listed in the table, one measurement was chosen for the matrix by as many different profiler designs as were available. If more than one profiler of a given design measured a section, a measurement was chosen from a device that was at least as reliable as the rest of its kind. Of the 10 repeat measurements from each device, a single measurement was chosen that had an IRI value near that of the other repeats. Thus, measurements that were known to contain large anomalies were excluded. Table 17 shows the coverage of profiler designs in the matrix.

In addition to investigating portability to specific profiler designs, this matrix was used to experimentally assess the effects of sample interval and sensor type on various analysis methods. Table 18 lists the devices included in the matrix, with the sensor type and sample interval of each. Inspection of tables 17 and 18 reveals that all 30 sections in the matrix were measured by at least one system with optical, laser, and ultrasonic height sensors. Twenty-four of the sections were also measured by the Dipstick. In addition, the effects of sample interval can be investigated. However, each sensor type usually implies a certain range of sample interval. Only the K.J. Law Profilometers have optical sensors, and they all record at 6-in (152 mm) intervals. Most laser devices record at a sample interval of less than 6 in (152 mm). All of the ultrasonic devices have a sample interval of about 12 in (305 mm).

Table 16. Sections measured in the 1993 RPUG study.

Region	Section Number	Surface Type	Finish	IRI Left Wheel Path (in/mi)
Mississippi	1	Asphalt Concrete	Smooth	80
	2	Composite	Smooth	57
	3	Composite	Rough	161
	4	Asphalt Concrete	Rough	217
	5	Portland Cement Concrete	Smooth	187
	6	Portland Cement Concrete	Smooth	81
	7	Portland Cement Concrete	Smooth	172
	8	Portland Cement Concrete	Rough	107
Nevada	1	Asphalt Concrete	Medium	177
	2	Asphalt Concrete	Smooth	51
	3	Asphalt Concrete	(old chip seal)	225
	4	Portland Cement Concrete	Smooth	113
	5	Portland Cement Concrete	Smooth	107
	6	Portland Cement Concrete	Smooth	70
Pennsylvania	1	Asphalt Concrete	Smooth	166
	2	Asphalt Concrete	Smooth	67
	3	Asphalt Concrete	Rough	135
	4	Asphalt Concrete	Rough	150
	5	Portland Cement Concrete	Smooth	176
	6	Portland Cement Concrete	Smooth	205
	7	Portland Cement Concrete	Smooth	120
	8	Portland Cement Concrete		89
South Dakota	1	Asphalt Concrete	Rough	247
	2	Asphalt Concrete	Medium	83
	3	Asphalt Concrete	Medium	90
	4	Asphalt Concrete	Smooth	69
	5	Portland Cement Concrete	Medium	97
	6	Portland Cement Concrete	Medium	87
	7	Portland Cement Concrete	Rough	110
	8	Portland Cement Concrete	Smooth	93

Table 17. Coverage of profiler designs in the portability matrix.

Region	Sections Measured by each Profiler Design							
	K.J. Law	Dipstick	ICC (U)	Pave Tech	SDType	ICC (L)	ARAN	PRORUT
Mississippi	1-8	1-8	1-8	1-8		1-6, 8		
Nevada	1-6		1-6			1-6		
Pennsylvania	1-8	1-8	1-8			1-8	1-8	1-8
South Dakota	1-8	1-8	1-8	1-8	1-8		1-7	

Table 18. Specific devices selected for the portability matrix.

Region	Inst. Number	Make	Model	Sensor Type	Sample Interval (ft)	Sections Measured
M	DS	Dipstick		I	1.000	1-8
	01	ICC	MDR 4090	U	1.072	1-8
	03	ICC	MDR 4087 L	L	0.542	1-6, 8
	05	Pave Tech		U	0.864	1-8
	06	K.J. Law	6900 DNC	O	0.500	1-8
N	06	ICC		U	0.992	1-6
	07	ICC	MDR 4090 L	L	0.524	1-6
	09	K.J. Law	6900 DNC	O	0.500	1-6
P	DS	Dipstick		I	1.000	1-8
	01	PRORUT		L	0.164	1-8
	04	ARAN	4900 LaserSDP	L	0.330	1-8
	05	K.J. Law	690 DNC	O	0.500	1-8
	08	ICC	MDR 4087 L	L	0.542	1-8
	76	ICC	MDR 4195	U	1.117	1-8
S	DS	Dipstick		I	1.000	1-8
	01	ICC		U	1.060	1-8
	02	South Dakota		U	1.000	1-8
	03	Pave Tech		U	1.085	1-8
	08	K.J. Law	6900 DNC	O	0.500	1-8
	10	ARAN	4300 LaserSDP	L	0.668	1-7

M - Mississippi N - Nevada P - Pennsylvania S - South Dakota
I - Inclinometer O - Optical U - Ultrasonic L - Laser

MEASUREMENT ERROR MATRIX

The entire data set from the 1993 RPUG calibration study was used to detect, study, and demonstrate common profile measurement errors. This data set is called the measurement error matrix. Unlike the portability matrix, described above, all of the measurements from all of the profilers that participated in the calibration study were analyzed (a total of 2,458 measurements). The complete set of data from the study was supplied by the contractors who performed the data analysis for the RPUG.[24] Tables 16 and 19 describe the sections and profilers included. The presence of multiple measurements of each section by each device allowed more effective use of plotting to pick out measurement errors and assess the relative repeatability of each profiler. Measures from the Pennsylvania region were used the most, because the data set included the largest number of different profiler designs. In addition, the PRORUT measured the Pennsylvania sections at a very close sample interval of about 2 in (50 mm). The Pennsylvania data could not be used exclusively, however, because it did not include a Pave Tech device, or an agency-built South Dakota type profilometer. Either a Dipstick measurement or a measurement by a K.J. Law Profilometer was used as a reference in most analyses.

Table 19. Devices participating in the 1993 RPUG calibration study.[24]

Region	Inst. Number	Make	Model	Sensor Type	Sample Interval (ft)	Sections Measured
M	DS	Dipstick		I	1.000	1-8
	01	ICC	MDR 4090	U	1.072	1-8
	02	ICC	MDR 4087	U	1.088	1-8
	03	ICC	MDR 4087 L	L	0.542	1-6, 8
	05	Pave Tech		U	0.864	1-8
	06	K.J. Law	6900 DNC	O	0.500	1-8
N	03	ICC	MDR 4090	U	1.068	1-6
	04	ICC	MDR 4097	U	1.077	1-6
	06	ICC		U	0.992	1-6
	07	ICC	MDR 4090 L	L	0.524	1-6
	08	K.J. Law	690 DNC	O	0.500	1-6
	09	K.J. Law	6900 DNC	O	0.500	1-6
P	DS	Dipstick		I	1.000	1-8
	01	PRORUT		L	0.164	1-8
	02	ICC	MDR 4090	U	1.092	1-8
	03	ICC		U	1.085	1-8
	04	ARAN	4900 LaserSDP	L	0.330	1-8
	05	K.J. Law	690 DNC	O	0.500	1-8
	06	ICC	MDR 4097	U	1.048	1-4, 6-8
	07	K.J. Law	6900 DNC	O	0.500	1-8
	08	ICC	MDR 4087 L	L	0.542	1-8
	73	ICC	MDR 4195	U	1.123	1-8
	74	ICC	MDR 4195	U	1.121	1-8
	75	ICC	MDR 4195	U	1.124	1-8
	76	ICC	MDR 4195	U	1.117	1-8
S	DS	Dipstick		I	1.000	1-8
	01	ICC		U	1.060	1-8
	02	South Dakota		U	1.000	1-8
	03	Pave Tech		U	1.085	1-8
	04	South Dakota		U	1.000	1-8
	05	K.J. Law		O	0.500	1-8
	06	South Dakota		U	1.000	1-8
	08	K.J. Law	6900 DNC	O	0.500	1-8
	09	Cal High Speed		U	1.037	1-8
	10	ARAN	4300 LaserSDP	L	0.668	1-7
	11	Pave Tech		U	1.100	1-8
	12	South Dakota		U	1.000	1-8

M - Mississippi N - Nevada P - Pennsylvania S - South Dakota
I - Inclinometer O - Optical U - Ultrasonic L - Laser

OTHER DATA

In an effort to collect enough profile data for the correlation matrix (described earlier) a large number of profiles of GPS sections was obtained from the LTPP study. Not all of these sections were used in the matrix, but they were sometimes used during the project. For example, each profile was supplied with the IRI reported to the LTPP data base by the regional contractors. These data were used to deduce the exact nature of the algorithm in use for calculating IRI by the LTPP program.

LTPP Study Sections

Profiles obtained for the on-going LTPP study provide a data base of profiles measured under conditions that are generally well controlled. Table 20 lists the nine types of pavements used in the GPS. Table 21 shows the distribution of the GPS sites in the North Central LTPP region that are located within States participating in this study. The only pavement types that are not readily available are the asphalt concrete over bound base and unbonded PCC overlay sections. The distribution of the current IRI levels was assembled from data provided by LTPP regional contractors and is shown in table 22. Generally, the predominant roughness levels are in the smooth and medium rough categories.

State DOT Data

In addition to the LTPP study data obtained for the project, several of the participating States supplied profiles, measured with their own equipment, of GPS sections and non-GPS sections in their State. These measurements were also used in specialized studies throughout the project. For example, the measurements of GPS sections by those States that have not participated in recent RPUG correlation studies provided alternate means of assessing their measurement practice. Some of the data was also supplied with additional information, such as distress measurements, truck traffic estimates, texture estimates, etc. Table 23 summarizes the data supplied by the States and the LTPP Regional Contractors. All of the measurements listed in the table are of known location and surface type.

Table 20. Types of LTPP GPS pavement types.

Key	Description
GPS 1	Asphalt Concrete (AC) on a Granular Base
GPS 2	Asphalt Concrete on Bound Base
GPS 3	Jointed Plain Concrete (JPC)
GPS 4	Jointed Reinforced Concrete (JRC)
GPS 5	Continuously Reinforced Concrete (CRC)
GPS 6	AC Overlay on AC
GPS 7	AC Overlay on JPC/JRC
GPS 9	Unbonded PCC Overlay on JPC or JRC

Table 21. Distribution of GPS test sections of participating States.

State	GPS Surface Type								Total
	1	2	3	4	5	6	7	9	
Illinois	2			2	6	1	7		18
Indiana	2	2	4	1	3	1	3	1	17
Iowa	1	1	5		2	1	2		12
Kansas	3		3	6		2	2	1	17
Louisiana		1		1					2
Minnesota	9		2	8	1	1	1	2	24
Mississippi	3	6	2	1	4	5	3	1	25
Nebraska	1		6	1	1	1	5		15
Ohio			1	2	1		3	3	10
Pennsylvania	3		1	2	2	2	7	2	19
Tennessee	3	6				6			15
South Dakota	1		7		3	2	1		14
Total	28	16	31	24	23	22	34	10	188

Table 22. IRI ranges for different GPS experiments.

Pavement Type	Total Sections	Roughness Range (in/mi)				
		0-50	50-100	100-150	150-200	>200
GPS 1	28	1	12	11	4	—
GPS 2	16	1	12	2	1	—
GPS 3	31	—	15	13	3	—
GPS 4	24	—	9	14	1	—
GPS 5	23	—	12	9	2	—
GPS 6	22	3	14	5	—	—
GPS 7	34	—	22	9	2	1
GPS 9	10	—	3	6	1	—
Total	188	5	99	69	14	1

Table 23. Data supplied by LTPP Regional Contractors and State DOTs.

Agency	Number of Sections	Number of Repeats	Length (mi)	GPS	Alternate Information
North Central	163	5	1/10	yes	IRI reported by LTPP, RMSVA, slope variance, Mays output
	3	1	1-2	no	surface texture
North Atlantic	15	1	1/4 - 3/4	no	surface texture, IRI, RMSVA, slope variance, Mays output
Western	17	5-10	1/10	yes	IRI reported by LTPP, RMSVA, slope variance, Mays output
	5	1	1/2 - 2	no	
Southern	14	1	1 - 10	no	IRI
Idaho	5	5	1/10	yes	rut depth, skid number, cracking index, traffic estimates of some sections
	3	1	2 - 4	no	
Iowa	5	1	1/10	yes	detailed surface texture estimates, skid number
	5	1	1/4	no	IRI, detailed surface texture estimates, structural and distress ratings, rutting and faulting, skid number, traffic estimates
Kansas	5	1	1/10	yes	
	8	1	~1	no	IRI, distress estimates, traffic estimates, Mays meter output
Minnesota	6	1	1/10	yes	
Nebraska	4	1	1/10	yes	height sensor measurements
	7	1	1 - 4	no	IRI, Serviceability Index, accident data, height sensor measurements, traffic estimates, cracking, rutting, faulting
Oregon	3	1	1/10	yes	micro and macrotexture, grooving
Wyoming	4	1	1/5	no	traffic estimates, skid number, distress, rut depth

APPENDIX D. REVIEW OF OLD RIDE NUMBER ALGORITHMS

This appendix provides a review of two algorithms for calculating RN that existed before this project. Both algorithms were developed to estimate panel rating from measured profile. The first, proposed by Dr. Michael Janoff in two NCHRP reports, uses PSD functions to predict panel rating.[3,4] The method is complex, and a ready-to-run algorithm was not provided. The second, developed by Spangler and Kelly, is more fully explained and is intended for use with profiles measured with K.J. Law Profilometers.[15] Technical limitations found during the study led to the development of a third algorithm. The study is described in appendixes H and I. The recommended algorithm is described in appendixes E and F.

NCHRP (JANOFF) STUDIES

The NCHRP sponsored two projects in the 1980s that investigated the effects of road surface roughness on ride comfort.[3,4] The primary goal of these projects was to develop and refine a transform that converts objective measures of pavement roughness to subjective measures of the public's perception of ride comfort. Estimates of ride comfort were called Rideability Number or Ride Number (RN), and were calculated from a PI.

Because several versions of RN and PI are described in this appendix, a convention is used where the name RN implies the generic RN concept (a roughness index ranging from 0 to 5, based on profile analysis). More specific indices are indicated with subscripts. For example, RN_{275} is the index defined in NCHRP Report 275. A similar convention is adopted for PI. PI is taken to mean a profile-based index involving mainly short wavelengths. A specific instance is identified with a subscript (e.g., PI_{275}).

Janoff and others employed statistical techniques to find the spatial frequency bands of measured longitudinal pavement profile roughness that correlate to subjective panel ratings of ride quality. Subjective panel ratings were collected using a modified version of the Weaver/AASHO scale associated with PSR and PSI, covering a range of 0 (impassable) to 5 (perfect).[53] The experimental design included studies of the effects of rating panel regionality, rating panel training, vehicle size, vehicle speed, and road surface type. The results of the study showed that the content of the road profile in the frequency band from 0.125 to 0.630 cycles/ft (0.410 to 2.07 cycles/m), or 10 to 50 Hz at 55 mi/h (24.6 m/sec), correlated the most highly with the mean value of subjective panel ratings.

These findings yielded a predictive transformation for the MPR expected for a given road site. The recommended estimate of MPR is rideability number, determined as a function of a PI:

$$RN_{275} = -1.74 - 3.03 \log(PI_{275}) \quad (8)$$

where PI_{275} (profile index from NCHRP Report 275) is computed from two profiles (left and right) with an algorithm that will be described later and which must have units of inches.

RN, like the Weaver/AASHO scale, was intended to range from 0 to 5. Note that PSI, which also ranges from 0 to 5, is based on a similar concept, but represents pavement structural defects as well as user comfort.[39] RN, on the other hand, is strictly meant to estimate ride comfort.

The second NCHRP project (Report 308) included pavement sections from five States in various regions of the country (Ohio, Michigan, New Jersey, New Mexico, and Louisiana). This study further addressed the effects of regionality, road surface type, and vehicle size, as well as road class and roughness level on the results obtained in the first study. It was determined that the results were relatively independent of surface type, road class, roughness level, and vehicle size. The correlation equations between PI and MPR for the individual States were only slightly different. The relevant band of frequencies was the same as in the earlier study.

Based on the results of the second study, Janoff proposed a new logarithmic transformation from PI_{275} (in inches) to RN:

$$RN_{308L} = -1.47 - 2.85 \log(PI_{275}) \quad (9)$$

This transformation applies to RN values in the range of 0.4 to 4.5.

Eqs. 8 and 9 can yield RN values less than 0 or greater than 5 if used to extrapolate beyond the typical range of PI values. Between the two NCHRP studies, Weed suggested an alternative form for the transformation:[54]

$$RN_W = 5\, e^{-a\,(PI)^b} \quad (10)$$

This transformation provides a relationship that satisfies the constraint that RN equals 5 for a PI of 0 (no roughness), and approaches 0 as PI becomes very large. In response, Janoff provided the exponential relationship between PI and RN:

$$RN_{308E} = 5\, e^{-11.72\,(PI_{275})^{0.89}} \quad (11)$$

Figure 45 shows that both eqs. 9 and 11 accurately fit the data from NCHRP Report 308 in the range of RN from 0.4 to 4.5 which represents nearly all roads and includes all roads of practical interest. (No road with an RN above 4.5 is considered to need repair, and all roads with an RN below 0.4 are likely to need repair.)

Although eq. 11 is more reasonable than eq. 10 for very smooth and very rough surfaces, it has not been compared with panel ratings at the extremes. Vibrations from within the vehicle (engine noise, tire imbalance, etc.) may cause panel rating for a perfectly smooth road to be lower than 5. A user may consider a road with a small (but greater than 0) level of roughness to be perfect. Thus, neither transform resolves the issue of predicting RN at extreme values.

Profile Measurements

In the original NCHRP study, two instruments were used to measure road profiles: a K.J. Law Inertial Profilometer, owned by the Ohio DOT, and a laser device owned by PSU. (The PSU system was manufactured by K.J. Law, but had been modified

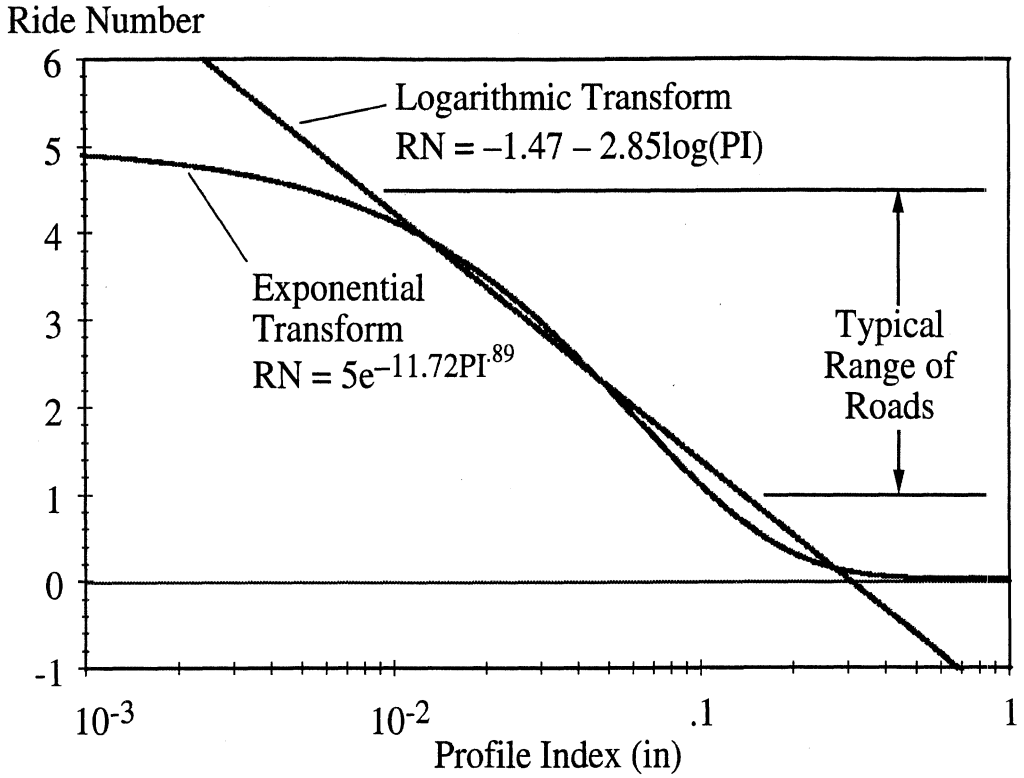

Figure 45. Transforms from PI to RN proposed in NCHRP Report 308.

extensively by the time the study was done. The profile calculation software was from PSU, not K.J. Law.)

The Law system measured at 1-in (25.4-mm) distance intervals, applied a 12-in (305-mm) moving-average low-pass anti-aliasing filter and recorded elevation values each 6 in (152 mm). The influence of the 12-in (305-mm) moving average is plotted as a function of wave number in figure 46. The plot shows:

- The filter has essentially no effect for wave numbers less than 0.1 cycles/ft (0.33 cycles/m), or wavelengths longer than 10 ft (3.05 m).
- Wavelengths of 2.23 ft (0.68 m), corresponding to a wave number of 0.45 cycles/ft (1.47 cycles/m), are attenuated by 30 percent.
- Wavelengths of 1.66 ft (0.51 m), corresponding to a wave number of 0.60 cycles/ft (1.98 cycles/m), are attenuated by 50 percent.
- Wavelengths of 1.0 ft (0.305 m) are completely eliminated.
- Wavelengths shorter than 1.0 ft (0.305 m) are attenuated but not eliminated.

PSD functions for profiles measured with Law systems also demonstrate the effects of this filtering. Figure 47 compares PSD plots for measures of a profile made using the PRORUT, a Law system, and a Dipstick. The figure illustrates the low-pass filtering in the Law measurement for high wave numbers (above 0.3 cycles/ft).

This filtering has a small but beneficial influence on analyses such as the IRI, where most of the roughness is coming from wave numbers less than 0.1 cycles/ft (0.33 cycles/m). However, for analyses that emphasize higher wave numbers, potentially

useful information is being filtered out. Computed results from the filtered profiles are expected to be systematically lower than those obtained from the unfiltered profile, sampled with the same interval.

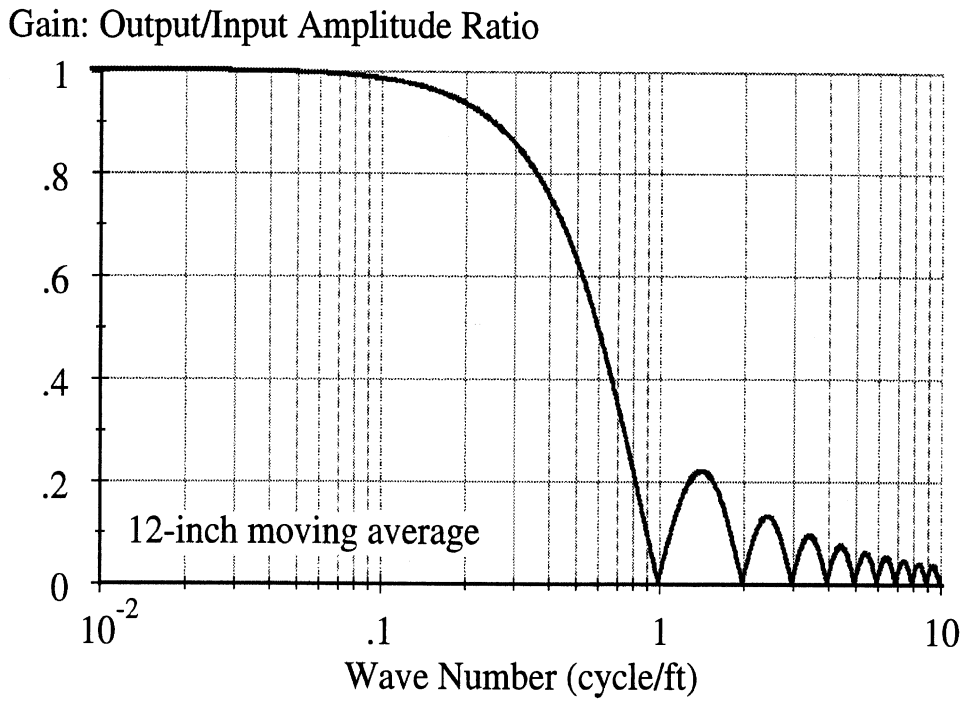

Figure 46. Filtering of a 12-in moving average.

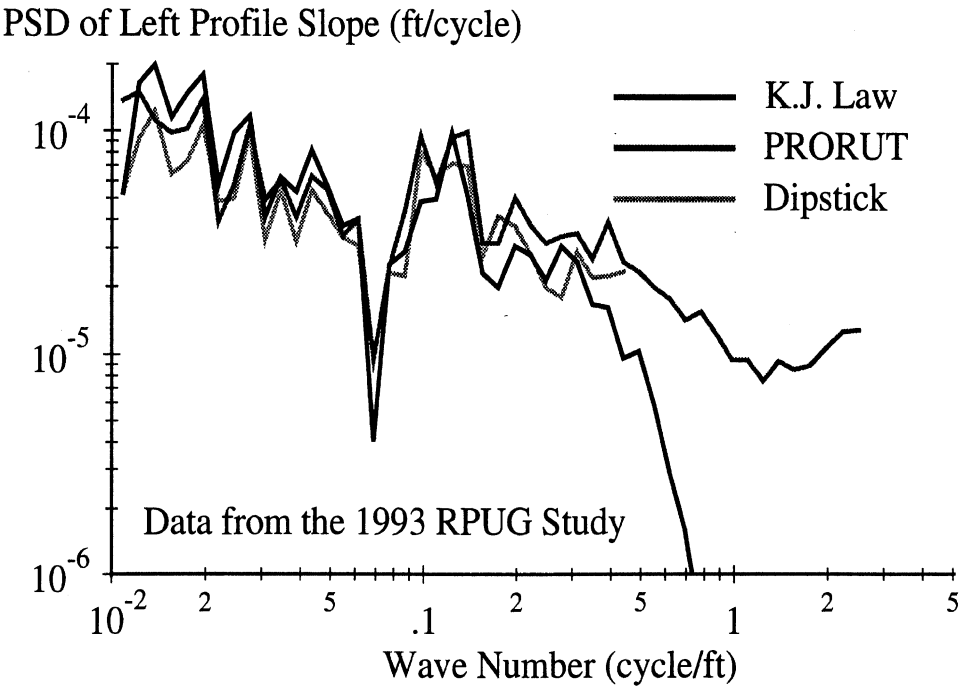

Figure 47. PSD plots from the multiple devices.

Algorithm for Calculating Profile Index

In the NCHRP studies, researchers used an FFT to calculate PI. Different methods were used for the profiles, depending on whether they were measured with the Ohio DOT (Law) system or the PSU profiler.

The profiles from the Ohio DOT (K.J. Law) system were preprocessed by subtracting the average value from the signal and windowing with a raised cosine Hamming window. The PI was then found using the following procedure. For each wheel track, (1) Fourier-transformed the profile records and squared all of the Fourier coefficients; (2) split the available bandwidth into one-third octave bands and summed the squares within each band; and (3) summed the one-third octave mean squares over the range of 0.125 to 0.630 cycles/ft (0.410 to 2.07 cycles/m). PI is the square-root of the sum of the squares of the two individual profiles.(55)

$$PI_{275} = \sqrt{PI_{275L}^2 + PI_{275R}^2} \tag{12}$$

This method does not account for the possibility that only one profile might be available. In general, the roughness properties are similar for the profiles of the left- and right-hand wheel tracks. If they have equal roughness, then the individual wheel track PI values will be about 29 percent ($100[1 - 2^{-1/2}]$) lower than the combined PI_{275} value.

The PSU profiler measured and recorded at 1-in (25.4-mm) intervals. Fourth-order low-pass Butterworth filters (with their 3dB frequency set at one-fourth the sampling frequency) were applied to the analog signals. After digitizing, the measurements were preprocessed by subtracting the average values from the accelerometer and height sensor samples. The Fourier coefficients were calculated for the accelerometer and height signals separately, then combined to yield the Fourier coefficients for profile. This result was then used to estimate the mean-squared profile heights in each one-third octave band. The mean squared components were convoluted with the transfer function of the Hamming window before calculating PI.

The two computational methods are theoretically equivalent. The PSU processing applied the same transforms but in a different order. Assuming the report accurately described the processing, then differences in the PI values from the two systems are due solely to (1) measuring error in the transducers used in the profilers; (2) differences in the ways the raw signals were filtered; and (3) the 12-in (305-mm) moving-average filter applied to the Ohio profiles after they were calculated but before they were recorded.

In the first study (NCHRP Report 275), 52 of the sections were measured by the Ohio DOT device and 12 by the PSU device. Data from 11 sections measured by both instruments were compared. The PI values for the PSU device were systematically high compared to the Ohio DOT data. In the report, the author guessed that the lack of agreement is due to filtering performed by the Law device at the time of data collection.[1] To account for this, measures of PI from the two devices were correlated:

---

[1] In NCHRP Report 275, Janoff states: "It is suspected, but not proven, the filters in the ODOT profilometer reduce the actual measured PI, thus providing uniformly lower readings than the PSU profilometer but almost perfect correlation between the two instruments in the frequency band of interest."

$$E[PI_{Ohio}] = 0.84\ PI_{PSU} \quad (13)$$

where E[x] means expected value of variable x. This equation was then used to adjust the PI values computed from PSU data.

The second study included data from three systems: (1) the sections from the Ohio DOT Profilometer used in the first NCHRP study; (2) a Minnesota Profilometer (also K.J. Law), used in Michigan; and (3) the PSU Profilometer, used in New Mexico, New Jersey, and Louisiana. The PSU data were again correlated with the Ohio DOT Profilometer using 12 sections in Ohio and adjusted using the following regression equation:

$$E[PI_{Ohio}] = 0.817\ PI_{PSU} \quad (14)$$

Although the measures are highly correlated, at best, only one of the measures can be correct. Regression slope coefficients between true profiling systems should be very near to unity. The 18-percent difference casts doubt on the reproducibility of PI: given a perfect profile, should PI computed from an FFT be used directly or multiplied by 0.817?

Figure 48 compares three weightings for PI_{275}. The published weighting is unity for wave numbers covering the third-octave bands in the range of 0.125 to 0.630 cycles/ft (0.410 to 2.07 cycles/m), and zero elsewhere. The PSU weighting is multiplied by 0.817, according to eq. 14. The Ohio (Law) weighting is multiplied by the wave number response function of the 12-in (305-mm) moving average that was applied to all measures from that device.

The figure might seem to offer an explanation for the discrepancy between the Ohio and PSU data. However, for typical profiles the bias because of the filtering in the Law system accounts for only about a 5-percent difference in the PI. This is not enough to fully explain the 18-percent difference observed in the NCHRP study.

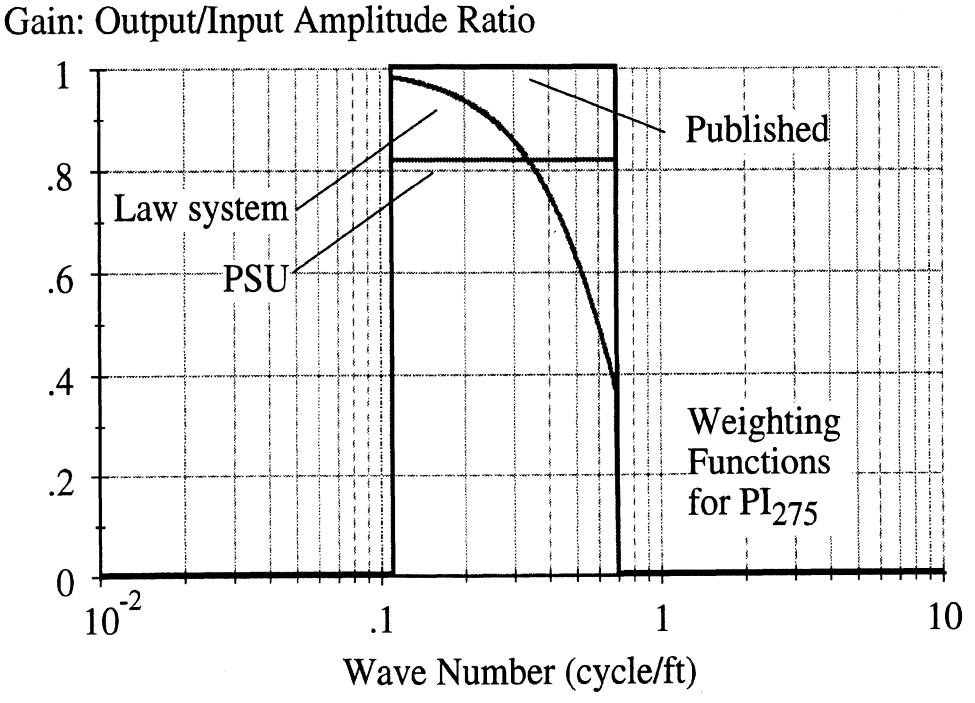

Figure 48. Total weighting functions used in the NCHRP studies.

SURFACE DYNAMICS (SPANGLER/KELLY) STUDY

At about the same time as the NCHRP projects, Surface Dynamics, Inc., performed a research project for the Ohio DOT that included developing a ride quality transform.[15] This project used methods very similar to those in the NCHRP projects and also yielded a transform from PI to MPR:

$$MPR_{SD} = 4.54 - 20.56(PI_{SD}) \tag{15}$$

This transform was refined in a subsequent study intended to evaluate the time stability of the subjective panel ratings.[16] As in the NCHRP work, this preferred transform took an exponential form to ensure that extreme cases took on reasonable values. The transform was revised to:

$$RN_{SD} = \frac{5e^{-20PIL_{SD}} + 5e^{-20PIR_{SD}}}{2} \tag{16}$$

where PIL_{SD} and PIR_{SD} are PI (as defined by Surface Dynamics) for the left and right wheel track measurement, respectively.

Algorithm for Calculating Profile Index

Theoretical Filter

In the Ohio DOT studies, PI is calculated as the RMS value of a filtered profile. The desired transfer function of the filter used in the studies (a second-order high-pass Butterworth) is:

$$H(s) = \frac{F(s)}{P(s)} = \frac{s^2}{s^2 + 2\xi\omega_n s + \omega_n^2} \tag{17}$$

where s is the Laplace operator, F(s) is the filtered profile, P(s) is the original profile, ξ (dimensionless damping ratio) has a value of 0.707, and ω_n (natural frequency) has a value of $2\pi/B$, where B is a base length.

This filter attenuates long wavelengths, and leaves short wavelengths, as shown by the plot in figure 49. (The function is plotted by replacing s with $j2\pi\nu$, where ν is wave number.) The first Ohio DOT study included an investigation of the effects of the spatial natural frequency ($\omega_n = 2\pi/B$) on the correlation between MPR and PI. The investigation found that the best correlation was obtained using a base length of 10 ft (3.05 m). The results were only slightly different for 8 and 12 ft (2.44 and 3.66 m). The second study recommended the use of 8 ft (2.44 m).

The results of both Ohio DOT studies are summarized in an ASTM STP paper.[56] The paper suggests the use of the high-pass filter for calculating PI, but relies on the 12-in (305-mm) moving average built into Law systems for the high wave number cutoff. The methodology presented by the paper also requires a system with a sample spacing of 6 in (152 mm). Application of the Ohio DOT algorithm to profiles from other sources was not studied.

The full theoretical filtering applied to the profile for the calculation of PI is the product of the low-pass moving average shown in figure 46 and the high-pass filter described by

eq. 17. Figure 49 shows a plot of the function in eq. 17, together with the full effect obtained by combining the two. The figure shows that short wavelengths (high wave numbers) are filtered out if the 12-in (305-mm) moving average is applied, as in the case of the Law systems. However, if the moving average is not applied, the short wavelengths do contribute to the computed PI.

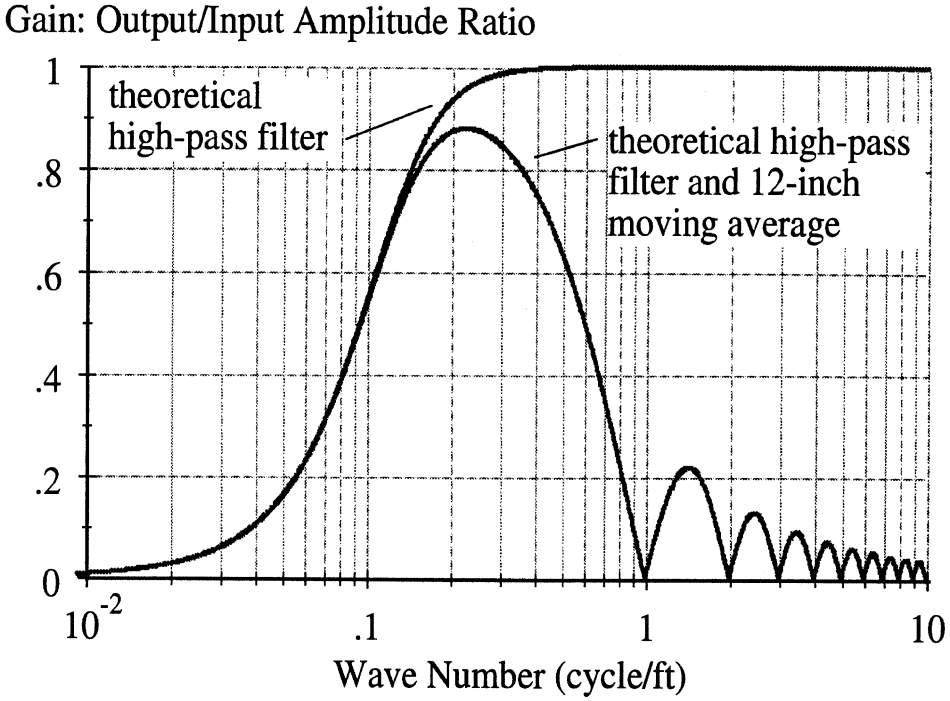

Figure 49. Theoretical wave number response of Spangler/Kelly PI with and without 12-in moving average.

The curves in figure 49 do not properly indicate the significance of the different wave numbers. Real roads generally have about 10 times more roughness at 0.1 cycles/ft (0.33 cycles/m) than they do at 1 cycle/ft (3.3 cycles/m). Thus, large differences in the responses of the algorithms at high wave numbers can mean less than small differences at low wave numbers.

Although road elevation variance decreases rapidly with increasing wave number, the variance of profile slope is approximately uniform over wave number. Figure 50 was prepared to show approximately the significance of the moving average when taking into account the distribution of profile variance over wave number. The gains of the filters were re-computed to show response to profile slope. Also, the plot axes are linear with amplitude and wave number. Thus, the area separating the two curves corresponds roughly to the difference between PI^2 as defined with the theoretical transfer function of eq. 17 for systems with and without the moving average. Figure 51 shows the same curves, plotted on a log scale for wave number.

The differences in the curves shown in figures 50 and 51 indicate the error that would be introduced if the theoretical Butterworth filter were used on a perfectly measured profile

that had not been smoothed with the 12-in (305-mm) moving average. As a minimum, the algorithm should include the 12-in (305-mm) moving average as a part of the definition, which would be omitted if the profile were preprocessed as is done with Law systems. (The ASTM paper does state that the profile must be preprocessed with the moving average filter. However, the significance of this step is not discussed.)

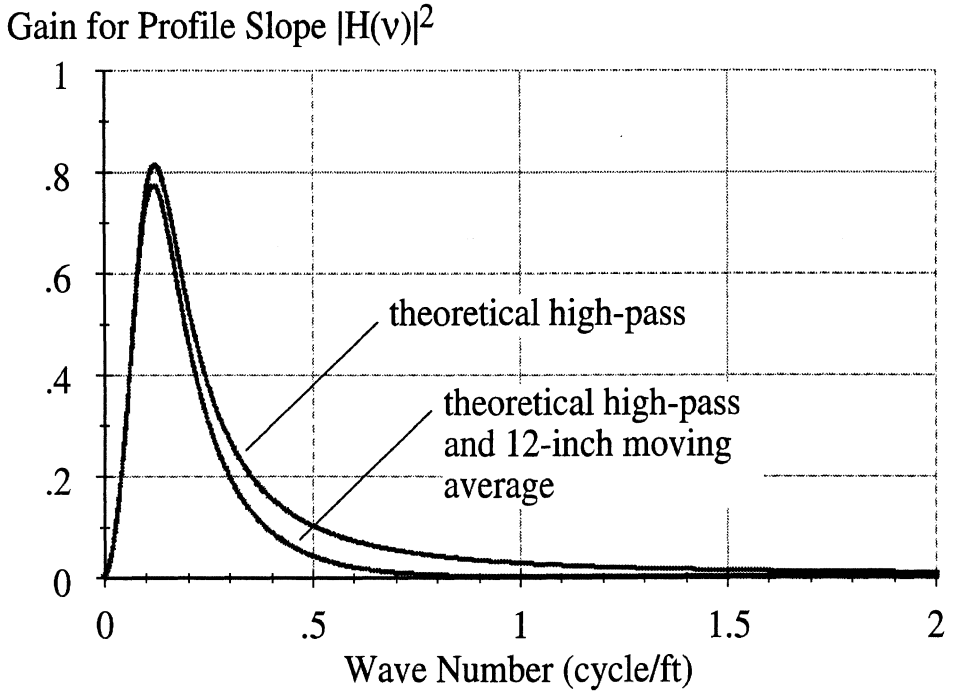

Figure 50. Theoretical Spangler/Kelly PI filters (linear plot axes).

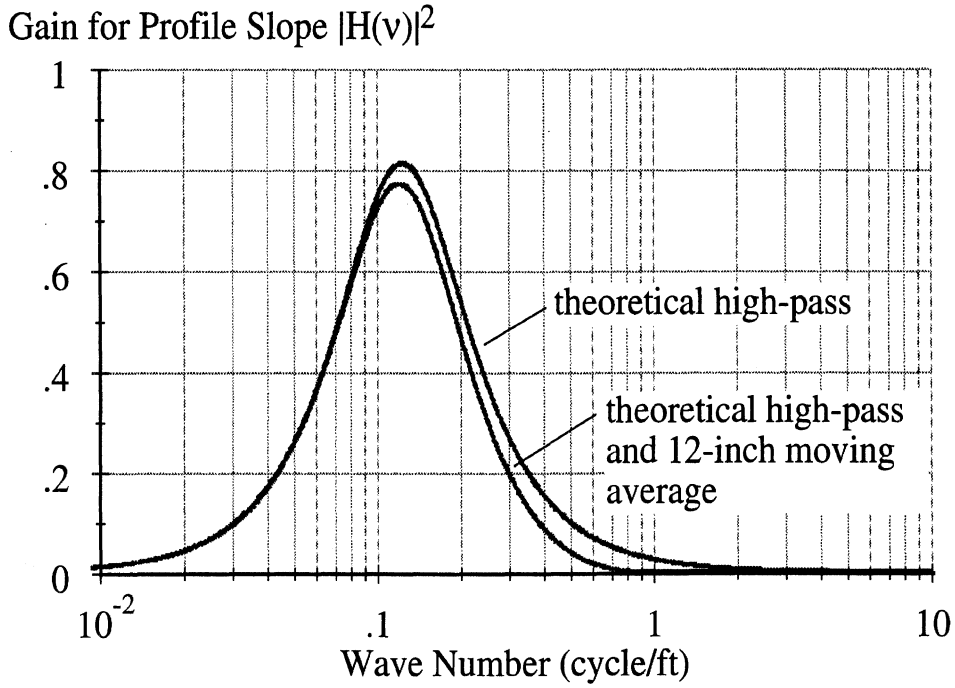

Figure 51. Theoretical Spangler/Kelly PI filters (semilog plot).

Spangler/Kelly Digital Filter Algorithm

Table 24 shows portions of the Fortran source code provided by Spangler and Kelly. The lines in bold are the essential calculations performed by the filter.

Table 24. Spangler/Kelly filter implementation.

```
018   c     DELFT ......... Interval between point pairs, ft.
020   c     PFTL .......... 'pftl' at current distance.
022   c     PFTLJ ......... 'pftl' at preceding point.
023   c     PFTLK ......... 'pftl' at 2nd preceding point.
025   c     DPFTL ......... 1st derivative of 'PFTL'.
026   c     DDPFTL ........ 2nd derivative of 'PFTL'.
027   c     PFTLF ......... Value of filtered 'PFTL' at current
029   c     DPFTLF ........ 1st derivative of 'PFTLF'.
030   c     DDPFLF ........ 2nd derivative of 'PFTLF'.
074   c     WLNGTH ........ Cutoff wave length, ft., of simulated
075   c                     2nd order highpass filter.
077   c     PK1,PK2,PK3 ... Filter coefficients.
098   c-Set filter constants:
100         WLNGTH=8.
103         PK1=1.
104         PK2=2.*.707*(2.*3.1416/WLNGTH)
105         PK3=(2.*3.1416/WLNGTH)**2
112   c  Set 'dynamic' initial conditions (use first 2 elevation pairs):
115         PFTLJ=DATA(2,2)
116         PFTLK=DATA(2,1)
117         DPFTLJ=(PFTLJ-PFTLK)/DELFT
123         DDPFLF=0.
126         PFTLF=0.
129   c- Loop to calculate filtered profile and sum
132         DO 10 I=3,NPTS
134         PFTL=DATA(2,I)
138   c- Calculate filtered profile:
140           DPFTL=(PFTL-PFTLJ)/DELFT
141           DDPFTL=(DPFTL-DPFTLJ)/DELFT
147   c- Save for the next pass:
149         PFTLJ=PFTL
152         DPFTLJ=DPFTL
156   c- Eight foot high-pass filter:
158           DPFTLF=DPFTLF+DDPFLF*DELFT
159           PFTLF=PFTLF+DPFTLF*DELFT
160            DDPFLF= PK1*DDPFTL-PK2*DPFTLF-PK3*PFTLF
187   10    CONTINUE
            ......
```

To understand the algorithm in table 24, first consider eq. 17 rewritten in the form:

$$Ps^2 = F(s^2 + 2\zeta\omega_n s + \omega_n^2) \qquad (18)$$

Then, replace s in the theoretical transfer function with the derivative operation: $sy = \frac{dy}{dx}$.

Using D to indicate first derivative and DD for a second derivative, eq. 18 is transformed to:

$$DDP = DDF + 2\zeta\omega_n DF + \omega_n^2 F \tag{19}$$

The source code in table 24 is based on eq. 19. The comments at the top describe the variables in the code, which correspond to symbols used in the equations below. The derivatives are approximated by using finite differences, and the filtered profile F is calculated by using numerical Euler integration:

(159) $$F_i = F_{i-1} + DF_{i-1/2}\,\Delta \tag{20}$$

where Δ is the sample interval, the subscript indicates the sample number, and the first number shown in parentheses, 159, is the line number in the listing. DF is calculated by numerical integration:

(158) $$DF_{i-1/2} = DF_{i-3/2} + DDF_{i-1}\Delta \tag{21}$$

The second derivative of profile, DDP, is estimated by the equation

(140, 141) $$DDP_{i-1} = \frac{P_i - 2P_{i-1} - P_{i-2}}{\Delta^2}. \tag{22}$$

(This equation is separated into two lines of code.)

Line 160 of the algorithm calculates the second derivative of the filter output:

(160) $$DDF_{i-1} = C_1\,DDP_{i-1} - C_2\,DF_{i-3/2} - C_3\,F_{i-1} \tag{23}$$

where C_1, C_2, and C_3 are based on the constants shown in eq. 19.

Line 160 contains a subtle error. Three of the four terms are taken for sample i-1, but one (DF) is taken at a position that would correspond to sample i-3/2 (halfway between sample i-1 and i-2). When terms are not all at the same sample, the response is modified by the artificial phasing between indices. For example, when the sample interval is 6 in (152 mm), the DF value from a point 3 in (76 mm) away from the correct location is used.

Although this might seem like a minor detail, the fact that $DF_{i-3/2}$ is used in line 160 rather than DF_{i-1} changes the behavior of the digital filter significantly from the target response. The wave number response function was obtained by combining the above equations to eliminate the derivatives, and replacing delays with the wave number equivalent:

$$Y_{i-1} = Y_i\,e^{-j\nu\Delta} \tag{24}$$

where ν represents wave number, to yield the following:

$$H(\nu) = \frac{C_1(1 - 2e^{-j\nu\Delta} + e^{-2j\nu\Delta})}{1 + (C_2\Delta + C_3\Delta^2 - 2)e^{-j\nu\Delta} + (1 - C_2\Delta)e^{-2j\nu\Delta}} \tag{25}$$

This function is plotted in figure 52 for profiles measured at 1-, 6-, and 12-in (25.4-, 152-, and 305-mm) intervals.

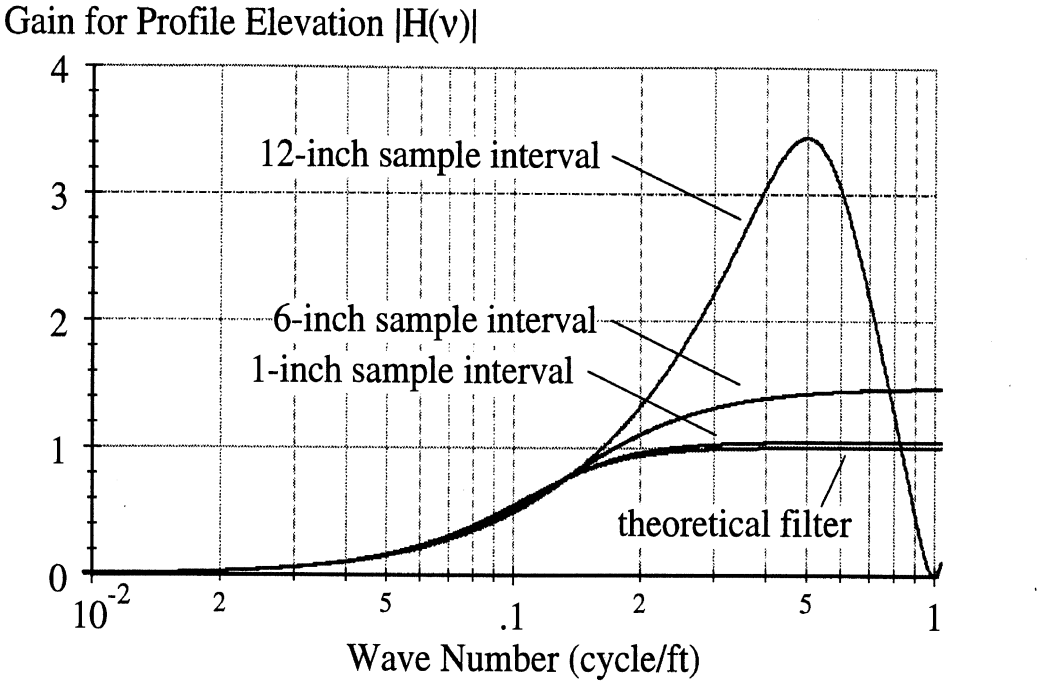

Figure 52. Spangler/Kelly algorithm applied to a profile sampled at various intervals.

The figure shows that the filter, as provided in the example code, behaves much differently than the intended filter, because of the indexing offset. At a sample interval of 6 in (152 mm), the filter has a maximum gain of approximately 1.45, instead of the unity gain defined in eq. 17. Even for the small sample interval of 1 in (25.4 mm), the filter differs noticeably from the intended response. For a 12-in (305-mm) sample interval, which is used by the Dipstick and many profilers, the filter as coded bears little resemblance to the intended function.

Modified Spangler/Kelly Method

The provided algorithm was studied to determine why there is such a big difference between theoretical and actual frequency response, leading to the analysis presented above. The source code was cleaned up to isolate the filter algorithm in a subroutine PIPROF, as shown in table 25. The subroutine PIPROF exactly duplicates the Spangler/Kelly algorithm when line 41 is commented out and line 46 is enabled.

The algorithm was modified to correct the error involving DDF. In the modified algorithm, the derivative of the filter at i-1 is used. It is estimated by taking the average of $DF_{i-3/2}$ and $DF_{i-1/2}$:

$$DDF_{i-1} = C_1 DDP_{i-1} - C_2 \frac{DF_{i-3/2} + DF_{i-1/2}}{2} - C_3 F_{i-1} \qquad (26)$$

Combining eq. 26 and eq. 21, then solving for DDF_{i-1} yields:

$$DDF_{i-1} = \frac{C_1 DDP_{i-1} - C_2 DF_{i-3/2} - C_3 F_{i-1}}{1 + C_2 \Delta / 2} \qquad (27)$$

The modified equation for DDF appears as line 41 in table 25.

Table 25. Source code for the two versions of the Spangler/Kelly PI algorithm.

```
C=======================================================================
      SUBROUTINE PIPROF(PROFIL, NSAMP, DX, FILT)
C=======================================================================
C  UMTRI-modified Spangler/Kelly profile analysis to filter profile.
C
C  --> PROFIL  Real    Elevation profile in inches.
C  --> NSAMP   Integer Number of samples of data.
C  --> DX      Real    Distance step in feet.
C  <-- FILT    Real    Filtered elevation profile in inches.
C
C  The RMS value of the filtered profile is "PI" (profile index) and is
C  transformed to RN through a conversion equation. This algorithm is
C  taken from ASTM draft standard "Standard Practice for Computing Ride
C  Number from Longitudinal Profile Measurements made by an Inertial
C  Profile Measuring Device", with a modification to improve frequency
C  response.
C
C  last modified: June 10, 1994 (UMTRI)

      IMPLICIT  NONE
      INTEGER   I, NSAMP
      REAL      PROFIL(NSAMP), DX, FILT(NSAMP)
      REAL      C1, C2, C3, CDEN, DX2, DDFILT, DFILT, DDPROF, PI2, WN
      PARAMETER (WN = 6.2831853070/8.0, C1 = 1.0, C2 = 2**0.5*WN)
      PARAMETER (C3 = WN*WN)

C  Initialize variables.
      DDFILT  = 0.0
      DFILT   = 0.0
      FILT(1) = 0.0
      FILT(2) = 0.0

C  Set constants based on DX
      DX2  = DX*DX
      CDEN = 1.0 + C2*DX/2.

C  Calculate filtered profile.
      DO 10 I = 3, NSAMP
        DDPROF = (PROFIL(I) - 2.*PROFIL(I-1) + PROFIL(I-2))/DX2
C--Use the following statement for the modified algorithm
          DDFILT = (C1*DDPROF - C2*DFILT - C3*FILT(I - 1))/CDEN
C--
        DFILT = DFILT + DDFILT*DX
        FILT(I) = FILT(I-1) + DFILT*DX
C--Use the following statement for the original ASTM algorithm
C         DDFILT = C1*DDPROF - C2*DFILT - C3*FILT(I)
C--
   10   CONTINUE
      RETURN
      END
```

The wave number response function for the modified algorithm is:

$$H(\nu) = \frac{C_1(1-2e^{-j\nu\Delta}+e^{-2j\nu\Delta})}{(C_2\Delta+C_3\Delta^2)e^{-j\nu\Delta} + (C_2\Delta)e^{-2j\nu\Delta} + (1+C_2\Delta)(1-2e^{-j\nu\Delta}+e^{-2j\nu\Delta})/2.} \quad (28)$$

Figure 53 shows the behavior of the modified algorithm for the same sample intervals used in figure 52. For a sample interval of 1 in (25.4-mm), the new filter matches the intended response almost exactly. For a 6-in (152-mm) sample interval, the full gain is only a few percent high (in contrast to the 45-percent error in the original). For a 12-in (305-mm) sample interval, the peak gain is 20 percent higher than that of the theoretical filter (rather than 240 percent, as is the case with the original algorithm). The remaining error is due to the approximation made in replacing differentials with finite difference equations.

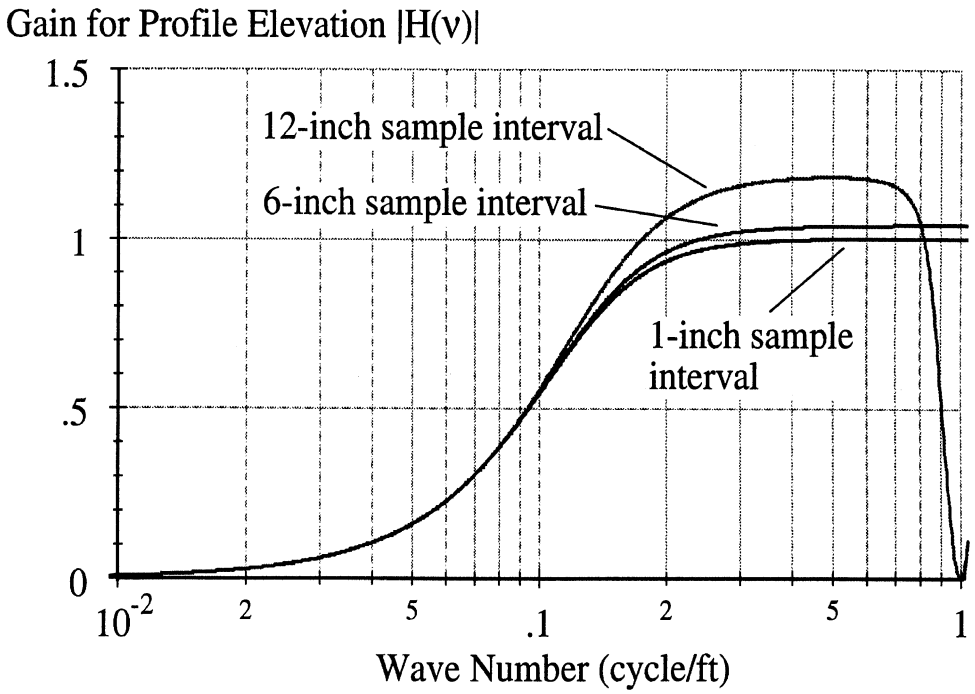

Figure 53. Wave number response of the modified Spangler/Kelly algorithm.

APPENDIX E. FILTER ALGORITHM THEORY

This appendix presents the technical details of two types of filters used in the research. One is based on a quarter-car model and is used to calculate the IRI and RN. The second is a four-pole Butterworth band-pass filter. Appendix F contains Fortran computer code for applying these filters to profiles. Working versions of the filters are included in the free RoadRuf software described in chapter 4.

QUARTER-CAR FILTER

This filter is defined by differential equations that relate motions of a simulated quarter-car vehicle to road profile inputs. Figure 54 shows a quarter-car model, which includes the major dynamic effects that determine how roughness causes vibrations of the car body. This system is described by four first-order ordinary differential equations that can be written in matrix form:

$$\dot{\mathbf{x}} = \mathbf{A}\,\mathbf{x} + \mathbf{B}\,h_{ps} \tag{29}$$

where **x** is an array of *state variables* (variables that, together, completely describe the state of the simulated system), and the **A** and **B** arrays have coefficients in the equations:

$$\mathbf{x} = [z_s,\ \dot{z}_s,\ z_u,\ \dot{z}_u]^T$$

$$\mathbf{A} = \begin{bmatrix} 1 & 0 & 0 & 0 \\ -k_2 & -c & k_2 & c \\ 0 & 0 & 1 & 0 \\ \dfrac{k_2}{\mu} & \dfrac{c}{\mu} & -\dfrac{k_1 + k_2}{\mu} & -\dfrac{c}{\mu} \end{bmatrix}$$

$$\mathbf{B} = [0,\ 0,\ 0,\ k_1/\mu]^T \tag{30}$$

The scalar constants and variables are defined as follows:

c_s = suspension damping rate
h_{ps} = smoothed profile elevation
k_s = suspension spring rate
k_t = tire spring rate
m_s = sprung mass (portion of mass of car body supported by one wheel)
m_u = unsprung mass (mass of the wheel, tire, and half of the axle/suspension)
z_s = height (vertical coordinate) of sprung mass
z_u = height (vertical coordinate) of unsprung mass
c = c_s/m_s
k_1 = k_t/m_s
k_2 = k_s/m_s
μ = m_u/m_s

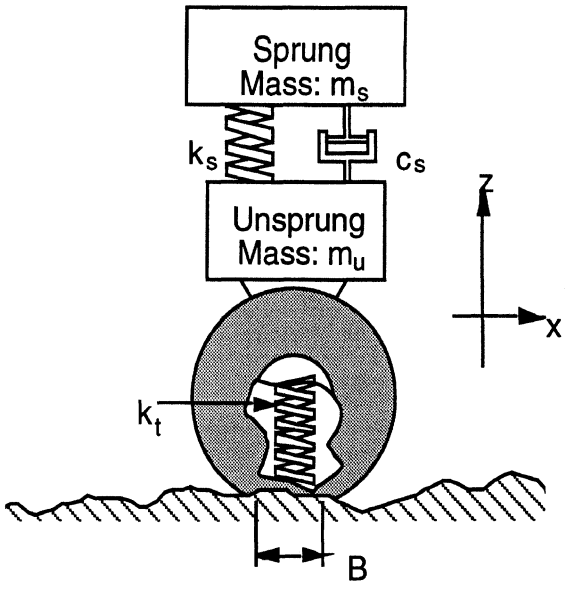

Figure 54. Quarter car model.

Time derivatives are indicated with a dot (e.g., $\dot{z}_s$). The time covered over each profile sample is related to longitudinal distance by the simulated speed of the vehicle:

$$t = X/V \tag{31}$$

where X is longitudinal distance and V is the simulated forward speed, expressed in units of length per second, where the length units match those of X.

State-Space Solution

For a set of linear equations such as eq. 29, the total response at point i is the sum of the *free response* (no input) of the system to its state at a previous point i-1, plus the *forced response* to an input over the interval between points i-1 and i. In the case that the input is a constant, the response can be written

$$\mathbf{x}_i = \mathbf{S}\,\mathbf{x}_{i-1} + \mathbf{P}\,u \tag{32}$$

where **S** is a 4×4 *state transition* matrix that defines the free response as a linear combination of the four variables in **x** at point i-1, and **P** is a 4-element *partial response* array that defines the forced response as a linear function of a constant u that is the input over the interval from i–1 to i. **S** and **P** are solutions of the equations, calculated from the matrices in eq. 29:

$$\mathbf{S} = e^{\mathbf{A}\,\Delta/V} \tag{33}$$

$$\mathbf{P} = \mathbf{A}^{-1}\,(\mathbf{S} - \mathbf{I})\,\mathbf{B} \tag{34}$$

where e is the base of the natural logarithms, Δ is the interval between profile samples, and **I** is a 4×4 identity matrix. Eq. 33 requires taking e to a matrix power. One method is to use a Taylor series expansion:

$$e^{\mathbf{A}\,\Delta/V} = \mathbf{I} + \sum_{i=i}^{N} \frac{\mathbf{A}^i(\Delta / V)^i}{i!} \tag{35}$$

where N is a number large enough to obtain the required accuracy.

Research of different interpolation methods showed that the best approximation is the assumption that the profile slope is constant between samples.[5] This means that to obtain the best accuracy, the assumed constant input *u* in eq. 32 should be profile slope.

Replacing profile height with profile slope in eq. 32 changes the physical meaning of the state variables. As written in eq. 30, with no scale factors, the units of z_s and z_u are the same as those of the input, h_{ps}. Because the describing equations (eq. 30) are linear, they can be applied to other types of inputs, such as smoothed profile slope:

$$\dot{\mathbf{x}} = \mathbf{A}\,\mathbf{x} + \mathbf{B}\,s_{ps} \tag{36}$$

where s_{ps} is smoothed profile slope, and the array **x** is redefined in terms of filtered slope variables s_s and s_u

$$\mathbf{x} = [s_s,\ \dot{s}_s,\ s_u,\ \dot{s}_u]^T \tag{37}$$

Profile slope over an interval B (see figure 54) is computed with the difference equation:

$$s_{ps,i} = \frac{h_{p,i+k} - h_{p,i}}{k\Delta} \tag{38}$$

where

$$k = \max[1,\ \mathrm{nint}(B/\Delta)] \tag{39}$$

The function *max* means "take the maximum of the two arguments," and the function *nint* means "round off to the nearest integer." B is the moving average base length. For example, if the sample interval is Δ=6 in (152 mm) and the base length is 9.8 in (250 mm), the ratio (B/Δ) is 1.64, which is rounded to 2. The number 2 is larger than 1, so the value of k would be 2.

To solve differential equations such as eq. 29, one must know or estimate the values of the state variables at some starting time. The response obtained over a profile includes a response of the transition from the assumed initial values to the profile-induced response. The effect of the initialization diminishes as the simulated car covers more of the profile. The best way to deal with the initialization is to measure the profile for some distance ahead of the site and start the simulation there. However, a requirement that extra profile be measured and stored is not always practical. Therefore, z_s and z_u are initially set to match the height of the first profile point, and $\dot{z}_s$ and $\dot{z}_u$ are set to match the average change in profile height per second over some length of profile at the start.

To initialize the algorithm, the elements of the **x** array for i=1 are set as:

$$\mathbf{x}_1 = [(h_{p,Lo/\Delta} - h_{p,1})/L_o,\ 0,\ (h_{p,Lo/\Delta} - h_{p,1})/L_o,\ 0] \tag{40}$$

where L_o is the initialization length.

Accumulator

In order for the quarter-car filter to yield a summary index, some combination of the calculated responses (the z's) must be accumulated over the length of the simulation as follows:

$$PI = \left(\frac{1}{L} \int_0^{L/V} |r|^p dt \right)^{\frac{1}{p}} \tag{41}$$

where PI is a summary profile index, r is some combination of the vehicle response variables, L is the length of the profile, V is velocity, t is time, and p is some exponent. The vehicle response variables oscillate about zero, and have zero as their average values. The absolute value in eq. 41 is needed in case the exponent, p, is less than 1.

INTERNATIONAL ROUGHNESS INDEX

The IRI is calculated using the quarter-car model described in the previous section. The vehicle properties used for the IRI are known as the *Golden Car* parameters:

c =	6.	(1/s)
k_1 =	653.	($1/s^2$)
k_2 =	63.3	($1/s^2$)
μ =	0.15	(-)
V =	80	(km/h)

Other parameters specific to the IRI are:

L_0 =	11.	(m)
B =	250.	(mm)

The IRI is accumulated using:

$$r = \dot{z}_s - \dot{z}_u \tag{42}$$

and p = 1. Thus, the IRI represents average rectified slope. Over a number of profile samples (n):

$$IRI = \frac{1}{n} \sum_{i=i}^{n} \left| s_{s,i} - s_{u,i} \right| \tag{43}$$

RIDE NUMBER

RN is calculated using the quarter-car model described in the eqs. 29 through 41. The following parameters are used for RN:

c =	17.	(1/s)
k_1 =	5120.	($1/s^2$)
k_2 =	390.	($1/s^2$)
μ =	0.036	(-)
V =	80	(km/h)

Other parameters specific to the RN are:

L_o = 19. (m)

B = 250. (mm)

RN is accumulated using eq. 42 and p = 2. Thus, the RN represents root mean squared slope.

FOUR-POLE BUTTERWORTH FILTER

Another filter considered in developing RN and used as a general band-pass filter in this research was a four-pole Butterworth filter. The theoretical transfer function of the band-pass filter is:

$$H(s) = \frac{s^2\Omega_h^2}{(s^2 + 2\zeta\Omega_l s + \Omega_l^2)(s^2 + 2\zeta\Omega_h s + \Omega_h^2)} \tag{44}$$

where Ω_h and Ω_l are the high- and low- spatial frequency cutoffs (in radians/length), respectively, and ζ is the dimensionless damping ratio set to 0.707 for a Butterworth filter. Figure 55 shows the theoretical frequency response of eq. 44.

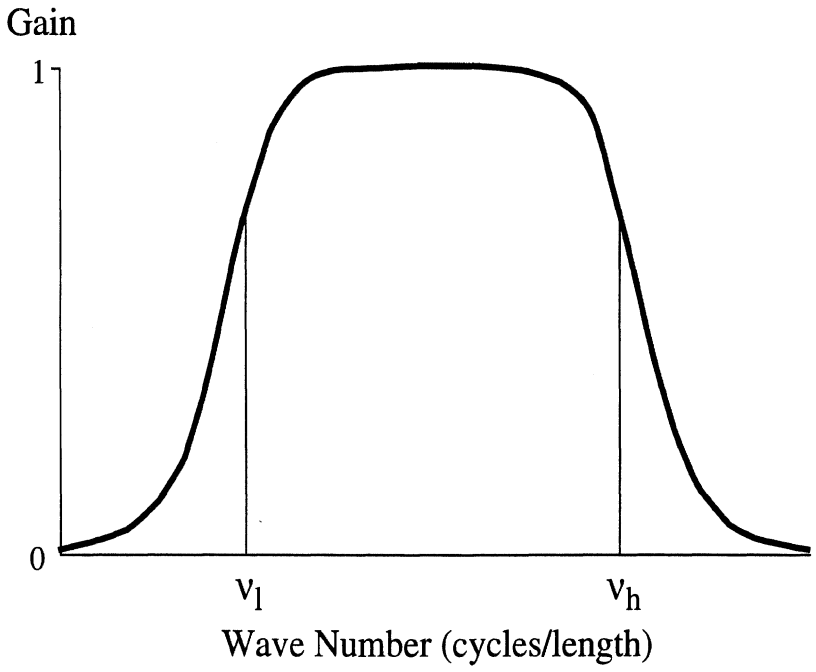

Figure 55. Wave number response of the four-pole Butterworth filter.

The cutoffs are usually specified using a wavelength, rather than a spatial frequency:

$$\Omega = \frac{2\pi}{\lambda} = 2\pi\nu \tag{45}$$

The theoretical frequency response from eq. 44 can be re written as:

$$P(s^2\Omega_h^2) = F((s^2 + 2\zeta\Omega_l s + \Omega_l^2)(s^2 + 2\zeta\Omega_h s + \Omega_h^2)) \tag{46}$$

where P(x) is the input profile and F(x) is the filtered profile. Then replace s in the theoretical transfer function with the derivative operation:

$$s\,y = \frac{dy}{dx}. \tag{47}$$

Using D to indicate first derivative, DD for a second derivative, etc., eq. 46 is:

$$b_2\text{DDP} = \text{DDDDF} + a_1\text{DDDF} + a_2\text{DDF} + a_3\text{DF} + a_4\text{F} \tag{48}$$

where $b_2 = \Omega_h^2$,

$a_1 = 2\zeta(\Omega_l + \Omega_h)$,

$a_2 = \Omega_l^2 + 4\zeta\Omega_l\Omega_h + \Omega_h^2$,

$a_3 = 2\zeta\Omega_l\Omega_h(\Omega_l + \Omega_h)$, and

$a_4 = \Omega_l^2\,\Omega_h^2$.

The matrix representation of eq. 48 is:

$$\mathbf{DF}(x) = \mathbf{A}\,\mathbf{F}(x) + \mathbf{B}\,P(x) \tag{49}$$

where $\mathbf{F}(x)$ is a vector of four state variables that include filtered profile and its three derivatives, and

$$\mathbf{A} = \begin{bmatrix} 0 & 1 & 0 & 0 \\ 0 & 0 & 1 & 0 \\ 0 & 0 & 0 & 1 \\ -a_4 & -a_3 & -a_2 & -a_1 \end{bmatrix}$$

$$\mathbf{B} = [0,\ b_2,\ -a_1 b_2,\ (a_1^2 - a_2)b_2]^T \tag{50}$$

State-Space Solution

The state transition matrix, described earlier for the quarter-car equations, can also be used to solve the differential equations for the Butterworth filter. The response is

$$\mathbf{F}_i = \mathbf{S}\,\mathbf{F}_{i-1} + \mathbf{P}\,P_i \tag{51}$$

where **S** and **P** are computed as before with eqs. 33 and 34, but using the **A** and **B** matrices for the Butterworth filter (eq. 50). As with IRI, profile is transformed from an elevation to a slope, using a base length B, to reduce the sensitivity of the filter to sample interval. To initialize the Butterworth algorithm, the elements of the **F** array for i=1 are set as:

$$\mathbf{F}_1 = [0,\ 0,\ -\Omega_h^2(p_{Lo/\Delta} - p_1)/L_o,\ 2\zeta\Omega_h^2(\Omega_h + \Omega_l)(p_{Lo/\Delta} - p_1)/L_o]. \tag{52}$$

Other than the initialization, the solution algorithm for the Butterworth filter is identical to that used for the quarter-car equations.

APPENDIX F. SOURCE CODE LISTINGS

This appendix provides tested Fortran source code for implementing most of the analyses described in chapter 2, including the IRI, RN, a generic quarter-car filter, and a four-pole Butterworth filter.

QUARTER-CAR FILTER

The IRI and RN filters both use the same basic equations, which have been coded in the form of a generalized quarter-car filter. By changing settings, the same code will calculate IRI or the PI needed for RN. With different coefficients, the filter properties can be altered for research applications.

Definition

The quarter-car filter described in appendix E has the following properties:

- The filter is initialized using state variables that are calculated from a segment of the profile at the start. The length of that segment is adjustable.
- The profile is converted to slope.
- The profile is smoothed with a moving average filter.
- The smoothed profile is filtered by solving differential equations.
- The simulated response is accumulated using an arbitrary exponent:

$$PI = \left[\frac{1}{N} \sum_{i=1}^{N} abs(F_i)^p \right]^{1/p} \tag{53}$$

where PI is a summary index computed from the filtered profile F, N is the number of points in the filtered profile, and p is the adjustable accumulator exponent. Use p=1 for the IRI or to simulate a ride meter. Use p=2 to get an RMS value.

Implementation

The quarter-car filter is implemented by calling subroutine QCAR (see table 26):

```
      CALL QCAR(PROF, NSAMP, DX, BASE, UNITSC, PI, XLEAD, XEXP,
     &          K1, K2, C, MU)
```

Subroutine QCAR should be applied to a profile represented as a one-dimensional array of floating-point numbers. In addition to computing a summary output value PI, the subroutine replaces the original profile with a profile filtered with the moving average and quarter-car filters. Subroutine QCAR calls three other subroutines:

1. Subroutine QCABC set coefficients in matrices A, B, and C (see table 27).

2. Subroutine SETSTM computes state transition and primary response matrices given the A and B matrices and a time step dt (see table 28). Subroutines INVERT, LUDCMP, and LUBKSB are supporting routines needed to invert a matrix in SETSTM (see tables 32 through 34).[57]

3. Subroutine STFILT filters the profile using the state transition method (see table 29).

The listed code is written for clarity, rather than being optimized for efficiency. The algorithm itself is so fast that coding efficiency is usually not an issue with modern computers. Fully operational profile analysis software is available including the source files shown in the listings (see chapter 4).

THE INTERNATIONAL ROUGHNESS INDEX

This section provides instructions for calculating the IRI. Further details about the IRI are provided by Sayers.[5]

Definition of the IRI

- IRI is computed from a single longitudinal profile. For systems that measure several profiles simultaneously, the IRI is calculated independently for each. The general recommendation is that the profiles should be measured in two traveled wheel tracks, with the IRI values for each being averaged to obtain a summary for the lane.
- The sample interval should be no larger than 11.8 in (300 mm) for accurate calculations. The required resolution depends on the roughness level, with finer resolution being needed for smooth roads. A resolution of 0.020 in (0.5 mm) is suitable for nearly all conditions.
- The profile is assumed to have a constant slope between sampled elevation points.
- The profile is smoothed with a moving average whose base length is 9.8 in (250 mm).
- The smoothed profile is filtered using a quarter-car simulation, with specific parameter values (Golden Car), at a simulated speed of 49.7 mi/h (80 km/h).
- The simulated suspension motion is linearly accumulated and divided by the length of the profile to yield the IRI. Thus, the IRI has units of slope, such as in/mi or m/km.

Note: The software in the digital K.J. Law Profilometers has always included a moving average of 12 in (305 mm). The difference between a 9.8-in (250-mm) and 12-in (305-mm) moving average on IRI is negligible. Thus, the moving average part of the IRI results in a high degree of compatibility with Law Profilometers. However, it is important that users realize that the smoothing has already been done. When processing data to obtain IRI, they should not perform this averaging a second time. In the source code presented below, the argument BASE should be set to 0.0 when processing profiles obtained with K.J. Law Profilometers.

Implementation

To get the IRI, call the routine QCAR (see table 26) as follows:

```
      CALL QCAR(PROF, NSAMP, DX, BASE, UNITSC, IRI, 11., 1., 653., 63.3,
     &          6., .15)
```

The last six values in this call to QCAR are critical. If any other values are used, the output of the routine will *not* be IRI.

RIDE NUMBER

This section provides instructions for calculating the RN. Further details about RN are provided in chapter 2 of this report and in a forthcoming TRB paper.[6]

Definition of RN

- The profile is smoothed with a moving average whose base length is 9.8 in (250 mm).
- The profile is further filtered with a band-pass filter. The filter uses the same equations as a quarter-car model but with a specific set of coefficients defined for RN.
- The filtered profile is reduced to yield an RMS value called PI, that should have units of dimensionless slope (ft/ft, m/m, etc.).
- PI is transformed to RN. RN is defined as an exponential transform of PI according to the equation:

$$RN = 5e^{-160(PI)} \tag{54}$$

  If a single profile is being processed, its PI is transformed directly. If profiles for both the left and right wheel tracks are processed, values for the two are averaged with the following equation, and then the transform is applied.

$$PI = \sqrt{\frac{PI_L^2 + PI_R^2}{2}} \tag{55}$$

Note: When using profiles from digital K.J. Law Profilometers, the moving average filter has already been applied. (See the earlier note in the definition of IRI.)

Implementation

To get PI, call the routine QCAR (table 26) as follows:

```
      CALL QCAR(PROF, NSAMP, DX, BASE, 1., PI, 19., 2., 5120., 390.,
     &          17., 0.036)
```

The last six values in this call to QCAR are critical. If any other values are used, the output of the routine will *not* be the appropriate PI for transformation to RN. To process one profile, apply subroutine QCAR as shown to get the PI, then apply the transformation in

eq. 54. To process two profiles, apply subroutine QCAR to each. Combine the PI values for each profile using eq. 55, then transform the result to the RN scale using eq. 54.

BUTTERWORTH FILTER

The Butterworth filter provided in the appendix is a four-pole, band-pass filter. The underlying theory is described in appendix E.

Description

The filter has the following properties:

- The filter is initialized using state variables that are calculated from a segment of the profile at the start. The length of that segment is adjustable.
- The profile is converted to slope.
- The profile is smoothed with a moving average filter with an adjustable base length.
- The smoothed profile is Butterworth filtered with adjustable short and long wavelength cutoffs.
- The simulated response is accumulated using eq. 53.

Implementation

The Butterworth filter is implemented by calling subroutine BUTTER (see table 30):

```
      CALL BUTTER(PROF, NSAMP, DX, BASE, UNITSC, PI, XLEAD, XEXP,
     &            FP1, FP2)
```

Note that the adjustable parameters listed above are passed in as arguments to BUTTER. Subroutine BUTTER calls three other subroutines:

1. Subroutine BWABC defines the model matrices A, B, and C for the Butterworth filter (see table 31).
2. Subroutine SETSTM computes the state transition and primary response matrices given the A and B matrices and a time step dt (see table 28). It requires a routine INVERT for inverting a 4×4 matrix (see listings 32 through 34).[57]
3. Subroutine STFILT filters the profile using the state transition method (see table 29).

Table 26. Code to filter a profile with the quarter-car equations.

```
C=======================================================================
      SUBROUTINE QCAR(PROF, NSAMP, DX, BASE, UNITSC, PI, XLEAD, XEXP,
     &                K1, K2, C, MU)
C=======================================================================
C Quarter-car filter a longitudinal road profile and calculate PI.
C
C <-> PROF   Real     On input, an array of profile height values.
C                     On output, an array of filtered PI profile values.
C <-> NSAMP  Integer  Number of data samples in array PROF. The filtered
C                     profile has fewer points than the original.
C --> DX     Real     Distance step between profile points (m).
C --> BASE   Real     Distance covered by moving average (m).
C                     Use 0.250 for unfiltered profile input, and 0.0
C                     for pre-smoothed profiles (e.g. K.J. Law data).
C --> UNITSC Real     Product of two scale factors: (1) meters per unit
C                     of profile height, and (2) PI units of slope.
C                     Ex: height is inches, slope will be in/mi.
C                         UNITSC = (.0254 m/in)*(63360 in/mi) = 1069.34
C <-- PI     Real     The average PI for the entire profile.
C <-- XLEAD  Real     Initialization base length.
C <-- XEXP   Real     Power weighting (1. = ARS, 2. = RMS).
C <-- K1, K2, C, MU   Filter coefficients.

      INTEGER   I, IBASE, ILEAD, NSAMP
      REAL      AMAT, BASE, BMAT, C, CMAT, DX, K1, K2, MU, PI, PR
      REAL      PROF, SFPI, ST, UNITSC, V, XEXP, XIN, XLEAD
      DIMENSION AMAT(4, 4), BMAT(4), CMAT(4), PR(4), PROF(NSAMP),
     &          ST(4,4), XIN(4)

C  Set parameters and arrays.
      CALL QCABC(K1, K2, C, MU, AMAT, BMAT, CMAT)
      CALL SETSTM(DX/(80./3.6), AMAT, BMAT, ST, PR)
      IBASE = MAX(NINT(BASE/DX), 1)
      SFPI = UNITSC/(DX*IBASE)

C  Initialize simulation variables based on profile start.
      ILEAD = MIN(NINT(XLEAD/DX) + 1, NSAMP)
      XIN(1) = UNITSC*(PROF(ILEAD) - PROF(1))/(DX*ILEAD)
      XIN(2) = 0.0
      XIN(3) = XIN(1)
      XIN(4) = 0.0

C  Convert to averaged slope profile, with PI units.
      NSAMP = NSAMP - IBASE
      DO 10 I = 1, NSAMP
   10   PROF(I) = SFPI*(PROF(I + IBASE) - PROF(I))

C  Filter profile.
      CALL STFILT(PROF, NSAMP, ST, PR, CMAT, XIN)

C  Compute PI from filtered profile.
      PI = 0.0
      DO 20 I = 1, NSAMP
   20   PI = PI + ABS(PROF(I))**XEXP
      PI = (PI/NSAMP)**(1./XEXP)
      RETURN
      END
```

Table 27. Code to set model matrices for the quarter-car filter.

```
C=====================================================================
      SUBROUTINE QCABC(K1, K2, C, MU, AMAT, BMAT, CMAT)
C=====================================================================
C Set the A, B and C matrices for the a 1/4 car model.
C
C -->  K1     REAL   Kt/Ms = normalized tire spring rate (1/s/s)
C -->  K2     REAL   Ks/Ms = normalized suspension spring rate (1/s/s)
C -->  C      REAL   C/Ms  = normalized suspension damper rate (1/s)
C -->  MU     REAL   Mu/Ms = normalized unsprung mass (-)
C <--  AMAT   REAL   The 4x4 A matrix.
C <--  BMAT   REAL   The 4x1 B matrix.
C <--  CMAT   REAL   The 4x1 C matrix.

      INTEGER        I, J
      REAL           AMAT, BMAT, CMAT, K1, K2, C, MU
      DIMENSION      AMAT(4, 4), BMAT(4), CMAT(4)

C  Set default for all matrix elements to zero.
      DO 10 J = 1, 4
        BMAT(J) = 0
        CMAT(J) = 0
        DO 10 I = 1, 4
   10     AMAT(I, J) = 0

C  Put 1/4 car model parameters into the A Matrix.
      AMAT(1, 2) = 1.
      AMAT(3, 4) = 1.
      AMAT(2, 1) = -K2
      AMAT(2, 2) = -C
      AMAT(2, 3) = K2
      AMAT(2, 4) = C
      AMAT(4, 1) = K2/MU
      AMAT(4, 2) = C/MU
      AMAT(4, 3) = -(K1 + K2)/MU
      AMAT(4, 4) = -C/MU

C  Set the B matrix for road input through tire spring.
      BMAT(4) = K1/MU

C  Set the C matrix to use suspension motion as output.
      CMAT(1) = -1
      CMAT(3) = 1
      RETURN
      END
```

Table 28. Code to set the coefficients in a state transition matrix.

```
C=======================================================================
      SUBROUTINE SETSTM(DT, A, B, ST, PR)
C=======================================================================
C Compute ST and PR arrays. This requires INVERT for matrix inversion.
C
C -->  DT    REAL   Time step (sec)
C -->  A     REAL   The 4x4 A matrix.
C -->  B     REAL   The 4x1 B matrix.
C <--  ST    REAL   4x4 state transition matrix.
C <--  PR    REAL   4x1 partial response vector.

      INTEGER   I, ITER, J, K
      LOGICAL   MORE
      REAL      A, A1, A2, B, DT, PR, ST, TEMP
      DIMENSION A(4, 4), A1(4, 4), A2(4, 4), B(4), PR(4), ST(4, 4),
     &          TEMP(4, 4)

      DO 20 J = 1, 4
        DO 10 I = 1, 4
          A1(I, J) = 0
10        ST(I, J) = 0
        A1(J, J) = 1.
20      ST(J, J) = 1.

C  Calculate the state transition matrix ST = exp(dt*A) with a Taylor
C  series. A1 is the previous term in the series, A2 is the next one.
      ITER = 0
30    ITER = ITER + 1
      MORE = .FALSE.
      DO 40 J = 1, 4
        DO 40 I = 1, 4
          A2(I, J) = 0
          DO 40 K = 1, 4
40          A2(I, J) = A2(I, J) + A1(I, K)*A(K, J)
      DO 50 J = 1, 4
        DO 50 I = 1, 4
          A1(I, J) = A2(I, J)*DT/ITER
          IF (ST(I, J) + A1(I, J) .NE. ST(I, J)) MORE = .TRUE.
50        ST(I, J) = ST(I, J) + A1(I, J)
      IF (MORE) GO TO 30

C  Calculate particular response matrix: PR = A**-1*(ST-I)*B
      CALL INVERT(A, 4)
      DO 60 I = 1, 4
        PR(I) = 0.0
        DO 60 K = 1, 4
60        PR(I) = PR(I) - A(I, K)*B(K)
      DO 90 J = 1, 4
        DO 70 I = 1, 4
          TEMP(J, I) = 0.0
          DO 70 K = 1, 4
70          TEMP(J, I) = TEMP(J, I) + A(J, K)*ST(K, I)
        DO 80 K = 1, 4
80        PR(J) = PR(J) + TEMP(J, K)*B(K)
90      CONTINUE
      RETURN
      END
```

Table 29. Code to filter profile.

```
C=======================================================================
      SUBROUTINE STFILT(PROF, NSAMP, ST, PR, C, XIN)
C=======================================================================
C Filter profile using matrices ST, PR, and C.
C
C <->  PROF   REAL      Input profile. Replaced by the output.
C -->  NSAMP  INTEGER   Number of data values in array PROF.
C -->  ST     REAL      4x4 state transition matrix.
C -->  PR     REAL      4x1 partial response vector.
C -->  C      REAL      4x1 output definition vector.
C -->  XIN    REAL      4x1 vector of initial values of state variables.

      INTEGER   I, J, K, NSAMP
      REAL      C, PR, PROF, ST, X, XIN, XN
      DIMENSION C(4), PR(4), PROF(NSAMP), ST(4, 4), X(4), XIN(4), XN(4)

C  Initialize simulation variables.
      DO 10 I = 1, 4
   10   X(I) = XIN(I)

C  Filter profile using the state transition algorithm.
      DO 40 I = 1, NSAMP
        DO 20 J = 1, 4
          XN(J) = PR(J)*PROF(I)
          DO 20 K = 1, 4
   20       XN(J) = XN(J) + X(K)*ST(J, K)
        DO 30 J = 1, 4
   30     X(J) = XN(J)
        PROF(I) = X(1)*C(1) + X(2)*C(2) + X(3)*C(3) + X(4)*C(4)
   40   CONTINUE
      RETURN
      END
```

Table 30. Code to filter a profile with the Butterworth equations.

```
C=======================================================================
      SUBROUTINE BUTTER(PROF, NSAMP, DX, BASE, UNITSC, PI, XLEAD, XEXP,
     &                  FP1, FP2)
C=======================================================================
C Butterworth filter a longitudinal road profile and calculate PI.
C
C <-> PROF   Real     On input, an array of profile height values.
C                     On output, an array of filtered PI profile values.
C <-> NSAMP  Integer  Number of data samples in array PROF. The filtered
C                     profile has fewer points than the original.
C --> DX     Real     Distance step between profile points (m).
C --> BASE   Real     Distance covered by moving average (m).
C                     Use 0.30 for unfiltered profile input, and 0.0
C                     for pre-smoothed profiles (e.g. K.J. Law data).
C --> UNITSC Real     Product of two scale factors: (1) meters per unit
C                     of profile height, and (2) PI units of slope.
C                     Ex: height is inches, slope will be in/mi.
C                         UNITSC = (.0254 m/in)*(63360 in/mi) = 1069.34
C <-- PI     Real     The average PI for the entire profile.
C <-- XLEAD  Real     Initialization base length.
C <-- XEXP   Real     Accumulator exponent (1. = ARS, 2. = RMS).
C <-- FP1, FP2        Filter coefficients.
      INTEGER   I, IBASE, ILEAD, NSAMP
      REAL      AMAT, BASE, BMAT, CMAT, DX, FP1, FP2, FP3, PI, PR
      REAL      PROF, SFPI, ST, UNITSC, V, XEXP, XIN, XLEAD
      PARAMETER (FP3 = .70711)
      DIMENSION AMAT(4, 4), BMAT(4), CMAT(4), PR(4), PROF(NSAMP),
     &          ST(4,4), XIN(4)

C  Set parameters and arrays.
      CALL BWABC(FP1, FP2, FP3, FP3, AMAT, BMAT, CMAT)
      CALL SETSTM(DX, AMAT, BMAT, ST, PR)
      IBASE = MAX(NINT(BASE/DX), 1)
      SFPI = UNITSC/(DX*IBASE)

C  Initialize simulation variables based on profile start.
      ILEAD = MIN(NINT(XLEAD/DX), NSAMP)
      XIN(1) = 0.0
      XIN(2) = 0.0
      XIN(3) = -FP2**2.*(PROF(ILEAD) - PROF(1))/(DX*ILEAD)
      XIN(4) = -2.*FP3*(FP1 + FP2)*XIN(3)

C  Convert to averaged slope profile, with PI units.
      NSAMP = NSAMP - IBASE
      DO 10 I = 1, NSAMP
   10   PROF(I) = SFPI*(PROF(I + IBASE) - PROF(I))

C  Filter profile.
      CALL STFILT(PROF, NSAMP, ST, PR, CMAT, XIN)

C  Compute PI from filtered profile.
      PI = 0.0
      DO 20 I = 1, NSAMP
   20   PI = PI + ABS(PROF(I))**XEXP
      PI = (PI/NSAMP)**(1./XEXP)
      RETURN
      END
```

Table 31. Code to set model matrices for the Butterworth filter.

```
C=====================================================================
      SUBROUTINE BWABC(FP1, FP2, FP3, FP4, A, B, C)
C=====================================================================
C
C  This routine sets the A, B and C matrix for Butterworth PI.
C
C  <-- A    Real    The 4x4 A matrix.
C  <-- B    Real    The 4x1 B matrix.
C  <-- C    Real    The 4x1 C matrix.
C  Last modified 10/17/94.

      IMPLICIT NONE
      INTEGER        I, J
      REAL           A, B, C, FP1, FP2, FP3, FP4
      DIMENSION      A(4, 4), B(4), C(4)

C  Initialize A and B matrix.
      DO 10 J = 1, 4
        B(J) = 0
        C(J) = 0
        DO 10 I = 1, 4
   10     A(I, J) = 0

C  Put filter parameters into the A Matrix.
      A(1,2) = 1.
      A(2,3) = 1.
      A(3,4) = 1.
      A(4,4) = -2.*FP3*(FP1 + FP2)
      A(4,3) = -(FP1**2. + FP2**2. + 4.*FP3*FP4*FP1*FP2)
      A(4,2) = -2.*FP3*FP1*FP2*(FP1 + FP2)
      A(4,1) = -FP1**2.*FP2**2.

C  Put filter parameters into the B matrix.
      B(2) = FP2**2.
      B(3) = A(4,4)*B(2)
      B(4) = A(4,3)*B(2) + A(4,4)*B(3)

C  Set the C matrix.
      C(1) = 1
      RETURN
      END
```

Table 32. Code to invert a matrix.

```
C=======================================================================
      SUBROUTINE INVERT(Y1, N)
C=======================================================================
C  This routine will store the inverse of NxN matrix Y1 in matrix YINV.
C  It was copied from "Numerical Recipes."
C
C  Y1   --> Real     The matrix to be inverted.
C  YINV --> Real     The inverse of matrix Y1.
C
      INTEGER      N, INDX, I, J
      REAL*4       Y1, YINV, D, A
      DIMENSION    Y1(N, N), YINV(4, 4), INDX(4), A(4, 4)

      DO 8 I = 1, N
        DO 9 J = 1, N
    9     A(I, J) = Y1(I, J)
    8   CONTINUE
        DO 10 I = 1, N
          DO 20 J = 1, N
   20       YINV(I, J) = 0.0
          YINV(I, I) = 1.0
   10   CONTINUE
      CALL LUDCMP(A, INDX, D)
      DO 30 J = 1, N
   30   CALL LUBKSB(A, INDX, YINV(1, J))
      DO 40 I = 1, N
        DO 50 J = 1, N
   50     Y1(I ,J) = YINV(I, J)
   40   CONTINUE
      RETURN
      END
```

Table 33. Supporting code (LUDCMP) to invert a matrix.

```
C=======================================================================
      SUBROUTINE LUDCMP(A, INDX, D)
C=======================================================================
C  This routine was copied from "Numerical Recipes" for matrix
C  inversion.
C
      INTEGER      N, INDX, NMAX, I, J, IMAX
      REAL*4       A, TINY, VV, D, AAMAX, SUM, DUM
      PARAMETER    (NMAX = 100, TINY = 1.0E-20, N = 4)
      DIMENSION    A(N, N), INDX(N), VV(NMAX)

      D = 1.0
      DO 10 I = 1, N
        AAMAX = 0.0
        DO 20 J = 1, N
20        IF(ABS(A(I,J)).GT.AAMAX) AAMAX=ABS(A(I,J))
        IF(AAMAX.EQ.0.0) PAUSE 'Singular matrix'
        VV(I) = 1.0/AAMAX
10      CONTINUE
      DO 30 J = 1, N
        DO 40 I = 1, J-1
          SUM = A(I, J)
          DO 50 K = 1, I-1
50          SUM = SUM - A(I, K)*A(K, J)
          A(I, J) = SUM
40        CONTINUE
        AAMAX = 0.0
        DO 60 I = J, N
          SUM = A(I, J)
          DO 70 K = 1, J-1
70          SUM = SUM - A(I, K)*A(K, J)
          A(I, J) = SUM
          DUM = VV(I)*ABS(SUM)
          IF(DUM.GE.AAMAX)THEN
            IMAX = I
            AAMAX = DUM
          ENDIF
60        CONTINUE
        IF(J.NE.IMAX)THEN
          DO 80 K = 1, N
            DUM = A(IMAX, K)
            A(IMAX, K) = A(J, K)
            A(J, K) = DUM
80          CONTINUE
          D = -D
          VV(IMAX) = VV(J)
        ENDIF
        INDX(J) = IMAX
        IF(A(J, J).EQ.0.0) A(J, J) = TINY
        IF(J.NE.N)THEN
          DUM = 1.0/A(J, J)
          DO 90 I = J+1, N
90          A(I, J) = A(I, J)*DUM
        ENDIF
30      CONTINUE
      RETURN
      END
```

Table 34. Supporting code (LUBKSB) to invert a matrix.

```
C=======================================================================
      SUBROUTINE LUBKSB(A, INDX, B)
C=======================================================================
C  This routine was copied from "Numerical Recipes" for matrix
C  inversion.

      INTEGER      N, INDX, I, II, LL
      REAL*4       A, B, SUM
      PARAMETER    (N = 4)
      DIMENSION    A(N, N), INDX(N), B(N)

      II = 0
      DO 10 I = 1, N
        LL = INDX(I)
        SUM = B(LL)
        B(LL) = B(I)
        IF(II.NE.0)THEN
          DO 20 J = II, I-1
20          SUM = SUM - A(I, J)*B(J)
        ELSEIF(SUM.NE.0)THEN
          II = I
        ENDIF
        B(I) = SUM
10    CONTINUE
      DO 30 I = N, 1, -1
        SUM = B(I)
        IF(I.LT.N)THEN
          DO 40 J = I+1, N
40          SUM = SUM - A(I, J)*B(J)
        ENDIF
        B(I) = SUM/A(I, I)
30    CONTINUE
      RETURN
      END
```

APPENDIX G. PSD ANALYSIS OF RIDE DATA

This appendix reports the details of the PSD analyses performed on panel rating data in which MPR were obtained for roads that were also profiled in both the left- and right-hand traveled wheel tracks. The data cover three experiments. Two of the experiments were linked to NCHRP projects: a rideability study held in 1983 and a follow-up study held in 1988.[3,4] All of the sites were measured by the Ohio DOT. The third experiment was made in the fall of 1993 by Fred Maurer of the Minnesota DOT. These data sets are described in appendix C.

As was done in the NCHRP rideability studies, PSD analyses were used to identify the waveband of road roughness that correlates best with MPR. PSD functions were converted to a series of RMS values over one-third octave bands. Correlations between the RMS values and the associated MPR values were calculated, duplicating results reported by NCHRP and confirming that the correct sections of profile were being processed.

For the new analyses, PSD functions were used to calculate RMS profile slope, rather than elevation. The reason for doing so is illustrated in figure 56, which compares the RMS slope and elevation in one-third octave bands for a sample section. Figure 56 shows that the RMS elevation associated with the smallest wave number in a band is numerically much larger than the amplitude associated with the highest wave number—the range spans three orders of magnitude. The large difference in amplitude can complicate statistical analyses because side effects of the numerically large values mask the significance of the smaller values. In contrast, the RMS slope is fairly uniform over the entire range of wave numbers, covering just one order of magnitude.

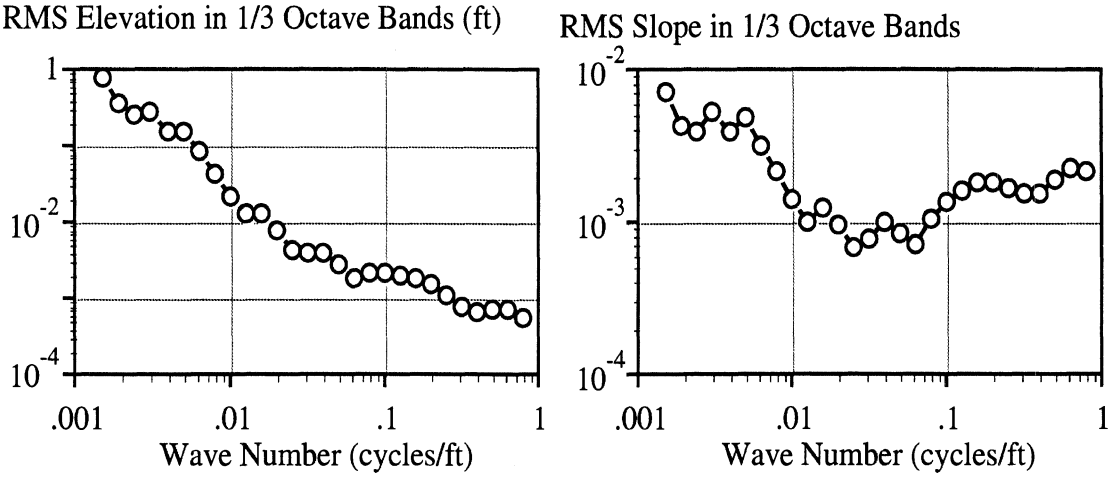

Figure 56. Sample RMS slope and elevation in one-third octave bands.

The profiles from the Ohio Profilometer were filtered with a 12-in (305-mm) moving average when the measures were made in the 1980s. The filter smoothed the profiles, causing complete attenuation of roughness at the 1-ft (0.305-m) wavelength and significant attenuation for wavelengths up to 3 ft (0.914 m), or wave numbers of 0.33 cycles/ft (1.08 cycles/m). As part of the PSD analysis reported in this appendix, the PSD functions

were mathematically transformed to compensate for the smoothing filter and to provide the PSD functions for the profile that would have been obtained without filtering. The motivation for making this transform was to reduce a measurement effect that was specific to the instrument used to collect the profile data, and thus deal with PSD functions that are closer to those of the true profiles.

For each road site, five sets of RMS slope values were calculated: (1) the left wheel-track profile alone; (2) the right wheel-track profile alone; (3) the point-by-point average of the two profiles; (4) the point-by-point difference between the two profiles; and (5) the RMS average of the RMS values computed for the left and right wheel-track profiles. As a first cut, data from each of the five sets of RMS values were correlated with the MPR for the Ohio DOT sections. Figure 57 shows the best correlations (with the RMS average of the RMS values of the left and right profiles). The correlation is not particularly good: R^2 never exceeds 0.64. A completely unexpected finding was that significantly different correlation plots were obtained for the left and right profiles. Taken at face value, they implied that the MPR was linked to different wavebands in the left and right wheel tracks.

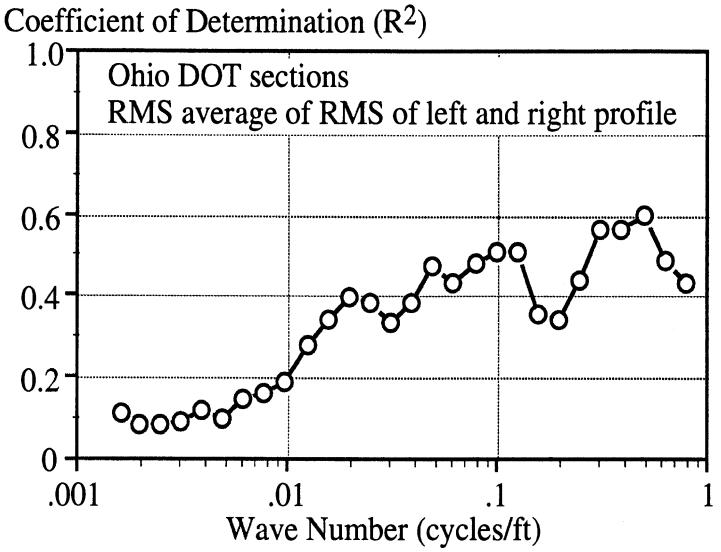

Figure 57. Linear correlation between RMS in one-third octave bands and MPR.

The odd finding about left versus right profiles turned out to be a meaningless artifact of the assumed linear relation between the RMS values and the panel ratings. The problem is illustrated in figure 58. Figure 58a shows a scatter plot between MPR and RMS slope for the third-octave band centered at the 0.125 cycles/ft (0.410 cycles/m) wave number, or an 8-ft (2.44-m) wavelength. The linear regression line is a poor approximation to an underlying relationship between the variables that is clearly nonlinear. The nonlinear relationship exists because the RMS values are proportional to profile amplitude, while the MPR numbers fit into a 0-to-5 psychological scale.

Several nonlinear models have been proposed to link profile statistics to MPR. An exponential transformation proposed by Weed was used for this work:

$$RN = 5\, e^{-A(PI)^B} \tag{56}$$

where RN is the predicted mean panel rating using a PI.[54] The transform in eq. 56 can be manipulated so that coefficients A and B are calculated using standard linear regression software. Consider the linear model:

$$y' = A' + B\, x' \tag{57}$$

where

$$x' = \ln(PI) \qquad y' = \ln(\ln(5/MPR)) \tag{58}$$

To determine the coefficients A and B, transform PI to x' and MPR to y', then obtain the linear fit of eq. 57 to obtain A' and B. Finally, calculate A from A' using the transform:

$$A = e^{A'} \tag{59}$$

Figure 58b shows a scatter plot of the same data seen in figure 58a after applying the exponential transformation. When regressions were done this way, correlation coefficients were much higher, and some of the odd relations disappeared. For example, with the transformed data, nearly identical results were obtained with left- and right-hand wheel-track profiles. Of the five sets of RMS values computed for each pair of profiles, the best correlations were obtained for both the Minnesota and Ohio DOT data sets with two of the five sets of RMS values: (1) the RMS average of the RMS of the left and right profiles; and (2) the RMS of the averaged profiles.

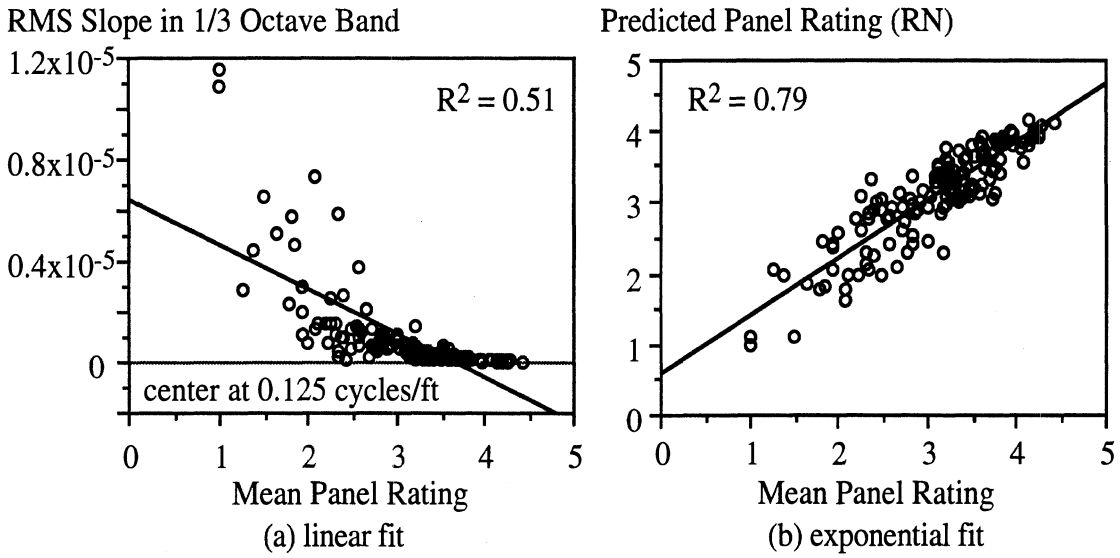

Figure 58. Linear versus exponential fit between profile-based index and MPR.

Figure 59 shows a typical plot of the coefficient of determination (R^2) versus wave number for the Ohio DOT sections, obtained using the average of the RMS of the left and right profiles. High correlation ($R^2 > 0.65$) is obtained for wave number higher than 0.05 cycles/ft (0.16 cycles/m), corresponding to wavelengths shorter than 20 ft (6.10 m). Lesser agreement ($0.30 < R^2 < 0.65$) is obtained for wavelengths up to 64 ft (19.51 m), and very little correlation is shown for longer wavelengths. For the range of wave numbers covered, the high wave numbers are clearly more important for predicting MPR than the low wave numbers. This finding corroborates the conclusions of Janoff, Spangler, and others.

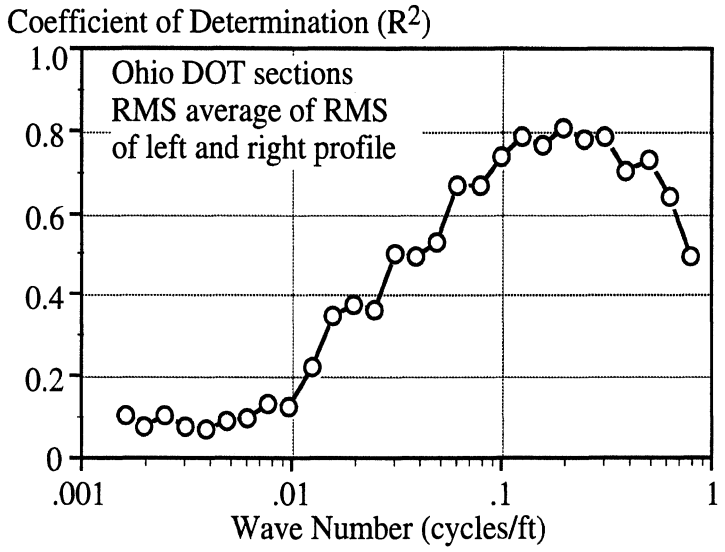

Figure 59. Correlation between MPR and third-octave RMS slope.

Having established correlations between MPR and individual third-octave RMS values, the next step in the analysis was to roughly determine the range of wave numbers that should be included in a single PI that is intended to predict MPR. The strategy was to define a PI calculated from the highest third-octave waveband, then define a second PI that includes lower wave numbers to include two-thirds of an octave, and then a third PI that includes a full octave, and so on. Figures 60a and 60b compare the correlations for over 28 and 25 PIs, respectively, differing by the lower limit (longest wavelength, λ). The PI for the highest one-third octave band alone shows correlation of $R^2 = 0.54$ for the Ohio DOT sections and 0.79 for the Minnesota DOT sections. As the bandwidth is extended to include longer wavelengths, the correlation with MPR improves up to a point, after which roughness because of the longest wavelengths degrades the correlation. The best results for the Ohio DOT sections ($R^2 = 0.85$) are obtained using the range of wavelengths from 1.1 to 36 ft (0.34 to 10.9 m). For wavelengths longer than 250 ft (76.2 m) the correlation drops rapidly. The results from the Minnesota data also show that correlation begins to drop when roughness is included from wavelengths longer than 100 ft (30.5 m). However, for the Minnesota data, the drop is much less significant. The Ohio profiles were filtered during measurement to attenuate wavelengths longer than 300 ft (91.4 m), so the observed drop-off in correlation is not a surprise.

Given an approximate limit for the longest wavelength that should be included for predicting panel rating, the question then becomes "What is the shortest wavelength that should be included?" The same general sensitivity study was repeated, except that this time the PI was initially defined for the optimum long wavelength band alone, and higher third-octave bands were added until the highest wave numbers were included. As shown in figure 60c, correlation improved for the Ohio DOT sections until the highest band was added. This suggests that an RN algorithm should include wavelengths ranging from 1.1 to 36 ft (0.34 to 10.9 m). On the other hand, results for the Minnesota DOT sections indicate the algorithm should have a short wavelength cutoff of 4.5 ft (1.4 m). (See figure 60d).

The goal of the PSD analysis was to guide the development of a digital filter for calculating RN. Thus, further searching was conducted to identify an optimal frequency weighting function that could be applied to the PSDs to increase the level of correlation to a panel rating for both data sets. An optimal shape was found for each of four types of weighting function: a box-car, a triangle, a trapezoid, and arbitrary weighting in each one-third octave band. The results for the box-car are illustrated in figures 60b and 60d. Figure 61 shows the optimal shapes for the other three types of weighting function for the Ohio DOT and Minnesota DOT data, respectively.

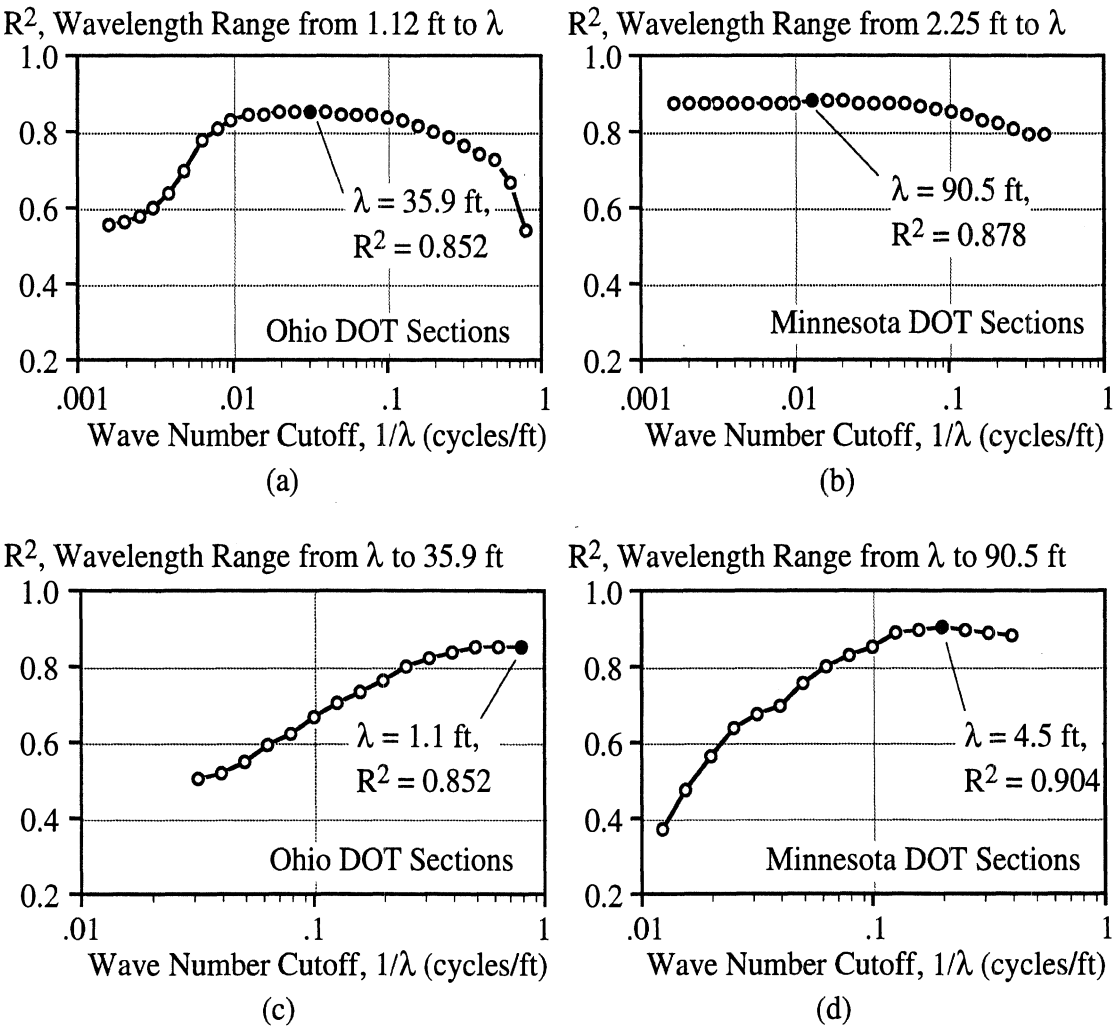

Figure 60. Correlation between MPR and PI for various bandwidths.

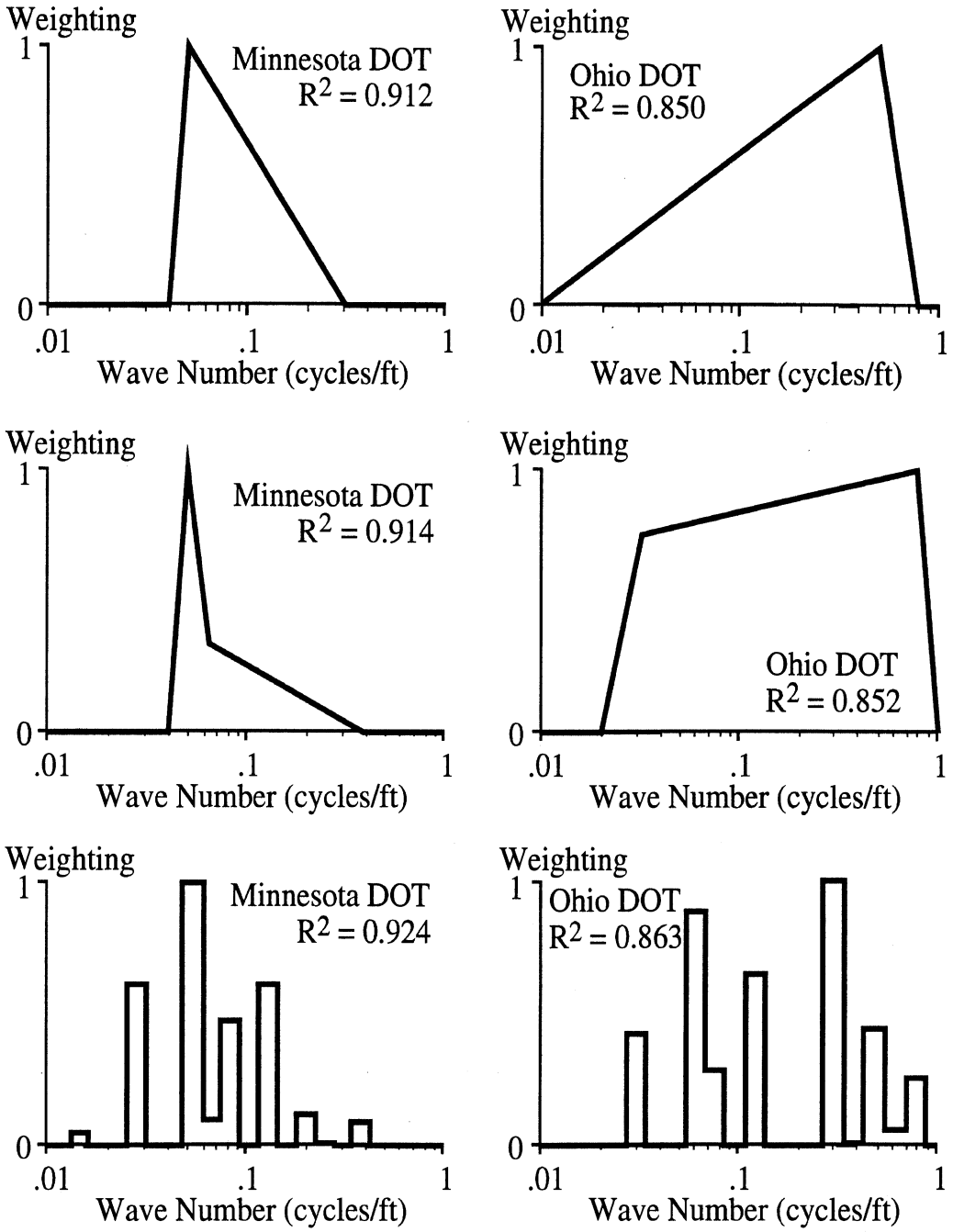

Figure 61. Optimal weighting functions of various shapes.

The triangular and trapezoidal weighting functions do not improve the correlation for the Ohio DOT data over that achieved by the box-car. For the Minnesota DOT data, they improve the coefficient of determination by less than 0.01. The arbitrary weighting function offers a slight improvement of about 0.01. However, the wave-number weighting cannot be easily approximated with a simple filter algorithm.

APPENDIX H. COMPARISON OF RIDE NUMBER ALGORITHMS

This appendix compares four methods for computing RN. RN is a transform of a summary profile index that has been called PI in past work. Four versions of PI that will be considered in this appendix are:

PI_{275}: The algorithm described in NCHRP Report 275.

PI_{SD}: The algorithm developed by Surface Dynamics, Inc., that was considered for an ASTM standard.[48]

PI_{MSD}: A modified version of the Surface Dynamics algorithm (see appendix D).

PI_{QC}: The quarter-car algorithm recommended in this report (see chapter 2).

The IRI is also included in the analysis as a benchmark.

The methods are compared in four stages: (1) comparison of the theoretical wave number response of each algorithm; (2) statistical comparison of each algorithm when applied to measurements of profile that cover a range of roughness values and surface types; (3) statistical evaluation of the ability of each algorithm to predict panel rating; and (4) statistical evaluation of the recommended algorithm to predict panel rating on a range of surface types.

THEORETICAL WAVE-NUMBER RESPONSE

The theoretical spatial frequency response of each algorithm was derived by hand, and plotted by a commercial matrix manipulation program (MatLab). This was done using matrix algebra as described in appendix E. Each frequency response was verified experimentally by filtering some profiles with typical frequency response characteristics and obtaining the PSD function of the output profile. Figure 62 illustrates the frequency response of each filter.

The figure shows that all of the algorithms have a maximum sensitivity for wave numbers between 0.1 and 1 cycle/ft (0.33 and 3.3 cycles/m), or wavelengths from 1 to 10 ft (0.305 to 3.05 m). Yet, within this range, the shapes of the responses are quite different. In the figure, all of the plots provide gain for profile elevation. This form of plot is the most obvious when considering the details of each transform to a sinusoidal input, giving a ratio ($|H(\nu)|$) of PI output for each unit of sinusoidal elevation amplitude. However, the magnitude of profile elevation for typical roads is not uniform. Amplitudes in real roads are approximately inversely proportional to wave number (i.e., proportional to wavelength). For example, the input amplitude to the PI filter for a 10-ft (3.05-m) wavelength is approximately 10 times that for a 1-ft (0.305-m) wavelength.

To better show the significance of the various PI filters to wave number, the theoretical responses are plotted in figure 63 as ratios of PI output for a sinusoidal slope input. By comparing the plots in figures 62 and 63, it can be seen that the three PI responses show

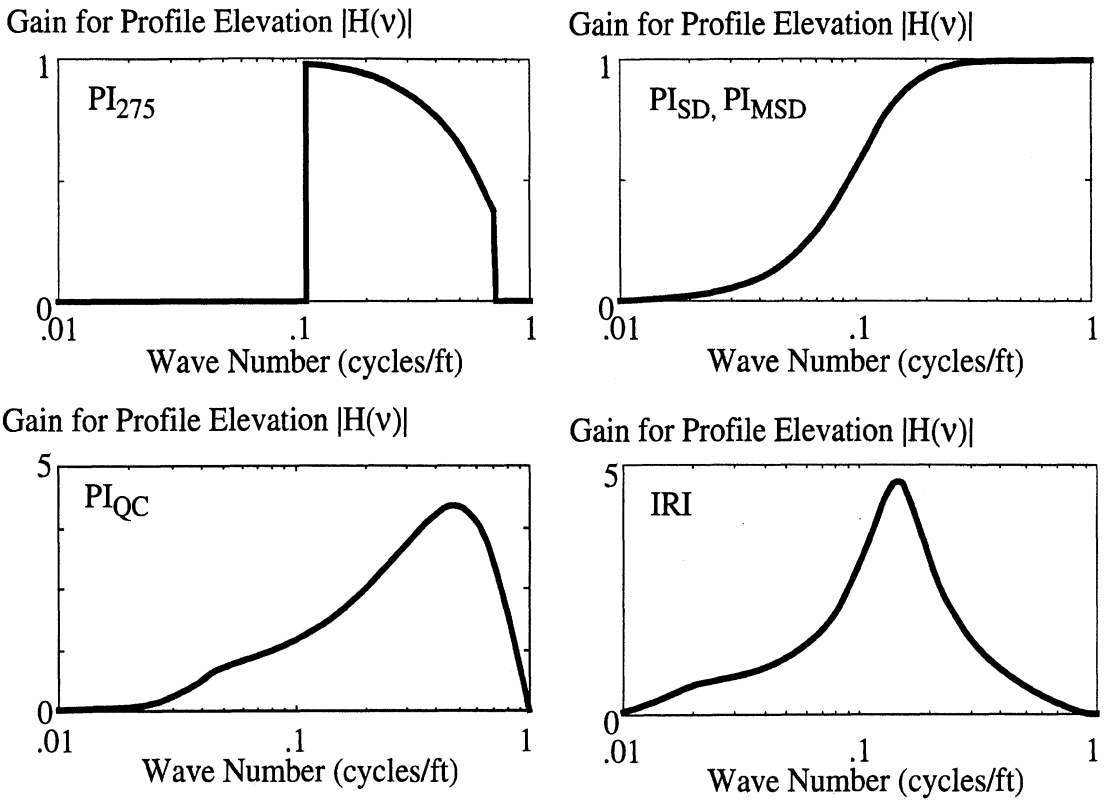

Figure 62. Theoretical frequency weighting functions for PI algorithms.

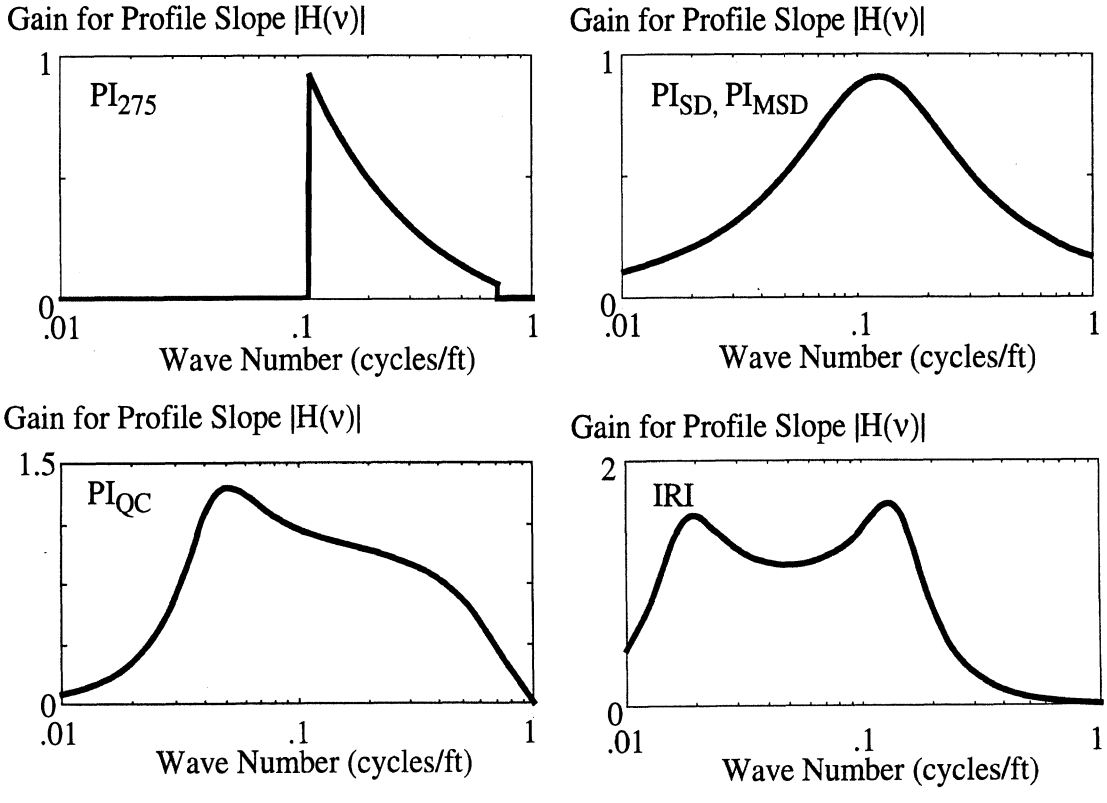

Figure 63. Theoretical frequency weighting functions for PI filters for a slope input.

more commonality when prepared for a slope input. Further, there is a more pronounced distinction between the three PI filters and the IRI filter—the IRI is the only filter that is sensitive to wave numbers less than 0.02 cycles/ft (0.066 cycles/m), or wavelengths longer than 50 ft (15.2 m).

The weighting functions in figures 62 and 63 represent the theoretical behavior of each algorithm for an infinitely small sample interval. Thus, they do not include sensitivity to sample spacing. The sensitivity of these algorithms to sample interval is shown in appendix I. Note that the frequency response for PI_{275} includes the 12-in (305-mm) moving average that was applied to most of the profiles used in its development.

STATISTICAL COMPARISON

Each algorithm for computing profile index was programmed and applied to the correlation matrix of profile measurements (see appendix C). The matrix was specifically designed to cover a range of roughness and surface type for the purpose of developing correlations between profile indices. All of the profiles in the matrix were measured by K.J. Law Profilometers.

Table 35 summarizes R^2 values between PI values obtained with each method. Although results will eventually be needed on the nonlinear 0-to-5 RN scale, the scatter plots prepared in this section show the values of PI for comparison to the IRI. The table shows that all of the variations of PI correlate to each other better than they do to the IRI. This should not be surprising, given that the algorithms for PI were developed to predict panel rating, whereas the IRI was developed to correlate to the output of response-type road roughness measuring systems. Also, the theoretical response plots shown in figure 62a show that, relative to the PI filters, IRI is influenced less by wave numbers above 0.2 cycles/ft (0.66 cycles/m) and more by wave numbers less than 0.02 cycles/ft (0.066 cycles/m).

Table 35. Summary of R^2 values, correlation matrix.

	IRI	PI_{QC}	PI_{MSD}	PI_{SD}
PI_{275}	.791	.900	.919	.906
PI_{SD}	.806	.990	.994	
PI_{MSD}	.857	.986		
PI_{QC}	.819			

Correlation among the four alternatives for PI was very high (R^2 >.9), but not as high for PI_{275} as for the others. One reason for this, which is not evident in the frequency response plots, it that the PI_{275} algorithm includes a cosine taper window. The cosine taper weights the profile highly in the middle and ignores features at the ends. Thus, any significant features that contribute to roughness at the beginning or the end of a profile affect all of the PI algorithms except PI_{275}. Note that PI_{SD}, PI_{MSD}, and PI_{QC} are very highly correlated ($R^2 \approx 0.99$).

Figures 64 through 73 compare the values of the indices for the matrix. Each plot shows a regression line and the R^2 value.

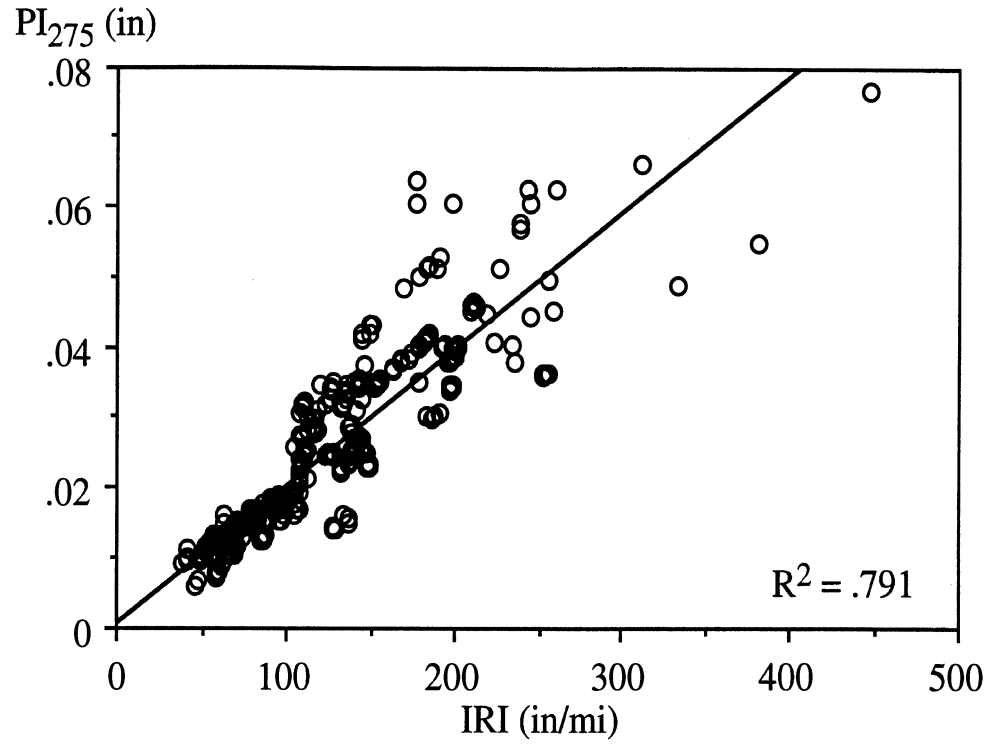

Figure 64. Statistical comparison of IRI and PI_{275}.

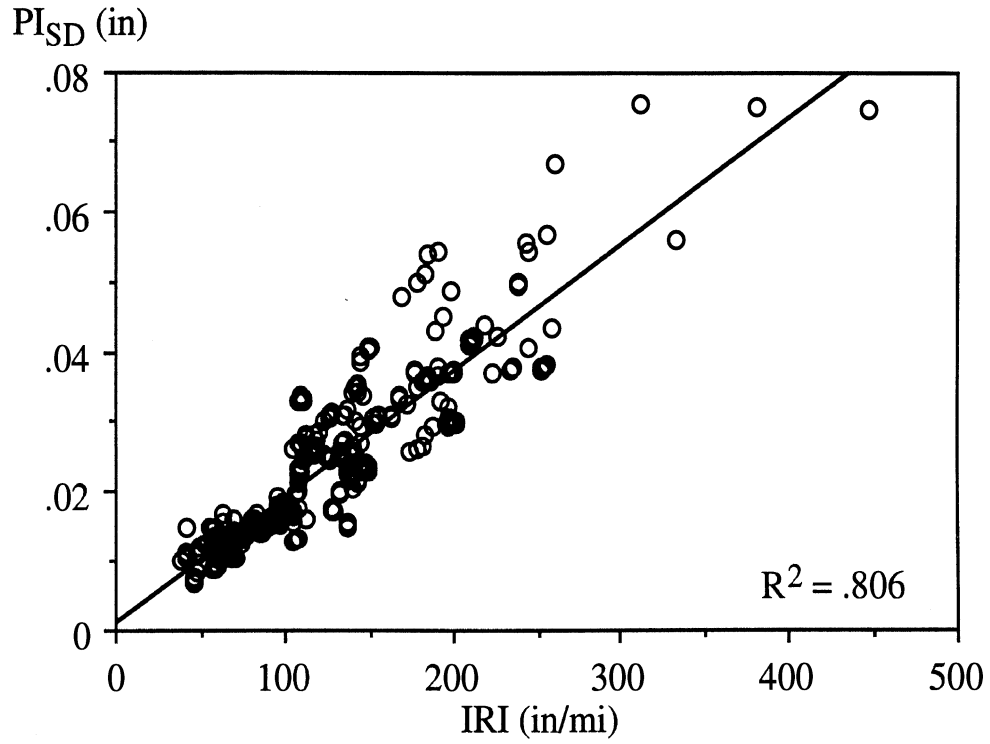

Figure 65. Statistical comparison of IRI and PI_{SD}.

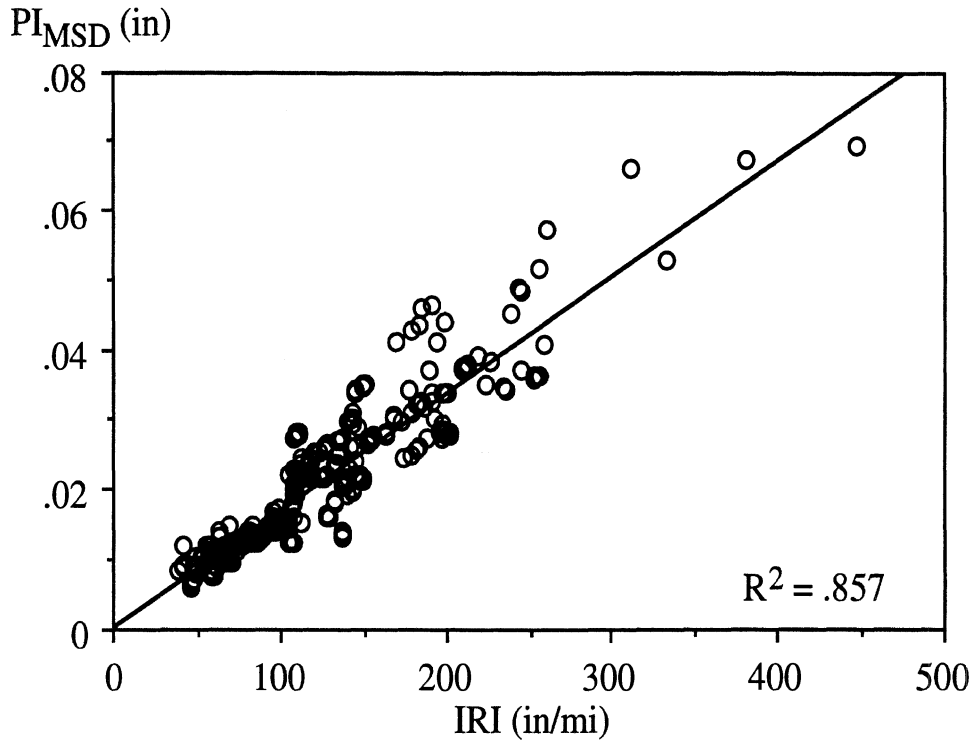

Figure 66. Statistical comparison of IRI and PI_{MSD}.

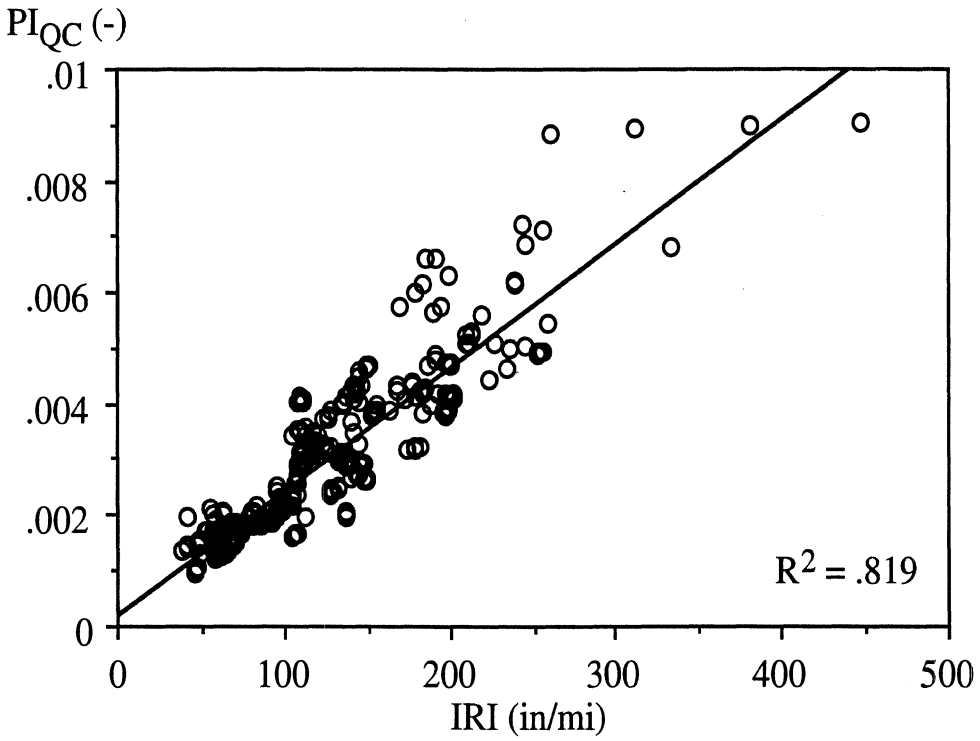

Figure 67. Statistical comparison of IRI and PI_{QC}.

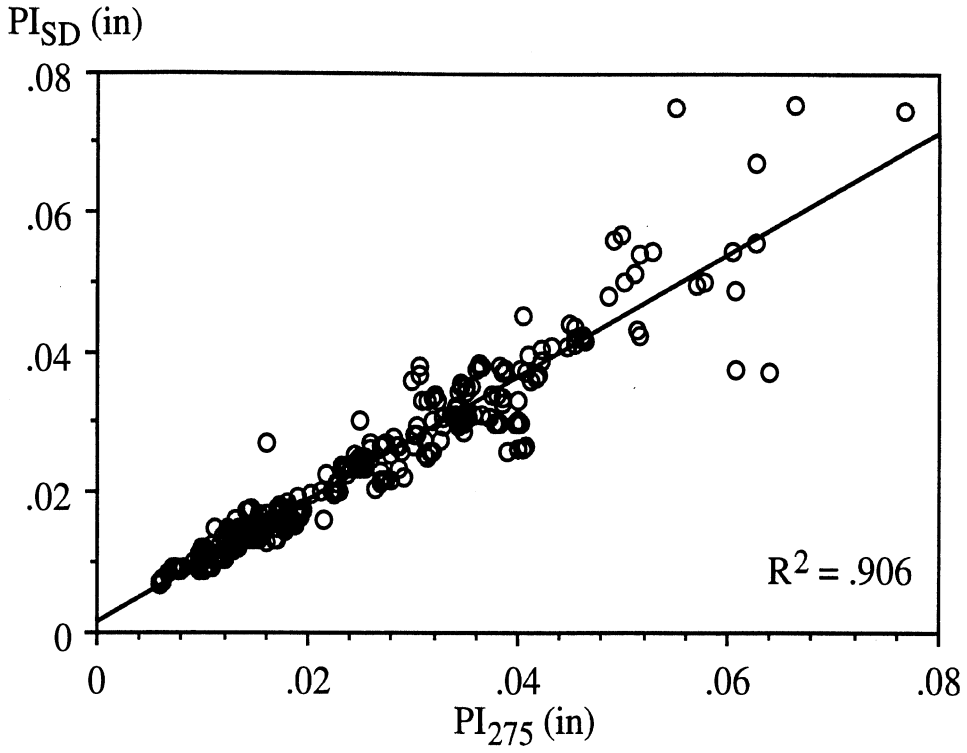

Figure 68. Statistical comparison of PI_{SD} and PI_{275}.

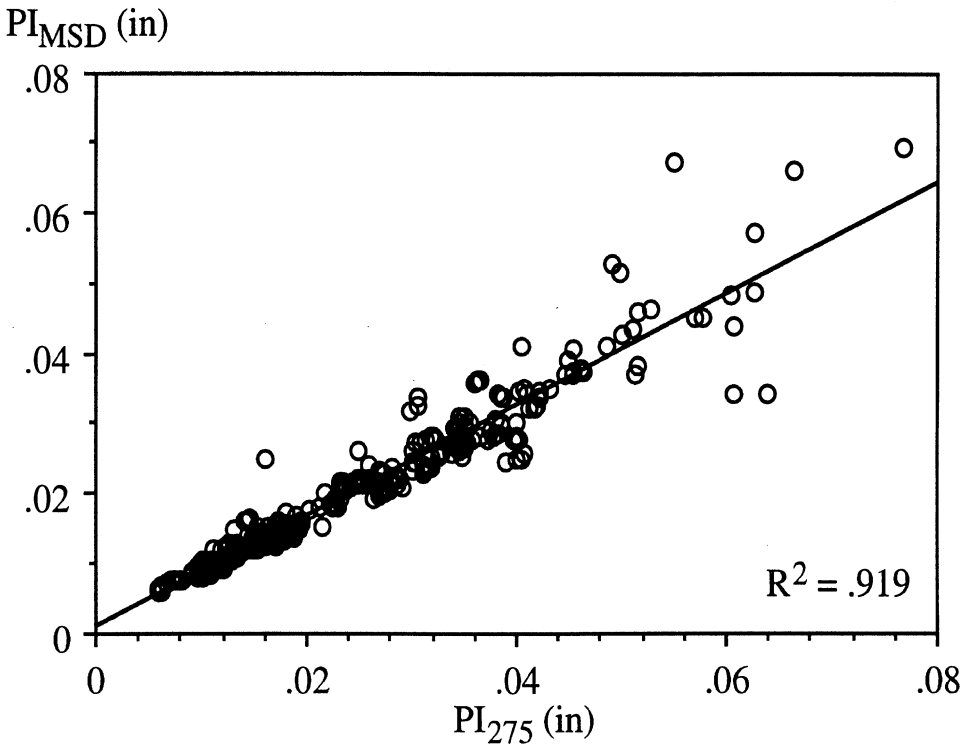

Figure 69. Statistical comparison of PI_{MSD} and PI_{275}.

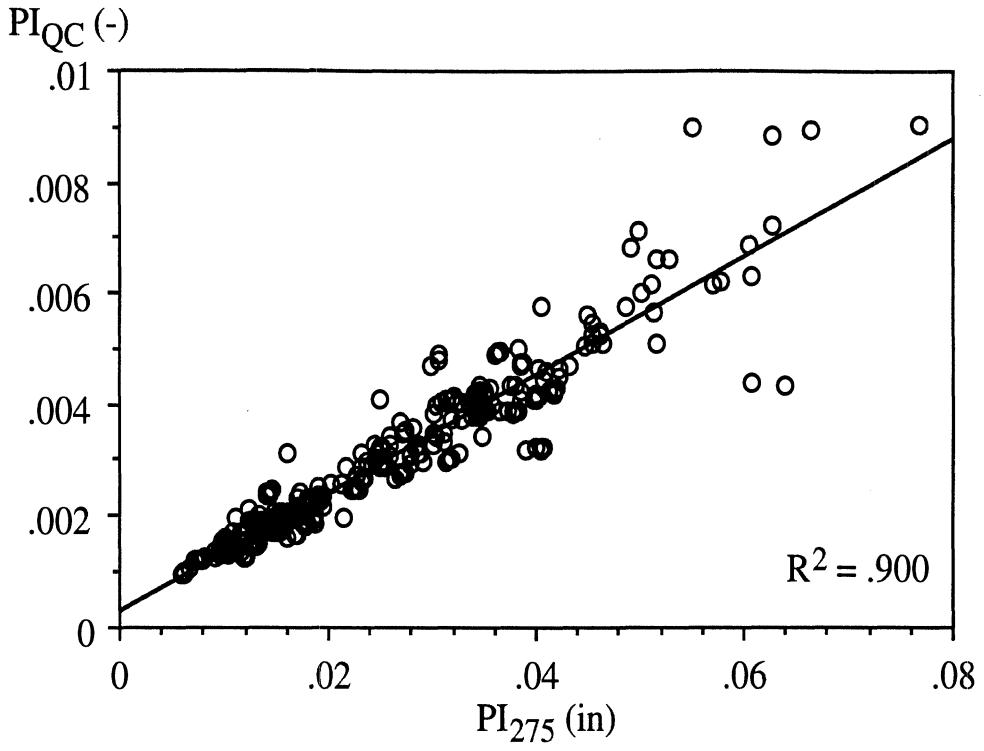

Figure 70. Statistical comparison of PI_{QC} and PI_{275}.

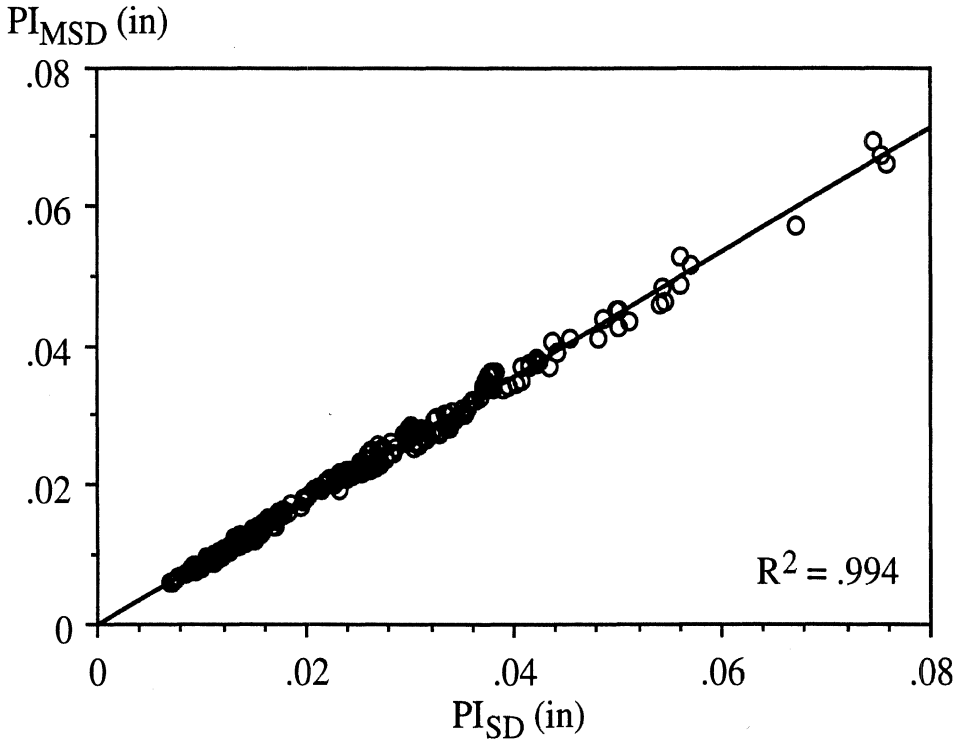

Figure 71. Statistical comparison of PI_{MSD} and PI_{SD}.

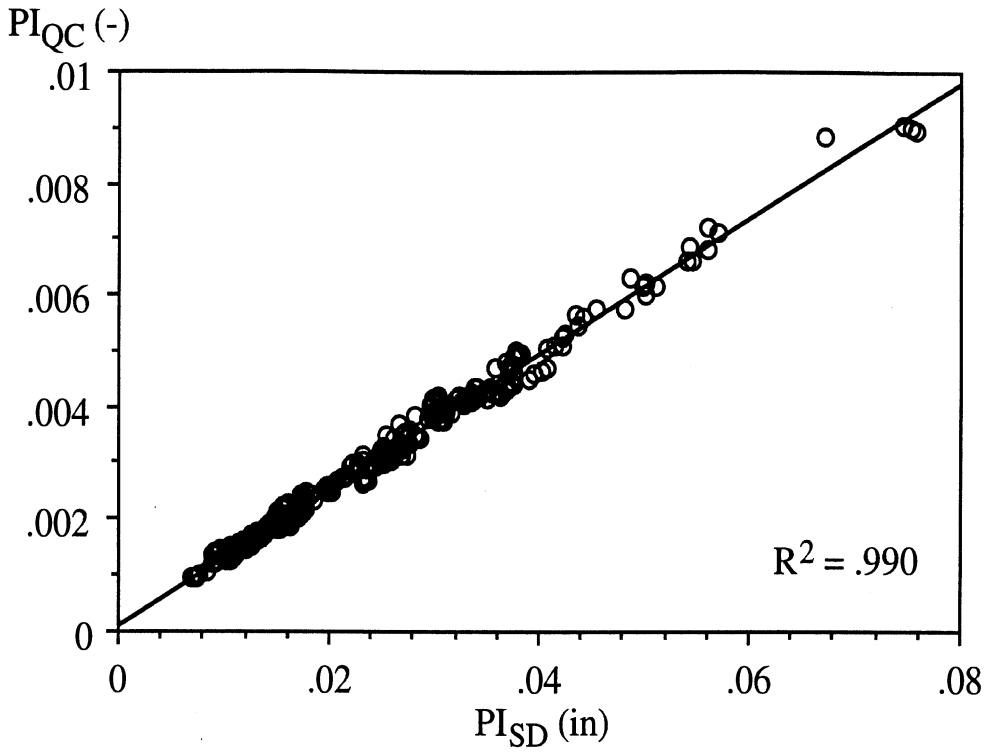

Figure 72. Statistical comparison of PI_{QC} and PI_{SD}.

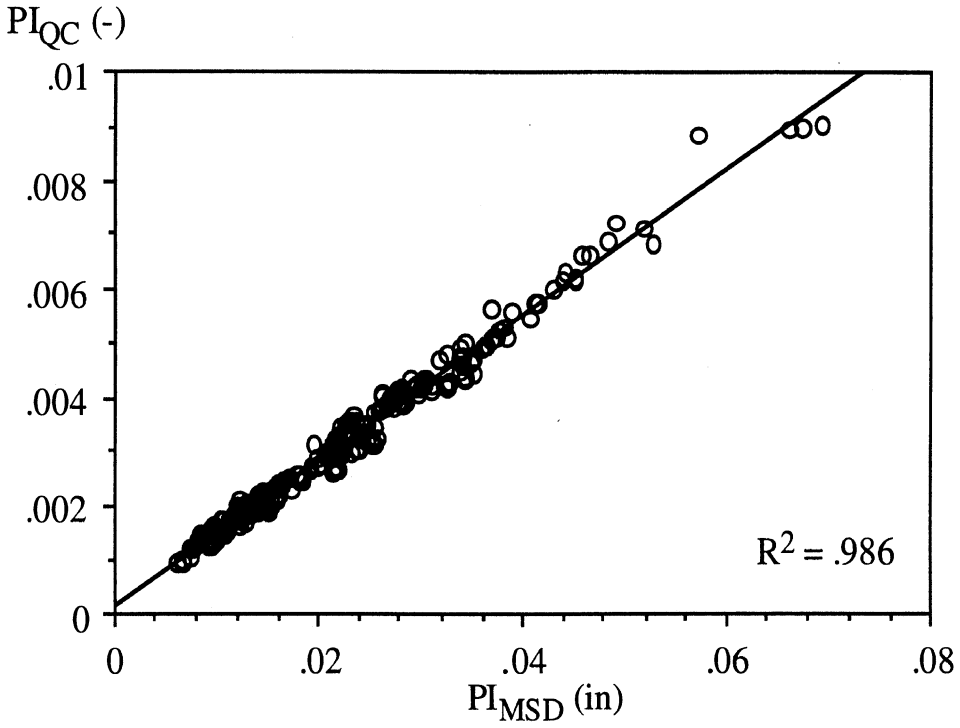

Figure 73. Statistical comparison of PI_{QC} and PI_{MSD}.

RELEVANCE TO RIDE QUALITY

The relevance of each algorithm to ride quality can be quantified by its ability to predict MPR. Each algorithm was applied to two sets of measured road profiles whose rideability was judged by rating panels: one for Ohio used in the development of RN_{275} and RN_{SD} in the 1980s, and another recent study performed in Minnesota. (Appendix C described the two data sets.)

Given that we are ultimately interested in results on the 0-to-5 RN scale, each type of PI was transformed to RN before it was compared to MPR. RN_{275} and RN_{SD} were calculated using the transforms recommended by their developers. RN_{QC} was calculated using the formulas given in chapter 2. PI_{MSD} was transformed to RN as follows:

$$RN = 5\, e^{-A(PI)^B} \tag{60}$$

where PI is a combination of the values for the left and right wheel track:

$$PI = \sqrt{\frac{PI_L^2 + PI_R^2}{2}} \tag{61}$$

The constants A and B were selected to provide optimal agreement with MPR for the Ohio sections. The IRI was transformed to a 0-to-5 scale using the same method, with the exception that "PI" in eq. 60 was replaced with the average of the IRI of the left and right wheel track.

Table 36 summarizes the standard error and coefficient of determination (R^2) for both data sets. Figures 74 through 78 compare the predicted values of RN for each algorithm to the actual values. Each plot shows a regression line and a line of equality.

Table 36. Summary of the relevance of RN algorithms to panel rating.

	Ohio Panel Data		Minnesota Panel Data	
Index	Standard Error	R^2	Standard Error	R^2
RN_{275}	.347	.788	.342	.869
RN_{SD}	**.292**	.845	1.212	.834
RN_{MSD}	.339	.829	.382	.879
RN_{QC}	**.292**	**.846**	**.288**	.879
RN_{IRI}	.431	.649	.400	**.894**

Overall, RN_{QC} predicts MPR with the lowest error level for the two data sets. RN_{SD} was developed using the Ohio data only. It predicts MPR as well as RN_{QC} for the Ohio data, but very poorly for the Minnesota data. Note that although the R^2 value looks good, the standard error is very high (> 1.2). The reason, illustrated in figure 75, is that a bias exists in the data. The bias is caused by the sensitivity of the algorithm to sample interval as described in appendix D. The algorithm acts differently for the Ohio data, which was recorded at a 6-in (152-mm) interval, than it does for the Minnesota data, which was recorded at an interval of about 13 in (330 mm). (Sensitivity to sample interval is covered in appendix I.) RN_{MSD} also predicts MPR with a bias for the Minnesota data (see figure 76), but the error is reduced significantly. RN_{275} predicts MPR fairly well for both the

Ohio and Minnesota data, but is prone to errors when significant roughness features appear at the beginning or end of a road section.

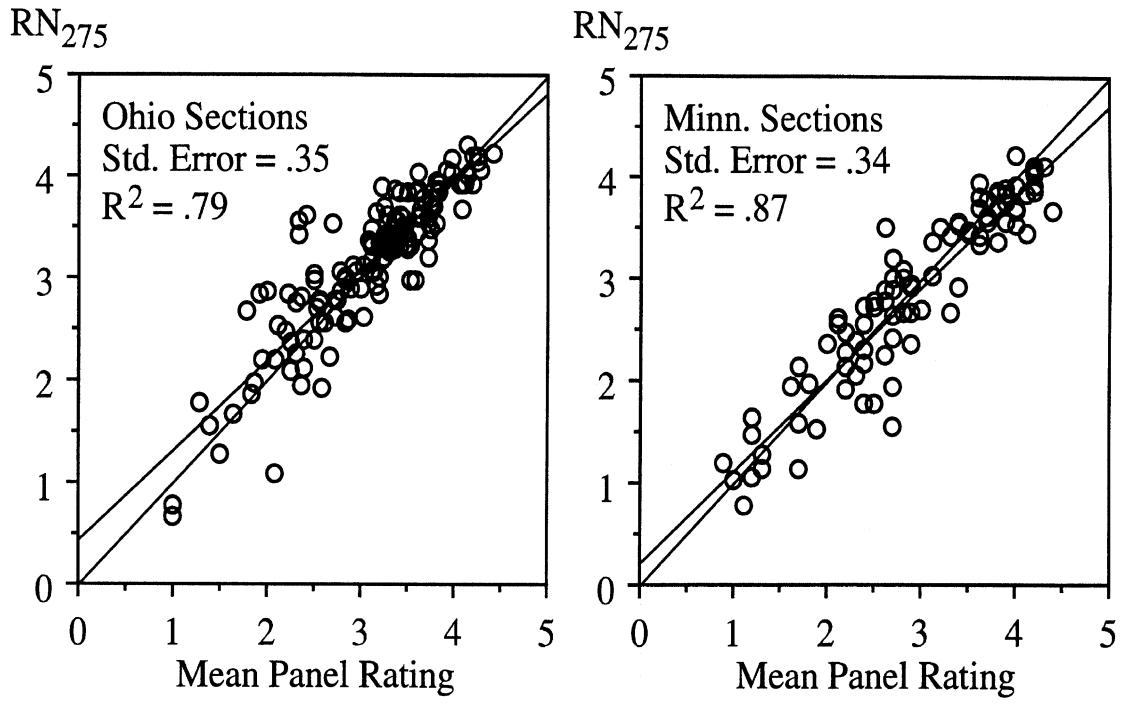

Figure 74. Prediction of MPRs by RN_{275}.

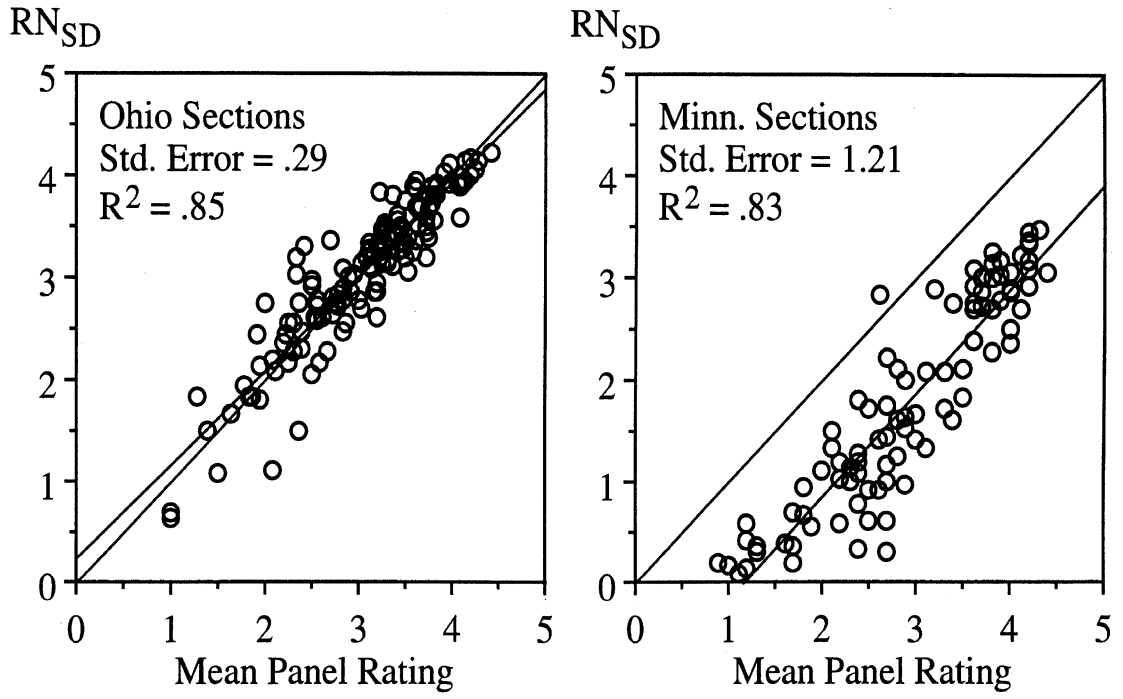

Figure 75. Prediction of MPRs by RN_{SD}.

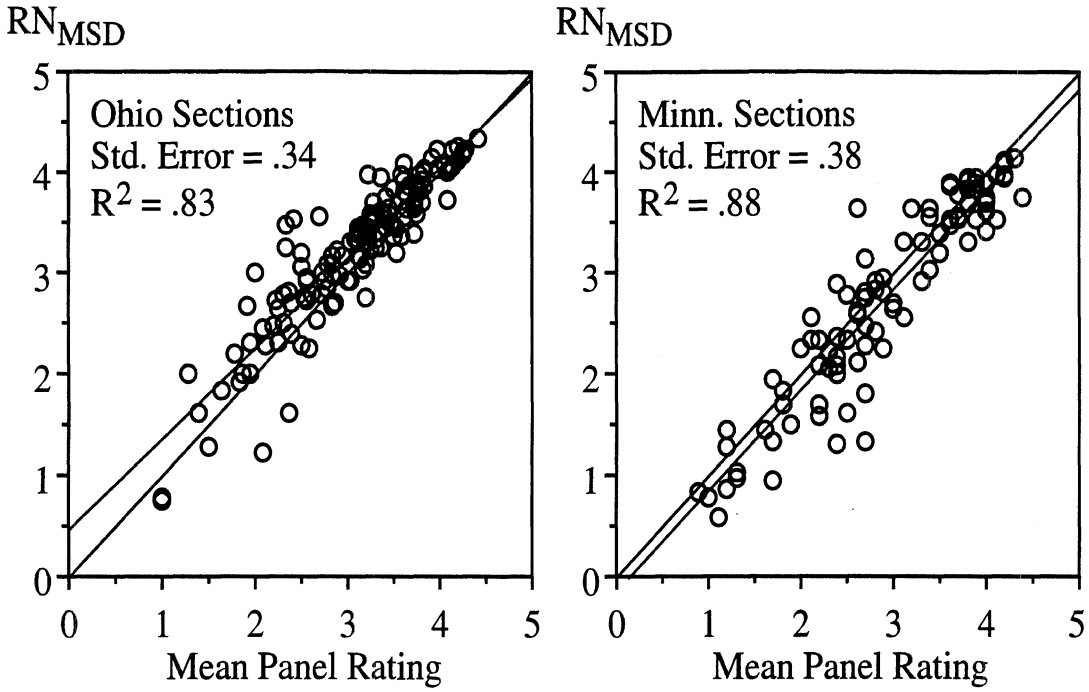

Figure 76. Prediction of MPRs by RN_{MSD}.

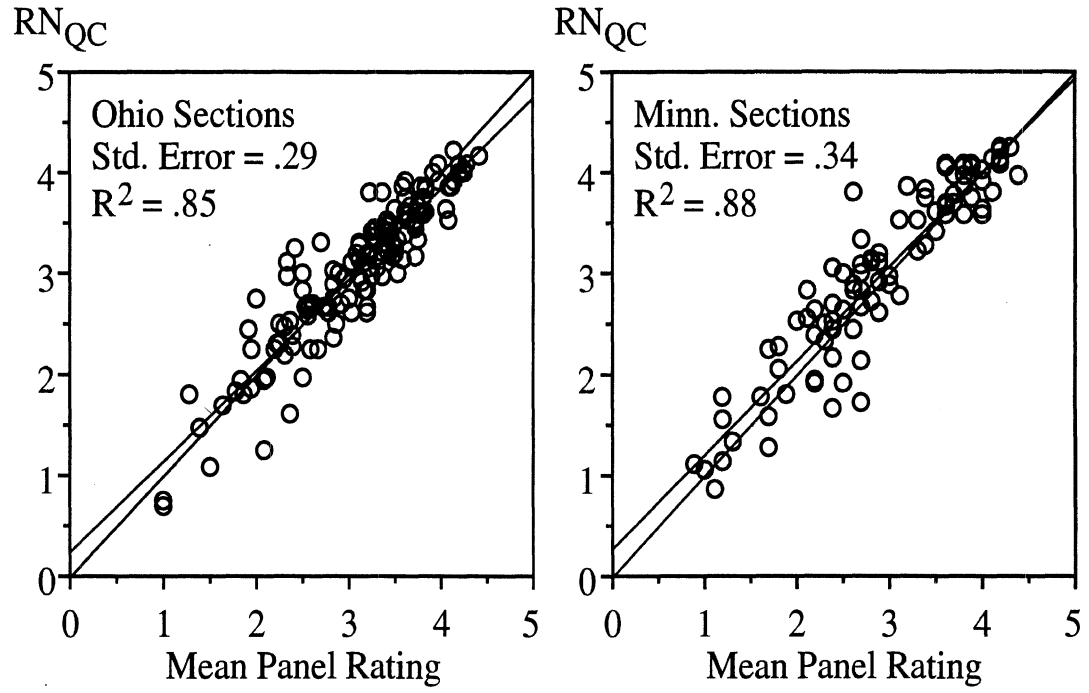

Figure 77. Prediction of MPRs by RN_{QC}.

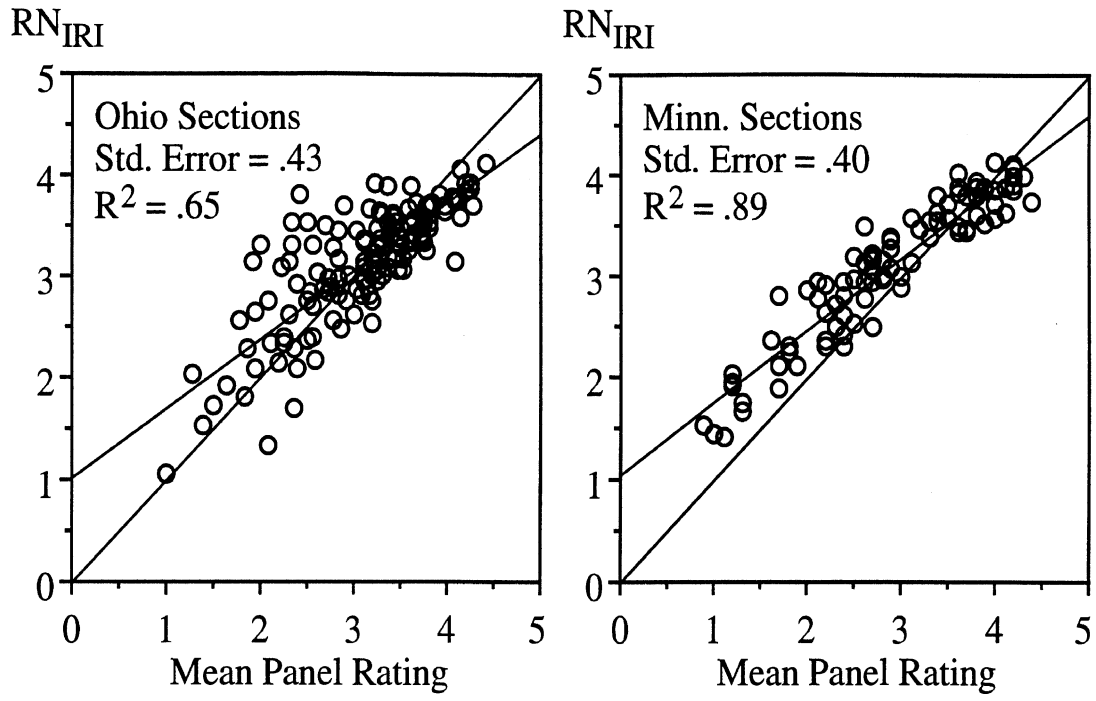

Figure 78. Prediction of MPRs by RN_{IRI}.

SENSITIVITY OF RN_{QC} TO SURFACE TYPE

Overall, the last three sections demonstrate:

- The four methods for calculating PI are statistically equivalent for profiles obtained with a K.J. Law Profilometer. Calculating any one of them provides the same type of information as the others.
- PI_{QC} (transformed to RN) is valid for both the Ohio and Minnesota data. It predicts panel rating with the lowest standard error for the panel ratings data used in the study (see appendix C).
- The IRI provides information that is unique to the other indices. It is relevant to different properties of profile, involving lower wave numbers (longer wavelengths).

PI_{QC} was developed to meet two objectives: (1) correlation with MPR; and (2) portability. Appendix I demonstrates that PI_{QC} is also the most portable of the algorithms.

Another study was made to determine if the relation between PI_{QC} and MPR depends on surface type. Table 37 summarizes the performance of PI_{QC} for the two sets of panel data on each surface type. The Ohio sections were classified as asphalt concrete, PCC, or composite. The Minnesota sections are classified as asphalt concrete or PCC. The table shows that PI_{QC} performs adequately on all three surface types, although more scatter (error) exists for the Ohio PCC sites.

Figures 79 and 80 compare the predicted and actual values of MPR for each surface type for the two data sets. Each plot shows a regression line and a line of equality. Note that asphalt concrete is the only surface type for which a broad range of MPR values are covered by both sets of panel data.

Table 37. Performance of PI_{QC} by surface type.

Surface Type	Ohio Panel Data		Minnesota Panel Data	
	Standard Error	R^2	Standard Error	R^2
Asphalt Concrete	.297	.911	.347	.898
PCC	.333	.772	.242	.891
Composite	.233	.853		

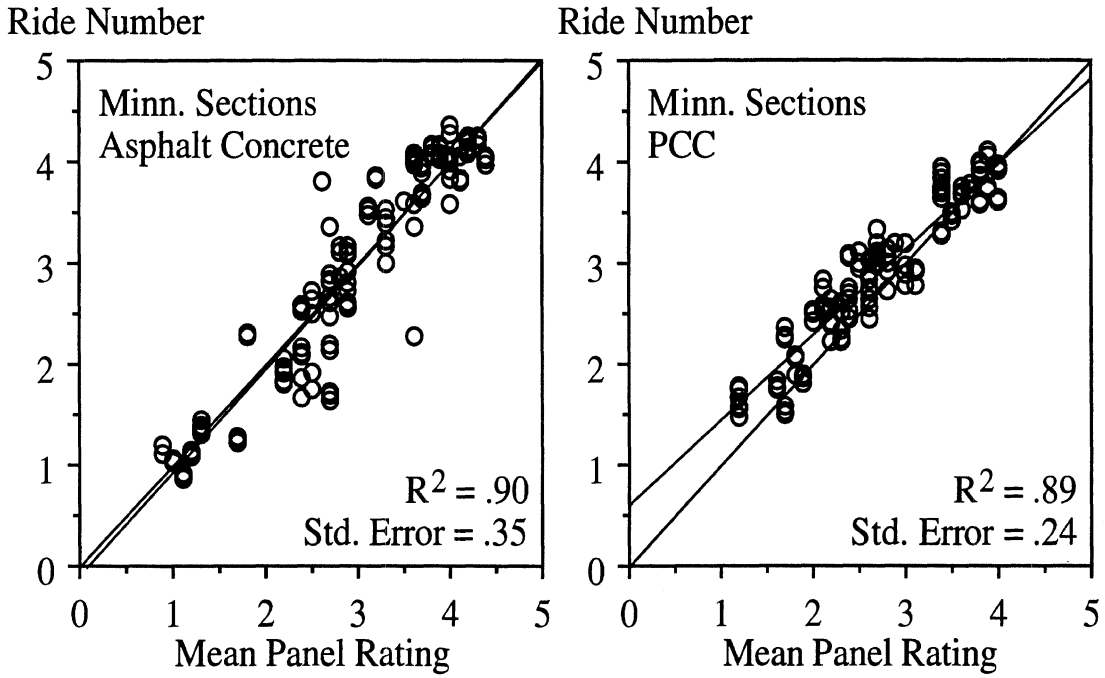

Figure 79. Prediction of MPR by PI_{QC} for the Minnesota data by surface type.

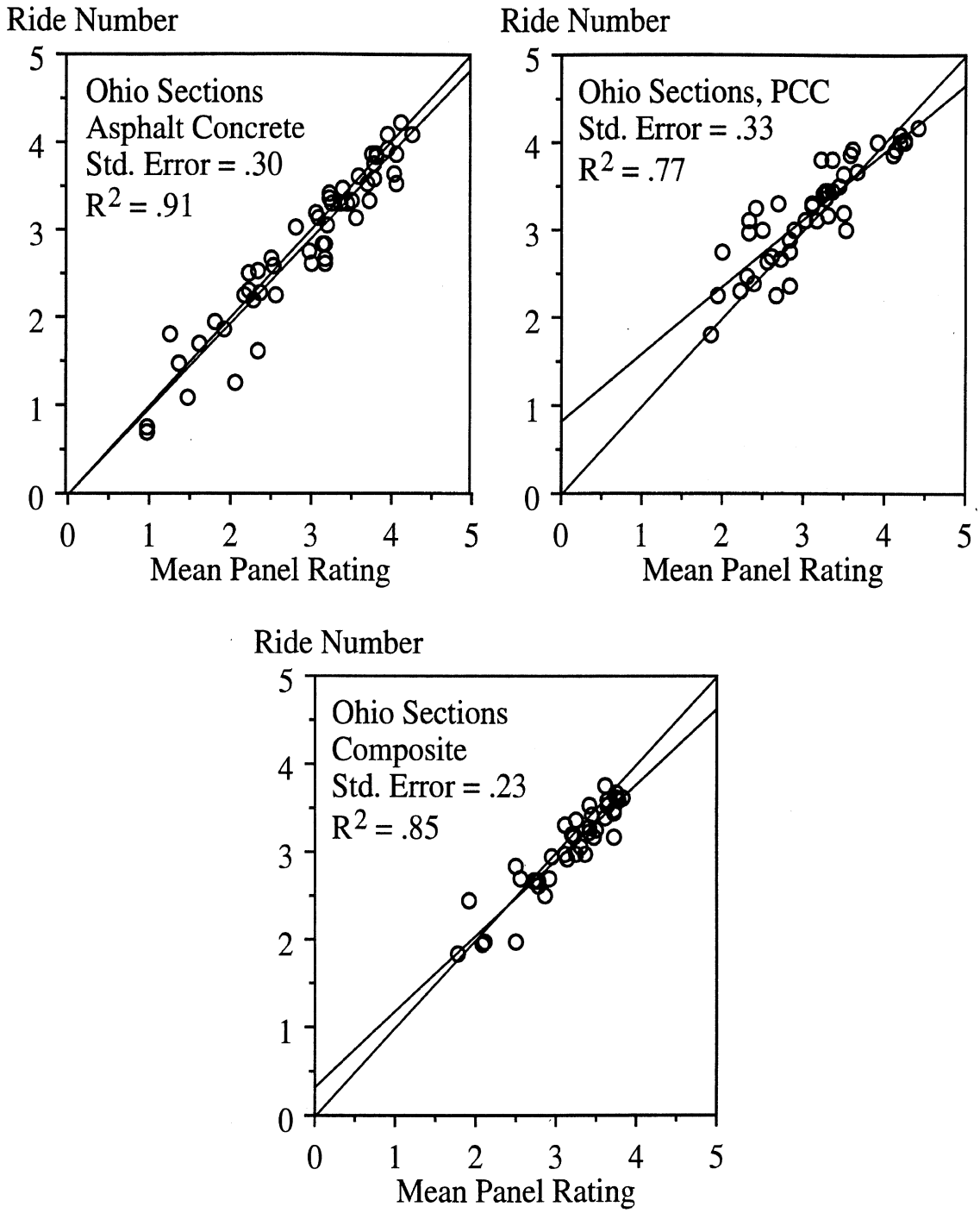

Figure 80. Prediction of MPR by PI_{QC} for the Ohio data by surface type.

APPENDIX I. RIDE NUMBER PORTABILITY

This appendix compares four methods for computing RN. RN is a transform of a summary profile index that has been called PI in past work. Four versions of PI that will be considered in this appendix are:

PI_{275}: The algorithm described in NCHRP Report 275.

PI_{SD}: The algorithm developed by Surface Dynamics, Inc., that was considered for an ASTM standard.[48]

PI_{MSD}: A modified version of the Surface Dynamics algorithm (see appendix D).

PI_{QC}: The quarter-car algorithm recommended in this report (see chapter 2).

The IRI was also included in the analysis as a benchmark. The abbreviations are provided for convenient identification of the algorithms throughout this appendix. The two existing algorithms (by NCHRP and Surface Dynamics) for PI_{275} and PI_{SD} were found to lack portability. Modification of PI_{SD} (PI_{MSD}) improved its portability, but not to the extent that is possible using a different type of solution. The algorithm recommended in this report was the most portable but not as portable as the IRI.

The portability of the alternatives for PI was evaluated in two ways: (1) by calculating the theoretical sensitivity of each algorithm to sample interval; and (2) through statistical evaluation of the performance of each algorithm when applied to measurements of the same profiles by several types of equipment.

THEORETICAL SENSITIVITY TO SAMPLE INTERVAL

The theoretical spatial frequency response of each algorithm was derived by hand and plotted by a commercial matrix manipulation program (MatLab). This was done using matrix algebra as described in appendixes D and E. Each algorithm for calculating PI acts as a filter with a characteristic transfer function that describes the ratio of an output to an input for a sinusoidal profile. The RMS value of a filtered profile can be estimated by applying the transfer function of the filter to the PSD function of the profile and integrating the result. This is basically how PI_{275} is calculated. The relation is shown in figure 81.

The transfer functions were constructed for each algorithm for a range of sample intervals. They were then applied to a white-noise slope profile and resulting RMS PI values were calculated. In the figure, the square root of the area under $G_{out}(\nu)$ provides the RMS value of filtered profile.

For a range of sample intervals, the theoretical RMS values were calculated and compared to the RMS that would be obtained in the limit using an infinitely short interval. Figure 82 provides the results for the IRI. The figure shows the expected output of the algorithm as a function of sample interval, normalized by the limit value. (The limit when the sample interval goes to zero is considered as the true reference response.) Note that the

error level of the IRI algorithm does not exceed 5 percent until the sample interval is greater than 4 ft (1.22 m).

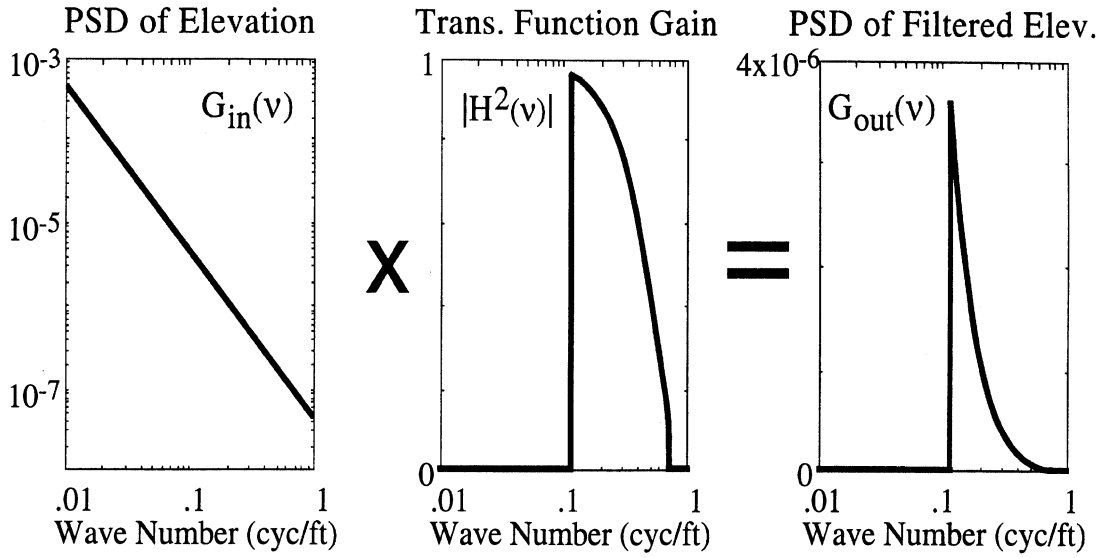

Figure 81. Theoretical calculation of filtered RMS elevation for PI_{275}.

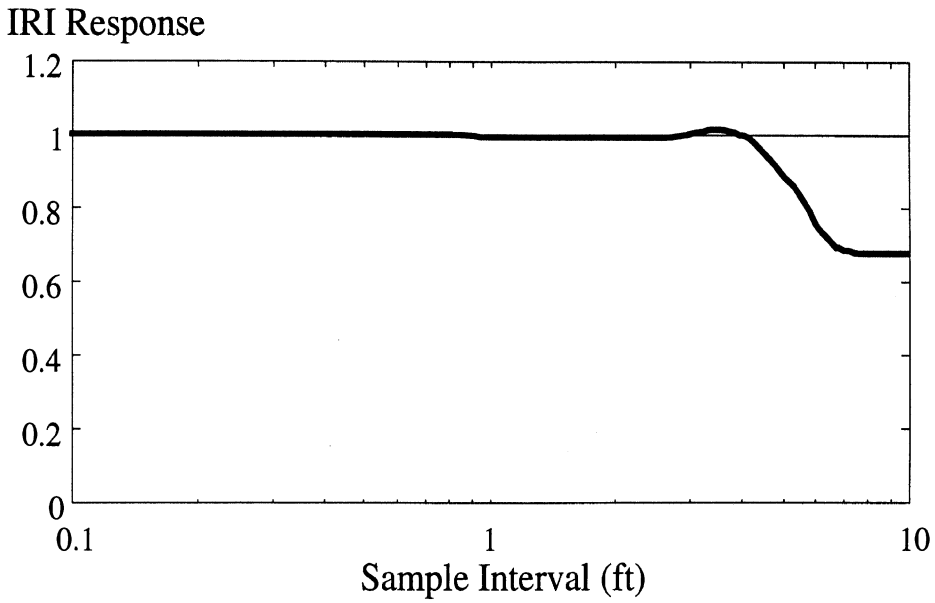

Figure 82. Sensitivity of IRI to sample interval.

Figure 83 shows the sensitivity of PI_{275} to sample interval. The response of the algorithm begins to drop off at a sample interval of about 8.5 in (216 mm). This is because the PSD of a road profile is only defined for wavelengths that are equal to or longer than twice the sample interval, and PI_{275} has a low-wavelength cutoff of about 17 in (432 mm). The response drops off slowly at first, then more rapidly at the larger sample intervals. (The contribution to PI is greater for the longer wavelengths.) Since much of the data used in the NCHRP studies was collected using K.J. Law Profilometers, the profiles were

filtered with a 12-in (305-mm) moving average. However, the moving average is not included in the description of the algorithm provided in the report.[4] Thus, a second line is included in figure 83 that shows the consequences of omitting the moving average.

Figure 84 compares the PI_{SD} and PI_{MSD} algorithms for a range of sample intervals. The response of the algorithm for PI_{SD} rises sharply even for very short sample intervals. Both the PI_{SD} and PI_{MSD} algorithm blow up over part of the range shown in the figure. PI_{SD} has an error of greater than 100 percent for sample intervals of 12 to 19 in (305 to 483 mm). PI_{MSD} only shows this level of error for sample intervals over 2 ft (610 mm), but it shows significant errors for any interval greater than 13 in (330 mm).

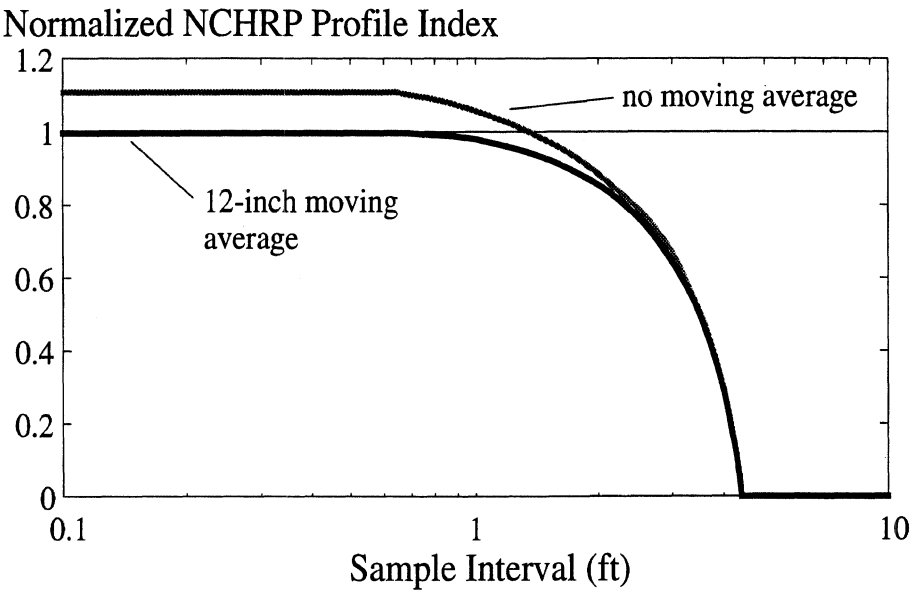

Figure 83. Sensitivity of PI_{275} to sample interval.

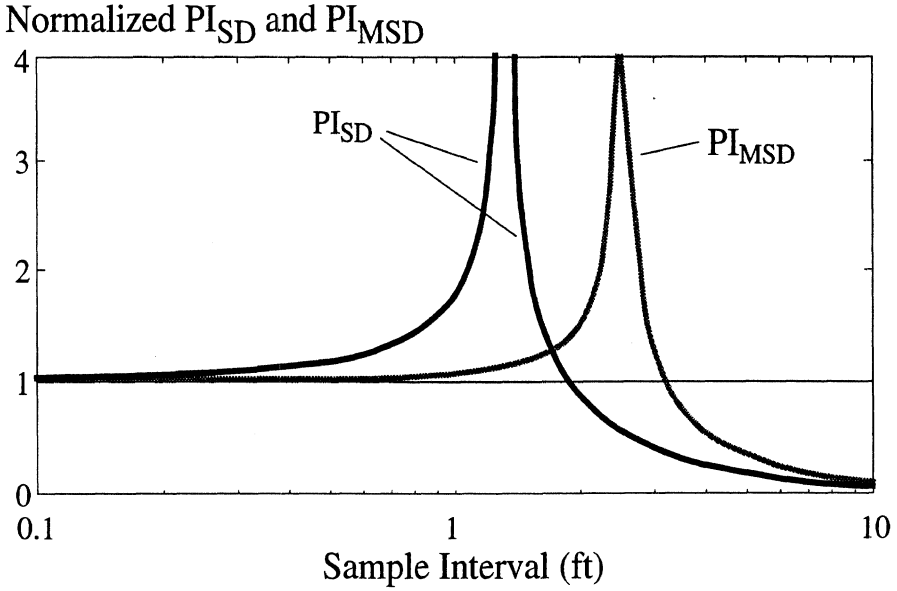

Figure 84. Sensitivity of PI_{SD} and PI_{MSD} to sample interval.

Figure 85 shows the sensitivity of PI_{QC} to sample interval. Next to the IRI, PI_{QC} is the least sensitive to sample interval.

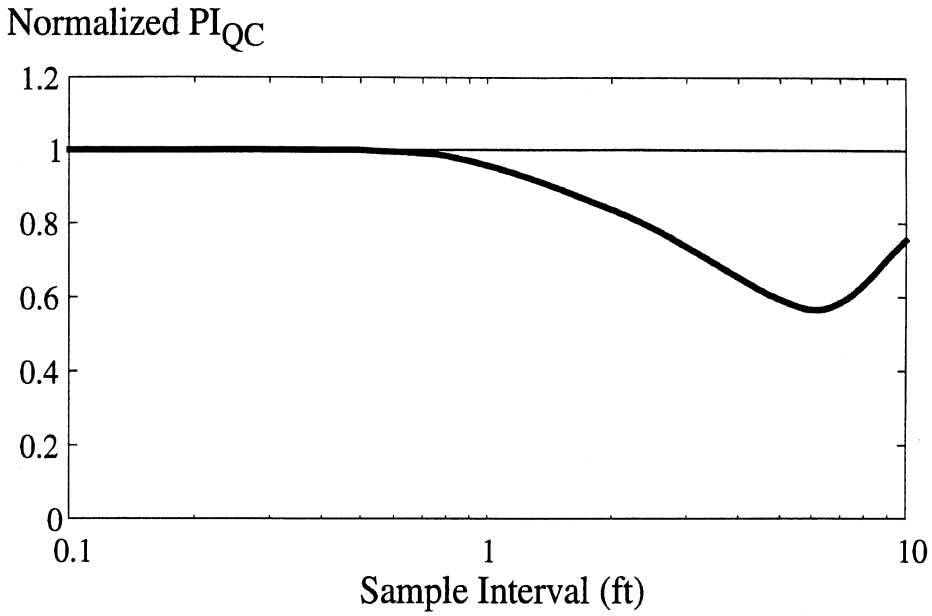

Figure 85. Sensitivity of PI_{QC} to sample interval.

STATISTICAL EVALUATION

The theoretical sensitivities show errors caused by a change in sample interval. They are inherent in the mathematics of the filters. Additional errors result from measurement errors in the profiling systems. To determine the total error, which includes the analysis method plus the limitations of a particular profiler and its human operator, a statistical evaluation was made. The algorithms for computing PI were programmed and applied to a matrix of profile measurements. This portability matrix is composed of repeated measures made on 30 sites by multiple profilers (see appendix C).

For each profile analysis, the summary roughness values from the various profilers were compared to those from the Law systems. The analysis was also done for the IRI to provide a benchmark. For example, figure 86 shows IRI results for the PRORUT. The figure shows a pair of IRI measures from the PRORUT and a Law system for each of eight sections. The figure shows both a regression line and a line of equality. The points in the plot follow the line of equality fairly closely. The R^2 value of 0.975 suggests that measures of IRI from the PRORUT and the Law system are compatible. However, the R^2 value alone does not indicate whether bias exists. The more appropriate indicators of the agreement between two profilers are the bias and random error of one set of measures relative to another.

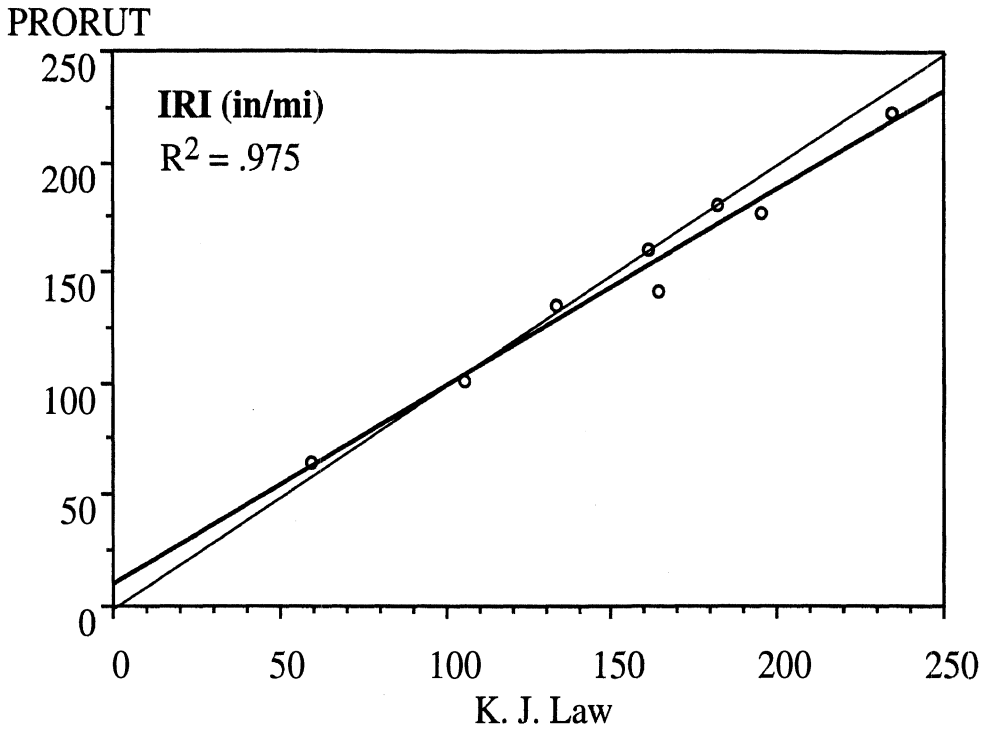

Figure 86. Comparison of IRI measures from the PRORUT and Law system.

Let the measures of roughness from the Law system on site *i* be X_i and the measure from another profiler be Y_i. Bias is defined as the average value of $(Y_i - X_i)$ for all sites. This statistic indicates, in absolute units (in/mi for IRI), by how much another system is high or low, relative to the Law system. For example, on the average, the measures from the PRORUT were lower for the eight test sites than those of the Law system, by 7 in/mi (0.11 m/km).

The normalized bias percentage is defined as 100 times the average value of the following expression computed for each site:

$$\frac{Y_i - X_i}{X_i} \tag{62}$$

In this case, the bias is normalized by the roughness ranges. For the example eight test sites, the PRORUT data were lower than the Law data by about 3 percent.

The RMS difference is the square root of the average value of $(Y_i - X_i)^2$ for all sites. It is approximately the difference that can be expected in a single pair of measurements and includes both random error and bias. For example, the RMS difference between the PRORUT and the Law system was 11 in/mi (0.17 m/km).

The normalized RMS difference in percent is defined as 100 times the square root of the average value of the following expression computed for each site:

$$\left[\frac{Y_i - X_i}{X_i}\right]^2 \tag{63}$$

For example, when expressed as a percentage, the average RMS difference that can be expected between the PRORUT and the Law system is about 7 percent.

The normalized bias and normalized RMS difference provide a clear means of assessing the relative portability of an algorithm for a profile index. They represent the level of systematic error and random scatter, respectively. They also, by virtue of normalization, allow comparison of unlike indices. For example, the statistics for a 0-to-5 scale can be compared to those for a 0-to-300 scale. One must be careful, however, to use measurements with a broad range of roughness and apply each set of algorithms to the same set of measurements.

Tables 38 and 39 provide a summary of the normalized bias and normalized RMS difference values for each algorithm. The first two rows of the tables show the sensor type and sample interval (Δ) associated with the profiler. Because the devices with ultrasonic sensors were problematic to all of the algorithms, including the IRI, it is suspected that some of the bias and scatter is caused by measurement error.

Table 38. Experimental normalized bias (in percent).

	Dipstick	ICC	PRORUT	ARAN	ICC	Pave Tech	SDType
Sensor	Static	Laser	Laser	Laser	U-sonic	U-sonic	U-sonic
Δ (ft)	1.00	0.54	0.16	0.33	1.08	0.86, 1.08	1.03
IRI	-5.6	-1.3	-3.1	0.3	16.3	26.6	6.5
PI_{275}	8.6	9.1	4.9	11.3	49.0	106.3	62.6
PI_{SD}	86.0	24.6	21.7	24.9	179.7	268.2	199.5
PI_{MSD}	21.0	16.8	26.7	23.9	61.7	113.9	80.6
PI_{QC}	0.3	-1.9	2.2	9.6	20.0	71.6	45.4

Table 39. Experimental normalized RMS difference (in percent).

	Dipstick	ICC	PRORUT	ARAN	ICC	Pave Tech	SDType
Sensor	Static	Laser	Laser	Laser	U-sonic	U-sonic	U-sonic
Δ (ft)	1.00	0.54	0.16	0.33	1.08	0.86, 1.08	1.03
IRI	10.6	13.3	6.9	10.4	35.0	51.1	17.1
PI_{275}	21.5	21.1	11.6	21.4	105.8	167.5	73.5
PI_{SD}	94.6	39.8	31.8	33.4	315.3	407.5	222.3
PI_{MSD}	28.5	31.0	35.1	31.1	122.4	177.8	95.2
PI_{QC}	15.6	23.4	8.5	16.2	122.6	78.6	59.5

International Roughness Index

The IRI shows the best portability of the five analyses because it has the lowest normalized bias and RMS difference. The bias values are exceptionally low for the Dipstick, PRORUT, ARAN, and laser ICC. The statistical results support the theoretical finding that the IRI should be the least sensitive to sample interval.

NCHRP Profile Index (PI_{275})

The results for PI_{275} fit into two categories: ultrasonic and non-ultrasonic systems. The wave numbers that affect PI_{275} range from 0.125 to 0.630 cycles/ft (0.410 to 2.07 cycles/m). A sample interval of 9.6 in (244 mm) is required to fully cover this range. The Dipstick has a sample interval of 12 in (305 mm), causing it to miss some of the wave numbers contributing to the PI_{275}. Even so, values of PI_{275} computed from the Dipstick are higher than those from the Law system, by an average of 9 percent. The bias seen in the laser profilers ranges between 5 percent (PRORUT) and 11 percent (ARAN). This bias is caused by the 12-in (305-mm) moving average filter applied in the Law data.

Overall, the agreement between the Law system, the Dipstick, and the three laser profilers is much closer than the 18-percent difference observed between the Law system and the PSU profiler in the NCHRP studies (see appendix D). The wide discrepancy between the two systems in the original study is still not explained. The Law systems have been verified repeatedly over the years through comparison with static measures, so the PSU measurements are assumed to be in error.

The generally low bias between the Law reference and the non-ultrasonic profilers shows that standardization of the RN might be possible, motivating the development of PI_{QC} in this project. However, the algorithm used to compute PI_{275} is not developed past the research stage. Although it was sufficient to establish correlation with MPR, there are some undesirable side effects of the analysis:

- The cosine taper window function eliminates inputs from the beginning and end of a profile. This is valid only when the roughness properties are uniform throughout a road section (seldom the case with real-world data).
- The FFT algorithm transforms a finite length of a profile at one time, in contrast to other algorithms that march through the data, processing the profile point-by-point. Algorithms that march can be used to show the distribution of roughness versus station number. This is not possible with an FFT.

Surface Dynamics Profile Index (PI_{SD})

The bias and RMS difference are significantly worse for PI_{SD} than was seen for the IRI or PI_{275} analyses. Agreement with the ultrasonic devices is nonexistent. Normalized bias and RMS errors are much larger than with the other analyses.

PI_{SD} is sensitive to all wave numbers above 0.125 cycles/ft (0.410 cycles/m) because the algorithm for estimating PI_{SD} has no high-frequency cutoff. Thus, in the absence of a moving average filter, the range of wave numbers that contribute to PI_{SD} will go as high as

the device can measure. This effect causes devices with a wider bandwidth than the Law reference to measure systematically high. However, a second effect is that the computer program for PI_{SD} has a wave number response function that increases its gain as the sample interval is increased (see appendix D). The second effect causes devices with sample intervals shorter then 6 in (152 mm) to measure systematically low, and those with larger sample intervals to measure systematically high.

The ICC laser system has almost the same sample interval as the Law reference: 6.48 in (165 mm) versus 6 in (152 mm). Its PI values are high on the average by 25 percent. At least part of the difference is due to a wider bandwidth in the ICC system.

The PRORUT has an even larger bandwidth, which would cause even more bias upward. However, the shorter sample interval means that the gain of the PI_{SD} algorithm is closer to unity (for the Law system it approaches 1.45), causing a bias downward. The two factors cancel somewhat, reducing the cumulative bias to 22 percent.

The best agreement is obtained by the PRORUT, in which the average RMS error is 32 percent. (For PI_{275}, the error was 12 percent.) This is unacceptably high. The other devices have even larger differences: 95 percent for the Dipstick, 40 percent for the ICC laser system, and 33 percent for the ARAN.

Modified Surface Dynamics Profile Index (PI_{MSD})

Agreement for PI_{MSD} improved considerably in comparison to PI_{SD}, but the errors are still unacceptably high. Although the PI_{MSD} algorithm reduces the sensitivity to sample interval, it still does nothing to limit the range of wave numbers above 0.125 cycles/ft (0.410 cycles/m). Systems that can measure roughness down to short wavelengths still produce numbers that are higher than those obtained from a Law system.

Quarter-Car Profile Index (PI_{QC})

PI_{QC} shows the lowest bias and RMS difference among the PI analyses. For the Dipstick and the laser systems, the bias and RMS difference are comparable to those of the IRI. For ultrasonic systems, the bias errors are lower than those of the PI algorithms, but are generally unacceptable. The bias is also greater than that predicted by the theoretical analysis described above. This is because the algorithm is sensitive to short wavelengths that are not measured accurately by the ultrasonic systems.

REFERENCES

1. Spangler, E.B. and W.J. Kelly, "GMR Road Profilometer - A Method for Measuring Road Profile." Highway Research Record 121, (1966) pp. 27-54.

2. Sayers, M.W., et al., "Guidelines for Conducting and Calibrating Road Roughness Measurements." World Bank Technical Paper Number 46, (1986) 87 p.

3. Janoff, M.S., *Pavement Roughness and Rideability Field Evaluation.* National Cooperative Highway Research Program Report 308, (1988) 54 p.

4. Janoff, M.S., et al., *Pavement Roughness and Rideability.* National Cooperative Highway Research Program Report 275, (1985) 69 p.

5. Sayers, M.W., "On the Calculation of IRI from Longitudinal Road Profile." Transportation Research Record 1501, (1996) pp. 1-12.

6. Sayers, M. and S.M. Karamihas, "Evaluation of Rideability by Analyzing Longitudinal Road Profile." Presented at the 75th Annual Meeting of the Transportation Research Board, Washington, DC, (1996).

7. *A Summary of Pavement Performance Data Collection and Processing Methods Used by State DOTs.* Federal Highway Administration Report FHWA-RD-95-060, (1994) 62 p.

8. Gillespie, T.D., et al., *Calibration of Response-Type Road Roughness Measuring Systems.* National Cooperative Highway Research Program Report 228, (1980) 81 p.

9. Sayers, M.W., et al., "The International Road Roughness Experiment." World Bank Technical Paper Number 45, (1986) 453 p.

10. *Highway Performance Monitoring System, Field Manual, Appendix J.* U.S. Department of Transportation, Washington, D.C. FHWA Publication 5600.1A, (1990).

11. Sayers, M.W., "Two Quarter-Car Models for Defining Road Roughness: IRI and HRI." Transportation Research Record 1215, (1989) pp. 165-172.

12. Gramling, W.L., *Current Practices in Determining Pavement Condition.* National Cooperative Highway Research Program Synthesis of Highway Practice 203, (1994) 57 p.

13. Hveem, F.N., "Devices for Recording and Evaluating Pavement Roughness." Highway Research Board Bulletin 264, (1960) pp. 1-26.

14. Holbrook, L.F., *Prediction of Subjective Response to Road Roughness Using the General Motors-Michigan Department of State Highways Rapid Travel Profilometer.* Michigan Department of State Highways Report R-719, (1970) 65 p.

15. Spangler, E.B. and W.J. Kelly, *Integration of the Inertial Profilometer in the Ohio DOT Pavement Management System.* Ohio Department of Transportation Report FHWA/OH-87/005, (1987) 122 p.

16. Spangler, E.B., et al., *Long-Term Time Stability of Pavement Ride Quality Data.* Federal Highway Administration Report FHWA/OH-91/001, (1990) 99 p.

17. Darlington, J., *A Roughness Wavelength Band Determined by Subjective Response.* Michigan Department of Highways unpublished report, (1976) 6 p.

18. McKenzie, D.W. and W.R. Hudson, "Road Profile Evaluation for Compatible Pavement Evaluation." Transportation Research Record 893, (1982) pp. 17-19.

19. "Guide for the Evaluation of Human Exposure to Whole-Body Vibration." International Standards Organization, International Standard 2631-1974, (1974).

20. Leatherwood, J.D. and L.M. Barker, "A User-Oriented and Computerized Model for Estimating Vehicle Ride Quality." National Aeronautics and Space Administration Technical Paper 2299, (1984) 42 p.

21. Pradko, F., et al., "Theory of Human Vibration Response." American Society of Mechanical Engineers 66-WA/BHF-15, (1967) 13 p.

22. Harness, M.D., et al., *A Comprehensive Study of Roadmeter Roughness Number With Riding Comfort for Indiana Pavements.* Indiana Department of Highways Report DRT-85-1, (1985) 298 p.

23. Loizos, A., et al., "Effects of User Characteristics and Vehicle Type on Road Roughness Perception." *Road and Transport Research,* Vol. 3, No. 4, (1994) pp. 57-65.

24. Perera, R.W. and S.D. Kohn, *Road Profiler User Group Fifth Annual Meeting. Road Profiler Data Analysis and Correlation.* Soil and Materials Engineers, Inc. Research Report No. 92-30, (1994) 87 p.

25. Hutchinson, B.G., "Principles of Subjective Rating Scale Construction." Highway Research Record 46, (1964) pp. 60-70.

26. Bendat, J.S. and A.G. Piesol, *Random Data: Analysis and Measurement Procedures.* Wiley-Interscience, New York, (1971).

27. Dodds, C.J. and J.D. Robson, "The Description of Road Surface Roughness." *Journal of Sound and Vibration*, Vol. 31, No. 2, (1973) pp. 175-183.

28. Robson, J.D., "Deductions from the Spectra of Vehicle Response due to Road Profile Excitation." *Journal of Sound and Vibration,* Vol. 7, No. 2, (1968) pp. 156-158.

29. Sayers, M., "Characteristic Power Spectral Density Functions for Vertical and Roll Components of Road Roughness," *Symposium on Simulation and Control of Ground Vehicles and Transportation Systems. Proceedings.,* L. Segel, J. Y. Wong, E. H. Law and D. Hrovat ed., American Society of Mechanical Engineers, New York, (1986) pp. 113-139.

30. Hayhoe, G.F., "Spectral Characteristics of Longitudinal Highway Profiles as Related to Ride Quality," *Vehicle, Tire, Pavement Interface, ASTM STP 1164,* J. J. Henry and J. C. Wambold ed., American Society of Testing and Materials, Philadelphia, (1992) pp. 32-53.

31. Perera, R.W. and S.D. Kohn, *Road Profiler User Group Sixth Annual Meeting. Road Profiler Data Analysis.* Soil and Materials Engineers, Inc., (1995) 87 p.

32. Sayers, M.W. and C. Mink, "A Simulation Graphical User Interface for Vehicle Dynamic Models." Society of Automotive Engineers Paper Number 950169, (1995) 10 p.

33. Sayers, M.W., *ERD Data-Processing Software Reference Manual. Version 2.00.* Univeristy of Michigan Transportation Research Institute Report UMTRI-87-2, (1987) 109 p.

34. Ervin, R. D., et al, *Influence of Truck Size and Weight Variables on the Stability and Control Properties of Heavy Trucks.* Federal Highway Administration Report FHWA-RD-83-030, (1983) 179 p.

35. Sweatman, P.F., "Effect of Heavy Vehicle Suspensions on Dynamic Road Loading." Australian Road Research Board ARR 116, (1980) 15 p.

36. Sweatman, P.F., *A Study of Dynamic Wheel Forces in Axle Group Suspensions of Heavy Vehicles.* Australian Road Research Board SR27, (1983) 56 p.

37. Gillespie, T.D., et al., *Effects of Heavy Vehicle Characteristics on Pavement Response and Performance.* National Cooperative Highway Research Program Report 353, (1993) 126 p.

38. *The AASHO Road Test, Report 5, Pavement Research.* Highway Research Board Special Report 61E, (1962) 352 p.

39. Carey, W.N. and P.E. Irick, "The Pavement Serviceability-Performance Concept." Highway Research Board Bulletin 250, (1960) pp. 40-58.

40. Novak, E.C. and L.E. DeFrain Jr., "Seasonal Changes in the Longitudinal Profile of Pavements Subject to Frost Action." Transportation Research Record 1362, (1992) pp. 95-100.

41. Perera, R.W., et al., "Comparative Testing of Profilometers." Transportation Research Record 1435, (1994) pp. 137-144.

42. Huft, D.L., "South Dakota Profilometer." Transportation Research Record 1000, (1984) pp. 1-7.

43. Lucas, J. and A. Viano, *Systematic Measurement of Evenness on the Road Network: High Output Longitudinal Profile Analyser.* Laboratoire Central des Ponts et Chaussees Report Number 101, (1979).

44. Still, P.B. and P.G. Jordan, *Evaluation of the TRRL High-Speed Profilometer.* Transport and Road Research Laboratory Report LR 922, (1980) 45 p.

45. Sayers, M.W. and T.D. Gillespie, *The Ann Arbor Road Profilometer Meeting. Final Report.* Federal Highway Administration Report FHWA/RD-86/100, (1986) 237 p.

46. Hudson, W.R., et al., "Root-Mean-Square Vertical Acceleration as a Summary Roughness Statistic," *Measuring Road Roughness and Its Effects on User Cost and Comfort, ASTM STP 884,* T. D. Gillespie and M. W. Sayers ed., American Society of Testing and Materials, Philadelphia, (1985) pp. 3-24.

47. Bertrand, C., "Field Evaluation of the Auto-Read Version of the Face Dipstick as a Class I Profiling Device." Presented at the 69th Annual Meeting of the Transportation Research Board, Washington, DC, (1990) 22 p.

48. "Standard Test Method for Measuring Road Roughness by Static Rod and Level Method." *Annual Book of ASTM Standards,* Vol. 04.03, E1364, (1991) pp. 667-701.

49. Donnely, D.E., et al., *Pavement Profile Smoothness Seminar Proceedings, Ft. Collins, Colorado, October 5-8 1987. Volume II: Data Collection Equipment.* Federal Highway Administration Report FHWA-DP-88-072-004, (1988) 307 p.

50. Croteau, J.R., *Pavement Roughness Evaluations Using a Mays Ride Meter.* Federal Highway Administration Report FHWA-NJ-82-003, (1981) 111 p.

51. Kulakowski, B.T., "Critical Evaluation of the Calibration Procedure for Mays Meters." Transportation Research Record 1084, (1986) pp. 17-22.

52. Lively, F. (1969) "Mays Road Meter Smooths the Way." Texas Highways. Feb. 1969, pp 11-13.

53. Weaver, R.J., *Quantifying Pavement Serviceability as it is Judged by Highway Users.* New York DOT (1978).

54. Weed, R.M. and R.T. Barros, "Discussions of Paper: 'Methodology for Computing Pavement Ride Quality from Pavement Roughness Measurements'." Transportation Research Record 1084, (1986) pp. 13-16.

55. Janoff, M.S., "The Prediction of Pavement Ride Quality from Profile Measurements of Pavement Roughness," *Surface Characteristics of Roadways: International Research and Technologies, ASTM STP 1031,* W. E. Meyer and J. Reichert ed., American Society of Testing and Materials, Philadelphia, (1990) pp. 259-267.

56. Spangler, E.B. and W.J. Kelly, "Development and Evaluation of the Ride Number Concept," *Vehicle-Road Interaction, ASTM STP 1225,* B. T. Kulakowski ed., American Society of Testing and Materials, Philadelphia, (1994) pp. 135-149.

57. Press, W.H., et al., *Numerical Recipes: The Art of Scientific Computing.* Cambridge University Press, Cambridge, (1986) 700 p.